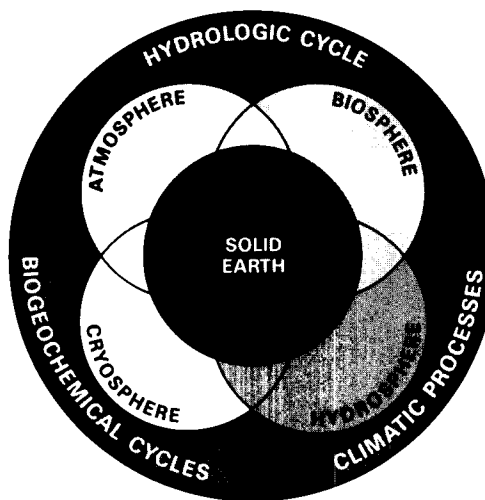


From Pattern to Process: The Strategy of the Earth Observing System

ORIGINAL CONTAINS
COLOR ILLUSTRATIONS



Eos Science Steering Committee Report

Volume II



National Aeronautics and
Space Administration

EARTH OBSERVING SYSTEM REPORTS

Volume I	Science and Mission Requirements Working Group Report
Volume II	From Pattern to Process: The Strategy of the Earth Observing System Science Steering Committee Report
Volume IIa	Data and Information System Data Panel Report
Volume IIb	MODIS Moderate-Resolution Imaging Spectrometer Instrument Panel Report
Volume IIc	HIRIS High-Resolution Imaging Spectrometer: Science Opportunities for the 1990s Instrument Panel Report
Volume IId	LASA Lidar Atmospheric Sounder and Altimeter Instrument Panel Report
Volume IIe	HMMR High-Resolution Multifrequency Microwave Radiometer Instrument Panel Report
Volume IIf	SAR Synthetic Aperture Radar Instrument Panel Report
Volume IIg	LAWS Laser Atmospheric Wind Sounder Instrument Panel Report
Volume IIh	Altimetric System Panel Report

**SCIENCE STEERING COMMITTEE
FOR THE
EARTH OBSERVING SYSTEM**

Dixon M. Butler, Chairman
Richard E. Hartle, Executive Secretary
Mark Abbott
Robert Cess
Robert Chase
Philip Christensen
John Dutton
Lee-Lueng Fu
Catherine Gautier
John Gille
Robert Gurney
Paul Hays
John Hovermale
Seelye Martin
John Melack
Donald Miller
Volker Mohnen
Berrien Moore, III
John Norman
Stanley Schneider
John Sherman, III
Verner Suomi
Byron Tapley
Raymond Watts
Eric Wood
Paul Zinke

PREFACE

Eos is dedicated to providing the observations and data and information system necessary to understand the way the Earth works as a natural system. The appearance of the Earth in these images is dominated by the blues of the oceans and the white of the clouds. These features are both the result of the abundant presence of water in the Earth's environment. These images contrast sharply with the desolate features of the lunar surface. They have become symbolic of the unity of our world and have encouraged the realization that our global environment is a precious thing which cannot be replaced. These images of Earth and our reaction to them are qualitative. With Eos, the Earth observations community hopes to quantitatively characterize our planet and provide the basis for a scientific understanding of the global system which is the Earth. This understanding will enable us to predict the future state of the environment and how it will respond to natural events and human activities. With this ability, our response to satellite images of Earth will have shifted from the emotional to the rational, from intuition to understanding.

Scientific study of the Earth has been a part of space flight from the beginning. The breadth of this challenge has made it difficult for some to accept while others have yearned for a personal understanding of Eos at a level of detail which was more readily achievable with less comprehensive missions. The intent of this report is to connect the specifics of the Eos mission with the overall study of the Earth system and to illustrate the utility of Eos in specific studies drawn from the traditional disciplines of Earth science.

The Eos Science and Mission Requirements Working Group issued its report in 1984. The fundamental recommendations of that group as to how the Eos mission should be carried out and what the elements of the mission should be have remained the foundation of continued Eos planning, and the work of this committee has been based upon them. In the ensuing three years considerable progress has been made in preparing for the implementation of Eos. The reports of the various Eos panels which have been issued over the last year and a half make this evident. This report integrates these better defined elements of Eos into a more detailed overall concept of the mission.

A critical step in the development of Eos has been the articulation of the overall strategy for Earth System Science and the recognition by the Earth System Science Committee of the NASA Advisory Council that Eos is the centerpiece of the implementation of this strategy. At the same time the International Council of Scientific Unions has adopted the International Geosphere-Biosphere Program as a major focus for worldwide cooperation in studying the Earth and the Space Station Program has been initiated. Both of these activities help to establish the international context within which Eos can happen.

During the considerable intellectual ferment which has accompanied the progress of the last three years, this committee has debated what the role should be for its report and who the audience is for this document. Eos is a part of a larger enterprise aimed at understanding global change and as such it is not necessary for us to articulate all aspects of the program for all audiences. This report is directed primarily at our colleagues in the international Earth observations community. This report summarizes the current Eos mission concept. It shows how this mission can provide the critical space observations needed to understand the integrated functioning of the global cycles of energy, water, and biogeochemicals. It illustrates by examples how this same set of observations will address the needs of various scientific investigations within the individual disciplines of Earth science. Finally, it recommends steps that must be taken now to prepare for Eos.

Many individuals have contributed to this report. Several significant contributions have come from outside of our committee. In particular, we wish to thank Drs. Tim Liu, Greg Wilson, and Jim Richman. The Eos project office at Goddard Space Flight Center headed by Chuck MacKenzie and the element of this project office at the Jet Propulsion Laboratory led by Jim Graf have provided excellent support to this committee and have been a pleasure to work with. Marty Donohoe of GSFC has contributed substantially to this report, particularly in the development of many of the figures. JoBea Cimino and Deborah Vane of JPL have also worked closely with this committee during the development of this report. These three individuals within the Eos Project have been outstanding to work with. We also must acknowledge the considerable support this committee has received from Dr. Shelby Tilford, Director of the Earth Science and Applications Division at NASA Headquarters and Alex Tuyahov, Program Manager for Eos within that division. Committee meetings have been made far more productive and enjoyable by the work of the team from Birch & Davis Associates, Inc., which has also provided the actual production of this report. This team has been led by Brenda Moldawer and she has been ably assisted by Dawn Cardascia and Angela Clark. Every report should be critically read by someone outside the group that develops it and this service was graciously provided to us by Dr. Sabatino Sofia of Yale University, along with the staff of the Earth Science and Applications Division at NASA Headquarters and the Chairmen and members of the various Eos panels.

CONTENTS

	Page
PREFACE	v
LIST OF TABLES	vii
LIST OF FIGURES	viii
ACRONYMS	xi
I. INTRODUCTION	1
II. Eos IMPLEMENTATION STRATEGY	5
Introduction	5
Overview	5
The Space Segment	8
Eos Data and Information System	25
International Involvement	29
Summary	29
III. MEASUREMENT STRATEGY FOR THE ENERGY, WATER, AND BIOGEOCHEMICAL CYCLES	30
The Energetic Planet	30
The Blue Planet	33
The Green Planet	41
Summary	49
IV. SYNERGISTIC MEASUREMENT STRATEGY	50
Introduction	50
Introduction to Solid Earth Processes	50
Geodynamics	52
Continental Geology	56
Introduction to Land Processes	62
Soils	62
Land Plant Productivity	65
Water Balance Dynamics from Local to Regional Scales	70
Inland Aquatic Environments	76
Introduction to Oceanic Processes	81
Ocean Biology	83
Oceanic Mesoscale Variability	90
Sea-Ice Dynamics	95
Air-Sea Interactions	103
Introduction to Atmospheric Processes	110
Use of Eos for Studies of Atmospheric Physics and Dynamics	112
Tropospheric Chemistry	116
Middle Atmospheric Ozone	122
Mesospheric Dynamics and Chemistry	128
V. CONCLUSIONS AND RECOMMENDATIONS	130
Recommendations	130
REFERENCES	135

LIST OF TABLES

Table		Page
1	Five Basic Recommendations Concerning Earth Science in the 1990s.....	2
2	Sequences of Research, Operational, and Commercial Satellite Missions Leading up to the Earth Observing System.....	6
3	Eos Instruments	10
4	Eos Instrument Descriptions	14
5	Eos Instrument Parameters	17
6	Eos Instruments for Determining Energy Fluxes at the Earth's Surface	34
7	Eos Instruments for Determining Elements of the Global Hydrologic Cycle	42
8	Annual Carbon Budget	43
9	Eos Instruments for Determining Elements of Earth's Primary Biogeochemical Cycles	49

LIST OF FIGURES

Figure		Page
1	Three views of the Earth from space photographed during the Apollo Program	1
2	Illustrates the coverage of the electromagnetic spectrum by the recommended Eos payload	9
3	Relationship between instrument functional capability and instrument concept	12
4	Principal measurements to be made by the Eos instruments	18
5	Scale drawing comparing one concept for an Eos payload on a platform with current generation spacecraft	20
6	Conceptualization of (a) platform carrying a significant subset of the Eos payload including the expanded SISP group of instruments and (b) platform carrying SAR and other Eos instruments	22
7	One- and two-day ground trace coverage of MODIS as a function of orbital altitude	23
8	SAR access coverage as a function of orbital altitude and actual SAR coverage at a specific altitude. One day surface coverage of a scatterometer as a function of orbital altitude	24
9	Surface coverage relationships for the MODIS and scatterometer instruments, each on two polar platforms	26
10	Common access coverage for SAR and HIRIS	27
11	Architectural concept for the Eos data and information system proposed by the Eos Data Panel	28
12	Schematic diagram of the disposition of absorbed solar energy in the Earth system	31
13	Important processes in the hydrologic cycle	35
14	Canopy model showing components of heat, radiation, and moisture balance at the soil surface	36
15	Schematic diagram of the air-sea interaction processes in the equatorial Pacific	39
16	The carbon cycle	43
17	Observed increases in atmospheric carbon dioxide and methane, resulting in part from human activities	44
18	Schematic of seven-box model of the global carbon cycle	45
19	The geologic cycle	51
20	SIR-A image of the Bolivian Andes	53
21	Topographic maps of the ocean floor produced from Seasat altimetry data	54
22	Baseline length difference between Haleakala Observatory, Hawaii and Yaragadee, Australia obtained during 4 years of laser ranging to Lageos	55
23	Sequence of events as spacecraft passes over network	56
24	Geologic structure of California and Western Nevada	57
25	Visible and near-infrared spectra of minerals	58
26	Thermal-infrared spectra of common rocks	59
27	A TIMS thermal-infrared image of the Kelso-Baker region, California	59
28	SIR-A radar image of the Pinacate volcanic field, Mexico	61
29	Thematic Mapper image of soils in the Death Valley region, California	63
30	Illustrates the factors that must be measured to estimate large-scale vegetation productivity	66
31	Collective effect of many leaves integrated over some spatial scale that might represent a pixel on a satellite image	67
32	Relative intensity of vegetation over North America using AVHRR data integrated from April to November 1982	68
33	The normalized difference varies from near zero (approximately 0.1) with no vegetation to near unity (approximately 0.9) for a full vegetation cover	68

LIST OF FIGURES (continued)

Figure		Page
34	Schematic of the hydrologic cycle	71
35	Illustrates the variability in saturated soil moisture areas during a rain event, depicts the level of heterogeneity that is typically found within a catchment	72
36	Schematic of modeling hydrologic responses at the catchment scale	73
37	Distributed hydrologic models represent the interactions of numerous processes through conservation equations on a horizontal grid	74
38	World-wide distribution of mires	77
39	Map of forested wetlands in Florida	78
40	Water surface of Lake Chad from a satellite photograph	78
41	Theoretical compiled transect of vegetation at the fringe of a swamp in the northern Sudd	78
42	Floating papyrus and <i>Salvinia</i> islands, Lake Naivasha, Kenya	79
43	Inputs and resulting physicochemical and biological processes that lead to methane emissions from the Amazon floodplain	81
44	Key biological and physical processes influencing primary production	84
45	Mean near-surface phytoplankton pigment concentrations obtained from 13 CZCS images during a 25-day period, May 22 to June 16, 1981	85
46	Key biological and physical processes affecting interannual variations in primary production	86
47	Distribution of useful ocean data during June 1981	89
48	Reduced Seasat altimeter data depicting meanders in the Antarctic Circumpolar Current induced by topographic effects of the Mid-Atlantic and Southwest Indian Ridges	90
49	AVHRR image of filaments associated with the California Current	91
50	A SAR image of a warm-core ring located about 100 km southeast of Delaware Bay	92
51	Interleaved water masses forming complex density fronts along the Mid-Atlantic Ridge	93
52	Mesoscale sea surface height variability based on Seasat altimetric data	93
53	CZCS image of the Western North Atlantic showing the Gulf Stream system, spin-off eddies, meanders, entrainment, and the Labrador Current	96
54	Geostrophic surface velocity derived of spaceborne altimetric measurements	97
55	Three-dimensional composite image of a Gulf Stream warm-core ring in the Western North Atlantic from AVHRR and expendable bathythermograph profile data	98
56	A system model for winter sea-ice behavior	99
57	Specific polynya processes	100
58	Passive microwave satellite images for 1974 of the Antarctic ice cover	101
59	Contours of the composite SST anomaly taken from ship track data and generated by the six El Niños between 1949 and 1981	104
60	The latent plus sensible ocean heat flux difference between December 1972 El Niño and December 1978 non-El Niño	105
61	The zonal mean latent heat flux for the northern hemisphere calculated from coincident ship reports and the Nimbus-7 SMMR for the year 1982	106
62	The combined monthly averages for January 1980 and 1981 of SST, wind speed, precipitable water, and latent heat flux	107
63	The combined monthly averages for January 1983 of SST, wind speed, precipitable water, and latent heat flux	108
64	Anomalies in sea surface temperature observed in four different ways for November 1979	109

LIST OF FIGURES (continued)

Figure		Page
65	Plot of vertical temperature distribution in Earth's atmosphere from surface to 100 km altitude, giving the nomenclature of atmospheric regions	111
66	Atmospheric "winds" derived from water vapor motions observed in Meteosat-1 6.7 μm radiance imagery	115
67	Example of machine-plotted vertical cross-section of potential temperatures and wind speed derived from conventional radiosonde data	116
68	Example of cloud wind vector height assignment made by stereo height determination	117
69	Cloud-top surface derived from observed high-resolution (AVHRR) IR image with the assumption of cloud-top cirrus emissivity equal to unity	117
70	Example of sea surface temperature obtainable by multiview, cloud-elimination algorithm process to be used as a refined boundary heat flux pattern for atmosphere model calculations	118
71	Example of vegetative index obtainable from an algorithm using a pair of high-resolution AVHRR bands in the visible and near-IR	118
72	Comparison of heavy rain estimates from SMMR on Nimbus-7 and ground-based radar	119
73	Example of a combined data product from a four-dimensional data base showing super-position of wind streamlines	120
74	The central role of OH in the oxidation of tropospheric trace gases	121
75	Carbon monoxide mixing ratio in the upper troposphere derived from measurements by the MAPS on the Space Shuttle	122
76	The stratosphere and mesosphere are complex atmospheric regions where radiative, chemical, and dynamical processes play significant roles	124
77	Shows the ozone distribution during a major stratospheric disturbance forced by planetary waves propagating up from below	125
78	Shows the nitric acid distribution during a major stratospheric disturbance forced by upward propagating planetary waves	125
79	Maps of total ozone for October 3 of the years (a) 1979 to 1982 and (b) 1983 to 1986 obtained by TOMS flown on Nimbus-7 satellite	126

ACRONYMS

ABLE	Amazon Boundary Layer Experiments
ADCLS	Advanced Data Collection and Location System
AGE	Amazon Ground Emissions
ALT	Radar Altimeter
AMRIR	Advanced Medium Resolution Imaging Radiometer
AMSR	Advanced Microwave Scanning Radiometer
AMSU	Advanced Microwave Sounding Unit
APACM	Atmospheric Physics and Chemistry Monitors
ARGOS 2	French Data Collection and Location System
ATN	Advanced TIROS-N
ATSR	Along-Track Scanning Radiometer
AVHRR	Advanced Very High Resolution Radiometer
CalCOFI	California Cooperative Oceanic Fisheries Investigations
CIS	Cryogenic Interferometer Spectrometer
CR	Correlation Radiometer
CZCS	Coastal Zone Color Scanner
DMSP	Defense Meteorological Satellite Program
DOPLID	Doppler Lidar, Laser Wind Measurement System
Eos	Earth Observing System
ERBI	Earth Radiation Budget Instrument
ERBS	Earth Radiation Budget Satellite
ERS-1	Earth Remote Sensing Satellite-1
ESA	European Space Agency
ESMR	Electronically Scanned Microwave Radiometer
ESSC	Earth System Science Committee
ESTAR	Electronically Scanned Thinned Array Radiometer
F/P INT	Fabry-Perot Interferometer
GARP	Global Atmospheric Research Program
GCM	Global Circulation Model
Geosat	Geodesy Satellite
GLRS	Geodynamic Laser Ranging System
GMS	Geostationary Meteorology Satellite
GOES	Geostationary Operational Environmental Satellite System
GOMR	Global Ozone Monitoring Radiometer
GPS	Global Positioning System
GREM	Geopotential Research Explorer Mission
HIRIS	High-Resolution Imaging Spectrometer
HIRS	High-Resolution Infrared Radiation Sounder
HMMR	High-Resolution Multifrequency Microwave Radiometer
IOC	Initial Orbital Configuration
IR	Infrared
IR-RAD	IR Radiometer

ACRONYMS (continued)

IRS	Indian Remote Sensing
ITCZ	Intertropical Convergence Zone
JERS	Japanese Earth Remote Sensing Satellite
LAGEOS	Laser Geodynamics Satellite
LAI	Leaf Area Index
Landsat	Land Remote Sensing Satellite
LASA	Lidar Atmospheric Sounder and Altimeter
LAWS	Laser Atmospheric Wind Sounder
LISS	Linear/Imaging Self Scanner Sensor
MAG	Magnetospheric Currents and Fields Detector
MAPS	Measurement of Air Pollution from Satellites
MEPED	Medium Energy Proton and Electron Detector
MLA	Multispectral Linear Array
MLS	Microwave Limb Sounder
MODIS	Moderate-Resolution Imaging Spectrometer
MODIS-N	MODIS-Nadir
MODIS-T	MODIS-Tilt
MOS	Marine Observatory Satellite
MPD	Magnetospheric Particle Detector
MSS	Multispectral Scanner
MSU	Microwave Sounding Unit
NASA	National Aeronautics and Space Administration
NCIS	Nadir Climate Interferometer Spectrometer
NOAA	National Oceanic and Atmospheric Administration
N-ROSS	Navy Remote Ocean Sensing System
N-SCATT	Navy Scatterometer
PAR	Photosynthetically Active Radiation
PEM	Particle Environmental Monitor
PMR	Pressure Modulated Radiometer
POES	Polar-orbiting Operational Environmental Satellites
SAM	Sensing with Active Microwaves
SAR	Synthetic Aperture Radar
SCATT	Scatterometer
SCM	Solar Constant Monitor
SEM	Space Environmental Monitor
SIR	Spaceborn Imaging Radar
SISP	Surface Imaging and Sounding Package
SLR	Satellite Laser Ranging
SMMR	Scanning Multifrequency Microwave Radiometer
SPCZ	South Pacific Convergence Zone
SPOT-1	Systeme Probatoire d'Observation de la Terre-1
SST	Sea Surface Temperature

ACRONYMS (continued)

SUB-MM	Submillimeter Spectrometer
SUSIM	Solar UV Spectral Irradiance Monitor
TDRSS	Tracking and Data Relay Satellite System
TED	Total Energy Detector
TIMS	Thermal Infrared Multispectral Scanner
TIROS	Television Infrared Operational Satellite
TM	Thematic Mapper
TOGA	Tropical Oceans and Global Atmosphere
TOMS	Total Ozone Mapping Spectrometer
TOPEX	Ocean Topography Experiment
TOVS	Tiros Operational Vertical Sounder
TREM	Tropical Rainfall Explorer Mission
UARS	Upper Atmosphere Research Satellite
VAS	VISSR Atmospheric Sounder
VIS/IR	Visible/Infrared
VIS-UV	Visible Ultraviolet Spectrometer
VISSR	Visible and Infrared Spin Scan Radiometer
WEPOLEX-81	Weddell Polynya Experiment
WCRP	World Climate Research Program
WOCE	World Ocean Circulation Equipment

I. INTRODUCTION

The most compelling images provided to us by the space program are those looking homeward at Earth floating in the void of space (Figure 1). The first scientific use of rockets provided *in situ* measurements of the outer reaches of the Earth's environment. Beginning in 1960, these were extended downward in focus through the use of satellite-based remote sensing to observe cloud patterns. After only a quarter century, these images are now a part of our daily lives.

Subsequent to these first steps, our ability to measure atmospheric properties has been greatly extended, particularly by the series of Nimbus and TIROS satellites. Satellite soundings of atmospheric temperature, along with measurements from a network of surface stations, form the backbone of global weather prediction models. This view of the atmosphere has been complemented by observations of the land surface by the Landsat series of satellites.

A glimpse of the potential of remote ocean observations was provided in 1978 by the abbreviated Seasat mission. The Coastal Zone Color Scanner (CZCS) carried onboard the Nimbus-7 satellite has provided a 7-year record of biological activity in ocean surface waters.

The Earth-looking satellites launched in the last 25 years have made important contributions to the understanding of our world and the various elements that it comprises. However, recent research has highlighted the need to study the Earth as a unified system; the Earth system of land, oceans, and atmosphere is linked together by energy, hydrologic, and biogeochemical processes. The significance of these interactions and of the specific processes involved depends upon the time and space scales of interest. Although considerable progress has been made (and will continue to be made) by single-discipline studies, a complete understanding of the

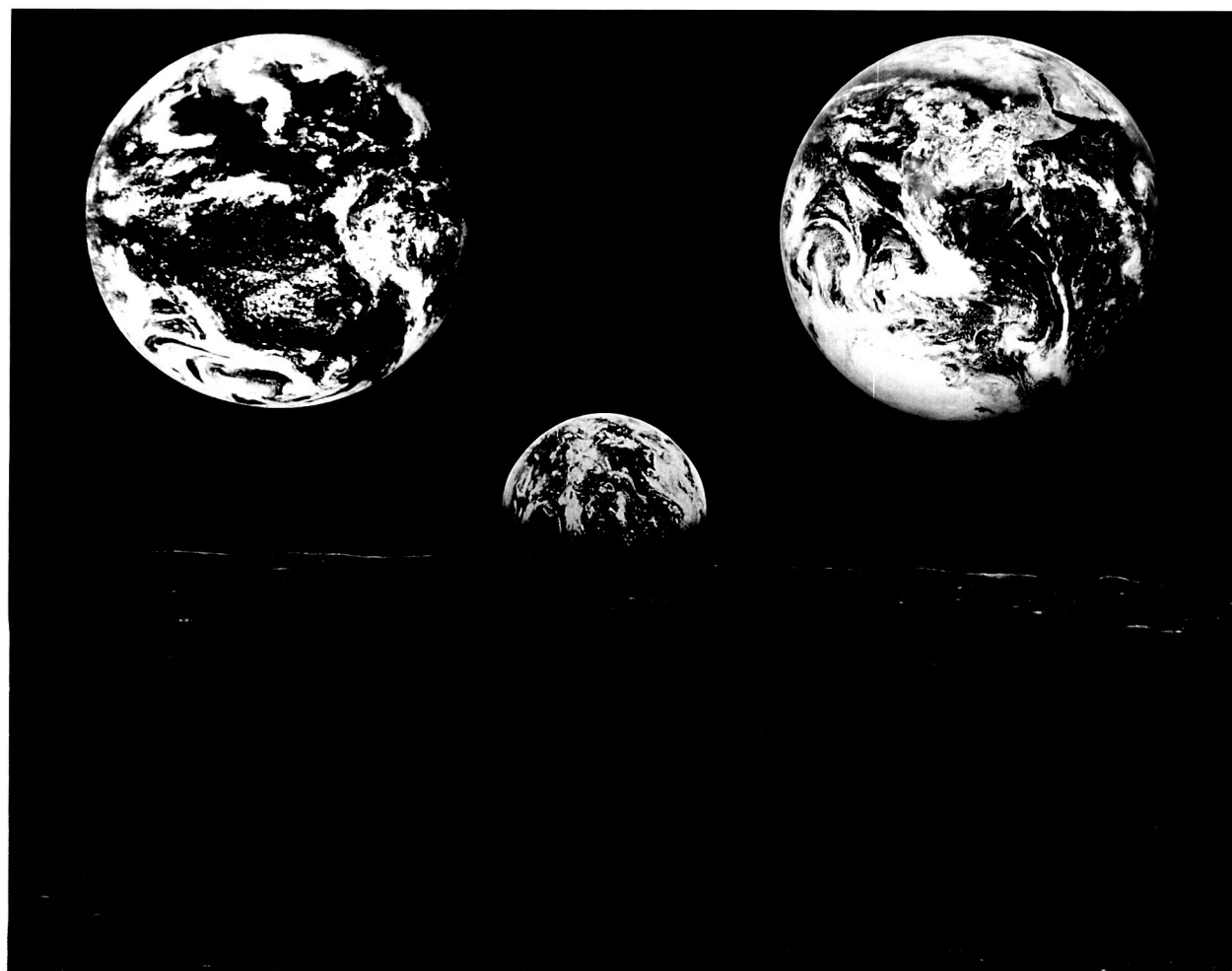


Figure 1. Three views of the Earth from space photographed during the Apollo Program.

Earth system requires multidisciplinary studies. The study of individual components in isolation will never replace studies of the complete system.

Eos, the Earth Observing System, is a natural outgrowth of the maturation of our ability to perform remote sensing, cope with the resulting data streams, and understand the coupled nature of the components of the Earth system. Eos will be built on the foundation laid by past and present Earth remote sensing satellites.

With the development of Eos, we will be able to observe (or infer) many of the key variables and processes of the global-scale cycles of energy, water, and biogeochemicals. At present, we often cannot describe even the mean field at the relevant time and space scales for many critical processes in the Earth system. Thus, the first goal is to obtain the various mean fields. Such information will be extremely useful, but the temporal and spatial variability of these fields and their correlations are of greater interest. For example, the variations catalogued as the El Niño event of 1982-83 greatly affected ocean energy fluxes, ocean productivity, precipitation over large areas of the world, and even the Earth's rotation rate; long-term changes in concentrations of atmospheric carbon dioxide may affect the Earth's radiative balance; large-scale changes in vegetation cover (desertification, conversion to agriculture) also affect the surface energy balance, as well as biogeochemical cycling. We need to understand the relevant forcing functions and how they create the observed temporal and spatial variability. If we know the Earth system well enough to describe these interactions, our ability to predict the system response to anthropogenic and natural perturbations will be greatly increased.

Our present state of knowledge is of varying quality. For the energy cycle we know the mean fields and some of the interactions fairly well (although the quality of this knowledge varies considerably from area to area); similar statements could be made about parts of the hydrologic cycle. On the

other hand, biogeochemical cycling is perhaps the least understood. In a general sense, our knowledge of a particular process decreases as the level of interaction between physical, chemical, and biological variables increases. Since the energy cycle is largely driven by physical interactions, we have more confidence in our knowledge of the energy cycle than in our current understanding of the biogeochemical cycles, where the interactions between physical, chemical, and biological processes are strong.

The Eos Science and Mission Requirements Working Group (Butler *et al.*, 1984) made five basic recommendations concerning Earth science in the 1990s (Table 1). Fundamental to them all is the need for an information system designed to collect, distribute, process, and facilitate the analysis of global data for a broad range of multidisciplinary and single-discipline studies of the Earth. Such a system must include the requisite human and intellectual resources, as well as instrument and computer hardware.

The first recommendation is that long time series of measurements are needed to resolve statistically some of the important low-frequency fluctuations of the parameters. This requirement argues for continuation of existing satellite data sets that are currently being used for Earth science studies. There are also several new measurement capabilities under development that will allow a significant number of additional variables to be observed and will enhance the quality and quantity of many existing measurements. It is gratifying to note that since the publication of the first Eos report, development by the National Aeronautics and Space Administration (NASA) of the Upper Atmospheric Research Satellite (UARS), the NASA Scatterometer (N-SCATT) to be flown on the Navy Remote Ocean Sensing System (N-ROSS), and Ocean Topography Experiment (TOPEX) has begun. Also, the National Oceanic and Atmospheric Administration (NOAA) has secured commitment to continue the polar orbiting NOAA satellite series.

Table 1. Five Basic Recommendations Concerning Earth Science in the 1990s

1. A program must be initiated to ensure that present time series of Earth science data are maintained and continued. Collection of new data sets should be initiated.
2. A data system that provides easy, integrated, and complete access to past, present, and future data must be developed as soon as possible.
3. A long-term research effort must be sustained to study and understand these time series of Earth observations.
4. The Earth Observing System should be established as an information system to carry out those aspects of the above recommendations which go beyond existing and currently planned activities.
5. The scientific direction of the Earth Observing System should be established and continued through an international scientific steering committee.

The second recommendation recognizes that progress in Earth science on the issues of the energy cycle, hydrologic cycle, and biogeochemical cycles, as well as on many important single-discipline questions, will only occur if scientists have easy access to past, present, and future data sets. This includes the ability to overlay a variety of remote sensing data sets from multiple sensors (and satellites) and *in situ* data. This recommendation goes beyond simply making data available. It requires ensuring that the data are provided in a generally useful form by the inclusion of user scientists' recommendations in the design and management of future data systems.

The third recommendation notes that the continued development of scientific infrastructure is necessary so that sufficient intellectual resources will exist to cope with the large-scale, complex, multidisciplinary problems of Earth science. This involves long-term research support for such investigations as well as training of new people. The ongoing fulfillment of these first three recommendations will lay the foundation for progress in understanding the Earth.

With the level of success currently being achieved in the areas described above, it is time to implement the final two recommendations. Eos, the Earth Observing System, will extend the measurement and data system capabilities currently available or in development to the levels that are required and achievable by the mid-1990s. It will also provide for an evolutionary system development within which new observing capabilities can be added as they become available. The fourth recommendation requires that Eos be planned as an information system to coordinate both continuing and new activities. Without such a focus, it is unlikely that the necessary coordination would be accomplished. The final recommendation of the Eos Science and Mission Requirements Working Group is that the sources of scientific guidance of Eos include the international community. This recommendation is made in recognition that there must be international cooperation in the study of the Earth system. Certainly, these issues transcend national boundaries; data from foreign satellite missions and research programs will be essential.

The Eos Science and Mission Requirements Working Group proposed a coordinated suite of new measurement capabilities. The Working Group noted that there was considerable scientific value in obtaining nearly simultaneous measurements of a variety of processes. For example, ocean productivity is strongly affected by wind-induced mixing; simultaneous measurements of wind stress and phytoplankton biomass are necessary to understand this process. The state of a crop or forest is strongly dependent on the incoming sunlight and available moisture in the soil; correct interpretation of ecosystem state requires nearly simultaneous measurements of plant and local environmental con-

ditions. In fact many, perhaps most, of the multidisciplinary studies will require a variety of contemporaneous measurements. There is also value in observing processes with a variety of techniques. For example, simultaneous radar and visible/infrared (VIS/IR) measurements of vegetation canopies will significantly increase the scientific return, as described in a subsequent chapter.

The suite of measurement capabilities can be roughly divided into two broad categories: monitoring (and mapping) and process studies. There are a number of variables that we wish to observe on a global basis for a long period of time. These will be used to derive maps of the mean fields, as well as to measure temporal and spatial fluctuations. Such variables include plant cover, continental rock units, ocean phytoplankton biomass, and atmospheric ozone. There are, on the other hand, process-oriented measurements that will be tightly focused on specific problems. For example, studies of the dynamics of specific ecosystem boundaries will require an ensemble of detailed *in situ* and satellite measurements. Results of these process studies will be used in model development of global-scale processes.

We note that there is a wide range of observable variables. For some, the physical basis of the measurements is well understood, and the relevant variable can be observed directly. For example, infrared measurements of surface temperatures, while subjected to difficult atmospheric correction and surface emissivity calculations, have a fairly well-understood physical basis. At the other end of the spectrum are variables that are less understood and can only be inferred from other measurements. For example, plant nutrient stress must be inferred from observations of the visible and thermal spectrum of vegetation, assisted by the use of models. The satellite instruments observe patterns in space and time of key variables. These patterns are the result of the forces and mechanisms at work in the Earth system. To understand the Earth system one must convert from pattern to process: The patterns revealed in the data must be transformed to quantitative determinations of the rates of various processes and the amounts of energy, momentum, water, or other chemicals exchanged among components of the system.

There are also important variables (and processes) that currently cannot be observed or inferred from space. There are many examples of this from both multidisciplinary and single-discipline studies. The Eos data and information system will provide information on these variables as obtained by *in situ* measurements that will be part of the overall program of Earth system observations.

To advance beyond a simple data collection program, Eos must support the development of models that incorporate these data and enable their interpretation. Such models will allow us to describe the

key processes in the Earth system and place them in a conceptual framework. There are several approaches to modeling. The simplest models are mere verbal descriptions of how we think a particular system operates, whereas the most complex ones are predictive models that allow us to infer the responses of the system to changes in the environment. Other models are of a statistical nature; they must reproduce the statistical properties of the system so that we can be assured that the system interactions are described correctly. Model building must follow an evolutionary sequence, from the simple to complex, with the ultimate objective of reaching the predictive stage for all important processes.

In summary, Eos presents a strategy for development of an information system for Earth science. This strategy is based on acquiring and distributing satellite data from the past, present, and future, assembling a suite of new measurement capabilities, and providing long-term research support for Earth science investigations. It is a difficult task and it will not answer every important scientific question in Earth science. However, it provides the potential for many important scientific breakthroughs in our understanding of a variety of single-discipline and multidisciplinary Earth science problems.

This report is intended for the Earth science community; it is designed to show how Eos will provide the tools for a significant advance in our understanding of the Earth system. As our title indicates, this report is intended to guide overall implementation strategy. There have been many clar-

ifications and refinements in the Eos concept since the publication of the Eos Science and Mission Requirements Working Group Report 3 years ago. Many of these are documented in this report. We begin by describing the observing system and its associated data and information system. Eos is motivated by the need for integrated study of the Earth. To show how this can be accomplished, the use of Eos to study the global-scale cycles is discussed. To illustrate the breadth of Eos' usefulness, examples of single-discipline studies using planned Eos resources are described. Finally, we focus our recommendations on the steps that need to be taken now in order to prepare for Eos.

Despite the scope of Eos, it does not stand alone. The Earth Observing System is a part of an integrated scientific study of Earth, which is already underway. The Earth System Sciences Committee (ESSC, Bretherton *et al.*, 1986, 1987) has laid out a broad strategy for progress in Earth science built upon the recommendations of the various boards of the National Research Council (NRC) and in particular on the reports of the Committee on Earth Sciences of the Space Science Board (NRC, 1982b, 1985). The ESSC report recognizes Eos as the centerpiece of the future implementation strategy. By proceeding to carry out the ESSC plan including Eos, we can move from the bits and pieces of single-discipline research to a comprehensive understanding of the Earth. This comprehension of the integrated Earth system will provide forecasting capability that can guide us in the wise development of our home planet.

II. Eos IMPLEMENTATION STRATEGY

INTRODUCTION

The concept of Eos, the Earth Observing System, has matured since the issuance of the report of the Eos Science and Mission Requirements Working Group (Butler *et al.*, 1984). Many of the essential aspects of Eos are inevitable consequences of its scientific goals. In addition, there are practical considerations that must be included in shaping the characteristics of such a major endeavor. This chapter will concentrate on the full observing system as it will exist by the year 2000, presenting both the concept and the essential components of the system.

The central recommendation of the Science and Mission Requirements Working Group is that Eos should be an information system designed to meet the needs of multidisciplinary Earth science; needs that go beyond the planned single-discipline space missions. The information system concept includes both a data and information system *per se* and the observing system located on platforms in low-altitude polar orbits. This remains the essential Eos concept.

As envisioned by the Science and Mission Requirements Working Group, Eos will be built upon a foundation of research and operational activities that are ongoing or will precede it. Within the NASA satellite program the UARS and the TOPEX are important precursors to Eos and will fly in non-sun-synchronous orbits in order to address specific measurement requirements. In particular, UARS will sample the diurnal variation of stratospheric constituents and winds. This variation must be understood in order for scientists to infer several aspects of the long-term behavior of the stratosphere from Eos observations always taken at the same specific times of day. Among other measurements TOPEX will determine the significant tidal components in the sea surface height field. This will permit these tidal effects to be taken into account in interpreting the Eos altimeter measurements taken at fixed times of day.

Two other research missions that must fly in non-Eos orbits are the Geopotential Research Explorer Mission (GREM) and the Tropical Rainfall Explorer Mission (TREM). The results of both will complement and extend the Eos observations and will be important in accomplishing the science being addressed by Eos. In addition to measuring the gravity field to study processes of mantle convection, the GREM determinations of the geoid will improve the accuracy and usefulness of ocean surface altimetry from Eos and TOPEX. The sampling of tropical precipitation rates at all local times by the Rainfall Mission is necessary to understand the diurnal variations of this key link in the hydrologic cycle. The rainfall observations, when used in conjunction with Eos and geostationary measurements, should

enable an extrapolation of directly measured precipitation from the tropics to higher latitudes and to all local times. There are also a number of important scientific satellite missions being undertaken outside the United States. Table 2 shows many of the research, operational, and commercial satellite missions that are planned or in progress and that lead up to or complement Eos.

In every area of Earth science there are space and time scales that are inaccessible to remote sensing and important processes that cannot be observed remotely. Suborbital remote sensing and *in situ* measurements from a variety of platforms have always been and will remain an essential complement to an extension of satellite observations. The responsibility for these may be outside of the Eos mission in the strictest sense, but Eos requires that these ongoing efforts continue and be expanded in order to maximize the return on the investment in space observations.

OVERVIEW

The study of Earth science today as described in Chapter I clearly requires that Eos obtain a long-term data record. Scientists cannot perform controlled experiments in the laboratory when dealing with the forces of the Earth, they must watch the Earth evolve over significant time periods to deduce from the patterns of change the processes that govern the Earth's behavior as a natural system. There are also important phenomena such as El Niño that only occur at intervals of several years and whose occurrence has not been predicted sufficiently in advance to permit mounting a specific observing effort.

Today there are events happening that are crucial to the long-term understanding of the Earth. They are being measured by a variety of operational and research satellites and by ground-based systems. Progress in understanding these phenomena can be greatly enhanced by ensuring that this irreplaceable information is preserved and is readily available for scientific study. Eos can begin now as an information system, building on and integrating these diverse data sources, and empowering the Earth science community to make maximum use of these measurements. It is also important to ensure the preservation of these data because they are an integral part of the required long-term data sets. Contemporary data form the baseline against which observations of change can be measured. By beginning now, Eos as an information system can provide the experience essential to prepare for the increased quantity and improved quality of data to be provided by the Eos space segment.

The Eos space segment will be deployed in the mid-1990s, with growth in the number and quality of

Table 2. Sequences of Research, Operational, and Commercial Satellite Missions Leading up to the Earth Observing System

Program	Objectives	Main Sensors	Orbit/ Maximum Altitude	Status/ Launch Date	
United States	POES Polar-orbiting Operational Environmental Satellites (also known as the NOAA series of satellites)	Environmental observations	Advanced Very High Resolution Radiometer; High Resolution Infrared Sounder; Stratospheric Sounding Unit; Microwave Sounding Unit; Solar Backscatter Ultraviolet Spectrometer; Earth Radiation Budget Instrument, Advanced Microwave Sounding Unit to be employed on 1990s follow-on missions	850 km altitude, sun-synchronous	NOAA/operational; follow-on missions planned
	GOES Geostationary Operational Environmental Satellite System	Environmental observations, wind speeds	Visible-Infrared Spin-Scan Radiometer; Atmospheric Sounder; Data Collection System; Space Environment Monitor; 1990s missions will feature separate sounding and imaging functions from a 3 axis stabilized platform	Geosynchronous	NOAA/operational; follow-on missions planned
	DMSP Defense Meteorological Satellite Program	Weather observations	Operational Linescan System; Special Sensor Microwave Imager; Infrared and Microwave Sounders	830 km altitude, sun-synchronous	USAF/operational
	LAGEOS-1 Laser Geodynamics Satellite	Geodynamics, gravity field	Laser Reflectors	6,000 km altitude, 110° inclination	NASA/operational; second satellite being built by Italy for 1991 launch
	Landsat Land Remote Sensing Satellite	Vegetation, crop and land use inventory	Multispectral Scanner; Thematic Mapper	705 km altitude, sun-synchronous	Eosat/operational; follow-on missions 6 & 7 approved for 1989 and 1991 launches
	GEOSAT Geodesy Satellite	Shape of the geoid; ocean and atmospheric properties	Radar Altimeter	800 km altitude, 108° inclination	U.S. Navy/operational
	GPS Global Positioning System	Geodesy, crustal deformation	Transmitters for precision location determination	Eventual system array of 21 satellites at 20,200 km and 55° inclination	USAF-NOAA-NASA-NSF-USGS
	UARS Upper Atmosphere Research Satellite	Stratospheric chemistry, dynamics, energy balance	Full Complement of Energy Input Spectrometers; Range of Spectrometers and Radiometers for Species and Temperature Measurements; Wind Measurement Interferometers	600 km altitude, 57° inclination	NASA/ launch 1991
	N-ROSS Navy Remote Ocean Sensing System	Ocean applications	Radar Altimeter, Wind Scatterometer, Special Sensor Microwave Imager; Low Frequency Microwave Radiometer	830 km altitude, sun-synchronous	Approved/launch 1990
	TOPEX/POSEIDON Ocean Topography Experiment	Ocean circulation	2-Frequency Radar Altimeter; Microwave Radiometer; Precise Positioning Systems	1,300 km altitude, 63° inclination	NASA-CNES/start 1987, launch 1991

Table 2. Sequences of Research, Operational, and Commercial Satellite Missions Leading up to the Earth Observing System (continued)

	Program	Objectives	Main Sensors	Orbit/ Maximum Altitude	Status/ Launch Date
United States (cont'd)	GREM Geo-potential Research Explorer Mission	Measure global geoid and magnetic field	Scalar Magnetometer; Vector Magnetometer	160 km altitude, polar orbit	Phase B complete/pending approval
	TREM Tropical Rainfall Explorer Mission	Tropical precipitation measurements	Multichannel Passive Microwave Radiometer; Visible Infrared Radiometer; Dual Frequency Radar	Free-flyer or attached to Space Station	Start 1991/launch 1994
Brazil	Remote Sensing Satellite	Land applications	Multispectral Pushbroom Imager	650 km altitude, sun-synchronous	Phase B in progress; 1990/1991
Canada	Radarsat	Ice and land monitoring	Synthetic Aperture Radar Wind Scatterometer	1,000 km altitude, sun-synchronous	Start 1987; launch 1994
China	Earth Resource Satellite	Land applications	Multispectral Scanner	400 km altitude, sun-synchronous	Phase B in progress; launch 1989
European Space Agency	METEOSAT	Weather observations	Multispectral Imaging Radiometer	Geosynchronous	Operational
	ERS-1 Earth Remote Sensing Satellite-1	Imaging of oceans, ice fields, land areas	Synthetic Aperture Radar; Wind Scatterometer; Radar Altimeter; Along-track Scanning Radiometer; Microwave Sounder; Precise Positioning Package	780 km altitude, sun-synchronous	Approved; launch in 1989/1990
France	SPOT-1 Systeme Probatoire d'Observation de la Terre-1	Land use, earth resources	High-Resolution Visible Imager (HRV)	832 km altitude, sun-synchronous	Operational
	SPOT-2	Land use, earth resources	High-Resolution Visible Imager	832 km altitude, sun-synchronous	Launch 1988
	SPOT-3	Land applications, ocean circulation	Improved HRV; Vegetation Monitoring Sensor; Radar Altimeter; Microwave Sounder; Precise Positioning System	832 km altitude, sun-synchronous	Funding assured; launch 1990
	SPOT-4	Land application	Improved HRV; Vegetation Monitoring Sensor	832 km altitude, sun-synchronous	Planning stages
India	IRS-1 Indian Remote Sensing Satellite	Earth resources	LISS I & II (Linear Imaging Self Scanner Sensor)	904 km altitude; sun-synchronous	Projected series; launch 1987
Japan	GMS Geostationary Meteorology Satellite	Weather observations	Visible & IR Radiometers; Data Collection System	Geosynchronous	Operational/NASDA
	MOS-1 Marine Observatory Satellite-1	State of sea surface and atmosphere	Multispectral Radiometer; Visible and Thermal IR Radiometer; Microwave Scanning Radiometer	909 km altitude; sun-synchronous	Operational
	JERS-1 Japanese Earth Remote Sensing Satellite-1	Earth resources	Synthetic Aperture Radar; Visible and Near-IR Radiometer	570 km altitude; sun-synchronous	Approved; launch 1991
	ADEOS	Environmental observations earth and ocean resources	Visible and near IR radiometer ocean color and temperature sensor payload of opportunity	Sun-synchronous	Planning stages; launch 1994

remote sensing capabilities through the year 2000. The full system would then operate for the next decade to obtain time series of at least 10 years duration for all of the requisite observables. Many of the crucial measurements would be obtained for a period of 15 years. The timely initiation of Eos observations will provide continuity in data records. By the mid-1990s, these data records will include the measurements of upper atmospheric chemical species, temperature and winds, sea ice extent, ocean color, the total and spectral irradiance of the sun, the radiative balance of the Earth, and measurements of sea surface characteristics including temperature, elevation, wind stress, and wave heights.

The same characteristics of Earth science research that require a long-term approach to observations also dictate the simultaneous use of a large set of observing capabilities to obtain the fullest possible description of the Earth. Passive observations in the visible and near-infrared regions of the electromagnetic spectrum detect the sunlight that is reflected from the atmosphere, clouds, and surfaces of the Earth. These reflections vary with the physical, chemical, and biological properties of the surface. Thermal IR and microwave emissions from the Earth are indicative of the temperature and composition of the surface and atmosphere, the amount of water present, and the properties of ice and snow. The trace chemicals of the atmosphere are revealed in narrow spectral features in virtually all spectral bands, from the ultraviolet to the microwave, with each chemical having a unique spectral signature at some wavelength.

Radars and laser-based instruments provide their own illumination and can be used to measure both the distance to a reflecting surface and the character of that surface. The coherence of radar signals can be used, together with the motion of the spacecraft, to synthesize a large aperture for high spatial resolution imagery. The strong interaction of water with microwave radiation is used in a variety of ways by radars. Radar altimeters reflect energy pulses off the ocean surface. They measure the distance to the average surface through the time delay in the return signal and detect such properties as surface roughness from the strength of the return and significant wave height from the shape of the return pulse. Scatterometers measure microwave energy reflected from small wavelets caused by wind. Wind stress is obtained from the amplitude of the return signal, and wind direction is determined by combining measurements from several antennas. Synthetic Aperture Radar (SAR) images those surfaces encountered by the radar signal where there is a significant change in dielectric constant. This information provides details on surface characteristics important for determination of landform evolution such as surface roughness and small-scale slopes. Lasers can detect atmospheric composition by measuring the strength of the laser

signal return. This can be done by comparing the signal return of lasers tuned on and off of a given spectral line. Lasers can also be used in a pulsed, lidar mode to provide range-resolved information using the time delay for receipt of the return pulse. The narrowness of the laser beam enables lidar techniques to measure the distance to targets significantly smaller than can be resolved with radar altimeters.

The extensive set of individual instruments in the Eos payload is required because of the different measurement capabilities needed to observe the various regions of the electromagnetic spectrum by passive and active remote sensing techniques. Figure 2 illustrates the coverage of the electromagnetic spectrum by the recommended Eos payload. The number of needed instruments is further increased by the impracticality of combining in a single instrument widely different spatial resolutions, swaths, and spectral resolutions. Likewise, it is generally impractical to combine in a single instrument simultaneous observations in different target directions—nadir, the Earth's limb, and the sun.

The Eos strategy, as articulated in the earlier report (Butler *et al.*, 1984), assumes the availability of morning and afternoon atmospheric soundings and morning surface images through continued flight of operational and commercial satellites similar to the NOAA and Landsat series. As the Eos concept has matured, the consideration of operational and commercial instruments has become more specific. The Eos Science Steering Committee is a joint activity of NASA and NOAA. In this context, NOAA has the responsibility of representing commercial as well as operational interests. The committee has considered the scientific uses of operational observations and the constraints placed on the overall observing system by collaboration between research and operational interests. The committee recommends that Eos be implemented in collaboration with future polar orbiting operational payloads to the extent that this collaboration strengthens the scientific return of Eos. The mission scenario presented in this report is based on an assumption that the resources of orbiting platforms will be shared by research, operational, and potentially, commercial instruments.

THE SPACE SEGMENT

Instruments and Payload

The consideration of the space segment of Eos must begin with the payload required to observe the Earth comprehensively. The Eos Science and Mission Requirements Working Group Report listed 13 conceptual instruments, each representing a block of functional capability (see Table 3).

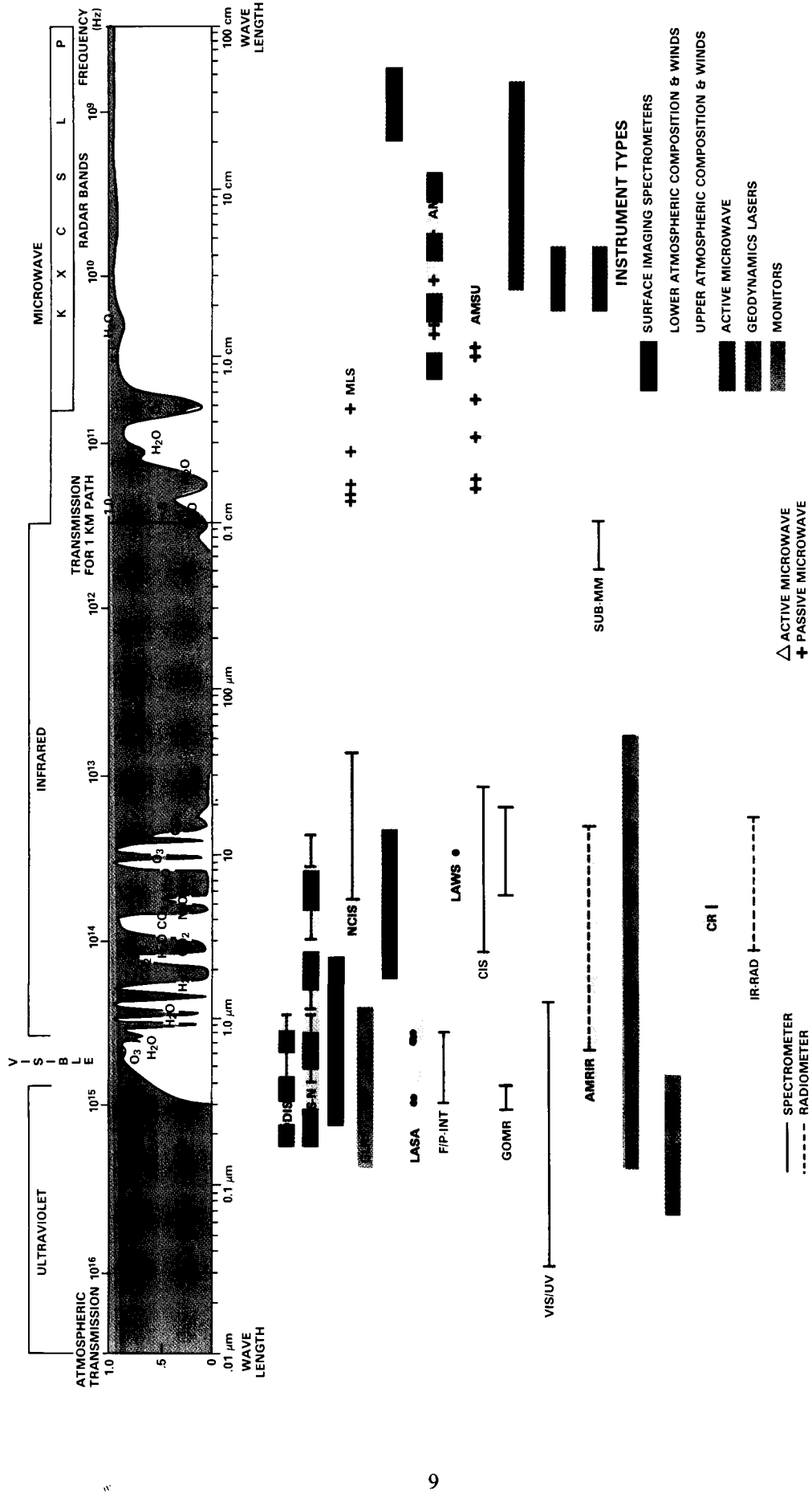


Figure 2. Illustrates the coverage of the electromagnetic spectrum by the recommended Eos payload.

Table 3. Eos Instruments

Instrument	Measurement
Advanced Data Collection & Location System (ADCLS)	Data and command relay and location of remotely sited measurement devices
	SISP—Surface Imaging and Sounding Package
Moderate-Resolution Imaging Spectrometer (MODIS)	Surface and cloud imaging in the visible and infrared 0.4 to 2.2 nm, 3 to 5 μ m, 8 to 14 μ m resolution varying from 10 nm to 0.5 μ m
High-Resolution Imaging Spectrometer (HIRIS)	Surface imaging 0.4 to 2.2 nm; 10 to 20 nm spectral resolution
High-Resolution Multifrequency Microwave Radiometer (HMMR)	1 to 94 GHz passive microwave images in several bands
Lidar Atmospheric Sounder and Altimeter (LASA)	Visible and near-infrared laser backscattering to measure atmospheric water vapor, surface topography, atmospheric scattering properties
	SAM—Sensing with Active Microwaves
Synthetic Aperture Radar (SAR)	L-, C-, and X-band radar images of land, ocean, and ice surfaces at multiple incidence angles and polarizations
Radar Altimeter	Surface topography of oceans and ice, significant wave height
Scatterometer	Sea surface wind stress to 1 m/s 10° in direction K_u band radar
	APACM—Atmospheric Physical and Chemical Monitor
Doppler Lidar	Tropospheric winds to 1 m/s doppler shift in laser backscatter
Upper Atmosphere Wind Interferometers	Upper atmospheric winds to 5 m/s doppler shift in O_2 thermal emissions
Tropospheric Composition Monitors	Trace chemical constituents of the troposphere
Upper Atmosphere Composition Monitors	Trace chemical composition passive emission detectors at wavelengths from UV to microwave
Energy and Particle Monitors	Solar emissions from 150 to 400 nm, 1 nm spectral resolution, Earth radiation budget, total solar irradiance, particles and fields environment

The payload was grouped into three packages plus a data relay capability to illustrate the synergistic relationships that exist among the instruments. A brief review of the payload is helpful in understanding the complete set of candidate instruments now being considered. The first package of Eos instruments was termed the Surface Imaging and Sounding Package (SISP). It included four capabilities—MODIS, HIRIS, HMMR, and LASA. The Moderate-

Resolution Imaging Spectrometer (MODIS) provides a comprehensive ability to observe the Earth from visible to thermal infrared wavelengths with high spectral resolution (10 nm in the visible) and with a wide swath ($\pm 45^\circ$ perpendicular to the satellite track). Its goal is to measure the entire daylight surface of the Earth every 2 days and observe the continuously changing patterns of physical and biological surface characteristics along with at-

mospheric observations of cloud properties and aerosol distributions. The spatial resolution of MODIS is about 1 km in order to provide frequent, extensive coverage while retaining adequate resolution to detect important spatial variations in the observed phenomena.

Many other phenomena, particularly on the land surface, vary on the scale of tens of meters. To observe these phenomena at selected locations, the MODIS capability is complemented by the High-Resolution Imaging Spectrometer (HIRIS). In addition to the higher spatial resolution, the HIRIS would retain high spectral resolution over a similar range of wavelengths with continuous spectral coverage. The swath width that can reasonably be covered at this higher resolution is about 30 km. Thus, the HIRIS will need to be pointable to focus on specific areas that require this type of coverage. The HIRIS observations are nested within the more extensive and frequent MODIS views.

HIRIS is also capable of looking forward or backward along the satellite ground track to exploit the extra observing power contained in the bidirectional reflectance variations of the radiation. The visible and infrared view taken by MODIS is further complemented by the presence of a wide swath, 1 to 10 km spatial resolution passive microwave capability known as the High-Resolution Multifrequency Microwave Radiometer (HMMR). This provides down-looking measurements of those surface and atmospheric phenomena observable in the microwave region of the electromagnetic spectrum. Many of these observations relate directly to the measurement of water and water-related properties of materials. The high spatial resolution microwave counterpart to HIRIS is the SAR, which is included in another package for reasons discussed below. The final capability in the SISP package is an aggregate of laser-based techniques for sounding the atmosphere and ranging to the surface called the Lidar Atmospheric Sounder and Altimeter (LASA). This capability provides vertically resolved measurements through the atmosphere that complement the surface images and precision determination of the topography of the Earth's surface. Key variables include the water vapor profile and aerosol characteristics. If flown together, this package of instruments will probe the same atmospheric conditions, which will enable their data to be compared and combined in detail to produce more information.

The second package consists of three radar techniques—altimetry, scatterometry, and synthetic aperture radar—and is called Sensing with Active Microwaves (SAM). The SAR can achieve spatial resolutions of 30 m. This provides the high spatial resolution microwave counterpart to the HIRIS visible/IR measurements. SAR primarily measures water-related phenomena, small-scale surface roughness, and large-scale structural features of the Earth's surface. The technique requires the instru-

ment to view to the side of the spacecraft track. Generally, observations cannot be taken within about 17° of nadir. The scientific desire to combine HIRIS and SAR observations and also HMMR and SAR observations of the same scenes under virtually identical conditions requires that the SAR be flown in a manner that enables its side-looking view to observe the same sites seen by HIRIS in the generally nadir view. This means that the SAR must fly on a separate platform from the SISP instruments. The SAR envisioned for Eos would contain three frequencies (L-, C-, and X-band) with quad-polarization and multiple-incidence and azimuth angles. The SAR can also be operated in a low-resolution (100 to 500 m) mapping mode with 1,000 km swath.

The other two radar techniques are altimetry (ALT) and scatterometry (SCATT). The ALT measures the elevation of the sea surface from which the geostrophic circulation of the ocean can be determined with knowledge of the geoid. ALT also measures significant wave height, sea surface wind speed, and the elevation and roughness of ice and land surfaces. The horizontal average of the height samples is taken over 2 to 20 km, depending on surface conditions. The vertical resolution can be as fine as a few centimeters. With long-term averaging, the TOPEX mission will produce accuracies of ± 2 cm. The level of accuracy obtainable is highly dependent upon the precise knowledge of platform location in space. The flight of ALT on an Eos platform requires that a precision location system be employed to enable measurements of the time-varying components of the ocean circulation. The SCATT measures sea surface wind stress, from which one can determine the velocity of the wind at the ocean surface. In general, the variables observed by SAR, SCATT, and ALT are sufficiently persistent to permit the three instruments of the SAM package to be flown in different orbits from one another without significant sacrifice of scientific return.

The third package is the Atmospheric Physics and Chemistry Monitors (APACM). The Eos strategy relies upon the operational payloads for soundings of atmospheric temperature, coarse vertical profiles of moisture, and general characterization of clouds. The remote sensing of the atmosphere can be broken down into measurements of the troposphere or lower atmosphere and of the stratosphere and mesosphere or upper atmosphere. It can also be divided into measurements of the temperatures, chemical species, and aerosols, which comprise the atmospheric composition and structure, and measurements of the winds. This pair of dichotomies in atmospheric variables to be measured results in four general instrument types being included in the Eos payload—Laser Atmospheric Wind Sounder (LAWS) measurements of the lower atmosphere, tropospheric composition measurements, upper atmosphere temperature and composition measurements, and Fabry-Perot Interferometry (F/P INT)

measurements of upper atmospheric winds. Within the APACM package there is a need to fly the upper atmospheric instruments together. These all use limb scanning to achieve sufficient vertical resolution. The tropospheric devices would point in the nadir direction and could be flown separately from the upper atmospheric devices.

There are also a number of general environmental monitors that round out the full measurement capability. These are the Earth Radiation Budget Instrument (ERBI), the total solar irradiance measurement (Solar Constant Monitor, SCM), the Solar Ultraviolet Spectral Irradiance Monitor (SUSIM), and the measurement of *in situ* plasma properties in the neighborhood of the platforms and the input of energetic particles into the upper atmosphere. This suite of measurements is summarized as one functional capability known as Environmental Monitors.

The Advanced Data Collection and Location System (ADCLS), while not an instrument per se, is an essential satellite link to a variety of automated devices deployed to make *in situ* measurements. These devices could vary from buoys floating in the open ocean to stream gauges to transmitters frozen into glaciers. In the future there will be a need to send commands to these devices as well as receiving their data and determining their location. This capability represents an indispensable link to the non-space measurements that are essential to completing the view of the Earth and should be implemented on the first Eos platform.

Following the issuance of the Science and Mission Requirements Working Group Report, consideration of how these functional capabilities might be realized as instruments has led to the identification of 30 individual devices. Figure 3 lists the functional

Functional Capability

Instrument Concept

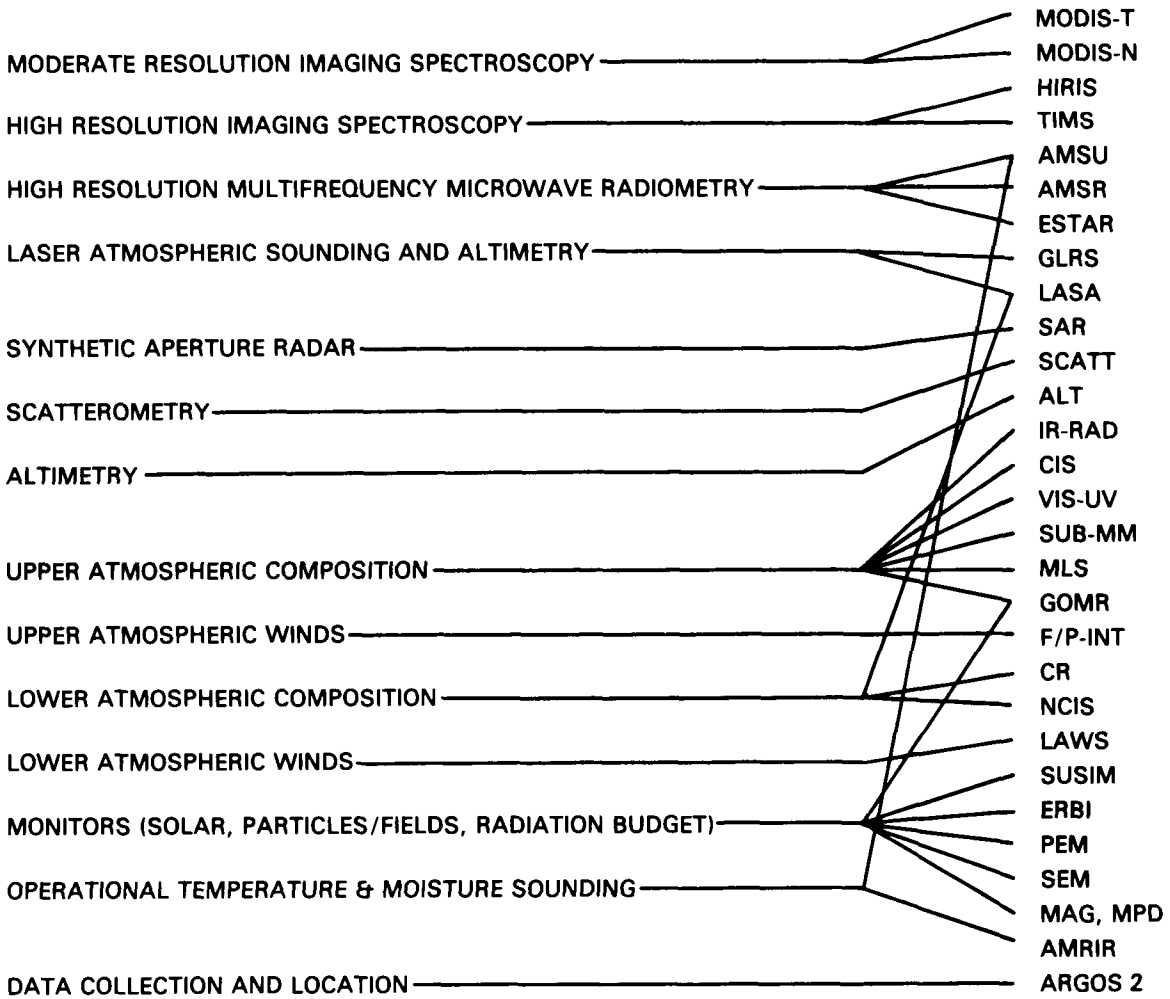


Figure 3. Relationship between instrument functional capability and instrument concept.

capabilities and the instruments now considered necessary to carry out these observing functions. One should keep in mind that some of the instruments included are quite modest in projected size and cost and greatly resemble instruments currently under development. It is not the number of instruments that is of significance but the integrated capability that they provide and their overall requirements for supporting resources. This expanded set of instruments is recommended at this time, but it is anticipated that the list will continue to evolve in response to the processes of payload development and technological innovation.

Table 4 gives brief descriptions of the complete candidate payload for Eos, including operational instruments. Table 5 shows some of the physical and operational characteristics of these instruments, while Figure 4 shows in matrix form the different types of observations provided by each device within the total payload. The matrix shows that many portions of the Earth system require several devices in order to provide the complete remote sensing characterization. In all cases, the full set of measurements needed by Earth science to characterize a part of the Earth system includes *in situ* observations. As Eos evolves there may be cases where the capabilities of an advanced sensor replace those of another instrument. Only the more advanced instrument concepts are listed here. The full observing set of instruments needs to be employed during the same time period, except in those cases of evolving measurement capability where a new instrument replaces one or more others.

Implementation Scenario

The degree of simultaneity required among the different instruments varies significantly. In order to maximize the synergism of the payload, various combinations of instruments should be flown on the same platform, as previously discussed with the SISP, SAM, and APACM packages. The current concept of Eos contains similar groupings of instruments. The first such grouping is essentially similar to the SISP described earlier. It is designed to achieve simultaneous observations of the surface and characterization of the atmospheric conditions that influence both surface conditions and their measurement through the interfering atmosphere. This combination includes the MODIS-T, MODIS-N, HIRIS, TIMS, and AMSR imagers of the surface together with the atmospheric sounders AMSU and LASA. (Infrared sounding capability is included in MODIS-N.) A second grouping combines those devices that measure the detailed chemical composition of the troposphere: CR, NCIS, and LASA. A third grouping includes all instruments making limb measurements of the stratosphere and mesosphere: IR-RAD, CIS, VIS-UV, SUB-MM, MLS, part of GOMR, and F/P INT. The flight of both the GLRS (Geo-

dynamic Laser Ranging System) and ALT on the same platform should improve the accuracy of range measurements from the satellite to the surface. Flight of LAWS with atmospheric sounders such as AMSU and MODIS-N or HIRS is also required to facilitate the combined incorporation of wind, temperature, and moisture data into atmospheric models. There are other, less stringent simultaneity requirements that the observing system should meet. For example, ESTAR measurements of surface soil moisture should be obtained within 1 hour of measurements characterizing the state of land surface vegetation. The system should provide the capability for SAR and HIRIS to make observations of a wide selection of sites also within 1 hour.

The operational logistics of producing and delivering timely forecasts and warnings give NOAA a strong preference for flying the operational payload as a complete unit. The ADCLS envisioned for Eos could be a part of this grouping, and its requirements could be met by an improved version of the current ARGOS system. The SCATT has relatively relaxed requirements for simultaneity but has coverage preferences similar to other wide-field-of-view instruments. There may be reasons for tight simultaneity between the SCATT and the LAWS, both of which provide direct wind measurements. The *in situ* devices to measure particles and fields conditions are generally small instruments and can be considered for flight on all platforms. The solar instruments can be flown on any Eos platform or in any other orbit that provides good solar viewing.

There are several reasons to consider flying multiple copies of some instruments. The current NOAA operational system includes morning and afternoon satellites. This dual capability is necessary to provide more frequent sampling of rapidly varying meteorological variables and to increase reliability of the measurement system through redundancy. Similar arguments are applicable to all tropospheric temperature, moisture, and wind sounders, including LASA, LAWS, and SCATT. An additional motivation for flight of multiple instruments is to obtain more complete daily or bidaily coverage with survey instruments having limited swaths or sampling patterns. This situation applies to both SCATT and ALT, particularly if they are to be used in an operational context. In general, it is recommended that for research the Eos payload should be built up until each type of measurement is being made with one instrument before multiple copies are flown of any instrument. NOAA operations require morning and afternoon copies of most instruments considered to be operational. Multiple copies of ALT and SCATT are recommended particularly if they are included in the operational payload.

Eos is conceived of as an evolving system that can incorporate new technology and the lessons of experience during its decade and a-half of anticipated operation. In addition to this requirement that an

Table 4. Eos Instrument Descriptions

ALT	ALTIMETER Radar system for the study of ocean topography and topographical measurements over ice. Dual frequency radar configuration with altitude precision less than 3 cm. Topex class altimeter.
AMRIR	ADVANCED MEDIUM RESOLUTION IMAGING RADIOMETER Visible/infrared radiometer for global measurement of cloud cover, sea surface temperature, measurement of snow and ice extent, plus measurement of vegetation cover and characteristics. Sensor will also provide atmospheric temperature and water vapor measurements and will be a follow-on instrument replacing the combined capability of the current AVHRR and HIRS instrumentation. Sensor will have a spatial resolution of 500 m at nadir and a ground swath of approximately 2,940 km.
AMSR	ADVANCED MICROWAVE SCANNING RADIOMETER Radiometer providing measurements of atmospheric water vapor, precipitation, and snow and ice extent. Multifrequency (5 to 40 GHz region) electronically scanned cylindrical parabolic antenna approximately 3 m × 6 m with a 3 m phased array. Field-of-view of 40° with a spatial resolution of 5 to 20 km. Anticipated radiometric performance of less than 1 K. Swath width of 1,000 to 1,500 km with an incidence angle of 45°.
AMSU	ADVANCED MICROWAVE SOUNDING UNIT (A and B) Microwave radiometer providing measurements of atmospheric temperature and humidity. Twenty-channel instrument divided into AMSU-A and AMSU-B subsystems. AMSU-A primarily provides atmospheric temperature measurements from the surface up to 40 km in 15 channels, i.e., 23.8 GHz, 31.4 GHz, 12 channels between 50.3 to 57.3 GHz and 89 GHz. Coverage is approximately 50° on both sides of the suborbital track, with an IFOV of 50 km. Temperature resolution equivalent to 0.25 to 1.3 K. AMSU-B primarily provides atmospheric water vapor profile measurements in five channels at 89 GHz, 166 GHz, and 183 GHz (3). Coverage is the same as AMSU-A, with an IFOV of 15 km and a temperature resolution of 1.0 to 1.2 K.
ARGOS 2	FRENCH DATA COLLECTION AND LOCATION SYSTEM (ADCLS) Data collection and location system for drifting platforms and balloons and remote <i>in situ</i> measurement sites. 401.650 MHz operating frequency for a drifting buoy location accuracy of 1 km and speed determination of 0.3 m/s.
CIS	CRYOGENIC INTERFEROMETER SPECTROMETER A combined cryogenically cooled Michelson interferometer and multichannel radiometer. Instrument views the Earth's limb and measures emissions in order to derive trace constituent abundances and temperatures in the wavelength region of 2.5 to 25 μ m.
CR	CORRELATION RADIOMETER Instrument for the measurement of constituents in the troposphere using selective absorption gas cell radiometry. Provides global distribution of carbon monoxide and other species, with limited vertical resolution.
ERBI	EARTH RADIATION BUDGET INSTRUMENT Multiple channel instrument for the measurement of the Earth's radiation budget on a regional, zonal, and global scale, using selected fields-of-view. Instrument response is from 0.2 to 50 μ m with selective filters. Instrument uses the sun as a calibration source. The instrument is divided into a scanning and non-scanning portion for the selective measurements.
ESTAR	ELECTRONICALLY SCANNED THINNED ARRAY RADIOMETER Microwave radiometer providing high-resolution soil moisture measurements using an aperture synthesis technique. Single frequency instrument at 1.4 GHz. Antenna size 18 m × 18 m covering a swath of 1,400 km. Approximate temperature resolution of 1 K.

Table 4. Eos Instrument Descriptions (continued)

F/P INT	FABRY-PEROT INTERFEROMETER Interferometer system measuring wind and temperature in the upper atmosphere by measuring Doppler shifts of absorption and emission features. Instrument views the limb in the 10 to 50 km altitude region to measure the absorption features of oxygen and scattered light bands and in the 60 to 300 km altitude region to measure the atmospheric emission features. Measures the vector wind field to less than 5 m/s.
GLRS	GEODYNAMICS LASER RANGING SYSTEM Laser system for the measurement of tectonic plate motion and ice sheet altimetry. It is a rapid scan, 18 cm diameter telescope instrument with integral star trackers. Laser energy per pulse, 10 mJ with a 10 Hz repetition rate. System uses retroreflecting cubes embedded in the surface target.
GOMR	GLOBAL OZONE MONITORING RADIOMETER Dual instrument consisting of a nadir viewing UV radiometer for the measurement of total ozone, and a limb-scanning IR radiometer for the measurement of the vertical distribution of ozone, temperature, and possibly other species. The UV instrument measures solar radiances and radiances reflected from the Earth-atmosphere system in six wavelengths between 305 and 340 nm in the near UV. It has a nadir field-of-view of $3^\circ \times 3^\circ$ equivalent to a spatial resolution of 43 km \times 43 km at nadir. A cross-track scanning mirror provides continuous coverage at all latitudes. The IR limb scanning radiometer has three or more channels, in the wavelength range from 6 to 18 μm for the measurement of ozone, temperature, and perhaps other species. The scan is in the plane of the orbit, from below the surface to above 100 km, with a vertical field-of-view at the limb of 2 km.
HIRIS	HIGH-RESOLUTION IMAGING SPECTROMETER Spectrometer providing highly programmable localized measurements of biological and geological processes at a spatial resolution of 30 m. Pointable instrument with a 30 km swath coverage, viewing accessible areas 25° off track and $+60^\circ$, -30° in track. Spectral coverage of 0.4 to 2.5 μm at 10 nm resolution. 196 spectral bands.
IR-RAD	INFRARED RADIOMETER Radiometer for the measurement of upper atmospheric temperature and certain atmospheric species. A multiband instrument that views the limb. Measures temperature, ozone, and trace species distribution with approximately 3 km vertical resolution over the altitude range from cloud tops to the mesopause.
LASA	LIDAR ATMOSPHERIC SOUNDER AND ALTIMETER Lidar system(s) for the measurement of water vapor total column content, water vapor profiles, aerosols and clouds, atmospheric state parameters, ozone, ice sheet mass balance, and land topography. System initially uses a 1.25 m diameter class telescope and multiple-wavelength selective laser systems tailored to specific measurement areas. Telescope is a fixed-nadir viewing system that may be modified for scanning and/or aperture size change.
LAWS	LASER ATMOSPHERIC WIND SOUNDER Doppler lidar system for direct tropospheric wind measurements. System consists of a 1.5 m diameter rotating telescope (approximately 3 rpm). Instrument covers a swath area of 300 km \times 300 km for radial velocity measurement of 1 m/s. Vertical resolution is 1 km.
MAG	MAGNETOSPHERIC CURRENTS AND FIELDS DETECTOR Magnetometer for the measurement of magnetospheric currents and fields.

Table 4. Eos Instrument Descriptions (continued)

MLS	MICROWAVE LIMB SOUNDER Microwave radiometer that detects and measures the distribution of trace chemical species in the upper atmosphere. Radiometer scans the Earth's limb and detects the thermal emission of trace species at selected frequencies in the range of 50 to 30 GHz. Nominal vertical resolution of 3 to 6 km.
MODIS-N	MODERATE-RESOLUTION IMAGING SPECTROMETER—NADIR Imaging spectrometer for the measurement of biological and physical processes and atmospheric temperature sounding on a 1 km × 1 km and an 0.5 km × 0.5 km scale. Scanning instrument covering 1,500 km swath centered at nadir. Spectral ranges of 0.4 to 2.3 μ m, 3 to 5 μ m, and 6.7 to 14.2 μ m. Total of 40 bands, 27 at 1 km and 13 at 0.5 km resolution available for readout.
MODIS-T	MODERATE-RESOLUTION IMAGING SPECTROMETER—TILT Imaging spectrometer for the measurement of biological and physical processes on a 1 km × 1 km scale. Scanning instrument covering a 1,500 km swath centered at nadir, with scan mirror tilt for sun glint avoidance. Spectral range of 0.4 to 1.04 μ m in 64 bands.
MPD	MAGNETOSPHERIC PARTICLE DETECTOR Detector consisting of an array of particle analyzers to measure magnetospheric energy sources.
NCIS	NADIR CLIMATE INTERFEROMETER SPECTROMETER Interferometer type instrument for the measurement of temperature profiles and tropospheric constituents, i.e., H ₂ O, N ₂ O, CH ₄ , etc. Approximate spectral coverage of 2 to 40 μ m.
PEM	PARTICLE ENVIRONMENT MONITOR Multiple instrument assembly for the local and global monitoring of energy input to the Earth's atmosphere by charged particles. Assembly includes particle energy spectrometers, an X-Ray Imaging Spectrometer, and electric and magnetic field detectors.
SAR	SYNTHETIC APERTURE RADAR Imaging radar for all-weather studies of small- and large-scale structural characteristics of the surface for application in geology, glaciology, plant physiology, hydrology, and oceanography. Resolution of 30 to 500 m over a selectable swath from 50 to 1,000 km located on either side of the subsatellite track. System variables include frequency (L-, C-, and X-band), polarization (quad for L- and C-, HH and VV for X-band), and imaging geometry (incidence angles of 15° to 55° and azimuth angles of 0° up to approximately 60°).
SCATT	SCATTEROMETER Microwave system for the measurement of wind stress over the oceans. System provides measurements along two parallel swaths from 120 to 700 km on either side of the subsatellite track, with a six stick antenna configuration. Wind speed to 2 m/s and 10° angular resolution are measurement goals.
SEM	SPACE ENVIRONMENTAL MONITOR (ADVANCED CONFIGURATION) A group of five sensors for <i>in situ</i> measurement of plasma, particles, and field parameters. Total Energy Detector (TED) measures total energy deposited by magnetospheric electrons and protons in the range of 0.3 to 20 kev. Medium Energy Proton and Electron Detector (MEPED) consists of four directional sensors and an omni-directional sensor for measuring protons, electrons, and ions in the range of 30 to greater than 60 kev. Three-Axis Magnetometer—Measurement of magnetospheric fields on 1-second intervals to 1 nT resolution. Instrument is boom mounted. Local Electric Field Instrument—Measures vector electric field to infer Joule heating in the thermosphere. Radio Beacon—Two frequency, 200 MHz and 400 MHz, phase, coherent radio beam for measurement of total ionospheric electron content, topside ionospheric profile, and plasma irregularities.

Table 4. Eos Instrument Descriptions (continued)

SUB-MM	SUB-MILLIMETER SPECTROMETER Scanning radiometer viewing the Earth's limb in the 0.1 mm spectral region to detect trace species through their emission spectra.
SUSIM	SOLAR UV SPECTRAL IRRADIANCE MONITOR Instrument system for the measurement of solar UV fluxes and their changes over a solar cycle. Full-disk solar spectral irradiance measurement. Wavelength coverage from 120 to 400 nm with spectral resolution varying from 0.1 to 5.0 nm.
TIMS	THERMAL INFRARED MULTISPECTRAL SCANNER Spectrometer providing high-resolution thermal imaging capability to the HIRIS for biological and geological measurements. Instrument will be bore sighted with HIRIS to provide 30 m resolution over a 23.3 km swath. Its spectral range will cover from 3 to 5 μ m and from 8 to 14 μ m, for a total of eight bands of 50 and 500 nm spectral resolution.
VIS-UV	VISIBLE-ULTRAVIOLET SPECTROMETER Multiple spectrometer system for measuring trace species in the upper atmosphere using selected emission lines. Instrument is high-resolution (0.3 nm) spectrometer covering the wavelength range of from 30 to 1,200 nm.

Table 5. Eos Instrument Parameters

Instrument	Mass (kg)	Operating Power (W)	Average Power (W)	Operating Data Rate (Mbps)	Daily Data Vol $\times 10^9$ (bits)	Pointing* Knowledge (arcsec)	Pointing* Accuracy (arcsec)
ALT	180	225	225	0.013	1.0	756	1,516
AMRIR	60	50	50	4.0	345	36	36
AMSR	320	300	300	0.1	8.6	18	36
AMSU	105	200	200	0.005	0.43	36	36
ARGOS 2	70	50	50	0.002	0.17	—	18,000
CIS	800	120	120	0.24	21	60	360
CR	100	100	100	0.001	0.08	300	360
ERBI	65	50	50	0.002	0.17	?	?
ESTAR	400	200	200	0.005	0.43	36	72
F/P INT	115	100	100	0.005	0.43	72	180
GLRS	340	800	240	0.1	2.6	20	20
GOMR	150	260	260	0.005	0.028	50	800
HIRIS	1,080	825	620	3.5 avg. 290 peak	140	0.75	626
IR-RAD	150	430	430	0.004	0.34	50	800
LASA	2,050	2,500	1,250	1.5	65	10	160
LAWS	800	3,000	800	1.0	26	20	20
MAG	10	10	10	0.002	0.17	2,052	—
MLS	400	500	500	0.01	0.86	180	1,800
MODIS-N	200	500	500	8.4	330	15	6,500
MODIS-T	100	200	100	8.5	240	250	250
MPD	10	10	10	0.001	0.08	900	900
NCIS	250	300	300	0.02	1.7	250	250
PEM	80	75	75	0.004	0.34	900	1,800
SAR	1,940	5,700 avg. 13,500 peak	2,300	100 290	3,030	360	1,800
SCATT	180	240	240	0.005	0.43	767	767
SEM	20	20	20	< 0.001	0.086	—	—
SUB-MM	500	100	100	0.003	0.24	20	60
SUSIM	110	20	20	0.002	0.11	90	180
TIMS	1,250	1,625	500	30	388	0.75	626
VIS-UV	250	220	220	2.0	100	50	300

*Boresight of instrument

INSTRUMENTS	MODIS-T	MODIS-N	HIRIS	TIMS	AMSR	ESTAR	GLRS	LASA	AMRIR	AMSU	SAR	SCATT	ALT	CR
MEASUREMENTS														
Surface soil moisture and wetlands extent						●					●			
Land surface composition	●	●	●	●										
Land surface biological activity, phenology and physiological state	●	●	●	●							●			
Surface topography			●					●			●			
Plate motion							●							
Surface temperature	●			●	●					●				
Snow and ice extent and character	●				●				●		●			
Sea ice extent character and motion	●				●				●		●			
Sea surface winds					●						●	●		
Ocean waves										●			●	
Ocean circulation	●	●										●		
Oceans and lakes biological activity	●	●	●											
Tropospheric winds														
Tropospheric composition									●					●
Aerosols	●	●	●						●					
Cloud properties	●	●	●						●					
Atmospheric temperature		●							●	●				
Atmospheric water content						●			●	●				
Precipitation rate					●									
Upper atmospheric winds														
Upper atmosphere composition														
Particles and fields environment														
Earth radiative balance	●	●								●				
Solar output														

Figure 4. Principal measurements to be made by the Eos instruments.

INSTRUMENTS	MEASUREMENTS
NCIS	Surface soil moisture and wetlands extent
LAWNS	Land surface composition
FIR/INT	Land surface biological activity, phenology and physiological state
IR-RAD	Surface topography
CIS	Plate motion
MLS	Surface temperature
SUB-MM	Snow and ice extent and character
VIS/UV	Sea ice extent character and motion
GOMR	Sea surface winds
ERBL	Ocean waves
SUSIM	Ocean circulation
PEM	Oceans and lakes biological activity
MPD	Tropospheric winds
MAG	Tropospheric composition
	Aerosols
	Cloud properties
	Atmospheric temperature
	Atmospheric water content
	Precipitation rate
	Upper atmospheric winds
	Upper atmosphere composition
	Particles and fields environment
	Earth radiative balance
	Solar output

NCIS, LAWNS, FIR/INT, IR-RAD, CIS, MLS, SUB-MM, VIS/UV, GOMR, ERBL, SUSIM, PEM, MPD, MAG

INSTRUMENTS

information system be capable of non-disruptive evolution in an age of rapid technological advance, this committee recognizes that the financial investment of such a significant undertaking would likely be unachievable over the typical 4- to 5-year development cycle of a NASA Space Science mission. Given the urgency of our need to understand the Earth and the key role of long-term data sets in enabling the development of this understanding, we assume that a significant subset of the capabilities we envision should be put in place while others are deferred for continuing financial investment in the system after its initial implementation. For the space segment of Eos, this may be made easier by the advent of orbital servicing and a generic design polar platform. It is also recognized that technological advance is required before some of our observational concepts are realized. These facts guarantee that the implementors of Eos will be confronted with crucial decisions on which instruments to develop for the initial orbital configuration (IOC) and which to defer.

This committee has considered several scenarios of instrument development and deployment. All are subject to substantial change by future events. Rather than endorse a specific scenario as illustrative

of how these decisions should be made, we recommend a set of guiding priorities. The top priority for Eos measurements is continuity in all ongoing satellite data sets that are essential for understanding the Earth system. This priority is a direct consequence of the first recommendation given in the Eos Science and Mission Requirements Working Group Report. The second priority is for instruments that address the broad multidisciplinary research questions of Earth science or that address the specific questions of a broad set of Earth science disciplines. This category is exemplified by the MODIS instrument and certainly includes the improved data relay capabilities of an advanced ARGOS. The third priority is for instruments that enable a specific key area of research in a single Earth science discipline. GLRS is one clear example. All other measurement capabilities may be regarded as sharing the fourth priority. These are the scientific priorities that must be incorporated with technological, financial, and programmatic constraints to arrive at the actual decisions on which instruments are placed in orbit as part of the Eos IOC and which are developed later.

As a direct consequence of the specific instrument characteristics and the payload grouping prin-

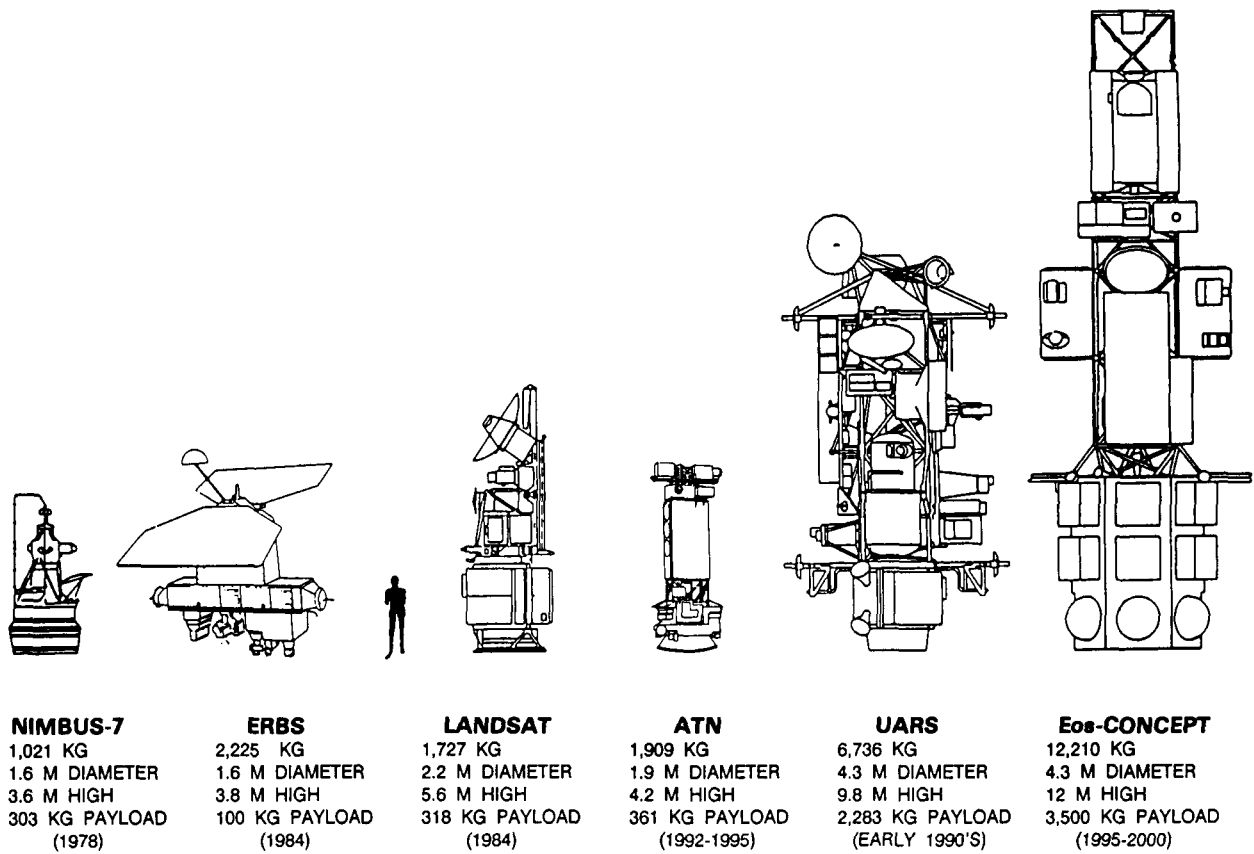


Figure 5. Scale drawing comparing one concept for an Eos payload on a platform with current-generation spacecraft.

ciples, Eos requires a new class of satellite bus to support the integrated deployment of subsets of the overall payload. Indeed, the resource requirements of the SAR instrument by itself exceed the power and weight capacities generally available on the current generation of Earth orbiting satellites (such as Landsat, UARS, and ATN). The need for a large payload and an extended-duration mission would be difficult to accommodate were it not for the capability to service instruments and satellite subsystems on orbit. This combination of expanded capabilities and on-orbit serviceability is a goal of the Space Station polar platform(s). Figure 5 illustrates the increased size of the platforms and payloads being discussed by comparing one concept for an Eos payload on a platform with current-generation spacecraft drawn to scale. The development and provision of at least the first afternoon polar platform as part of the U.S. Space Station program contribution will greatly facilitate the development of Eos. A similar contribution from the European Space Agency (ESA) will enable a fuller realization of the Eos system by the mid-1990s. Figures 6a and 6b show one concept of two such platforms carrying much of the afternoon Eos payload.

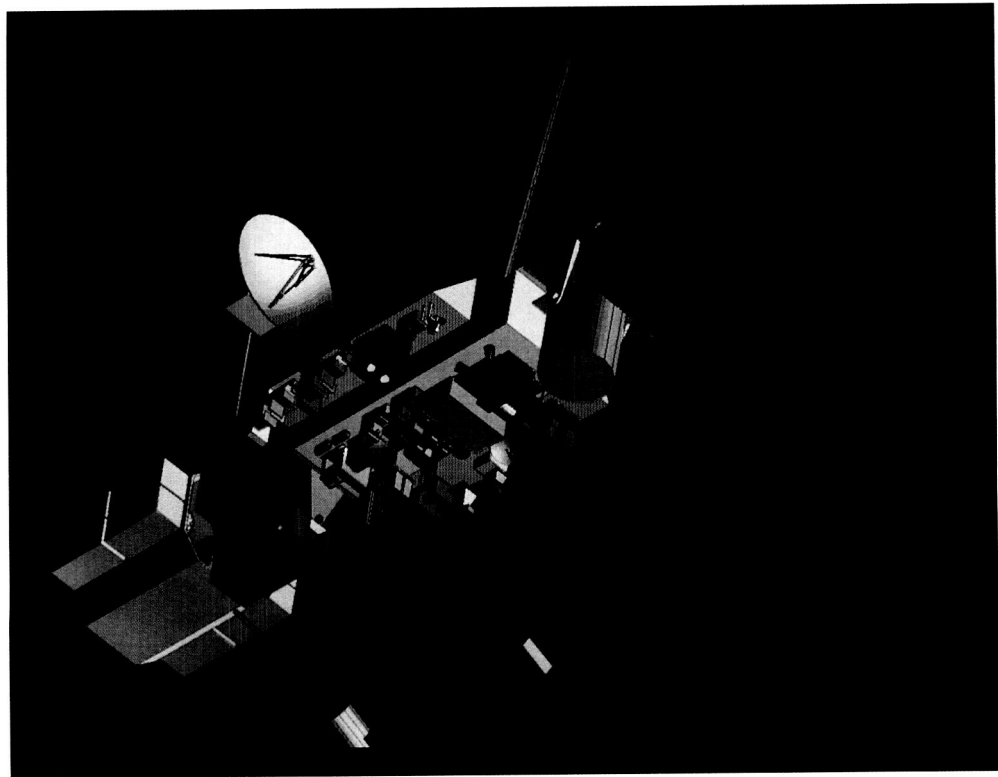
Orbit Selection

One conclusion of the first Eos Working Group report is that all of the needed observing capabilities included in this mission concept could be accomplished through use of sun-synchronous orbits at low altitudes. For most and potentially all Eos instruments, the specific equator crossing time preferred for the first copy is between 1:00 and 1:30 p.m. This time will provide observations of the land surface under extreme conditions of thermal and hydrologic stress and is sufficiently close to noon to provide ocean surface observations without excessive problems with sun glint. This afternoon crossing time is also acceptable because of the assumed continuation of morning observations similar to the current Landsat and NOAA capabilities. NOAA afternoon polar orbiting satellites have had equator crossing times between 2:00 and 2:30 p.m., but there are strong operational reasons dealing with the timely delivery of the major evening forecast for the continental U.S. that make a choice of 1:00 to 1:30 p.m. preferable for current and future systems. NOAA has also indicated a preference for a crossing time of 9:00 to 9:30 a.m. for the morning operational payload, and this time has been assumed in this report for any morning orbiting platform(s).

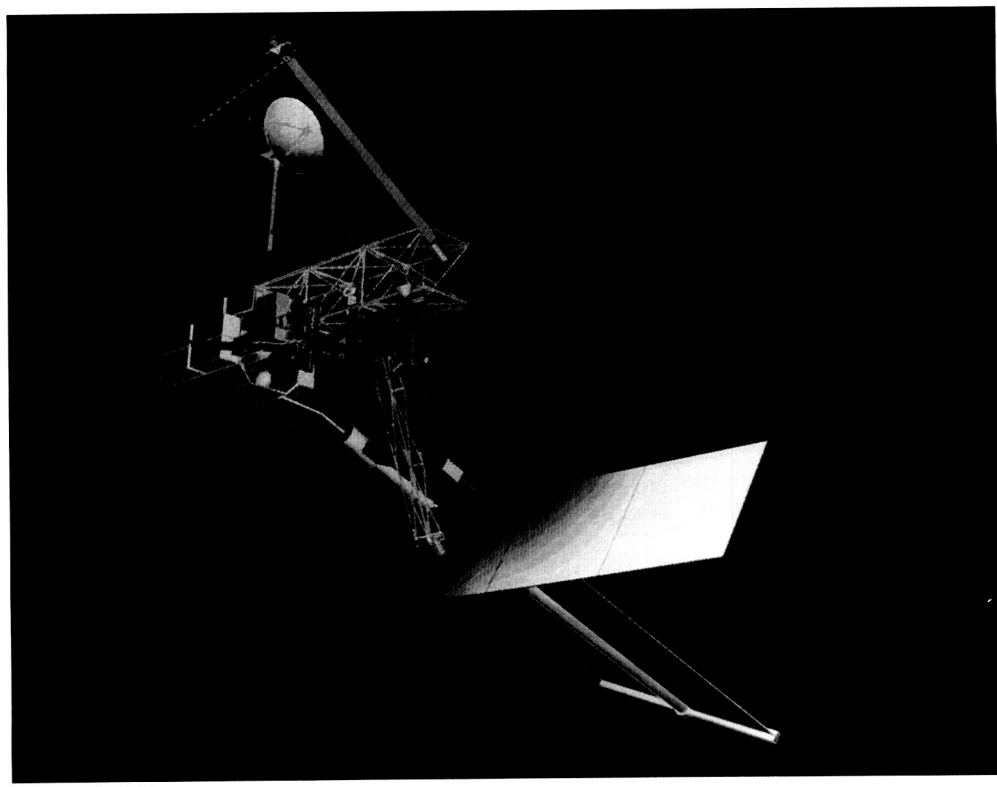
The other key element in the selection of an orbit or orbits for Eos is the altitude. The initial Eos concept assumed that all payload elements would be flown at an altitude of 705 km. Altitude affects several aspects of the observing capability of the instruments. First, greater distance from the Earth's

surface permits observation of a wider swath without the necessity of viewing through excessively long atmospheric paths and without the requirement of using data taken at very high look angles. Specifically, it is recommended that observations to be taken by the MODIS instruments should not be considered for scientific purposes beyond a 45° cross-track look angle. A second effect of altitude is on the size, power requirements, and cost of the instruments. The effects of altitude on these parameters vary with the type of instrument and range from a square root of altitude dependence for the optics sizes in limb scanning instruments to a cube of altitude dependence for the power required in a synthetic aperture radar instrument.

A subtle effect of altitude is on the repeat pattern of the ground traces of different orbits. Orbit can be adjusted to produce precisely repeating ground traces in different time intervals. For instance, the 705 km altitude chosen in the earlier Eos concept produces a ground trace that repeats every 16 days. It also produces an approximate repeat pattern every 2 days. This enables instruments that can look out to cross-track angles of 45° from nadir to obtain coverage of the entire Earth every 2 days. Figure 7 illustrates this and also shows the repeat patterns produced by two other orbital altitudes being considered for Eos platforms. All of these orbits produce precise repeats in 16 days. As indicated above, 705 km produces a pseudo 2-day repeat pattern that enables a number of wide-swath Eos instruments to obtain global coverage (both in daylight and at night) of the Earth's surface every 2 days. There is substantial scientific desire to obtain global coverage daily. When coupled with the $\pm 45^\circ$ look angle constraint stated above, realizing this desire would require an altitude in excess of 1,000 km. Such a significantly higher altitude is felt to be excessively costly and impractical for platforms that may be serviced at 2- to 3-year intervals, and also would severely constrain payload size given the available launch vehicles. Operational observations are generally made on NOAA spacecraft at altitudes that range from 780 to 860 km. The operational mandate requires that these satellites produce the best possible daily coverage for weather forecasts. This consideration has led the Eos Science Steering Committee to consider the 824 km altitude, which produces a pseudo 5-day repeat pattern and enables the Eos wide-swath instruments to obtain global coverage every 3 days and 90 percent coverage every 2 days (see Figure 7). A third orbit that was considered for some Eos instruments is a substantially lower altitude of 480 to 580 km. The example shown (540 km) produces a strict 16-day repeat pattern without a more frequent pattern of effective coverage to illustrate the full range of possibilities. Lower orbits exist that reproduce the repeat pattern characteristics of both the 705 and 824 km altitudes and a variety of other patterns as well. Low altitudes such as 540 km would be chosen to

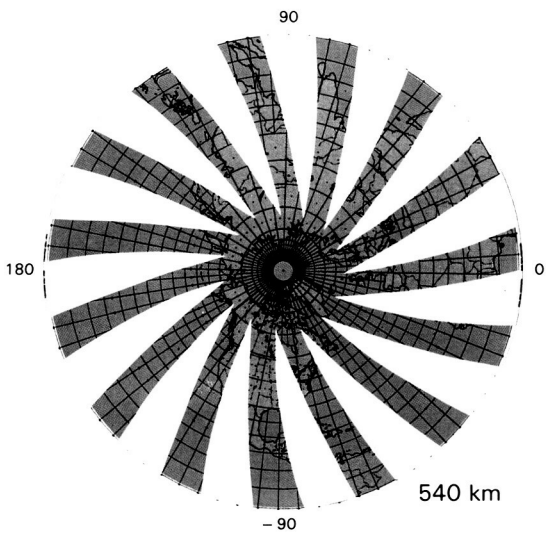
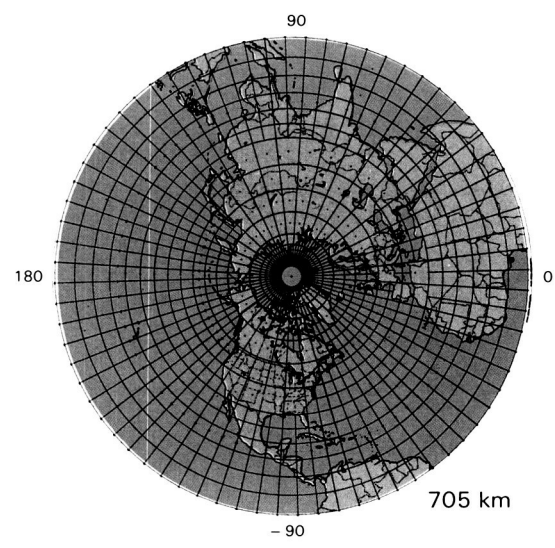
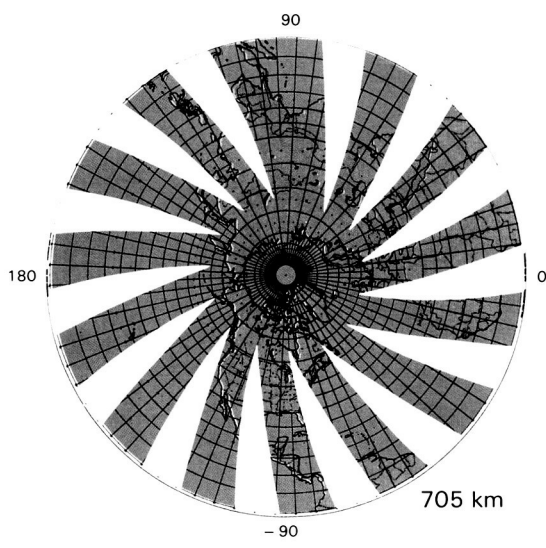
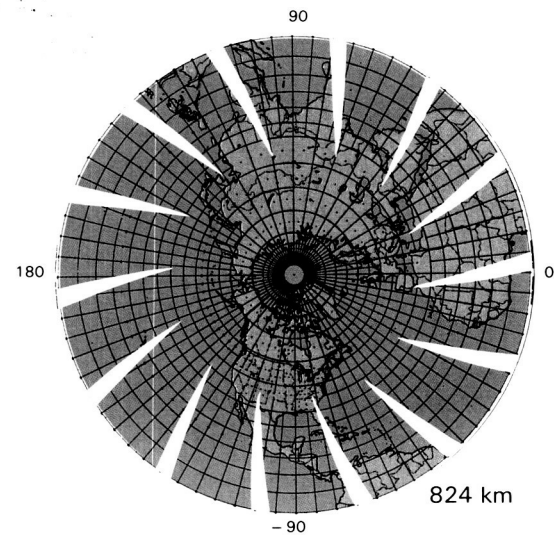
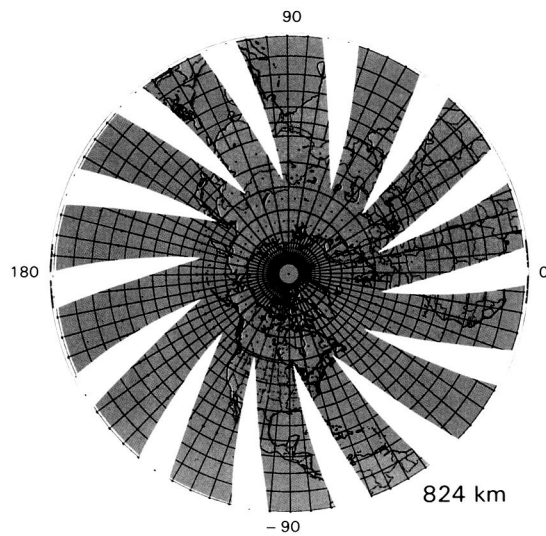


(a)

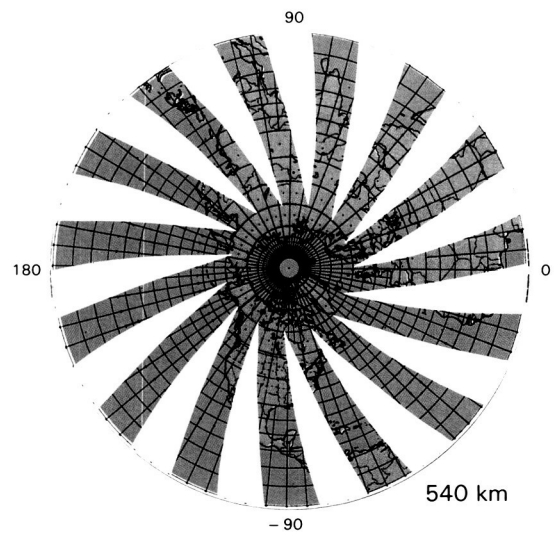


(b)

Figure 6. Conceptualization of (a) platform carrying a significant subset of the Eos payload including the expanded SISP group of instruments and (b) platform carrying SAR and other Eos instruments.



ONE DAY COVERAGE



TWO DAY COVERAGE

Figure 7. One- and two-day ground trace coverage of MODIS as a function of orbital altitude. The altitudes illustrated are 824, 705, and 540 km.

minimize cost, power, and other requirements for instruments that do not need to obtain wide-swath frequent coverage of the Earth's surface.

Figure 8 illustrates the coverage produced for various instrument swaths on the Earth's surface for the three particular orbital altitudes under consideration. Note that in these cases the amount of coverage is generally unaffected by choice of altitude. The specific amount of high-resolution SAR coverage that can be acquired even with continuous operation of the SAR (which is not anticipated) is much less, due to the roughly 100 km swath planned for this instrument in the high-resolution mode. As mentioned earlier, flight of some instruments on both morning

and afternoon platforms offers expanded measurement possibilities. Figure 9 illustrates this for MODIS-N and SCATT. For MODIS-N, assuming flight of both platforms at 824 km altitude, more than 95 percent of the Earth can be covered each day and about 65 percent of the surface is seen at both morning and afternoon local times. This should enable improved study of diurnal variations and vegetation responses to the onset of stress. For SCATT, flight of instruments in both morning and afternoon orbits enables greatly increased coverage every day. Eventual operational use of such measurements will likely require at least this much coverage. The Eos payload for flight in the afternoon orbit re-

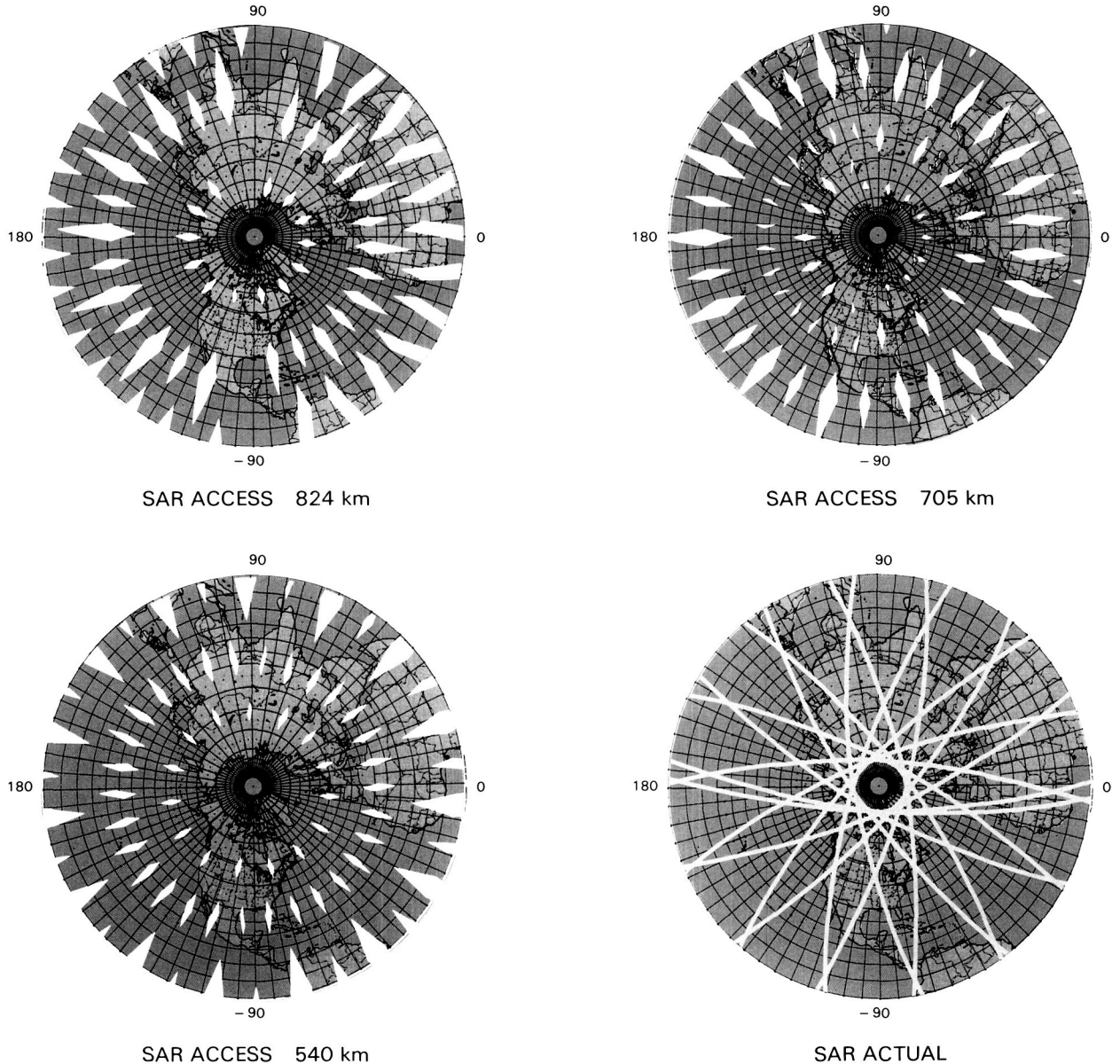


Figure 8. SAR access coverage as a function of orbital altitude and actual SAR coverage at a specific altitude (above). One-day surface coverage of a scatterometer as a function of orbital altitude (facing page). The altitudes illustrated are 824, 705, and 540 km.

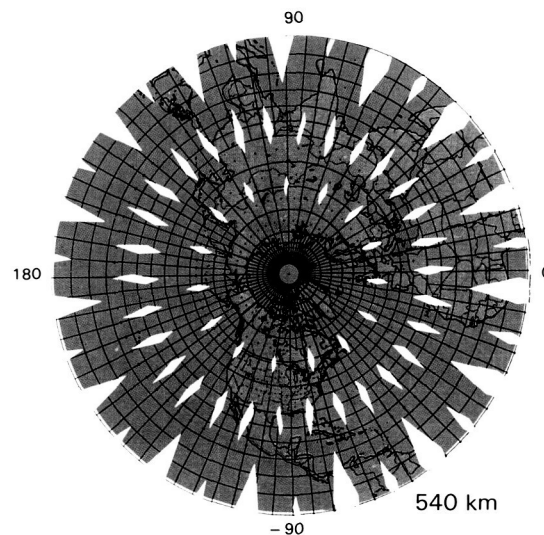
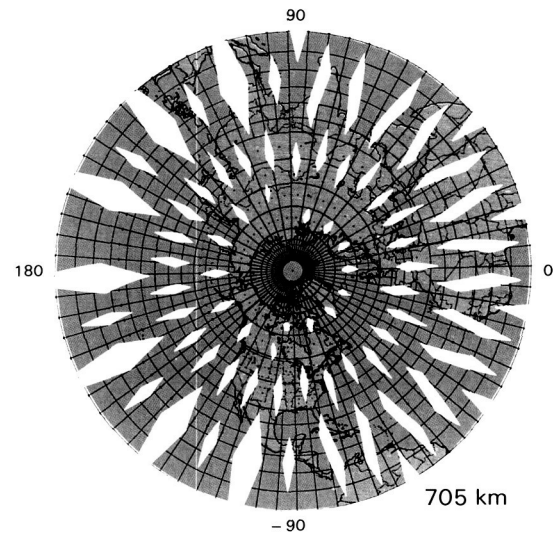
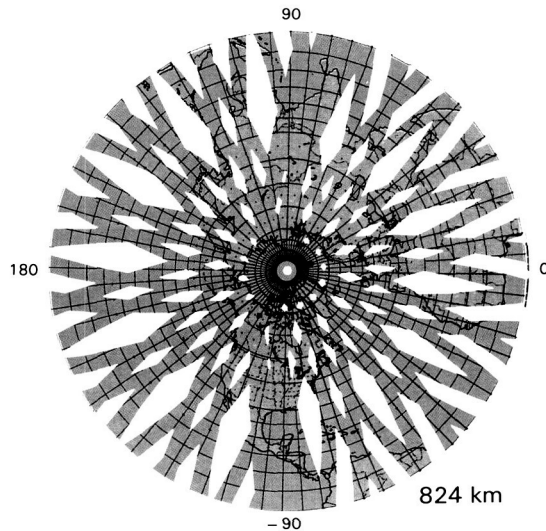
quires at least two platforms. If both platforms are at the same altitude and are phased in the same orbit so that they are roughly 25 minutes apart, a SAR instrument on one platform can view the same sites as seen by the HIRIS instrument on the other. This is illustrated in Figure 10 and fulfills one of the simultaneity requirements listed earlier.

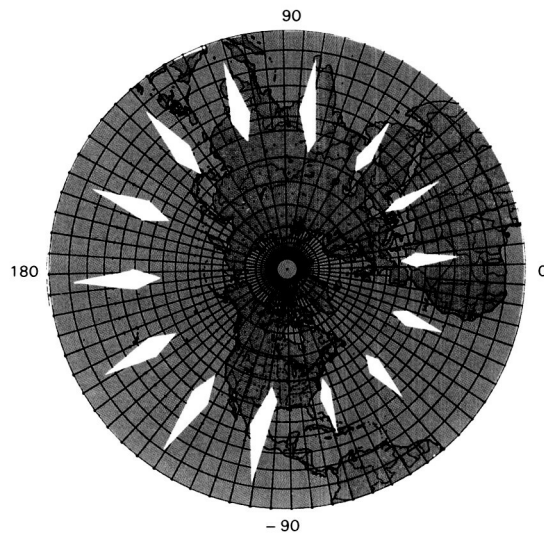
Orbital altitude also affects mission logistics. The effects of atmospheric drag must be compensated by boosts from the platform propulsion system. The amount of fuel required effectively limits the range of altitudes considered to those above about 475 km. Servicing of platforms and specifically the fuel required to move platforms or

servicing vehicles to and from operating altitudes and the orbits attainable by the Space Shuttle limit the range of Eos operational altitudes to no more than 850 km.

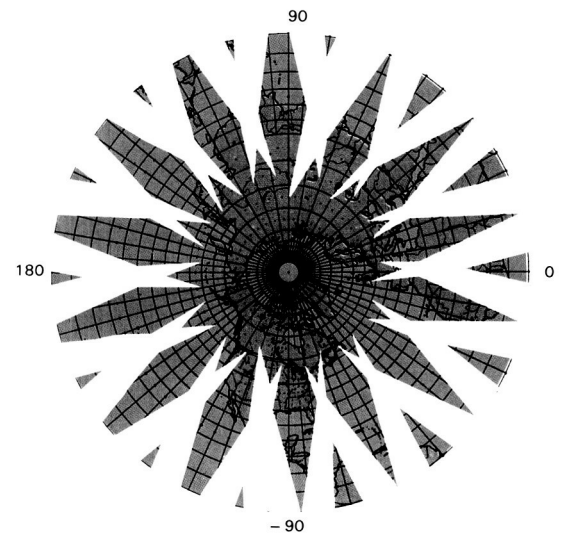
Eos DATA AND INFORMATION SYSTEM

The key to the Eos concept and to its ultimate success in meeting the needs of the Earth science community is the data and information system. This system must be the foundation upon which the rest

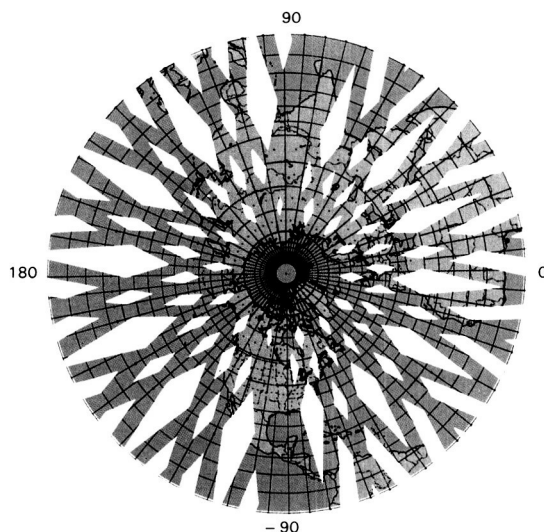




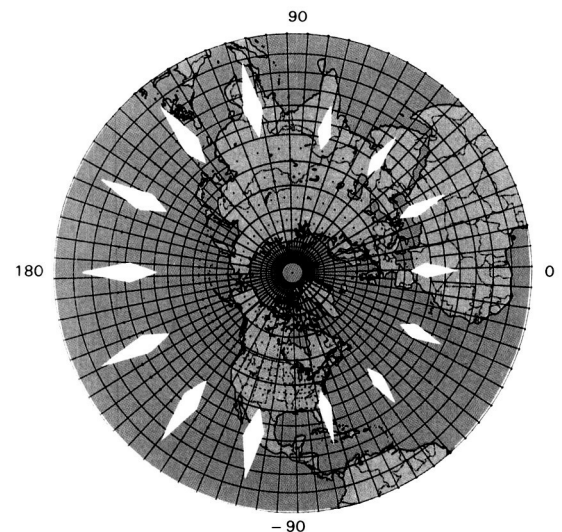
(a)



(b)



(c)



(d)

Figure 9. Surface coverage relationships for the MODIS and scatterometer instruments, each on two polar platforms. A.M. platform has a descending node and the P.M. platform has an ascending node. Illustration (1) shows the combined coverage achieved each day if MODIS instruments are flown on both morning and afternoon platforms (95 percent of the globe is covered), (b) for the same scenario as (a) shows the extent of the regions where both morning and afternoon MODIS observations would be obtained on the same day for comparison and examination of rapid diurnal changes. Illustration (c) shows one-day, single scatterometer coverage and illustration (d) shows dual scatterometer coverage for a single day.

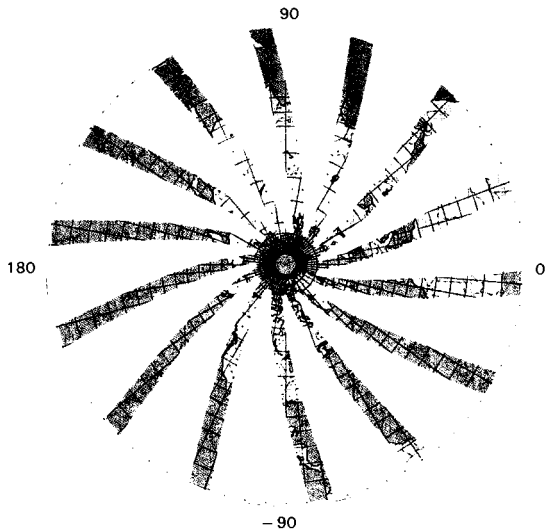


Figure 10. Common access coverage for SAR and HIRIS. Same surface area access coverage of HIRIS and SAR with HIRIS platform phased 25 minutes ahead of SAR platform.

of the mission is built; it will be the means by which all Eos results are collected and communicated. As with all other aspects of the Eos concept, the essential character of the data and information system is dictated by the nature of Earth science. Earth scientists must often take an eclectic approach to solving problems and assemble data of different types from a wide range of sources. The number of potential sources of useful data can, in some instances, be quite large. Thus, access to a wide range of data sources in a one-stop shopping mode of operation is essential to the productivity of the researcher. Another characteristic of the data is the fact that different aspects of the same data set are useful in different investigations. For example, the appearance of cloud images is important in predicting the likelihood and amount of precipitation that they may produce, while changes in their position provide a measure of wind velocity. Different research foci also lead to concern with different levels of detail in the data. A modeler of global climate may only be interested in general summary characteristics of the type of ecosystem in a region, while an investigator of the dynamics of that particular ecosystem will be concerned with variations within the area on space scales perhaps as short as a few tens of meters. This requires that the data and information system be capable of handling a wide range of data, including data on ranges of spatial and temporal resolution and averages of various kinds. This also requires the ability to store and retrieve the results of various research studies for use in other work. Taken together, these requirements dictate that the Eos data and information system be designed to include as

users a broad segment of the Earth science research community, and that users be closely involved in the development and subsequent management of the data and information system.

The Eos data and information system must also function in the more traditional sense as a data system for the Eos mission data. This function extends from the various instruments and platform subsystems through data downlink and ground-based distribution and processing to the storage of this data for the duration of the mission in a mission data base. Given the scope of the Eos mission, this is a formidable challenge. In the 1990s it is likely that the Eos data stream together with that from operational payloads will comprise in excess of 90 percent of all space science data. Table 5 has listed the data generation capabilities of the various instruments and the assumed average volumes of data that they will produce. Taken together they indicate that the research and operational data systems must be capable of handling an average data flow from space of up to 120 Mbps. The Eos data and information system must cope with roughly 1 terabyte of data each day and store this together with a host of derived products in a mission data base for up to 15 years. It is this scope, as well as the need to serve a community that extends beyond those directly involved in the mission implementation, that makes the Eos data and information system the challenge that it is.

Significant portions of the Eos payload will be acquiring data in a relatively routine fashion over the life of the mission, but major parts of the observing capability will be designed to allow for flexible experimentation in the acquisition of data. Choices of view angles, spectral channels, scan patterns, and other variables can be changed almost continuously to respond to the targets of observation and the nature of the science investigations being conducted. This necessitates an ability to command some instruments in a routine manner. It also implies that this ability to command be made available to many researchers over various periods of time in a manner analogous to the current mode of using major telescopes and particle accelerators. In order to do this, researchers must not only have input to the instruments command stream, but must have access to facilities for simulating the effects of their commands to refine their concepts. Such a testbed system could also be used to help resolve conflicts between potential observing scenarios.

The Earth science research community is quite large and widely distributed throughout the United States and the world. The Eos data and information system must put Eos in the hands of this extensive community as a research tool. Through contemporary data and information system technology, the researcher should be capable of accessing and interacting with a space mission from the researcher's home institution. Much of Earth science has and will

continue to require researchers to spend long stints in remote and often inhospitable environments. The data and information system should work to mitigate this necessity and certainly should not compound it.

As has been stressed repeatedly, virtually all quantitative data acquired about the Earth is useful for research. This is especially true of the long-term self-consistent acquisition of data for operational purposes. A cornerstone of the collaboration between NASA and NOAA in Eos is the easy ability for the research and operational data systems to interact and share data at all levels. To accomplish this, this committee recommends that the data and information systems required for research and operations be planned and implemented in parallel. The system should serve as a convenient means to aggregate interactive research demand for operational data, particularly in retrospective investigations. User friendly and efficient access to the operational data bases is a strong requirement in Earth science.

The Eos Data Panel (Chase *et al.*, 1986) has taken many requirements into account and has proposed one possible concept of an architecture for the

Eos data and information system. This concept takes into account the combined requirements of both research and operations and shows them as an integrated system; however, the actual implementation responsibilities for various elements within the system can easily be fulfilled by either NASA or NOAA. This implementation topology (see Figure 11) illustrates several key features that the system must include. First among these is the non-hierarchical nature of the concept. The Eos data and information system must avoid single point failures, including institutional bottlenecks in the flow of data. A second characteristic is inherent flexibility, where various nodes within the system can vary greatly in capability and can evolve without disrupting the overall system. A third key feature of the system is the preservation of the operational space-to-ground communications in use today while also making available the greater capabilities of the Tracking and Data Relay Satellite System (TDRSS). These two systems not only complement one another; they can be used to provide mutual backup and to increase both the research and operational data streams.

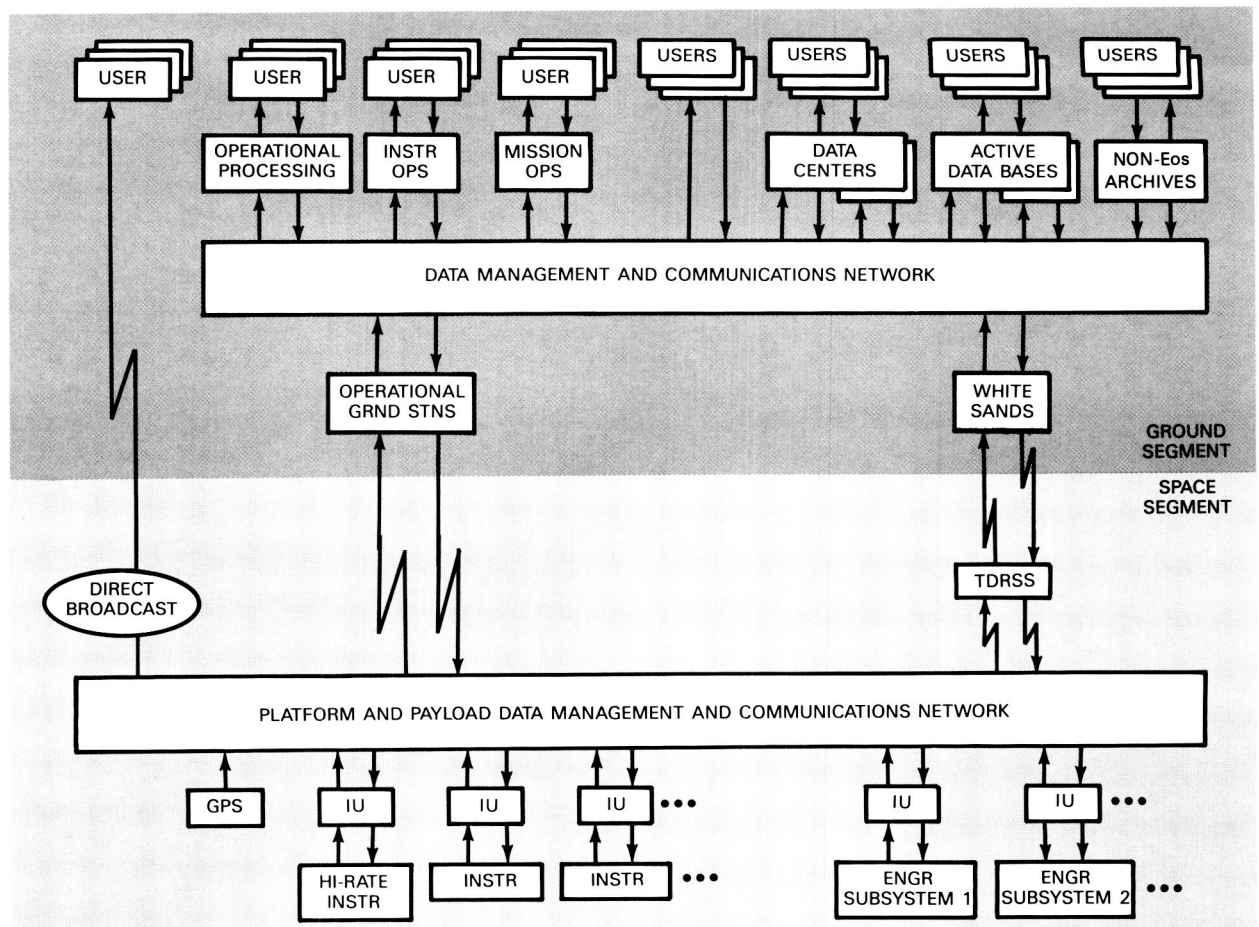


Figure 11. Architectural concept for the Eos data and information system proposed by the Eos Data Panel.

INTERNATIONAL INVOLVEMENT

The International Geophysical Year set the tone for multinational cooperation in efforts to understand the Earth. The commonality of interest and mutual benefit of shared cost bind the national efforts in Earth science together and have led to significant ongoing cooperation in satellite programs of Earth remote sensing. The Nimbus and operational NOAA satellites launched by the United States include non-United States instruments as essential payload elements. UARS and TOPEX are both proceeding on a multinational basis. Coordinated research programs such as the Global Atmospheric Research Program (GARP), World Ocean Circulation Experiment (WOCE), the World Climate Research Program (WCRP), and Tropical Oceans and Global Atmosphere (TOGA) continue to be major research foci coordinating international satellite and ground-based measurement efforts.

The successful implementation of the Earth Observing System will require resources of various kinds from many different nations. The object of the investigation certainly transcends national borders. The environmental quandaries that confront Earth scientists today generally have implications for public policy that are multinational in scope.

The first and most essential international resources required are intellectual resources. The Earth science community is global in extent, no longer dealing with a limited mission that will produce a few key discoveries by a small team of selected investigators. Instead there will be an abundance of data to support a vast number of studies ranging from the small site-specific work of perhaps a single scientist to the comprehensive modeling of major segments of the Earth system. The issue will not be one of controlling access to a small data set, but of attracting an adequate cadre of researchers to make full use of this research tool.

The second resource is financial. Eos will need several space platforms, a number of instruments, a revolutionary data system, and a significant team of scientists to be successful. The pace of progress will almost certainly be limited by funding. To the extent that this burden can be shared among nations, more

resources can be brought to bear on obtaining a comprehensive understanding of the Earth.

The third resource is access to specific areas that are of particular importance in gaining a scientific understanding of the Earth. With the exception of Antarctica, virtually all of the land surface of the Earth is under the control of individual nations. With the extension of the zone of economic interest to 200 miles from a nation's shore, much of the world's oceans are also under similar control. *In situ* data are essential to Earth science. This implies that information about many specific locations and the ability to make localized measurements are required.

Finally, the benefits to be derived from proceeding with Eos are for all of us who share this planet. The fundamental understanding of how Earth functions as a global system is not something that can be monopolized. In addition, observations of specific areas of local interest and significance can be obtained and put to use to the extent possible given the local infrastructure for using the information.

SUMMARY

The implementation of Eos should start with a data and information system that unites researchers and sources of data. This system must be able to grow to the capabilities required by the expanded set of remote sensing devices that can be brought to bear on the study of the Earth in the 1990s. Eos includes an extensive set of coordinated observations that will exhibit substantial synergy if carried out together. Eos will not have to replicate the set of observations being made on an operational basis, but can, through coordinated implementation of the research mission together with the NOAA operational mission, capitalize on this ongoing effort. Eos will make use of the new generation of spacecraft called space platforms being developed as part of the Space Station program. These platforms will provide expanded resources for the support of co-located instruments and more effective utilization of the investments made in instruments through on-orbit servicing. International cooperation in this venture is essential to its success. Eos must be a comprehensive system for the study of the Earth that can be sustained through the first decade of the next century.

III. MEASUREMENT STRATEGY FOR THE ENERGY, WATER, AND BIOGEOCHEMICAL CYCLES

Sunlight drives the outer part of the Earth system, maintaining life, motion, and physical and chemical transformations. The solar energy is used many times by the Earth's physical, chemical, and biological subsystems, being transformed and modified as it flows through the system and back to space. The multiple uses of the energy, the key role of water in energy storage and transport, and the physical and chemical planetary characteristics controlled and modified by the presence of life combine to determine the state of the Earth system.

The structure and motion of the inner part of the Earth system—the core, mantle, and crust—are determined by thermal processes driven by heat generated in the interior of the planet. The convection generated by this heat source moves the tectonic plates and shapes the continents. The processes produced by this internal energy form the geologic cycle, which is discussed in Chapter IV.

The environment of planet Earth is thus the result of interactions among energy, water, and life. Understanding the sensitivity of the system to disturbances, ascertaining the potential ranges of variability, and determining the possibility of irreversible change are the central questions of Earth System Science and are among the most crucial and urgent in all of modern science. Eos will address these questions.

THE ENERGETIC PLANET

The flux of solar energy through the Earth system is understood generally (Figure 12), but the far greater mastery of the specific rates and underlying processes is required before well-reasoned predictions about how the system will respond to change can be made, let alone trusted.

From the global perspective, the solar energy flux is most intense in the equatorial regions. This heats both the atmosphere and the ocean and evaporates considerable water from the surface. This moisture is then a large source of latent heat that drives atmospheric motions. The equatorial energy sources induce convective poleward flow and the Coriolis force turns this circulation into eastward flow at mid-latitudes. The atmospheric winds apply drag forces to the ocean surface and create the great gyres by which the oceans contribute to the exchange of heat between tropical and polar regions. In the polar regions, the relative input of solar heat is small, and the radiation of energy to space cools both the atmosphere and the surface leading to the growth of sea ice, atmospheric subsidence, and the formation of cold ocean bottom water.

The input and output energy are determined by the radiative properties of the atmosphere and the surface albedo. How the atmosphere transmits, absorbs, and reflects incoming and outgoing radiation depends critically on the presence of clouds and atmospheric chemical composition.

The amounts of carbon dioxide and other trace gases in the atmosphere and the surface albedo (all undergoing changes from human activity) control the infrared cooling of the Earth. Changes in average temperature in turn can cause shifts in the extent of cloudiness, vegetation, and snow and ice. These changes can then offset or amplify the initial warming. The extent to which this happens globally depends on the aggregate local response.

Thus, to understand the global energy cycle and predict how average regional and global climate will change, we must examine the energy cycle in detailed local and regional contexts all over the globe.

To obtain a detailed determination of the global energy cycle and the energy flux through any given location, measurements from the Earth Observing System and from geosynchronous satellites, and the principle of conservation of energy, can be combined to produce estimates of the various fluxes of energy. Energy conservation is typically applied to both the global energy balance and to the balance of local energy fluxes. To describe how Eos will contribute to the study of the energy cycle let us begin with energy transformations at the surface of the Earth, where the change in the energy stored below the surface must equal the difference between the incident solar energy and the sum of the radiative, sensible, and latent heat losses to the atmosphere.

Radiative Energy Fluxes

The radiative energy input to the surface can be determined by measuring the solar flux at the top of the atmosphere and accounting for the detailed atmospheric energy transmission characteristics, including clouds, aerosols, absorption, and scattering by the gases of the atmosphere. The Solar Constant Monitor (SCM) type of instrument will monitor the solar flux. The extent of cloud cover is the dominant factor in determining the amount of this energy reaching a given surface location. MODIS will measure the amount of cloud cover, but the sun-synchronous polar orbits of Eos will limit this measurement to four local times. The existing system of five geosynchronous satellites provides continuous observations of cloud cover between 50°N and 50°S latitude. The amount of energy transmitted through clouds cannot be measured directly from satellites and must be inferred from models based on observa-

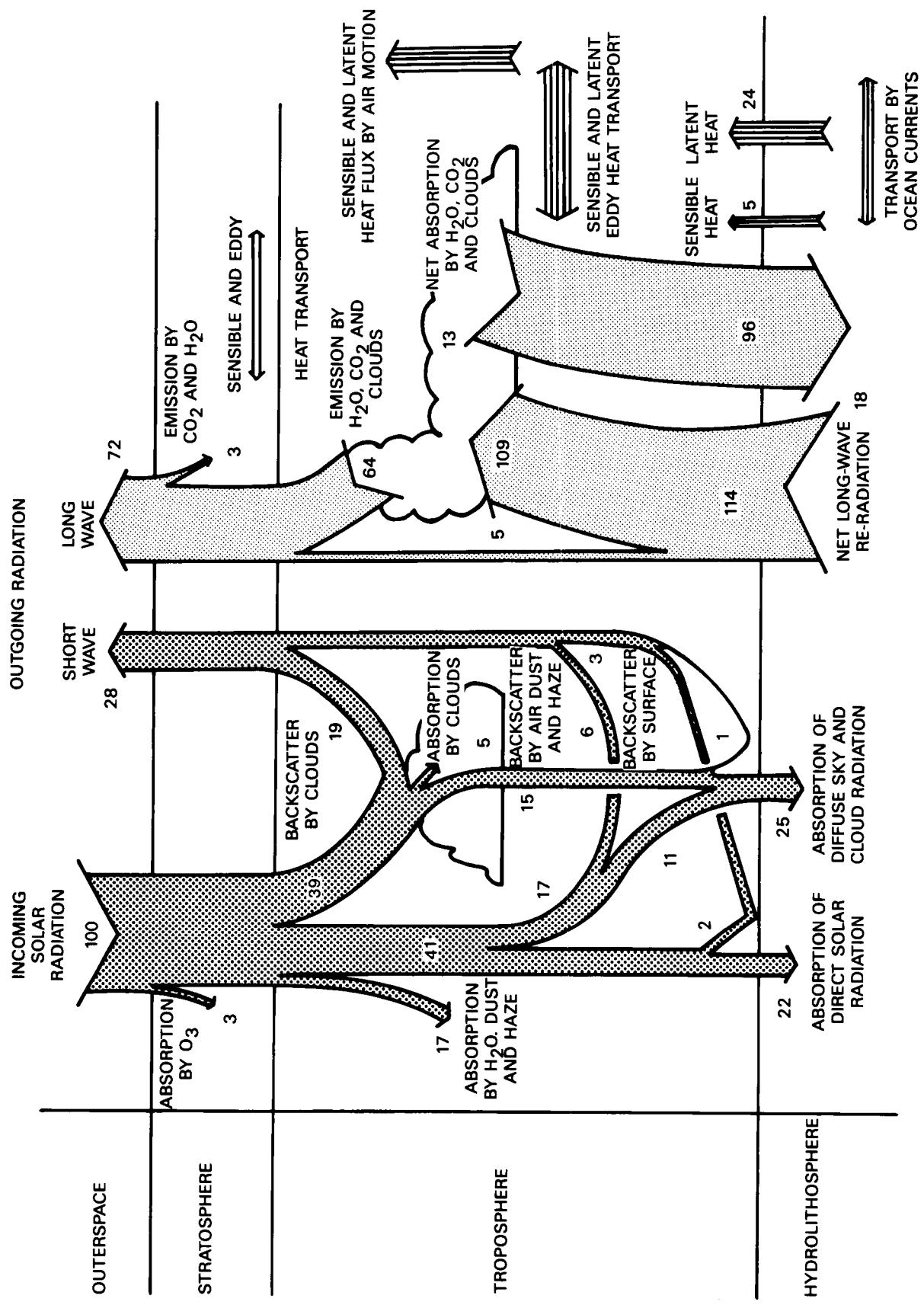


Figure 12. Schematic diagram of the disposition of absorbed solar energy in the Earth system.

tions of cloud properties. MODIS provides the capability to determine key cloud-top properties such as temperature and, by inference, height; the Advanced Microwave Scanning Radiometer (AMSR) will determine the total liquid water and ice content of the cloud; and LASA will sample the cloud-top height and temperature at a series of locations to improve the spatially continuous passive observations. The atmospheric sounding capability of geosynchronous satellites will be employed to make a somewhat less precise continuous measurement of these same cloud-top properties. The Advanced Microwave Sounding Unit (AMSU) soundings of atmospheric temperature and moisture and infrared temperature soundings from the High-Resolution Infrared Radiation Sounder (HIRS), MODIS, and the geosynchronous VISSR Atmospheric Sounder (VAS) taken through holes in the clouds will help determine the vertical extent and number of cloud layers. Aerosols and individual molecules of the atmosphere also scatter incoming radiation. The aerosol amounts and properties will be measured using the spectral capabilities of MODIS for broad areal coverage together with the spot measurements of aerosols by LASA. Finally, the amount of incoming solar energy that is absorbed at the surface depends on the surface albedo. This is measured by the MODIS, with the HIRIS offering the ability to sample the small spatial-scale variability within the individual MODIS pixels.

The radiative loss of energy from the surface by the emission of infrared radiation (IR) will be calculated from the temperature and emissivity of the surface and consideration of the IR absorbed and re-emitted by the atmosphere. The surface temperature will be measured from Eos by the MODIS, AMSU, AMSR, and AMRIR instruments. The Thermal Infrared Multispectral Scanner (TIMS) will provide sampling of small spatial-scale variations within the overall scene, as will the thermal IR channel(s) of commercial land remote sensing devices if they are onboard the polar platforms with Eos and operational instrumentation. In addition to surface temperature, the spectral richness of MODIS will provide the capability to make an independent measurement of surface emissivity. In regions where sea ice is present, AMSR will measure the fractional ice coverage, which is critical to the determination of the thermal emissivity of the polar ocean surfaces.

The determination of the radiative properties of the atmosphere depends not only on the factors discussed above for transmission of solar radiation through the atmosphere, but also on the amounts and vertical distributions of radiatively active (or greenhouse) gases. The three principal gases involved are CO_2 , H_2O , and O_3 , but N_2O , CH_4 , and chlorofluorocarbons are of increasing importance because they absorb IR radiation in the spectral regions where the other gases do not. CO_2 , N_2O , and the chlorofluorocarbons are sufficiently long-lived to be

well mixed both vertically and horizontally throughout the troposphere, and therefore their abundance is best determined by a network of ground-based stations. The distribution of water vapor will be measured to varying degrees of accuracy by AMSU, AMSR, and LASA. AMSU will provide a coarse vertical profile, AMSR will provide a measure of total column density, and LASA will provide high vertical-resolution profiles and information on the height of the boundary layer to augment the AMSU and AMSR measurements. The measurement of tropospheric O_3 from satellites will probably remain difficult, but measurements of the total column density by Global Ozone Monitoring Radiometer (GOMR) and of stratospheric profiles by IR Radiometer (IR-RAD), Microwave Limb Sounder (MLS), Submillimeter Spectrometer (SUB-MM), Cryogenic Interferometer Spectrometer (CIS), and GOMR will be of value in augmenting ground-based measurements. LASA may provide a direct measurement capability. CH_4 distributions will be measured by the combination of ground-based sampling and the Correlation Radiometer (CR) and Nadir Climate Interferometer Spectrometer (NCIS) instruments on Eos.

Sensible Heat Flux

The flux of sensible heat from the surface to the atmosphere depends on the surface temperature, the temperature of the atmospheric boundary layer, and the intensity of turbulent motion or convection in the boundary layer. The determination of surface temperature is discussed above. The direct measurement of boundary-layer properties from space is difficult because the vertical extent of the boundary layer is often smaller than the vertical resolution of the remote sensing technique. Consequently, when this is the case, boundary-layer properties must be inferred from the available suite of remote measurements, augmented by surface measurements where possible. A key variable is the height of the boundary layer; LASA will provide the first remote measurements of this variable on a global basis. Another important set of variables is the boundary temperatures which can be modeled from knowledge of the surface temperature and the average temperature over the lowest resolvable layer of the atmosphere.

Determination of the intensity of turbulent motion or convection in the boundary layer can also be inferred given a knowledge of the wind at the top of the boundary layer, the surface roughness, and the static stability of the boundary layer. The wind speed at the top of the boundary layer can be estimated from wind and temperature observations from Eos and geosynchronous satellites. Over the oceans, radar scatterometers and altimeters (SCATT and ALT within the Eos payload) provide measurements of sea surface wind speed. These surface winds can be used in combination with the lowest-layer winds measured by LAWS on Eos, with extratropical winds

calculated from atmospheric temperature soundings by AMSU and HIRS using the thermal wind equation, and with cloud track winds from geosynchronous images to determine the wind speed at the top of the boundary layer. The surface roughness over land can be estimated from Eos SAR images; over water the surface roughness is directly measured by SCATT and ALT to determine sea surface wind speed. A general indication of the static stability of the boundary layer can be inferred from the general meteorological conditions as observed in the satellite images from both Eos and geosynchronous instruments and from the wind speeds.

Latent Heat Flux

The loss of latent heat from the surface through evaporation and transpiration is the key variable shared by the energy and water cycles. Discussion of the strategy for determination of latent heat flux is given in the following section dealing with the water cycle. In addition to the consideration of latent heat flux at the Earth's surface, there is substantial exchange between latent and sensible heat within the atmosphere through the condensation of water vapor to form liquid and solid hydrometeors and their re-evaporation. Eos will provide some sampling of this energy exchange process as well. AMSR will measure the total column density of water vapor, liquid water, and the ice content of clouds. AMSU will provide soundings of water vapor, as will LASA. AMSR will also measure the rate of precipitation. Although Eos orbital characteristics will not permit these observations to be made over the lifetime of a storm, their instantaneous measurement should provide new insight into this element of the atmospheric energy cycle. Table 6 summarizes the observations required to study the energy balance at the Earth's surface and the Eos instruments and other measurements that will be used in this study.

THE BLUE PLANET

Introduction

Water in its three phases dominates the processes that control the planetary environment. The hydrologic cycle determines the distribution of water on the planet and, through phase changes from ice to liquid to gas, plays an important role in the planetary energy balance. For example, at the ocean surface, evaporation not only creates a moisture flux to the atmosphere, but also cools the ocean. In the atmosphere, condensation releases heat, which warms the atmosphere and contributes to vertical motions and the intensification of storms. In the polar regions, the heat released in freezing and absorbed in melting buffers the seasonal temperature extremes.

Furthermore, the patterns of evaporation and precipitation determine the sea surface distribution of salinity, which in part determines the circulation patterns of surface and intermediate waters. The moisture distribution in the atmosphere and the distribution of evapotranspiration at the surface help determine the development of weather systems and the patterns of precipitation over both land and ocean.

The global hydrologic cycle consists of the reservoirs of water including the oceans, snow, ice, lakes, rivers, ground water, aquifers, clouds, and atmospheric water vapor, and the fluxes between them (Figure 13). The time scales involved vary widely. Water vapor has an average atmospheric residence time of about 10 days, and the residence time of water in rivers is similar. In lakes, water typically resides for tens of years; while in deep aquifers and glaciers the time scale is centuries. The residence time in the oceans varies from 10 to 1,500 years. As with other aspects of the Earth system, there are elements that are essentially governed by the virtually instantaneous local situation and other components that respond to the long-term average of globally controlled conditions.

At the planetary scale, the total annual global evaporation and precipitation is equivalent to a water volume of 517,000 km³. The oceanic evaporation is equivalent to a global sea level change of 1 m per year. Of the total precipitation, about 400,000 km³, or 78 percent, falls over the ocean. Of the remaining 120,000 km³ that falls on land, 64 percent evaporates immediately, and 28,000 km³ goes to runoff, leaving just 12,000 km³ available for global freshwater storage, which is roughly 100 times the total annual U.S. water consumption.

Much of civilization is based on the availability of freshwater, which in turn depends on the patterns of precipitation, soil and vegetation, and the topographic routing of water flow. All of these are subject to change caused by shifts in the energy cycle and by human action. All of them also influence and respond to the water cycle itself through alteration in the processes of evapotranspiration, erosion, and life. To understand and predict even local conditions on time scales of more than a few days requires a global knowledge of the hydrologic cycle and its ties to geologic, energetic, and biological processes.

The Eos instruments will provide improved global determination of the fluxes of the hydrologic cycle and measurements of important properties of the various reservoirs. Among the fluxes, Eos will make a major contribution to quantifying evaporation and the global distribution of precipitation. For the storage areas, Eos will measure soil moisture; snowpack extent and water equivalent; glacier and ice cap properties; the global distribution of the different types of soil, rocks, and vegetation; the topography of river basins; and the varying extent and nature of wetlands.

Table 6. Eos Instruments for Determining Energy Fluxes at the Earth's Surface

Radiative Energy Input	
Direct Measurements	
Solar flux at top of atmosphere	SCM, SUSIM
Cloud cover	MODIS, VAS*
Aerosols	MODIS, LASA
Surface albedo	MODIS, HIRIS, AMRIR
Indirect Measurements to Determine Energy Transmitted Through Clouds	
Cloud temperature and height	MODIS, LASA, VAS*
Cloud total liquid and ice content	AMSR
Cloud vertical extent and number of layers	AMSU, AMRIR, MODIS, VAS*
Radiative Energy Lost from Surface	
Surface temperature	MODIS, AMSU, AMSR, AMRIR, TIMS, VAS*
Surface emissivity	MODIS, AMSU, AMSR
Fractional sea ice	AMSR, SAR
Greenhouse gases	
CO ₂	Ground-based monitoring
Water vapor	AMSU, AMSR, LASA, MODIS, VAS*
Ozone	GOMR, IR-Rad, MLS, SUB-MM, CIS
CH ₄ (troposphere)	NCIS, CR (maybe)
CH ₄ , N ₂ O, chlorofluorocarbons (stratosphere)	IR-Rad, SUB-MM, CIS, GOMR
Sensible Heat Flux	
Direct Measurements	(See above)
Indirect Measurements	
Temperature of atmospheric boundary layer based on boundary layer height	LASA
Tropospheric temperature profile	MODIS, AMSU, VAS*, LASA
Intensity of convection in boundary layer based on:	
Wind at top of boundary layer	LAWS, VAS*, cloud track winds*, atmospheric temperature
Surface winds (ocean)	SCATT, ALT
Surface roughness: land	SAR
ocean	SCATT, ALT
Latent Heat Flux	
Direct Measurements	
Atmospheric water vapor	(See above)
Atmospheric liquid water and ice	AMSR
Indirect Measurements	
Ocean surface evaporation	AMSR, AMSU, MODIS, AMRIR
Land surface evaporation	HIRIS, MODIS, SAR, ESTAR, TIMS

*Geostationary platform instruments

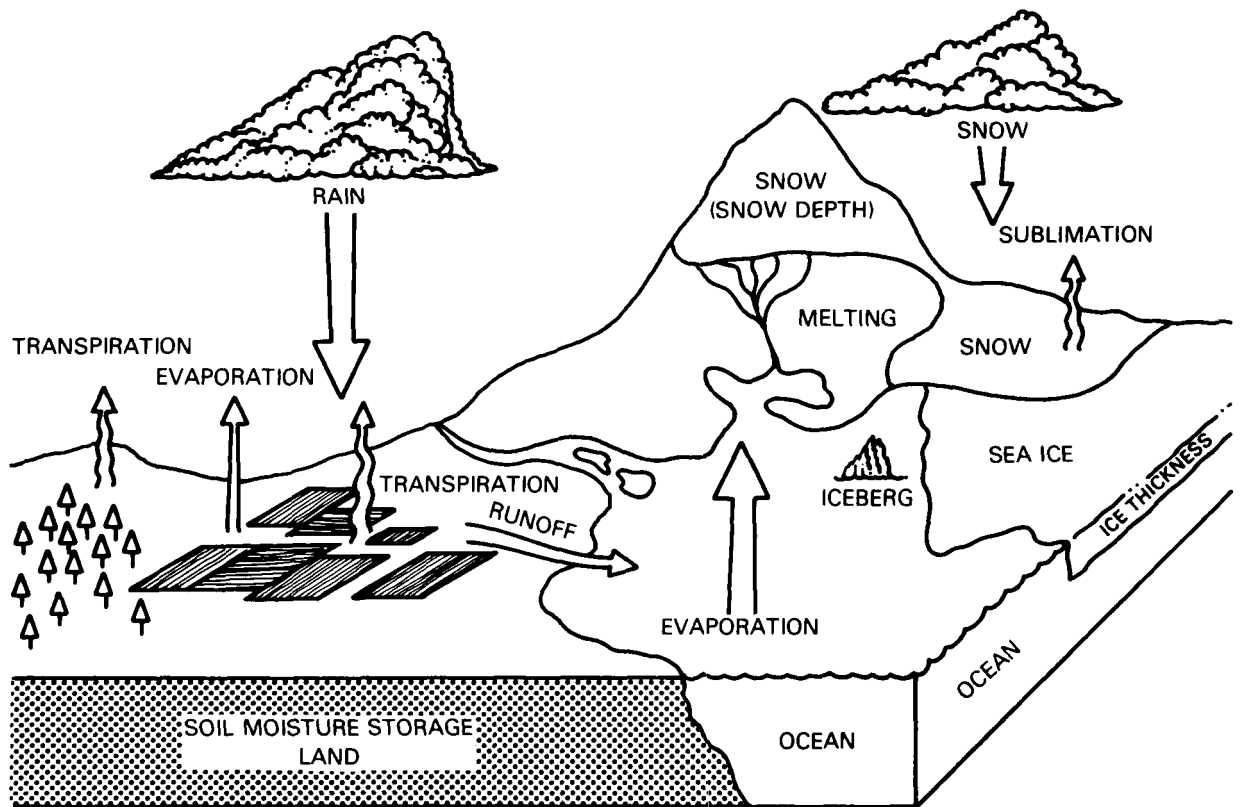


Figure 13. Important processes in the hydrologic cycle (adapted from Smagorinsky, 1982).

The Role of Eos

In the 1985 report (NRC, 1985) of the Space Science Board's Committee on Earth Science dealing with a strategy for Earth science from space in the 1985-2000 timeframe, the highest-priority measurement objective for the freshwater component of the hydrologic cycle is (in part):

"To measure the spatial distribution of runoff, soil moisture, precipitation and evapotranspiration over the Earth."

The primary objective for the study of the world's snow cover from space is:

"To measure its horizontal extent, depth, density, liquid water content, and albedo"

Eos can meet significant portions of these and other CES measurement objectives through the provision of new measurement techniques, primarily microwave, for the study of the surface and atmospheric components of the hydrologic cycle. In particular, Eos will provide better measurements from which to calculate evaporative fluxes over the oceans and evapotranspiration over land. It will also, for the first time, provide direct observations of surface soil moisture at 10 km resolution. The critical

Eos instruments for determination of the evaporative fluxes and the soil moisture will be the Electronically Scanned Thinned Array Radiometer (ESTAR), which will estimate soil moisture in the upper few centimeters of soil at 10 km resolution; the SAR, which will measure surface soil moisture and standing water at higher resolution of 30 to 500 m; and the AMSR, which will measure oceanic surface properties, the water-equivalent of snowpack, atmospheric water vapor, and precipitation. This section will describe some of the uses of these and other instruments in the study of the hydrologic cycle.

The Land

Evapotranspiration and Soil Moisture

Evapotranspiration is the combined loss of water through the process of evaporation and transpiration (Figure 14). Evaporation occurs from water surfaces and bare soil, while transpiration occurs from the canopy cover. The crucial role of evapotranspiration at regional or global hydrologic scales is only now becoming understood; we now know, for instance, that precipitation is sensitive to changes in regional evapotranspiration and soil moisture.

At least two methods exist for the estimation of evapotranspiration: (1) a modified Priestly-Taylor

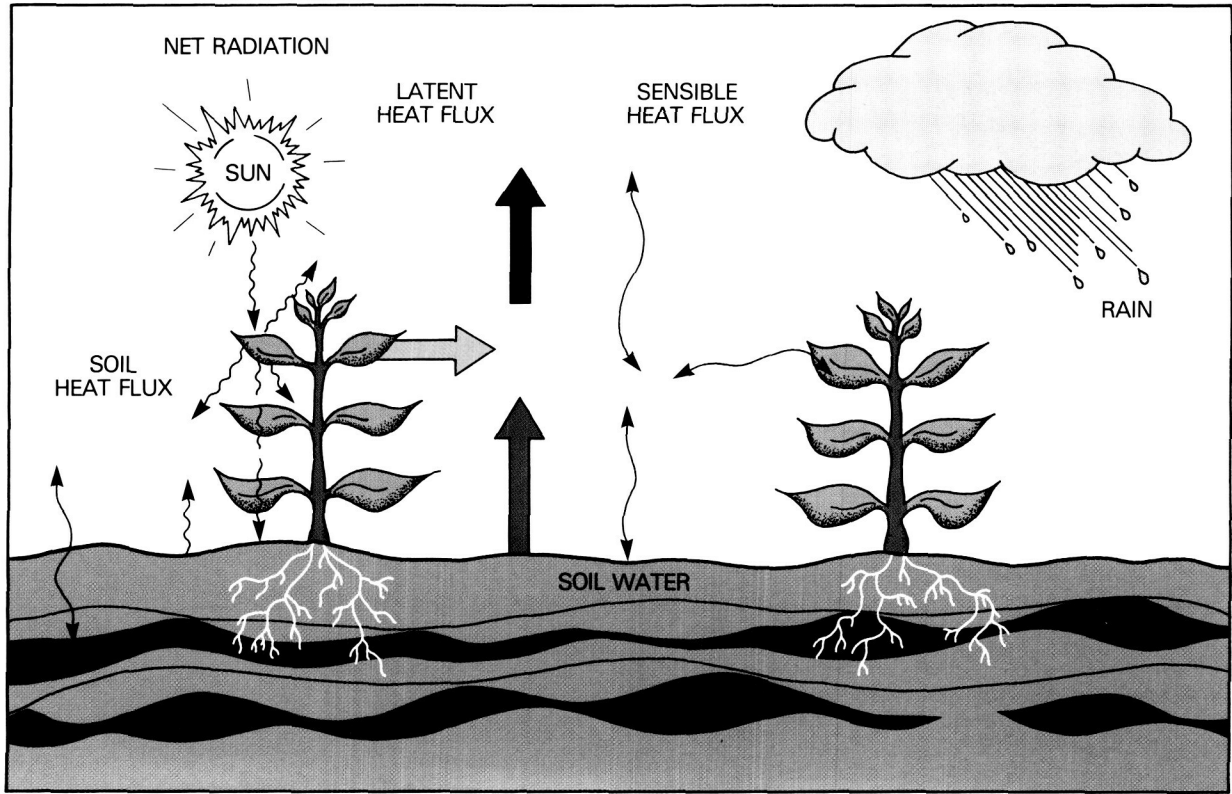


Figure 14. Canopy model showing components of heat, radiation, and moisture balance at the soil surface.

method that depends on surface radiation balance, and (2) a thermal-inertia-moisture availability method (here referred to as the TIMA method) that is based on day-night surface temperature differences and soil-plant-atmosphere models.

The Priestly-Taylor method assumes that an energy balance exists at the soil surface and then derives the potential evapotranspiration as proportional to the difference between the incident net radiation and the heat conducted into the soil. This equation can be modified to provide separate estimates of the evaporation and transpiration components of the evapotranspiration. This separation is particularly important when vegetation cover is sparse and much soil is exposed. The capability of ESTAR is essential to this separation of soil evaporation and transpiration because it provides the only direct, wide-area measurement of the surface soil moisture condition.

The variables in the Priestly-Taylor technique will be provided by the following observations. First, the net radiation can be determined from a combination of the following measurements: solar radiation from GOES, albedo from MODIS or HIRIS, sky radiation emission from a thermal radiation model that uses temperature and water vapor soundings from one of the profilers on Eos and/or geosynchronous satellites, and surface radiation emission

from surface temperature measurements with MODIS, TIMS, and GOES. Second, the soil heat conduction flux can be estimated empirically from hourly changes in surface temperature measured from geostationary satellites. Although soil heat flux usually is negligible on a daily basis, it is mainly daytime soil heat fluxes that affect evapotranspiration, so hourly surface temperature measurements from GOES can improve water availability estimates.

Eos is of additional use on the output side. As stated, the Priestly-Taylor method provides an estimate of the potential evapotranspiration (the amount of water flux that might occur); the actual transpiration is a function of the proportion of the surface that is covered with vegetation and the soil moisture, or saturation ratio, which varies from zero for a dry soil surface to unity for saturated soil. The saturation ratio will be measured by ESTAR on Eos at 10-kilometer spatial resolution.

In addition to direct measurement by ESTAR, if the soil type is known, the saturation ratio can be estimated from precipitation data and the square-root of time drying relation for the particular soil. If the soil is visible from space, HIRIS data will measure its geochemical composition. The structure of the soil can be measured *in situ* or inferred from the remotely observed response of the soil to wetting and heating.

An alternative method for estimating water availability is the thermal-inertia-moisture-availability (TIMA) method which is more complicated than the Priestly-Taylor method. The TIMA method combines simplified versions of an atmospheric planetary boundary-layer model, a land surface-layer model, a vegetation model, and a subsurface soil model. Each of these models is parameterized in terms of soil moisture and thermal inertia. If the soil type is known and sounding measurements are available to provide air temperature data, water vapor content, and wind speed above the planetary boundary layer, then evapotranspiration may be estimated.

Use of this technique will also be improved through direct measurement of soil moisture, and from improved observations of the planetary boundary layer through advanced temperature and moisture sounders such as LASA. Of these variables, soil moisture and surface temperature could be measured directly using microwave and thermal infrared data from ESTAR and MODIS, respectively. Visible and near-infrared reflectance measurements from MODIS and HIRIS will also be used to estimate vegetation type and photosynthesis rate, from which the stomatal resistance can be estimated. SAR may also give an indication of canopy state and data on soil and canopy moisture.

Soil moisture plays a critical role in plant productivity, water storage, and the determination of evapotranspiration from land. The soil water also alters the heat capacity and thermal conductivity of the soil, and the evaporation of this water cools the soil and buffers its temperature extremes.

From the perspective of storage and its effect upon vegetation and, hence, climate, it is surprising that we know so little about the global distribution of soil moisture. Currently, there are few measurements of changes in soil moisture because of spatial variation and the difficulties of conventional sampling. With Eos it will be possible using the ESTAR and subsampling with the SAR to determine soil moisture in regions of low vegetative density. Through use of MODIS and subsampling with HIRIS in areas of dense vegetation cover, soil moisture will be estimated from spectral characteristics of the canopy.

In addition to direct observation of surface soil moisture, an alternative approach is based upon the measurement of the diurnal surface temperature variations. Because the heat capacity and thermal conductivity of water are very different from those of dry soil, soil moisture can be estimated from the modulation of the diurnal surface temperature signal. This estimate may be obtained by calibrating a coupled energy and mass balance model of the upper soil using thermal infrared data from MODIS, and in certain areas from TIMS.

There are still some undetermined values—surface wind speed, aerodynamic resistance, and

humidity. Currently, these cannot be obtained from Eos instruments over land, but aerodynamic resistance can be roughly estimated from land cover classification. Surface wind speed and humidity may be extrapolated from the overall satellite soundings using approximate relationships determined by inter-comparison of space- and ground-based observations at a limited set of specific sites.

The root zone soil moisture and evapotranspiration parameters should be treated together because the microwave-observable surface soil moisture is not sufficient to satisfy all requirements and because the depth of the root zone is larger than the sampling depth of the ESTAR or SAR. Evapotranspiration is the major depletion mechanism for the root-zone soil moisture reservoir. Thus, determination of one leads to the estimation of the other.

In summary, through use of the Eos-derived data, specific *in situ* investigations, and what we know about the physics of the system, we shall be able to determine the global yet geographically specific and time-varying pattern of evapotranspiration. This will provide an important atmospheric boundary condition, as well as a perspective on the Earth never before available.

Snow

Accurate observations of the areal extent and albedo of snow are needed to determine the planetary radiation budget.

Snow areal extent is easily measured using MODIS. In addition to the visible bands, the middle infrared bands of MODIS are necessary to discriminate snow cover from low, cold clouds. Observations every few days are necessary because of the dynamic nature of the phenomenon and will help quantify the amount of snow added by each storm. The thermal MODIS bands can also be used to determine the surface temperature of the snowpack and estimate the extent to which the snow is melting. Visible and near-infrared data may be used to estimate the albedo, which varies by nearly a factor of two among different snowpacks, depending on their age and structure.

Given information about the snowpack age and structure and geographical location, the depth and water-equivalence of the snowpack can be estimated using multifrequency passive microwave emission data from AMSR. Because of the uncertainty introduced by major variation in snow properties within mountainous terrain, these passive microwave measurements alone will not be sufficient to characterize the snowpack. SAR will offer some improvement, particularly for snow water equivalence, because of its high spatial resolution. In these regions, additional surface measurements of snow depth and density will be necessary to model the extent and character of the global snowpack.

The Oceans

The oceans cover about 70 percent of the Earth's surface, with an average depth of 4 km. Of this depth, about 1 m per year is evaporated away and replaced by precipitation and runoff. Because of the vast extent of the ocean, and the small number of meteorologic stations scattered among islands and on ships, Eos will play a major role in the improvement of global estimates of oceanic evaporation. The following discusses how ocean evaporation is currently determined, and how Eos will provide improvements over the present technique. Other roles of Eos in probing other aspects of the ocean are discussed in the next section and in Chapter IV.

Evaporation

Air-sea interaction processes couple the atmosphere and ocean; this coupling determines the state and evolution of the atmosphere-ocean system. The critical exchanges across the interface include heat, moisture, and momentum. The heat fluxes, which include sensible, latent, and radiative fluxes, moderate the global climate; the moisture flux drives the hydrologic cycle, where the moisture given up by the ocean is deposited in part as precipitation on land; and the momentum flux from the wind to the ocean surface generates ocean surface currents and wind-waves. As the El Niño discussion in the Air-Sea Interactions section in Chapter IV shows, small changes in these fluxes can yield planetary-scale changes in weather.

Figure 15 shows in schematic form the processes that transfer heat, water vapor, and momentum between the ocean and atmosphere. The interfacial heat exchange has four major components: the incident solar radiation, the outgoing longwave radiation, the evaporation or latent heat flux, and the sensible heat flux. Over most of the oceans, and particularly over the tropical oceans, shortwave radiation and latent heat flux are much larger in magnitude than the others and have the greatest variability. The interaction of these fluxes with the ocean determines the oceanic heat storage. The momentum flux generates the ocean surface currents and the ocean wind-waves. Finally, the water vapor transfer into the atmosphere plays a critical role in the global hydrologic cycle.

The moisture flux from the ocean to the atmosphere both cools the ocean and supplies water vapor to the atmosphere; the net exchange determines, in part, the upper ocean stratification and the resulting circulation. The reason the moisture flux occurs is that immediately above the ocean surface, the air in contact with the water is fully saturated with water vapor. If at a height a few meters above the surface, however, the air is subsaturated, the vertical moisture flux occurs that causes evaporation and cools the ocean. Because of turbulent moisture

transfer, the transfer rate increases with the wind speed and is also a function of ocean wave height.

The classic modeling of these fluxes rests primarily on shipboard or island station observations. For instance, the present determination of the water vapor flux from these observations uses a bulk formula that depends on surface wind speed, the saturation humidity given as a function of the sea surface temperature, and the surface humidity. The latent heat flux is then the product of the moisture flux and the latent heat of evaporation. Because regular shipboard observations are limited to the great circle routes between the continents, there are large gaps in our data base, particularly in the equatorial Pacific. These gaps are just beginning to be filled by satellite observations, but difficulties still remain. For example, using the conventional bulk parameterization methods to determine moisture flux requires measurements of sea surface temperature, surface-level wind speed, and specific humidity, the sea state, and the vertical boundary layer stability. The stability further requires knowledge of the air temperature at some fixed height above the sea surface, the surface temperature, and the specific atmospheric humidity. For completeness, precipitation rates are also required.

Eos provides two methods for improvement of the accuracy and the temporal resolution of the moisture flux. First, Eos will allow the direct measurement of the specific humidity in the atmospheric boundary layer through the capabilities of the new sounders such as AMSU or LASA. The present Tiros Operational Vertical Sounder (TOVS) resolves the lowest-level humidity in the layer 1,000 to 700 mb. The AMSU and/or the LASA should provide the capability to reliably infer the humidity in the atmospheric boundary layer.

In addition to an improved measure of the surface humidity, Eos will also provide for improved measurements of sea surface temperature (SST) and winds. MODIS, for example, will provide a better spectral and spatial resolution of sea surface temperature. The improved SCATT on Eos will directly measure sea surface wind velocities. The combination of these measurements with the improved humidity measurement suggests that Eos will provide estimates of the moisture flux out of the ocean and measurements of the precipitation return at an improved time and space scale compared to present measurements.

Second, Eos will permit direct measurement of the moisture flux through AMSR. This capability has already been demonstrated using Scanning Multifrequency Microwave Radiometer (SMMR) data. With the proper choice of microwave frequencies, AMSR would eliminate the errors introduced through use of bulk formulas and in the retrieval of intermediate parameters such as SST, wind speed, and precipitable water. Although no spaceborne sensor scheduled for the near future would provide the

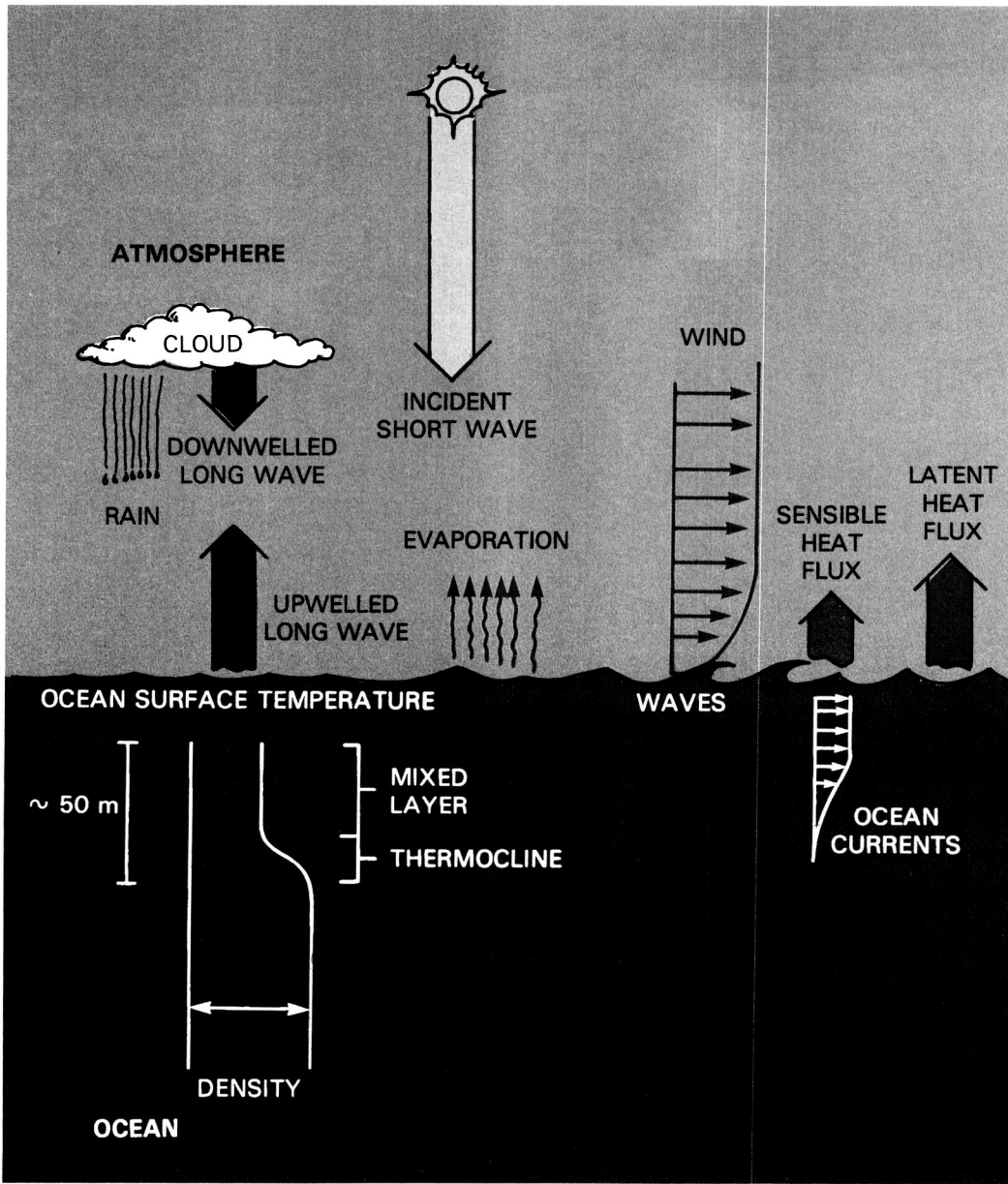


Figure 15. Schematic diagram of the air-sea interaction processes in the equatorial Pacific.

whole set of optimal frequencies, AMSR on Eos will provide the first opportunity to measure the necessary radiances at compatible coverage and resolutions.

The Atmosphere

Water Vapor and Rainfall

The transport of water from the oceans to the land depends entirely on water vapor distributions in the atmosphere and precipitation. A detailed quantitative understanding of how water vapor concentrates and condenses in clouds and where and how much it rains remains to be developed.

Measurements of water vapor as a crude function of altitude are now available from space, as are

extensive measurements of cloud extent and cloud-top temperature. Ground-based observations over land greatly augment this data for continental regions. To understand the role of the atmosphere in the global hydrologic cycle, these measurements must be extended. The vertical resolution of atmospheric moisture measurements must be increased. Clouds often occur in multiple layers and current space techniques only characterize the uppermost surface. Instruments are needed that can see through gaps in the upper layers and characterize the total column content of liquid water and water vapor.

The flight of the AMSU, beginning on the NOAA-K satellite and continuing into the Eos era, will improve the vertical resolution of atmospheric temperature and moisture sounding under both

cloud-free and cloudy conditions. The improved spatial resolution of the MODIS infrared sounding and thermal measurement channels will permit observations of lower cloud layers and high vertical-resolution temperature sounding to the ground through smaller cloud gaps. The AMSU, AMSR, and LASA will permit the characterization of total column content of liquid water and water vapor. LASA and perhaps other laser instruments will directly determine the height of cloud layers and LASA will be able to measure cloud-top temperature and pressure precisely.

For the hydrologic cycle, the integrated amount of rain that falls over a time period is the key parameter—not the instantaneous rate of rainfall. Rain gauge networks provide this data over much of the inhabited land area of the globe, but given the extreme heterogeneity of rainfall, the networks must be quite dense to provide accurate local or regional observations. Ground-based rain radars are beginning to improve this situation, but a truly global coverage system is unattainable without space measurements. Quantitative observation of global rainfall represents one of the severest challenges to both remote sensing and *in situ* measurements. The methods for measuring rain from low Earth orbit are as yet unproven, but the theoretical foundation for the technique has been laid and initial suborbital tests of the concept are under way.

The Eos strategy for obtaining global measurements of rainfall involves making use of the polar platform instrumentation, geostationary satellite capabilities, and a low-inclination orbiting payload known as the Tropical Rainfall Explorer Mission (TREM).

The first element is the ability of passive microwave instruments, specifically AMSR, to measure the integrated rain rate in an atmospheric column.

Rainfall may be estimated using AMSR passive microwave observations in several ways. Over ocean areas, the rainfall in an atmospheric column can be easily established because the emission from raindrops is large compared with the emission from the ocean background. Over land areas, the interpretation of microwave emission data is more difficult because the emission from the land is not small compared with that of raindrops, and the land background signal varies spatially. Some assumptions about the height of the freezing layer over land and of the droplet size distribution are needed to effectively determine rain rates. A spaceborne rain radar could prove helpful in refining rainfall algorithms.

Flight of AMSR on Eos will provide the only global measurements of rain rate; however, only about 60 percent of the atmosphere is covered every 12 hours and the measurement is only a snapshot of how much rain is falling at the time the platform flies over the storm. For a typical rainstorm this snapshot is a measure of the integrated rainfall for a

10-minute period (i.e., the time it will take the rain at the top of the atmospheric column to reach the ground). A second shortcoming of the Eos measurements is that the platform always comes over a site at the same time of day or night, and the sampling is thus systematically convoluted with the diurnal variation in rainfall, which is unknown. Flight of AMSR on both morning and afternoon platforms will help alleviate this problem, but this alone is not sufficient.

The second element of the rainfall observing strategy is the TREM. TREM will carry a passive microwave instrument, a rain radar, and a visible and infrared cloud imager similar to the AVHRR or geostationary VISSR. The passive microwave device will function in essentially the same way as AMSR, and assuming that the TREM mission and Eos are in orbit at the same time, the AMSR can be cross-calibrated with the TREM device during times when an Eos platform is over-flying the TREM. The radar on TREM will directly measure the height of the rainfall within the clouds and below, and offers an alternative measurement of rain rate that is range resolved. This technique is essentially similar to ground-based weather radars. The TREM will suffer from the same instantaneous sampling deficiencies as AMSR on Eos, but the TREM payload will be flown in a low-inclination orbit (i.e., 28.5°) and its samples of rainfall will not be aliased by the diurnal cycle. The combination of one or two AMSRs on Eos polar platforms and the TREM payload will provide the needed intense sampling of global rainfall.

The third element of the strategy addresses the fact that both Eos and TREM will only sample instantaneous rainfall amounts. Some rough indication of the intensity of rainfall is currently inferred from infrared and visible images of cloud-top conditions. These observations are currently available from the various geostationary meteorological satellites such as GOES. The geostationary observations have the advantage that they can monitor cloud conditions throughout the life of a storm. The direct rainfall measurements of Eos and TREM can be compared with visible/infrared imagery available on both missions and the geostationary satellites. This comparison can be used to build a statistical basis for inferring the amount of rainfall produced by different cloud conditions in different regions and meteorologic situations. The geostationary observations will then become useful as a quantitative extension of the low-altitude observations through the life of the storm.

An additional element in the set of techniques for determining integrated rainfall will be the use of ESTAR and SAR on Eos to measure surface soil moisture. Under many circumstances a frequent sampling of surface soil moisture will provide a good indication of the integrated precipitation that has fallen on a given area during the previous 12 to 36 hours. Where drainage patterns are understood, the

extent of wetlands and the size of lakes measured by SAR will also give an indication of antecedent precipitation.

The combination of the probability distribution over the diurnal cycle from TREM, continuous geostationary data, and the global Eos data will lead to a significant quantitative knowledge of global precipitation.

Summary

Eos will permit the determination of many of the factors in the hydrologic cycle to an improved accuracy. These include the evaporation from land and ocean, the distribution of atmospheric water vapor over the ocean, and improvement in our knowledge about the precipitation rates, especially over the ocean and over uninstrumented land regions.

Eos will permit determination of evaporation and transpiration from land, and these observations will allow improved characterization of the land, its topography, rock, soil, and vegetation characteristics, and the properties of its wetlands. By its determination of the soil characteristics, the topography of river basins, and the extent of wetlands, Eos will add greatly to our understanding of the land component of the water cycle.

The improved observations of the patterns of oceanic evaporation will permit a greatly improved accounting of this critical source term in the hydrologic cycle, as well as the critical latent heat flux. The combination of these improved heat and mass flux measurements should yield improved precipitation and weather forecasts for both the ocean and the adjacent land areas.

In sum, with the measurement capabilities provided by Eos we should begin to unravel the global hydrologic cycle. Table 7 summarizes the observations required to study the elements of the Earth's hydrologic cycle and the Eos instruments and other measurements that will be used in this study.

THE GREEN PLANET

As life has evolved over the last 3.5 billion years, biological processes have fundamentally modified the chemistry of the Earth's hydrosphere, lithosphere, and atmosphere. Early life forms developed oxygenic photosynthesis and thus created an oxygen-rich atmosphere that was hospitable to evolution of land plants, animals, and finally, humans. Now human activities appear to have the potential for further planetary change. We have altered the structure of vegetation and soils, shifted chemical resources, consumed large amounts of fossil fuels, and produced new combinations of organic and inorganic compounds. These alterations affect the Earth's biota by favoring one set of organisms over another and thus producing subse-

quent changes in the structure of major terrestrial biomes. Major alterations in the function of terrestrial biomes affect both the type and growth rate of vegetation. Ultimately, through modifications in energy, water, and material transport, such shifts in the functions of terrestrial ecosystems induce changes in the climate of the globe and the chemistry of the atmosphere and oceans.

The geologic record provides evidence of other biogenic changes in past epochs. In a temporal sense, however, the influence of humans is fundamentally different from other factors that have shaped the Earth; the rates of change tend to be far greater than those of other evolutionary processes.

In particular, human activity is sending measurable transients through the biogeochemical cycles of the planet—the Earth's metabolic system. Since even the most rapid processes of adjustment among the various chemical reservoirs take decades, new equilibria are far from being established. In a sense, therefore, these human-induced perturbations and the Earth system's subsequent responses constitute a potentially valuable class of ongoing metabolic experiments at the global level. If the right questions are asked and the appropriate data of sufficient accuracy are collected in a timely fashion, these experiments hold the promise of providing major new insights into the basic processes that support life on this planet.

The following are key questions concerning the planet's primary biogeochemical cycles drawn in large part from the report of the Committee on Earth Science of the Space Science Board (NRC, 1985).

- *Sulfur*—It is known from a comparison of the natural and anthropogenic fluxes of sulfur that the total amount of sulfur entering the atmosphere has doubled owing to human activity, but it is not known yet what the impact will be. What are the effects of increased levels of sulfate in precipitation? How do the effects vary? What is the role of sulfur in upland and tropical soils? Are these soils a source or sink for trace sulfur gases?
- *Phosphorus*—What are the mechanisms controlling availability of phosphorus in terrestrial soils, and how do these mechanisms respond to perturbations such as acid precipitation, fire, or deforestation? What is the flux of riverine phosphorus to the oceans; how has it changed in the past; how is it changing today? What are the consequences of these changes?
- *Nitrogen*—What is the magnitude of the nitrogen fixation rate in major biomes? How much of this fixation is determined by natural processes unaffected by man, and how much is under advertent or inadvertent control of

Table 7. Eos Instruments for Determining Elements of the Global Hydrologic Cycle

Land	
Evapotranspiration and Soil Moisture	
Priestly-Taylor technique	
Radiative energy input	See Table 6
Radiative energy lost from surface	See Table 6
Soil heat conduction flux (based on hourly surface temperature)	VAS*
Soil saturation ratio	ESTAR
Soil type	HIRIS
TIMA Method	
Soil moisture	ESTAR, SAR, MODIS, TIMS
Surface temperature	See Table 6
Vegetation type, photosynthesis rate	MODIS, HIRIS, SAR
Canopy state	SAR, MODIS, HIRIS
Inferred Parameters	
Surface wind speed, aerodynamic resistance, humidity, root zone soil moisture	Determined from land cover classification and site-specific satellite/ground comparisons
Snow	
Areal extent	MODIS
Temperature	MODIS
Albedo	MODIS
Depth, water equivalence	AMSR, SAR (some <i>in situ</i> measurements needed in mountainous terrain)
Runoff	ADCLS
Ocean Evaporation	
Moisture flux (direct)	AMSR
Moisture flux (indirect)	
Specific humidity in boundary layer	AMSU, LASA
Sea surface temperature	MODIS
Sea surface wind speed	SCATT
Atmospheric Water Vapor and Rainfall	
Temperature sounding	MODIS, AMSU
Water vapor sounding	MODIS, AMSU
Total column content of liquid water and water vapor	AMSU, AMSR, LASA
Cloud height, temperature, pressure	LASA
Integrated column rain rate	AMSR
Tropical rain rate	TREM
Total rainfall	VAS*

*Geostationary satellite instrument

humans? How is the fixation rate changing? Are stores of nitrogen in major soil systems deteriorating? What effect does anthropogenic nitrogen have on rivers and coastal biomes? Have NO, NO₂, and N₂O emissions from combustion and agricultural soils enhanced global concentrations of these gases? If so, what effects may be expected on

other important species, such as tropospheric ozone?

- **Carbon**—Why is methane increasing in the atmosphere? What is the role of terrestrial vegetation in the carbon cycle? What is the rate of the oceanic uptake of CO₂? Is global CO changing? If so, why?

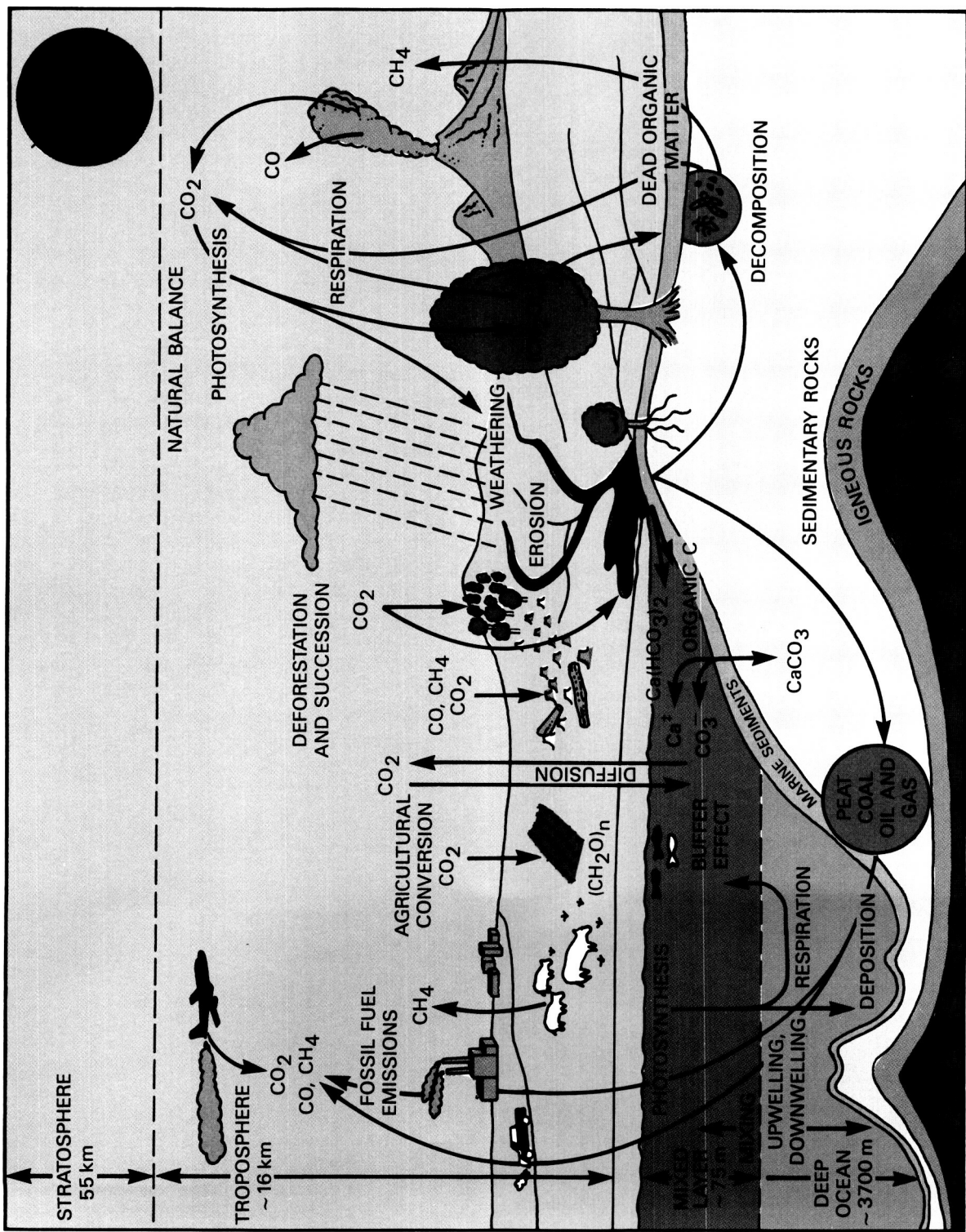


Figure 16. The carbon cycle.

For some of these questions Eos will be uniquely valuable; in others, our quest is more exploratory. In order to illustrate the measurement requirements that Eos should address in expanding our understanding of the Earth's metabolic system, we shall consider the carbon cycle (Figure 16) in detail.

The Carbon Cycle

There are four central biochemical processes in the carbon cycle: photosynthesis, autotrophic respiration, aerobic oxidation, and anaerobic oxidation. A positive difference between photosynthesis and autotrophic respiration defines the rate at which green plants accumulate carbon in the form of complex organic carbon compounds. The latter two processes, aerobic and anaerobic oxidation, are the route by which these complex organic carbon compounds are returned to simple inorganic states: CO, CO₂, CH₄. Increases in the rate of aerobic oxidation (including the abiotic processes of fossil fuel combustion) are the probable cause of the observed increases in atmospheric CO₂ and the potential increase in atmospheric CO; increases in the rate of anaerobic oxidation may be the cause of the observed buildup of CH₄.

Aerobic Oxidation

The human perturbations of the quasi-steady state cycle of carbon, created by burning fossil fuels, harvesting forests, and converting land to agriculture, are reflected most clearly by the phenomenon of the increasing concentration of atmospheric CO₂ (see Figure 17). If current trends of increasing CO₂ continue, by the year 2070 the atmospheric concentration will exceed 600 parts per million by volume (ppmv)—more than twice the pre-industrial level.

An increase in the amount of CO₂ will result in an even greater atmospheric retention of radiant heat

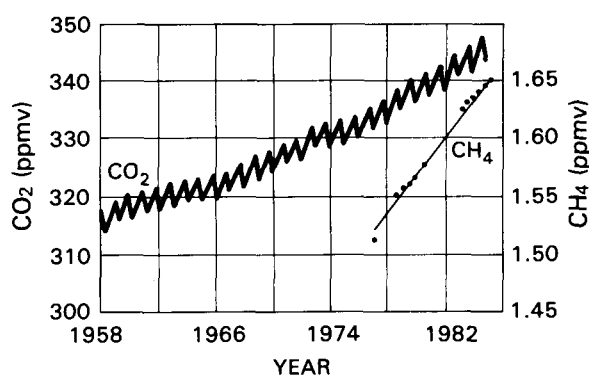


Figure 17. Observed increases in atmospheric carbon dioxide and methane, resulting in part from human activities.

from the sun and a higher equilibrium temperature for the Earth as a whole. If atmospheric concentrations of CO₂ rise to 600 ppmv, then the increase in temperature is expected to be important: 2 to 4°C for the entire Earth with an increase of approximately 10° at the poles. More important, rainfall patterns could be affected dramatically and thus could alter the global distribution of agriculture.

The relatively short lifetime of CO in the atmosphere makes the global picture for carbon monoxide more difficult to ascertain. Changes in the atmospheric concentration of CO would be important since CO is the primary control on the oxidation state of the atmosphere; furthermore, changes in atmospheric CO could reflect changes in terrestrial CH₄ emissions, which are discussed in subsequent sections.

At present, our ability to interpret the carbon cycle (Figure 16) and, thus, to predict future carbon dioxide concentrations in the atmosphere, is confounded by unresolved imbalances in the carbon budget. Simply stated, the annual budget (Table 8) does not balance, and other sinks—on land or in the oceans—must play a role. More specifically, the imbalance is diminished by reductions in the estimation of the rate of deforestation or increases in the regrowth, or if the oceanic uptake is underestimated, or if there are significant shorter-term natural variations in the concentration of carbon dioxide in the atmosphere that override the imbalances. The question of which combination of these possibilities is more likely is both important and fascinating.

Table 8. Annual Carbon Budget

Input of Carbon as Carbon Dioxide into Atmosphere	Flux*
Fossil Fuel:	5.0
Deforestation minus regrowth:	1.0
Total Input:	6.0
Uptake of Carbon Dioxide	
Atmospheric Increase:	2.5
Oceanic Uptake:	2.5
Fertilization Effects:	?
Total Uptake:	5.0

*Flux is given in units of 10⁹ metric tons per year or 10¹⁵ grams carbon per year.

The present average concentration of carbon dioxide in the atmosphere is about 346 parts per million, which is equivalent to about 740 billion metric tons (BMT). This is up from less than 600 BMT, which, based on ice core records, we believe was present in the atmosphere in the middle of the last century. Estimates of the amount of carbon in living organic matter on land vary between 450 and

600 BMT, and 1,000 to 1,500 BMT in the Earth's surface soils (see Figure 18).

The amount of carbon released globally from vegetation and soils as a result of deforestation remains uncertain, though much progress has been made in recent years. The difficulties in calculating this release center on two general but important factors: (1) the rate of land-use change, and (2) the response of biota to disturbances. It is surprising and frustrating that, even today, estimates of the current rate of conversion of closed-canopy tropical forests to agricultural land vary from 70,000 to 100,000 km² per year; the combined area of Massachusetts, New Hampshire, and Vermont is approximately 70,000 km². The biotic response to such disturbances has proven even more difficult to determine accurately.

Calculations of the net carbon loss from the global biotic inventory, which attempt to take into account the uncertainties concerning disturbance rates and biotic response, indicate that from 1860 to 1980 the total loss was between 100 and 200 BMT, which is roughly the amount of carbon dioxide that the combustion of fossil fuels has contributed. So over roughly the last 120 years as much CO₂ has come from deforestation as from fossil fuel combustion, though the present rates show that fossil fuel now is about three to five times more important (Figure 18). We should mention that this historical

estimate of about 150 BMT of carbon from deforestation is consistent with other calculations that use ratios of carbon isotopes, as found in ice cores and in tree rings, to infer how much CO₂ has come from deforestation; however, the temporal patterns from these two types of calculations do differ somewhat.

The oceans are by far the largest active reservoir of carbon. Recent estimates of the total amount of dissolved inorganic carbon establish an amount of about 38,000 BMT. Only a small fraction is carbon dioxide (0.5 percent); the bicarbonate ion, which makes up 90 percent, and the carbonate ion, at slightly less than 10 percent, are the major forms of dissolved inorganic carbon. There is far less dissolved organic carbon, about 1,000 BMT, and even less "particulate" organic carbon.

Although the oceans are the largest active reservoir of carbon and cover almost 70 percent of the globe, the total marine biomass contains only about 3 BMT of carbon, or just about 0.5 percent of the carbon stored in terrestrial vegetation. On the other hand, total primary production of marine organisms is 30 to 40 BMT per year, corresponding to 30 to 40 percent of the total primary production of terrestrial vegetation (Figure 18). However, only a relatively small portion of this production results in a sink for atmospheric carbon, primarily through the sinking

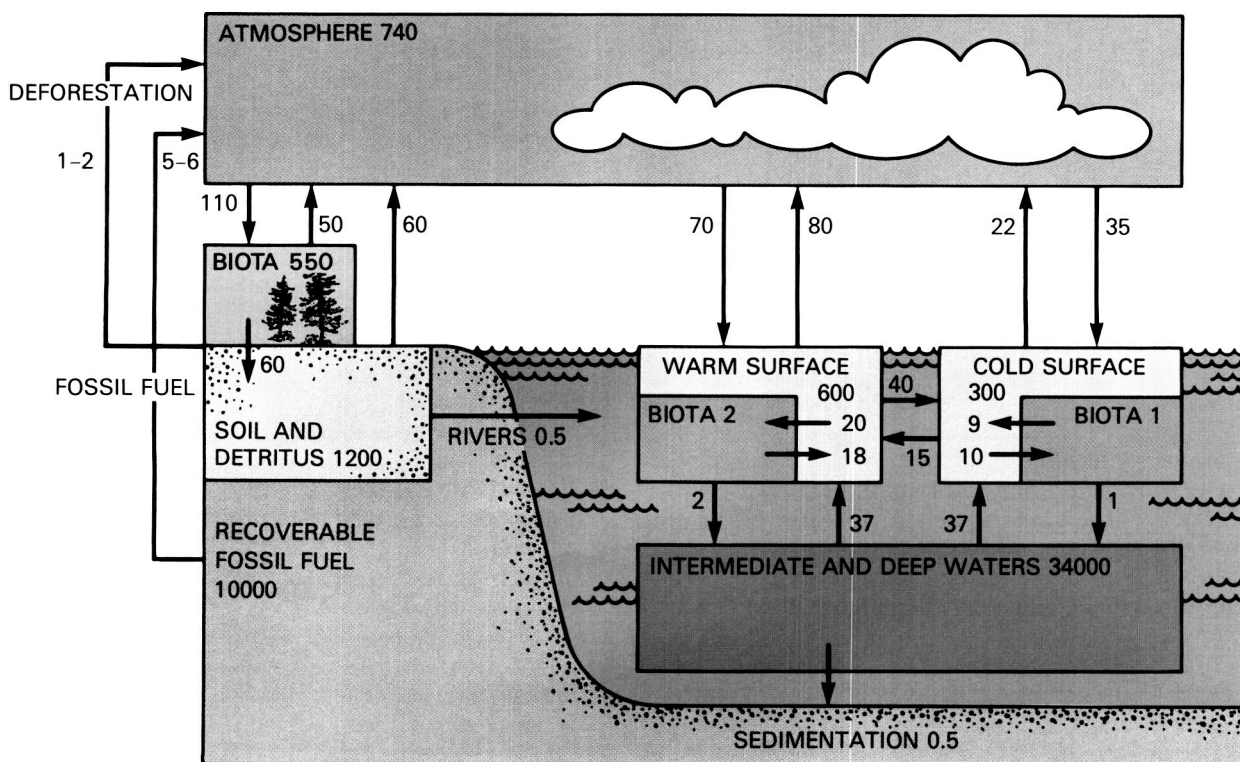


Figure 18. Schematic of seven-box model of the global carbon cycle, where fluxes are in units of 10^{15} g C yr⁻¹ and reservoirs 10^{15} g C.

of particulate organic carbon, which decomposes in deeper layers or is incorporated into sediments.

The net flux of atmospheric carbon dioxide into the oceans remains uncertain, although most current models suggest that between 40 and 50 percent of fossil fuel carbon dioxide is taken up by the oceans. If these calculations reflect actual oceanic uptake, then, as the imbalance implies, this result is inconsistent with the magnitude of the biospheric source for CO_2 estimated either directly from land clearing patterns or indirectly from tree ring and ice core records of carbon isotopes (Table 8). These issues are important and yet far from resolution.

The emissions of the biogenic and/or anthropogenic compounds CO , CH_4 , and higher hydrocarbons such as isoprene and terpenes, represent only a small fraction of the total carbon flux into the atmosphere. Nevertheless, these reduced carbon compounds play important roles in the chemical system that controls the levels of oxidizing species (OH , HO_2 , and O_3) in the atmosphere. Many of these compounds are also radiatively active and, thus, influence climate. And yet in comparison to our knowledge about CO_2 , the dynamical patterns that CO and CH_4 trace are even less well resolved.

Anaerobic Oxidation

As an alternate to aerobic oxidation, anaerobic oxidation provides another path back from complex organic carbon compounds to simple inorganic molecules. This path might be viewed as an “emergency” or “escape” route for the decomposition of complex molecules—a path to use when oxygen is not available. The anaerobic path tends to be less visible and somewhat more difficult to track because the planet is so oxygen rich. The sites for anaerobic oxidation tend to appear episodically or to be not often in full view, such as water-logged soils. In this route, the end carbon-product is methane, CH_4 , which is produced by microbes during the breakdown of organic material.

In addition to biogenic production, methane is produced during biomass burning (in the anaerobic zone of the fire) and also released to the atmosphere during the extraction of natural gas and coal.

Because the Earth has a strongly oxidizing atmosphere, the role of methane in the global carbon cycle is relatively minor from a bulk constituent viewpoint. The same holds true for CO . However, from the viewpoint of the Earth’s climate system and from the perspective of the chemical composition of the atmosphere, the role of methane is potentially crucial.

Methane, as mentioned, is a greenhouse gas, and molecule for molecule, it is 10,000 times more effective than CO_2 in blocking outgoing radiation. Furthermore, the photochemical oxidation of methane is an important source for CO . This is discussed more fully in the section on tropospheric chemistry in Chapter IV. The measured atmospheric

concentration of methane is increasing rapidly. in fact, during the last 10 years the rate of increase appears to have been more than 1 percent per year—more than twice as rapid as CO_2 .

At the present time we do not know what is causing this increase in CH_4 . It could be caused by either an increase in global biogenic CH_4 emissions or a decrease in global tropospheric OH levels (OH is the principal scavenger for CH_4), or a combination of both. Since OH is the single most important species involved in scavenging of both biogenic and anthropogenic species from the troposphere, a change in its concentration would have very significant consequences for future tropospheric composition and climate.

In order to gain an understanding of the changes in the biogeochemical cycles of the planet, the state of various components of the Earth system must be assessed. For instance, to understand the changing concentrations of atmospheric CO_2 , CO , or CH_4 , we need to understand the rates at which these compounds are being altered in the atmosphere, and, more important, to determine the rates of exchange between the atmosphere and biosphere and between the oceans and atmosphere. Obviously these exchanges will be governed in part by processes that are governed by other compounds and physical variables. Hence, diverse and extensive data sets will be required in order to understand these fluxes between components of the Earth system.

The Role of Eos

In 1986 the U.S. Committee for an International Geosphere-Biosphere Program (IGBP) of the National Research Council recommended a research program “to describe and understand the interactive physical, chemical, and biological processes that regulate the Earth’s unique environment for life, the changes that are occurring in this system, and the manner in which they are influenced by human actions” (NRC, 1986a). The issues associated with the global carbon cycle are, in a very real sense, canonical examples of the issues that confront the IGBP. Eos, initially through its data system and the associated modeling program and later during the expanded observational phase afforded by the polar platforms, will be critical to the successful execution of the IGBP.

To illustrate how Eos will help advance our understanding of the global carbon cycle, take a highly abstracted view by considering a simple box or budget model (Figure 18) of the Earth: an atmosphere, a warm and cold mixed layer of the ocean underlain by intermediate and deep layers, a box representing terrestrial vegetation, and finally one for detritus and soil carbon. Such models were popular devices in the early 1970s for exploring the global carbon cycle as expressed by the transfer of CO_2 . This simple construct has the major actors in the cycle and the important exchanges just discussed.

We have learned that such resolution is simply not sufficient to unravel the global carbon cycle. Today, geographically specific models of high dimension, models of terrestrial vegetation and detritus at 0.5° by 0.5° , models of ocean basin including the needed biotic and chemical interaction at 10° by 10° , and sub-basin scale models at far finer scales are all under development. However, the success of these models depends on the availability of greatly enriched data sets. Eos will provide much of this needed information.

Marine Biosphere-Ocean-Atmosphere Exchanges

Carbon dioxide exchanges between the atmosphere and the ocean surface are controlled by differences in partial pressure, $p(\text{CO}_2)$. Atmospheric $p(\text{CO}_2)$ can be considered as simply a function of concentration that is well-monitored *in situ*. In the ocean, the system is more complex since CO_2 is a non-conservative tracer: it dissociates in the carbonate cycle and is consumed and released by biota. Hence, these processes must enter any calculation, as must, obviously, the physical transport processes of advection and eddy diffusion.

To determine the oceanic net uptake in response to increasing levels of atmospheric CO_2 we need to consider a variety of variables, including oceanic circulation, sea surface temperature, wind stress and/or sea surface roughness, and biotic activity.

In the previous two sections (The Energetic Planet and The Blue Planet), we have discussed Eos' role in determining the ocean circulation. This is considered further in Chapter IV. Also in Chapter IV, we discuss the investigation of oceanic primary production using primarily the MODIS instrument interplayed with LASA, TIMS, SCATT, ALT, and AMSR. The central issues in the global carbon cycle as well as the physical climate system are (1) what is the role of the ocean in the carbon cycle; specifically what is the rate at which the oceans are taking up carbon dioxide; (2) how might the oceans change given a changing climate; (3) what is the feedback on climate, directly and indirectly; and (4) specifically, how might the uptake of CO_2 change in a changing climate. We need, in short, to know how the oceans operate at the global scale and, hence, obviously demand global data sets. However, in addition to such broad ocean-basin investigations using Eos, there is a need for important detailed studies of mesoscale systems, including *in situ* investigations that will clarify the relation between physical forcing and biotic activity (see Chapter IV). Key mesoscale issues associated with the understanding of the basin-scale distribution of primary production are:

- Where are the regions of high mesoscale variability?
- How does the mesoscale variability affect global productivity and biogeochemical cycling?

- What is the global climatology of productivity?

In the Eos era we will be able to observe and then link physical processes to the temporal and spatial variability of the biological patterns. For instance, the two separate processes of bottom water formation and intense upwelling appear not only to provide an opportunity to uncover important relationships between physical and biological phenomena, but also to give insight into specific important events that govern the broad aspects of the oceanic role in the cycling of carbon, nitrogen, sulfur, and phosphorus.

It is necessary to emphasize that measurements of physical processes are essential for understanding the biological processes in the ocean (and on land as well). Fortunately Eos will offer this observational capability. From Eos, important achievable measurements will be those that relate the distribution, in time and space, of primary production with temperature, wind, water turbidity, and sunlight variations all in the context of an overall pattern of oceanic circulation.

Terrestrial Biosphere-Atmosphere Exchange

The essential questions for the biosphere and the global carbon cycle are: At what rate is carbon being fixed in terrestrial vegetation? What is the pattern of allocation for this fixed carbon, and at what rate is it being released through the respiration of detrital material, and what is the form of this respired carbon?

Today, it appears that surprisingly good estimates of the temporal and spatial pattern of primary production (carbon fixation) can be made using the current AVHRR. The expanded spectral range of MODIS will extend this capability dramatically. HIRIS will provide the ability to make similar measurements on much finer spatial scales.

More generally, the canopy of a plant community contains a wealth of information about the state of the system. For instance, changes in water and nutrient availability are reflected in changes in the canopy development, structure, and the pattern of spectral reflectance. By using SAR and HIRIS, interplayed with LASA and MODIS, these parameters can readily be determined. Subtle changes in the vigor of vegetation and the rates of production and respiration are expressed through alterations of leaf chemistry.

This combined capability will not only provide better estimates of production, but of equal importance, with it we may better understand the allocation of the fixed carbon among the various parts of the plant and different chemical compounds. Understanding the form in which the carbon is produced is the key to determining the rate at which it will be respired later as detrital material. This is particularly important because it is the critical return path to the atmosphere.

It is necessary to distinguish between conditions of dry and wet soils. In the former case, primarily oxidized compounds (e.g., CO_2) are emitted; in the latter case some reduced gases are formed (e.g., CH_4), including from basic soils, NH_3 . Also, nitrous oxide (N_2O) is emitted from wet soils, though the precise chemistry is still unclear. Because of particular conditions that must prevail, the character and the release rate of the gases is an intermittent process very much dependent upon the wetness of the soils and the character of the organic material. Soil moisture has been discussed already and we simply note again its importance. Given the moisture estimate (which, as discussed in the preceding section on the Blue Planet, can be measured by Eos directly or treated as a spatially-varying function of precipitation, actual evapotranspiration, and soil type) and the temperature, the respiration rate and form can be calculated if we also know the chemical character of the detrital material, in particular its lignin-to-nitrogen ratio. This chemical composition is related to that of the plant material from which it is derived, and this has an expression in the canopy of the vegetation. There is strong evidence now that changes in lignin-to-nitrogen ratios can be determined through changes in the patterns of spectral reflectance that could be sensed by HIRIS.

There is now a growing urgency to include the key processes that regulate the flux and distribution of radiatively important trace gases other than carbon dioxide, such as methane and nitrous oxide. The magnitude and direction of the flux of these gases are determined in part by the geographic and time-varying patterns of temperature, nutrient status, and soil moisture and by the heterogeneous pattern of disturbance.

In addition to the state characteristics of various ecosystems (and as an aid in the determination of these state characteristics), we need a better understanding of the various perturbations to which components of the biosphere are being subjected. As previously stated, the conversion of forests to agriculture or pasture, and the harvest of forests for timber and fuelwood, cause a net release of CO_2 to the atmosphere. Deforestation also causes the release of trace gases other than carbon dioxide, such as methane and nitrous oxide. Such disturbances to ecosystem processes vary geographically, but are important global phenomena. Uncertainties in the estimates of the current and historical flux of carbon result in part from different assumptions concerning the types of ecosystems converted and the rates of tropical deforestation. Ecosystem characteristics are not spatially uniform, nor are disturbances. The HIRIS, TIMS, and SAR will enable major advances in the accurate specification of perturbation characteristics.

These new research initiatives in global ecosystem studies and landscape ecology demand models with improved spatial resolution and, most

important, data with georeferenced characteristics. The ecological data required to refine the magnitude and geographical pattern of biospheric carbon dioxide exchange include: the geographic distribution of the world's major vegetation zones and the amount of carbon stored in each zone, the geographic distribution of the world's soils and the amount of carbon stored in each, the state of the vegetation and soils, and the response of vegetation and soil to disturbance. The land use data required include: the time-varying and geographically-referenced rates of ecosystem conversion to agriculture and other land uses, the rate and location of forests degraded for timber harvest or fuelwood, the rate and location of afforestation and field abandonment, and the rate and structure and function through the modification of the processes of nutrient cycling.

Eos data offer great possibilities for obtaining the necessary spatially and temporally detailed data for global ecosystem models and for landscape models dealing with changes in the planet's biogeochemical system generally, as well as better resolving the global carbon cycle.

Terrestrial Biosphere–Ocean Exchange: Rivers

Disturbance patterns, and their relation to the periodicity and spatial patterning of hydrologic transport, are also important. With respect to the global carbon cycle, the organic carbon removed by soil erosion may be distributed to lower-lying areas, in which case its turnover rate is probably little affected. If, however, the organic carbon is transported to lacustrine or marine sediments, its turnover time may be significantly increased, thus leading to a misrepresentation in the magnitude and timing of carbon flux between the biota and the atmosphere. Presumably the loss of carbon by erosion and fluvial transport is small relative to the overall flux directly between the biota and the atmosphere. Nonetheless, this point has become sufficiently obscured in recent years to warrant an extended investigation. Moreover, for other nutrients, such as nitrogen, erosion and fluvial transport raises important biogeochemical issues, especially since this transport affects terrestrial-aquatic interactions.

In order for us to link ecosystem processes to fluvial and aquatic processes, detailed spatial data are required to capture the scale and dynamics of the hydrologic and geomorphologic characteristics of watershed and waterbasin processes. These data include topography, soil erosivity, precipitation, sediment delivery, fluvial transport and water routing, stream network topology, and other geographically detailed factors. Many of these issues are discussed in the section addressing the hydrologic cycle; however, a few additional points regarding observational opportunities afforded by Eos are summarized below.

For instance there are perhaps unexpected possibilities for hydrologic models to exploit remotely

Table 9. Eos Instruments for Determining Elements of Earth's Primary Biogeochemical Cycles

Marine Biosphere-Ocean-Atmosphere Exchange	
Surface wind field	SCATT, ALT, AMSR
Cloud cover	VAS*, MODIS
Surface air temperature	MODIS, AMSU, AMSR, AMRIR, TIMS, VAS*
Surface humidity	LASA, AMSR
Phytoplankton biomass, fluorescence	See Tables 6 and 7
Terrestrial Biosphere-Atmosphere Exchange Over Land	
Radiation and Leaf Area	
Atmospheric transmission	See Table 6
Reflected near IR	AMRIR, MODIS, HIRIS
Reflected PAR	AMRIR, MODIS, HIRIS
Vegetation Type	
Time sequences	MODIS, HIRIS, AMSR
Images	SAR
Multiview angles	MODIS-T, HIRIS
Plant Temperature	
Available Soil Water	MODIS-N, AMSU, TIMS
Methods shown earlier	See Table 7
Ratio of radiances	MODIS-N

*Geostationary platform instruments

sensed data traditionally used by vegetation models. We now know that there are strong correlations between vegetation indexes determined from remotely sensed data and runoff curve numbers. Remotely sensed thermal and microwave data can be used to estimate surface-soil moisture at a regional scale that can then be used to model soil moisture in the profile. Remotely sensed data also hold great promise for landscape-scale models of evapotranspiration. Finally, through its effect on hydrology and vegetation, topography greatly influences ecosystem properties. On Eos, the wide range of sensors, including microwave, laser profilers, and synthetic aperture radars, will allow great progress to be made in the determination of the Earth's topography. Table 9 summarizes the observations required to characterize the nature of global biological activity and the Eos instruments and other measurements that will be used to study the green planet.

SUMMARY

A primary observation about the Earth system is that energy flows and matter cycles. The fluxes of energy and the transformations of matter are the consequence of thermal imbalances created by differential heating by solar radiation falling on the surface and by the flow of energy outward from deep within the Earth's interior. The creation of thermal gradients develops dynamical and chemical forces that drive the evolution of the global system, creating energy flows, mass fluxes, and transformations in phase and composition of materials.

The Earth Observing System, in concert with models and *in situ* process studies, will provide a new and more profound level of understanding of the basic life-sustaining processes of our planet. In the next chapter, specific case studies further elucidate the value of this new Earth Observatory.

IV. EXAMPLES OF Eos MEASUREMENT STRATEGIES

INTRODUCTION

To illustrate possible applications of the Eos system, this chapter describes a set of 14 different hypothetical science investigations. In this exercise, our purpose is not to survey all of Earth science, but rather to give some specific examples that demonstrate the power and utility of the proposed satellite system.

We choose these studies from four general areas:

1. Geology and geodynamics,
2. Land processes,
3. Ocean processes, and
4. Atmospheric circulation and chemistry.

In terms of duration, these studies range from long-term monitoring projects to studies of transient events. An example of a long-term project is the decadal-scale monitoring of tropospheric chemistry; an intermediate-term project is the determination of the interannual variability of the plankton bloom in the California Current. A short study is the determination of the convective properties of an open water region in the Antarctic ice cover during winter, and a very short-term study is the measurement of the properties of breaking waves in the upper atmosphere. Certain of the Eos experiments are long-term measurement studies, which for their success depend on the continuity of the satellite-gathered data sets over long time periods. Other equally important experiments will study transient events in generally inaccessible regions of the Earth.

As well as illustrating the science potential of Eos, each of the 14 experiments has relevance to the general habitability of the Earth. The atmospheric chemistry studies should lead to an understanding of the changes in the ozone layer, which absorbs biologically destructive ultraviolet radiation. The ocean experiments will lead to an understanding of the relation of ocean heat storage to weather and climate. Even the short-term study of open water in the Antarctic pack ice will lead to an understanding of processes that keep the oceanic bottom water enriched in oxygen.

In summary, the following 14 sections are a sample of the scientific problems that will be addressed by Eos. These sections, and the problems they address, are not a closed set; rather, they illustrate the power and diversity of the Eos system.

INTRODUCTION TO SOLID EARTH PROCESSES

The first two sections of this chapter discuss the application of Eos observations to studies of solid Earth processes. The examples selected begin with

the interior motions of the mantle and crust, then move outward to include problems related to the surface rocks. Even this diverse set of topics, however, covers only a portion of the wide range of problems that can be addressed from spaceborne observations; it is intended to illustrate, rather than define, the Eos potential.

The solid Earth is classically divided into the core, mantle, and crust. It is a dynamic system, driven by internal heat to produce a wide range of geologic processes. This internal heating results in a continuous cycle of rock formation, tectonics and uplift, erosion, transport, deposition, metamorphism, and finally remelting (Figure 19). This rock cycle forms the basis for our understanding of geologic history and evolution, and ties together all of the different geologic processes that operate on the Earth. The formulation of plate tectonic theory has allowed this cycle to be placed into a global context in which all of the continental and oceanic plates can be seen to interact to produce the global distribution of tectonic features, volcanic terrains, and continental rock units. This global context provides an ideal perspective from which to study the solid Earth as a unified system.

The dynamic processes operating within the geologic cycle operate at very slow rates over very long time periods. For this reason they are more difficult to study than the dynamic processes occurring within the other major Earth cycles. Nonetheless, the effects of the changes produced by geologic evolution do represent major changes in the Earth system, from the initial genesis of continents, through the onset and variability of plate motions, to the evolution of continental and oceanic volatile reservoirs. In addition, geologic changes have major impacts on the other cycles, for example through the control of climate produced by the distribution of land masses and mountains.

Within the geologic cycle there are three major processes, each of which can be addressed using observations from space. These are:

1. The dynamic motions of the interior and the tectonic evolution of the Earth's crust as it is driven by these motions;
2. The compositional evolution of the crustal materials due to melting, differentiation, and reworking; and
3. Processes that occur at the surface, including erosion, transport, and deposition.

Dynamic motions occur within both the core and the mantle. Those within the core control the generation of the Earth's magnetic field, but otherwise have little observable effect at the surface. The motions and composition of the mantle, however, do

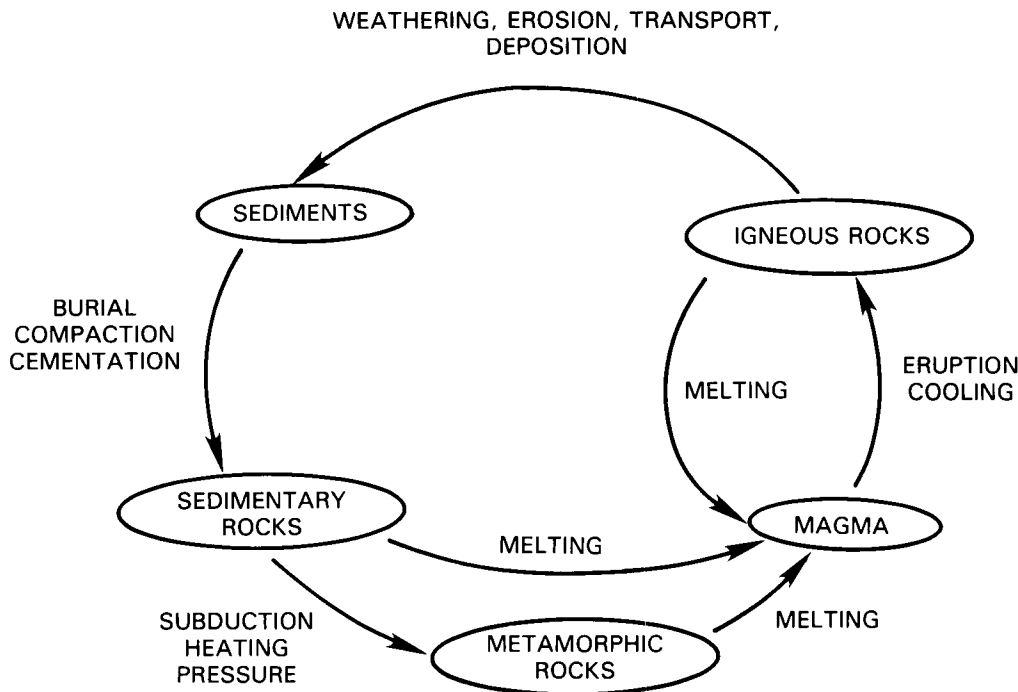


Figure 19. The geologic cycle.

play an essential role in shaping the observable surface, because many crustal rocks were derived directly from the mantle, and the convective motions within the mantle drive the motions and interactions of the crustal plates. Finally, the crust is of great interest, for it is that portion of the Earth on which we live.

The compositional evolution of crustal material is evidenced by the occurrence of two primary crustal rocks—oceanic and continental. Although the oceanic crust is not directly observable, a great deal can be learned about it from space, for example, using gravity perturbations of the ocean surface to determine the topography of the ocean floor. On the continents, the crustal rocks are exposed, providing a history of the growth and deformation of the continental plates. In addition, compositional variations provide information on a wealth of geologic processes such as volcanism and magma differentiation and sedimentary environments and history.

Surface processes, which include erosion, transport, and deposition, are active geologic processes occurring at the surface of the Earth. These processes are the result of the interaction between the solid surface and the atmosphere, hydrosphere, and biosphere. Thus, the geologic materials on the surface fit directly into the global cycles of energy, water, and nutrients. In addition to the role that surficial processes play in the dynamics of the Earth system, they also provide a means of determining the

Earth's recent history. The morphology and composition of the surface materials have been produced by the integrated effects of geologic processes acting over the past thousands to millions of years. The surface of the Earth therefore provides a record of these processes, and provides the means for determining how surface conditions have changed with time. This preserved record reveals important variations in climate, sea level, and polar ice extent, which have had a major impact on the evolution, productivity, and distribution of life on the Earth. Understanding this climate history is critical to understanding the changes currently under way. Comparison with past evolution is the only means available to test models that make long-term predictions. Finally, monitoring of active geologic processes will have important practical implications for mankind. Volcanic eruptions, floods, and desertification are examples of such processes that affect man on regional to global scales.

In summary, remote sensing of the solid Earth provides a means for understanding the Earth's evolution, and provides a snapshot of the slow processes that operate over geologic time. It provides information on a great variety of geologic topics, which are of substantial interest not only for an improved scientific understanding of the Earth system, but also for an improved ability to monitor and control the factors affecting the interaction and productivity of life on the Earth.

GEODYNAMICS

A comprehensive understanding of the dynamics of the complete Earth system depends in a critical manner on understanding each of its elements: atmospheric dynamics, ocean dynamics, and the dynamics of the solid Earth. The dynamics of the Earth encompass a broad spectrum of motions, including the orbital motion of the Earth-Moon system about the sun, the rotation of the Earth about its center of mass, and the motions of the core, mantle, and crust. The province of geodynamics focuses on questions related to the motions of the components of the Earth's surface relative to one another (tectonic motions, land subsidence, and/or uplift); the motions of the Earth as a whole (polar motion and Earth rotation); the motions of the core with respect to the mantle and the coupling torque involved in these motions; the solid Earth and ocean tidal deformations; the external gravity field, its changes, and its use to infer the internal structure of the mantle; and finally, the mapping of the Earth's surface topography, including both the land topography and the topography of the mean ocean surface.

The solid Earth is a dynamic system, whose energy is supplied by internal heat to produce a continuous cycle of rock formation, tectonics and uplift, erosion, burial and subduction, metamorphism, and finally remelting. Geodynamics is the branch of Earth science that deals with the forces and processes that take place in the Earth's interior. These processes play a fundamental role in the overall cycle of plate formation and destruction, for they control the motions of the continental and oceanic plates, which in turn control the origin, evolution, structure, and internal relations of the regional features of the Earth's crust. The development of plate tectonic theory within the past 30 years has provided a crucial conceptual link between the dynamic processes occurring within the Earth and the expression of these processes observable at the surface in the form of earthquakes, mountains, volcanoes, and troughs.

Remote sensing of the Earth through Eos will address important questions regarding the dynamics of the Earth system using observations of the structure and motions of the crust. Among the large number of questions to be addressed, several have been identified by the U.S. Geodynamics Committee (NRC, 1980), the Committee on Earth Science of the Space Science Board (NRC, 1982b), and the Board on Earth Sciences (NRC, 1983a). Examples of these include:

- What is the relationship between mantle and crustal dynamics?
- What is the nature of the continental to oceanic transition?
- What is the origin and evolution of continental and oceanic crust?

- What are the compositional and structural characteristics of plate boundaries and how do these relate to the record of earlier tectonic events?
- When did plate tectonics first begin?

Major advances in these areas require a global perspective that can best be obtained through global remote sensing. The crustal evolution characterized in the plate tectonic models begins at the spreading centers, located predominantly in the oceans. Therefore, contemporaneous study of both continental and oceanic evolution is necessary to understand the complete crustal dynamic process. Because the plate tectonics hypothesis and many of its important corollaries evolved from geophysical and geologic observations of the ocean floor, the hypothesis has been more successful in explaining oceanic phenomena. Consequently, there is a need for improving our measurements of continental structure, topography, and deformation. Measurements of tectonic features, together with dense grid measurements of deformation taken over broad geographical regions and repeated over extended time periods, will allow studies of plate boundary evolution. In particular, the relation of plate boundary strain fields to the onset of earthquakes and the deformation of the plate interiors can be addressed and placed in a regional and global context.

Critical requirement for current observation systems is to provide the requisite observations to refine our understanding of these processes. The importance of satellite-derived measurements in collecting a synoptic set of regional and global measurements to support these investigations was outlined in the Research Briefing 1983 prepared by the Committee on Science, Engineering and Public Policy (NRC, 1983b), and has been supported by numerous National Research Council reports. Eos provides a unique capability for space-based instruments to obtain measurements to facilitate many geodynamics studies.

The following sections describe the application of specific Eos sensors to particular geodynamic measurements. At the end of this section we discuss, as an example, how the integrated suite of Eos instruments could be combined to study the dynamics and structure of the San Andreas fault zone in Southern California.

During the past two decades, remarkable progress has been made in understanding geodynamic processes through the application of space techniques. Structural features have been identified from space platforms primarily by their morphologic expression on visual images. This capability will be continued on Eos by the HIRIS and TIMS instruments. The inclusion of an active SAR instrument will greatly enhance the mapping of surface structures by Eos because the SAR images often provide details not obtainable from visual imaging alone.

Finally, accurate determination of satellite orbits by laser and radar tracking systems has been developed as a technique for obtaining a detailed representation of topography, crustal motions, and the long wavelength components of the Earth's gravity field.

The Shuttle Imaging Radar (SIR)-A and -B missions have demonstrated the ability of spaceborne SAR instruments to identify geologic structures from space (Figure 20; Elachi *et al.*, 1982; Farr, 1982). Surface structural features such as lineaments, faults, domes, and layered rock outcrops can be imaged by a SAR instrument due to the subtle variations in topography and surface roughness that they produce. These features are often more easily recognized on radar images than on visual images alone, particularly in regions of moderate to heavy vegetation cover. The SAR instrument also allows mapping through cloud cover, which is an important advance for the geologic observation of many regions in the tropics. In addition, the SIR-A and -B experiments have demonstrated the important capability of 23 cm (L-band) radar to penetrate dry, alluvial layers and to reveal the subsurface structure. Observations in the Egyptian desert have mapped the

distribution of subsurface drainage patterns associated with ancient river channels. Such observations not only provide important structural measurements, but also provide important clues to recent environmental changes associated with active surface processes and possible climate change.

Variations in the height of the surface gravity equipotential (geoid) over the ocean, as determined by satellite altimetry, have been used to infer the mechanical strength of the crust and flow properties of mantle rock. The Eos radar ALT will provide measurements of sea surface heights to an accuracy of several centimeters. The Seasat experiment demonstrated that such measurements provide an important tool for studying the structure and density of the oceanic crust (Figure 21). Insight into the processes responsible for mountain building and convection within the mantle will be provided by the synergistic merger of space and ground gravity and geodetic data with seismic, geological, and thermal information.

In the satellite laser ranging (SLR) technique, ultrashort laser pulses transmitted from a ground-based ranging system are reflected off orbiting

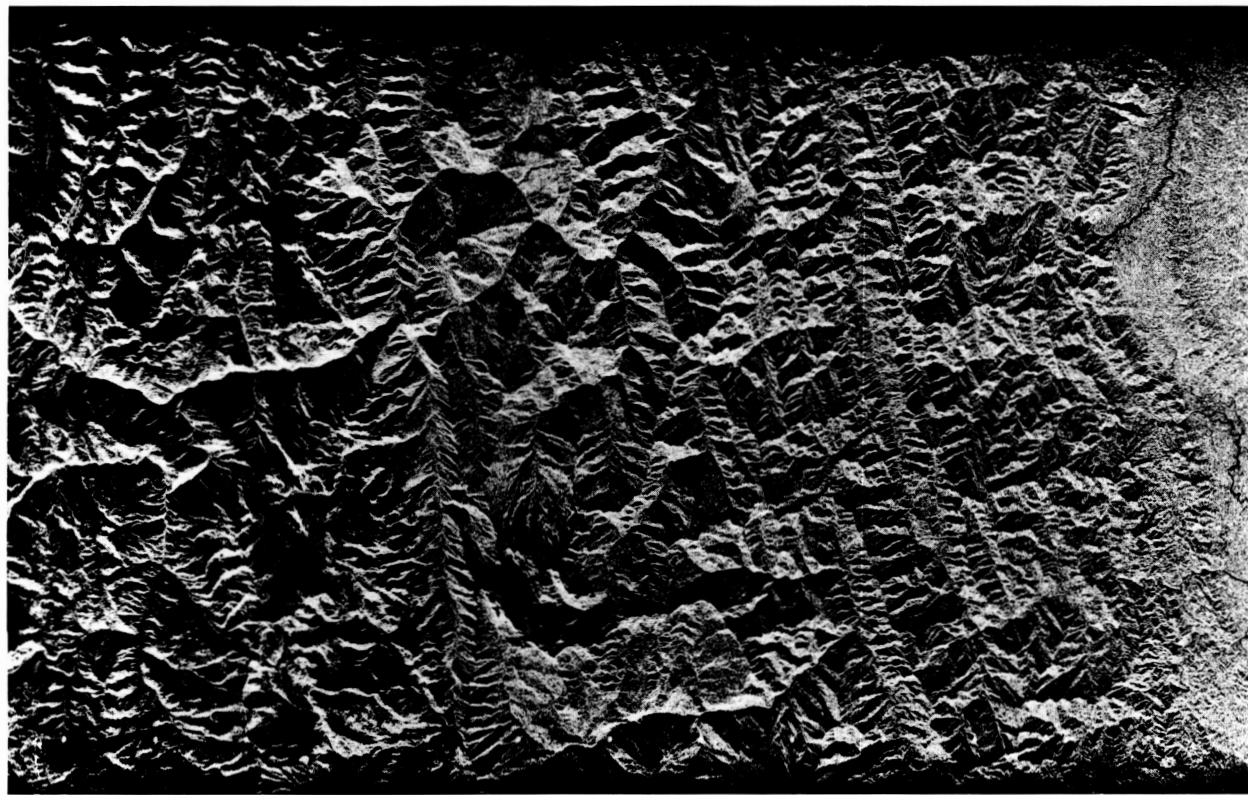


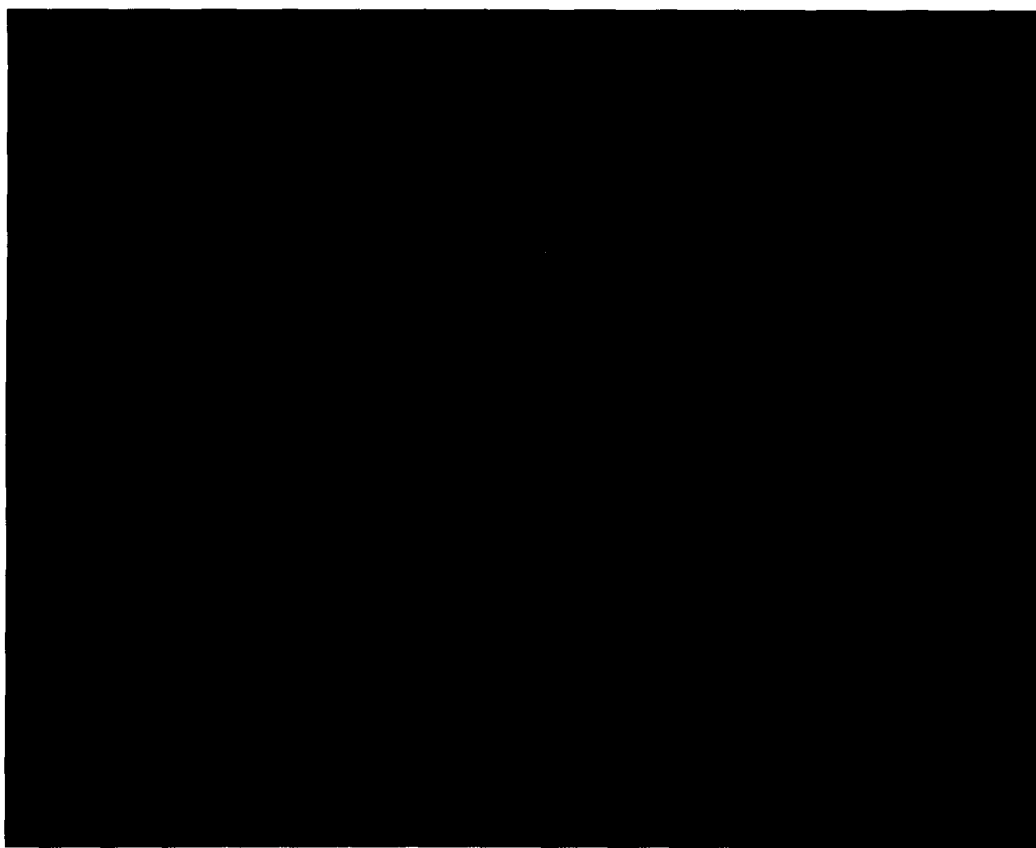
Figure 20. SIR-A image of the Bolivian Andes. On the western side (left) of this image, the mountains are composed of large fault blocks. In the central region the structural pattern is dominated by thrust faults, producing the distinctive pattern of north-south trending linear faults. At the eastern margin, these thrust faults overlap onto the Brazilian shield.

ORIGINAL PAGE
BLACK AND WHITE PHOTOGRAPH

ORIGINAL PAGE
COLOR PHOTOGRAPH



(a)



(b)

Figure 21. Topographic maps of the ocean floor produced from Seasat altimetry data. Combined with space and ground gravity and geodetic data, the Seasat data can provide insight into the structure and density of the oceanic crust.

satellites, and measurements of their time of flight are analyzed to yield centimeter-level precision range information (Kahn *et al.*, 1980; Von Bun *et al.*, 1977). Utilizing SLR data from a global network of ground-based stations and accurate models of the Earth's geopotential field to propagate the orbit of a high-altitude satellite such as the LAGEOS, the relative positions of the ground-based tracking stations have been determined with centimeter accuracies.

Repeated measurements from stations on different tectonic plates have been used to measure the relative velocities of the ground stations at the level of a few centimeters per year (Tapley *et al.*, 1985; Christodoulidis *et al.*, 1985). As an example, Figure 22 indicates the results obtained using 4 years of satellite laser ranging to LAGEOS collected by the SLR system at Haleakala Observatory, Hawaii, and Yaragadee, Australia. The rate of convergence between these two sites is estimated to be 63 mm per year and is in qualitative agreement with the 67 mm per year predicted by the Minster-Jordan AM1-2 model.

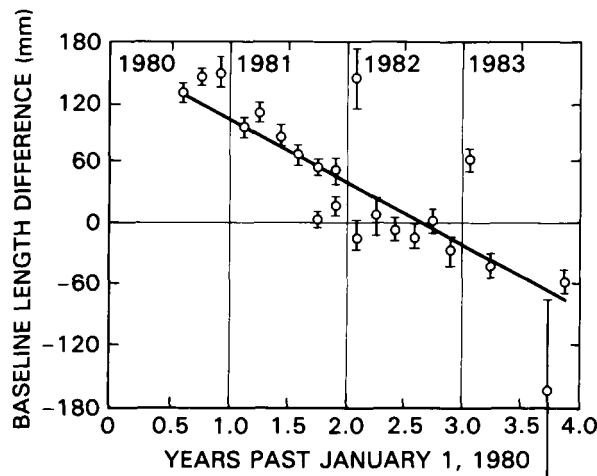


Figure 22. Baseline length difference between Haleakala Observatory, Hawaii and Yaragadee, Australia obtained during 4 years of laser ranging to LAGEOS (slope = -63 ± 33 mm/yr, rms = 32 mm).

Because of the high cost of fabricating and operating the SLR ground stations, fixed stations are rarely built. The GLRS instrument proposed for the Eos platform would invert the current SLR measurement scheme. The laser ranging and optical tracking equipment would be placed on the satellite and would range to inexpensive passive retroreflectors on the ground. The use of the GLRS would permit orders of magnitude more sites to be selected. In combination with ground-based systems, the measurements would provide a global, centimeter-accuracy geodetic data base for the study of plate

tectonics and regional crustal deformation and strain. The operation of a laser ranging instrument from Eos to ground-based retroreflectors, as Figure 23 shows, would permit dramatic improvements in the temporal and spatial resolution with which geodynamic processes can be studied. The measurements would expand current capabilities to measure tectonic plate motion and provide unique opportunities to search for time variations in the plate velocities. In particular, such a system could provide a capability to observe the precursory geodetic motions believed to occur prior to the onset of large earthquakes and, in a broad sense, provide significant information on the evolution of the Earth and other planets.

The increased density of crustal movement measurements provided by GLRS will lead to a substantial enhancement of the measurements obtained by the current network of ground-based laser systems. They would extend well beyond the capabilities of conventional local surveys, which are very labor-intensive and of limited utility in mountainous regions. The new networks of retroreflectors should be designed to complement, rather than compete with, those that will be surveyed with highly mobile receivers operating on microwave signals from the GPS (global positioning system) satellites.

The following case study describes how Eos data might be used to study the specific question of the structure and deformation at a plate boundary, such as along the San Andreas fault system in California.

Initially, SAR data would be used to define the regional structural setting using morphologic information. Tectonic features, including fault zones and deformations, would be identified and mapped. Compositional data from HIRIS and TIMS would also be used to study the regional structure. The trace of individual geologic units would provide a means of defining the deformation and folding of rock units throughout the fault zone. Matching of specific rock sequences across fault zones would be used to measure the offset along different segments of the fault system. These observed offsets would provide a means of identifying previously undetected faults that are not well expressed morphologically. *In situ* age dating of offset rock units would provide a measure of the time history of the displacement. Once the regional setting had been determined, specific sites for laser ranging and radar topographic studies would be selected. In the vicinity of major fault zones, where significant strain is accumulating and earthquake occurrence is likely, a greater density of sites and more frequent surveying would be performed. As shown in Figure 24, retroreflectors could be placed at sites separated by several tens of kilometers with the intersite separation increasing slowly with distance from the fault. Resurveying of the sites several times a year should be adequate for monitoring strain accumulation and plate motion

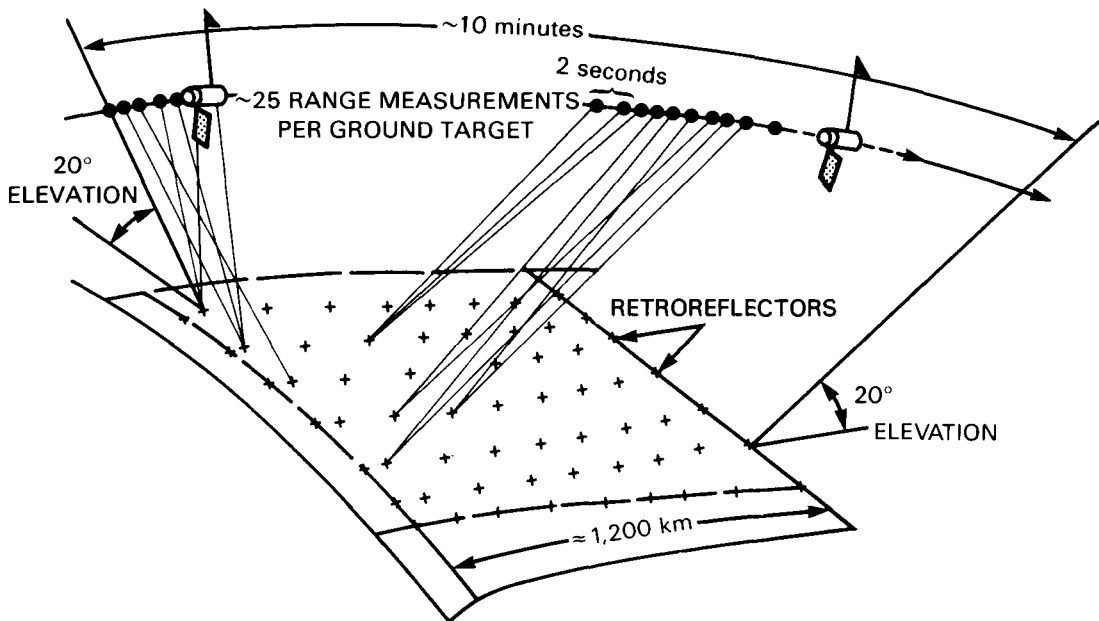


Figure 23. Sequence of events as spacecraft passes over network.

during major seismic events if no significant temporal variability is noted. When significant temporal variability and change in the rate of strain accumulation are detected, more frequent resurveying, on the order of a few days to a week, would be possible to assess the likelihood of an earthquake occurrence or to monitor a seismic deformation process. Similarly, frequent observations could be made subsequent to an earthquake to study how stress changes diffuse into a plate interior. Such studies would contribute to the knowledge of the driving mechanisms for plate motions and earthquakes and the rheology of the subsurface layers of the Earth.

Digital topographic maps would be produced from stereoscopic SAR imaging and from radar ALT observations. These data would be used to quantify the uplift and deformation, and to tie these to compositional, morphologic, and strain measurements. In the case of the San Andreas system, the substantial amount of information collected through seismic studies would be correlated with the surface expression of compositional units to refine our understanding of the subsurface structure.

In summary, the study briefly outlined above illustrates a potential use of the integrated suite of Eos instruments to address the question of the dynamic motions of the Earth's crust and mantle. The various sensors available will provide direct measurements of surface morphology, structure, composition, topography, and strain rate that can be used to characterize the tectonic and dynamic state of a given region. These measurements will provide a snapshot of the tectonic history reflected in the structure of the rocks exposed at the surface, which will allow de-

tailed models of the dynamic processes operating within the Earth to be tested and improved.

CONTINENTAL GEOLOGY

The study of continental geology provides a fundamental means for understanding the processes that control the formation and evolution of the Earth. These processes can be roughly divided into two classes: those operating within the Earth, which produce the large-scale motions and interactions of the Earth's crust and mantle, and those active at the surface, which rework surface materials. The geologic processes combine to form a cycle of formation, uplift, erosion, and deposition that produces the patterns of continental rock units exposed at the surface today. Thus, the continental rock record provides the best means for understanding many geologic processes occurring at very slow rates over very long periods of time and thereby unraveling the evolutionary history of the Earth. In addition, the study of recent surface geologic processes provides a means for studying the evolution of landforms and of determining recent climatic variations. Finally, monitoring active and often devastating geologic processes, such as volcanic eruptions and major floods, provides a means for determining how these events affect the total Earth system.

A major objective for Earth science in the 1990s is to determine the composition, structure, origin, and evolution of the continental rock units (NRC, 1982). To meet this objective, a wide range of specific geologic questions have been identified that

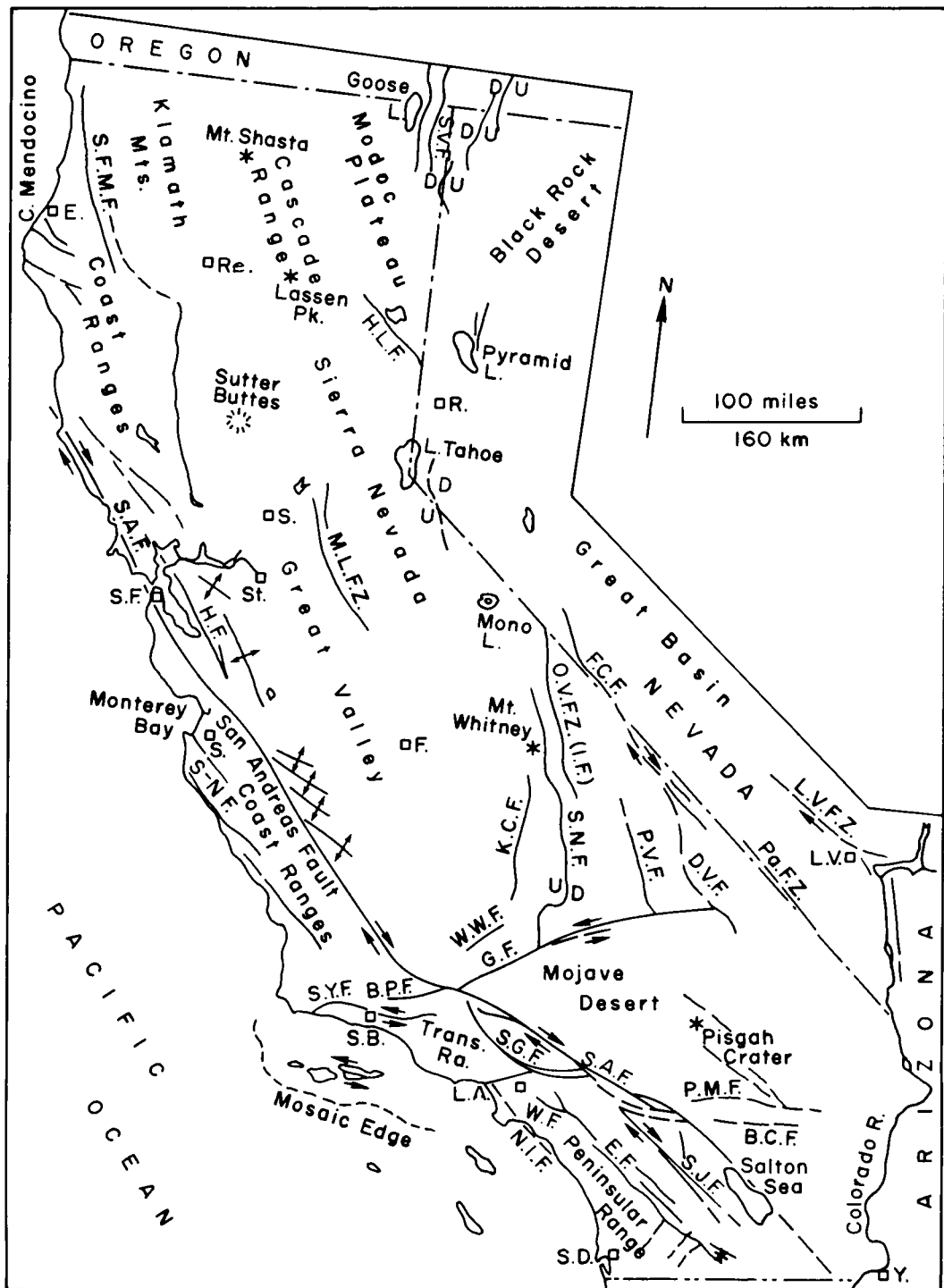


Figure 24. Geologic structure of California and Western Nevada (based on General Electric Co. ERTS-1 Mosaic, courtesy of P.D. Lowman, Jr.) November 1974.

can best be addressed through remote sensing observations (NRC, 1982). Examples of these questions include: (1) What is the deformational and depositional history of the continents? (2) What are the composition and global distribution of volcanic centers, and what is their relationship to active and

past plate motions? (3) What is the relationship of time-variable surface processes to the evolution of the continents? (4) What is the distribution of natural resources and natural hazards? and (5) What is the history of climatic variation as recorded in surficial weathering materials and landforms?

Understanding these questions on a global scale will be greatly enhanced by the integrated measurements to be provided by Eos. The rock and soil composition, the distribution of weathering products, the regional structural patterns, global topography, and surface textures at a range of scales can all be determined and used to fully interpret geologic processes and history. In addition, the integrated package of Eos instruments will provide a means of separating the effects of vegetation, atmospheric properties, and soil composition and moisture content, from rock composition. This separation will allow the distribution of the underlying rock units to be determined. The goal of the Eos approach is to integrate the measurement capabilities of the techniques emerging today into a long-term, synergistic observational campaign that will maximize the overall scientific return.

To illustrate the advantages provided by the combined suite of Eos instruments, the remainder of this section will describe the specific use of the Eos instruments to address the question of continental rock composition and structure. After discussing the contribution of the Eos instruments, a specific example will be given showing how the Eos approach could be applied to the study of the geologic evolution of an eruptive volcanic center associated with the San Andreas fault system in northern Mexico.

Eos will have three instruments—HIRIS, TIMS, and MODIS—that will directly determine mineralogy and lithology on regional and continental scales. Each instrument has different measurement objectives, and each will provide unique observational opportunities. MODIS will extend the type of global coverage obtained by the AVHRR instrument. It will have much better spectral resolution than is currently available. The increased spectral resolution will contribute to improved rock and mineral identification. The high temporal resolution of MODIS will allow surface variations due to vegetation changes and active geologic processes to be mapped. These changes must be understood in order to separate the spectral effects of surface moisture, vegetation, and atmospheric aerosols from the spectral character of the rock and soil materials. Finally, the thermal bands on the MODIS will allow concurrent measurement of surface temperature, which can be used to determine the distribution of rock and soil units based upon their thermophysical properties (Abrams *et al.*, 1984).

The HIRIS instrument will provide high spatial resolution (30 m) and increased spectral coverage (10 nm bands from 1 to 2.5 μm) not available from MODIS for specific regions of interest. The HIRIS spatial resolution is the same as that of the Thematic Mapper (TM), which has proven successful in resolving the distribution of geologic units at a scale necessary to construct detailed tectonic and lithologic maps. Solar radiation from 0.4 to 2.5 μm has sufficiently high energies to induce electronic transitions,

charge transfers, and molecular vibrations in surface minerals. The radiation reflected from the surface contains spectral signatures associated with these effects and thus provides information on mineral chemistry. HIRIS data can be used to identify minerals with transition elements (e.g., Fe, Ti, Mn) and minerals having carbonate, sulfate or hydroxyl ions, or minerals that contain bound water (Figure 25). The number of discrete bands and the spectral resolution needed for each band are governed by the locations, depths, and shapes of absorption features to be measured. HIRIS is designed to properly sample many surface mineral species in addition to properly sampling the reflective characteristics of vegetative canopies. For the first time on a global basis, HIRIS will provide geoscientists with the capability to directly map the composition of surface materials from space.

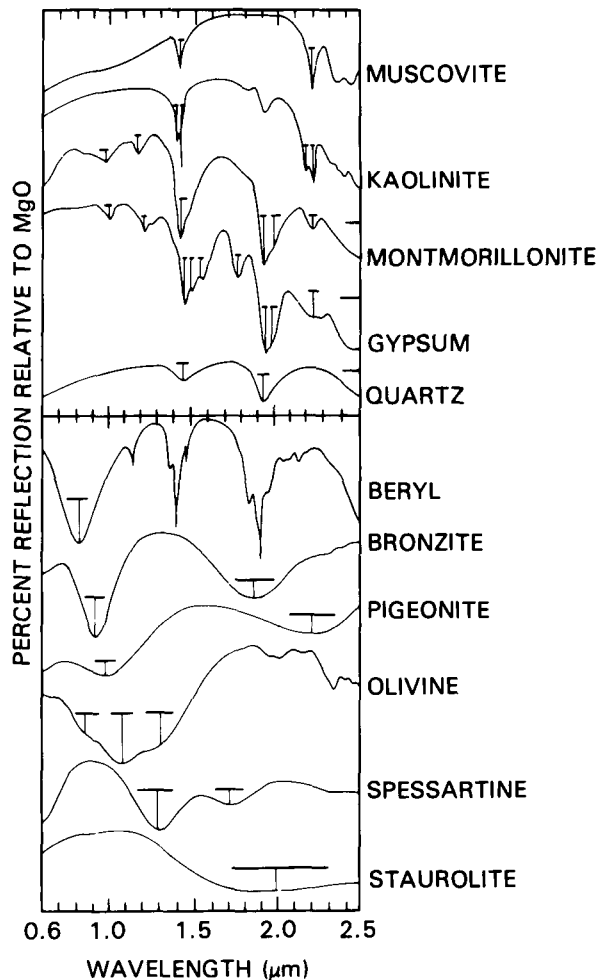


Figure 25. Visible and near-infrared spectra of minerals. These spectra provide a unique means of differentiating between many Fe and OH bearing minerals.

In addition to direct surface compositional determinations, the overall reflectance properties of vegetation can be used as surrogate measures of the underlying surface materials because the type and structure of the vegetation canopy are in part controlled by the soil properties. The emerging field of geobotany will benefit from this improved ability to map vegetation type, growth patterns, and distribution by relating these parameters to the composition of the underlying soil. For example, flat-topped and oak-hickory canopies found in the Ozarks are indicative of regions with porous or thin soils. This capability will be particularly important for compositional mapping in moderate to heavily vegetated areas. Geobotany promises to provide important new information, not only to the study of geology, but also to the understanding of ecosystems and the natural development of plant communities and species distribution.

The TIMS instrument will also provide a substantial capability for mapping the composition of primary silicate, carbonate, sulfate, phosphate, and hydroxide minerals and rocks (Figure 26).

The potential of thermal emission measurements for rock discrimination has long been known (Lyon, 1962; Hunt and Salisbury, 1974), but has only recently been demonstrated in remote sensing applications using an aircraft version of the TIMS instrument (Figure 27; Kahle and Goetz, 1983;

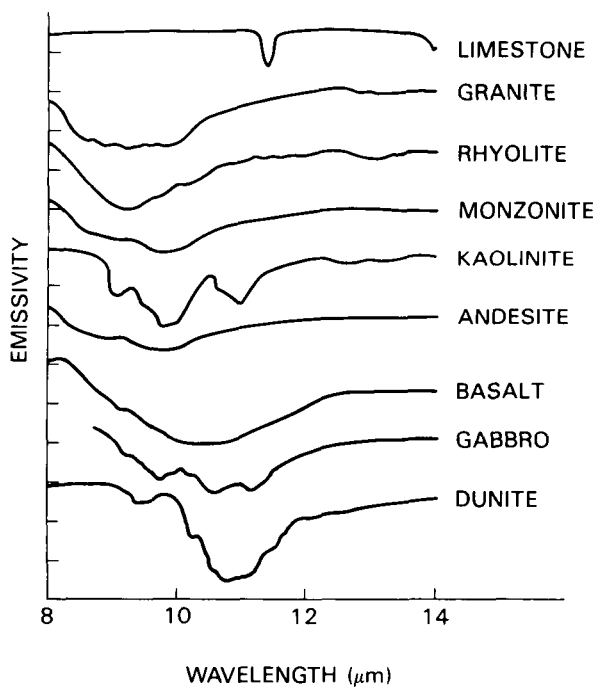


Figure 26. Thermal-infrared spectra of common rocks. These major rock types are readily distinguished using the thermal-IR spectral region.



Figure 27. A TIMS thermal-infrared image of the Kelso-Baker region, California. This false-color image can be used to identify and map numerous rock units and subtle differences in soil composition.

Gillespie *et al.*, 1984). This technique is highly complementary to visible and near-IR spectral measurements, such as those to be provided by HIRIS and MODIS, allowing a much broader range of geologic materials to be identified. Simultaneous measurements in the two spectral regions will allow better identifications to be made by using more than a single spectral feature. In addition, more sophisticated compositional mapping, such as the identification of primary and weathered materials, will allow weathering, transport, and depositional processes to be studied. The TIMS instrument will allow a separation of rock units based on subtle differences in composition. It has been shown that subtle differences in feldspar composition, silica content, and the abundance of mafic minerals can be recognized using thermal-IR observations (Figure 27). These measurements will be very useful for mapping compositional variations in eruptive volcanic materials. Such variations are often associated with the evolution of magma composition through time. Combined analysis of the TIMS and HIRIS data can also be used to study the hydrothermal alteration of primary volcanic rocks by volcanic and fumerolic activity (Rowan *et al.*, 1974).

All of the spectral measurements obtained by Eos will be improved by the simultaneous acquisition of atmospheric temperature and composition measurements obtained directly by HIRIS and MODIS and by atmospheric sounding instruments and LASA. These measurements will allow the complicating effects of water vapor, atmospheric aerosols, ozone, and other atmospheric components to be corrected for directly, rather than relying on ground or spacecraft data acquired at different locations or at different times as must usually be done at present. This capability represents a major advance and is necessary if unique compositional determinations are to be made using spectral data.

The study of surface textures produced by surface processes will also benefit from the synergistic approach of Eos. These observations are of particular importance because surface properties reflect the effects of present and past climates and provide clues to climate change. SAR measurements made at long (70 cm), medium (23 cm), and short (2 to 6 cm) radar wavelengths will provide surface texture information at widely different scales, ranging from a few centimeters for the shortest wavelengths to several meters for the longest (Figure 28; Elachi *et al.*, 1982; Schaber, 1976; Greeley *et al.*, 1985). Multiple polarization measurements will permit the specular (mirror-like) reflections from large-scale slopes and facets to be separated from volume scattering by surface and subsurface rocks, vegetation, and ice. This will provide a much improved measure of the surface texture (Farr, 1982). Additional surface texture information obtained from surface temperature measurements taken by MODIS, TIMS, and AMSU will allow the thermal inertia, and thus the average parti-

cle size, to be determined. The ESTAR instrument will provide measurements of soil moisture that can also be used to study soil properties. Thus, the SAR, ESTAR, and surface temperature measurements will provide a means of mapping soils and stratigraphy based on physical properties such as surface texture, dielectric constant, and moisture which will complement compositional mapping using the MODIS, HIRIS, and TIMS spectral measurements. The relationships between surface physical properties and composition can then be used to study the interplay of fluvial, aeolian, volcanic, and glacial and periglacial processes in controlling the development of the surface.

A final example of the synergism that can be applied to the study of continental geology using the Eos complement of instruments involves the measurement of global topography. Topographic measurements with a spatial resolution of 700 m and a vertical resolution of 10 cm will be provided over limited regions by the LASA instrument. Topography will also be determined from SAR stereo imaging over broader regions with higher horizontal resolution, but at a lower vertical resolution (Leberl, 1983). The data from all of these instruments will be combined with structural and compositional mapping to study a wide range of geologic processes. For example, tectonic deformations can be identified using SAR; the degree of uplift, faulting, and deformation can be quantified using LASA and SAR topographic measurements and GLRS precision ranging to corner reflectors; and the composition of associated magma bodies, volcanic extrusions, or metamorphic complexes can be related to their location within the tectonic environment. A second example would be the combined use of these data sets to study fluvial, glacial, and aeolian surface processes by quantifying the control and development of structural fabric (e.g., dunes or drainage patterns), erosional downcutting, isostatic rebound, or the formation of sedimentary basins, in relation to such properties as rock composition, regional slope, and climate.

The synergistic use of Eos data can be further illustrated by considering a specific research problem. The example discussed is to determine the composition, age, eruptive history, and relationship to plate boundary dynamics of a regional volcanic eruptive center. This problem requires knowledge of the regional structural and compositional characteristics, as well as the specific properties of the volcanic field. As an example, we will consider the Pinacate volcanic province associated with the San Andreas fault zone in northern Mexico.

The initial phase of the project will be to determine the regional structural and compositional setting. This characterization will be made using the SAR data to define the structural and topographic features, and Multispectral Scanner (MSS), TM, and MODIS data to discriminate regional rock and soil

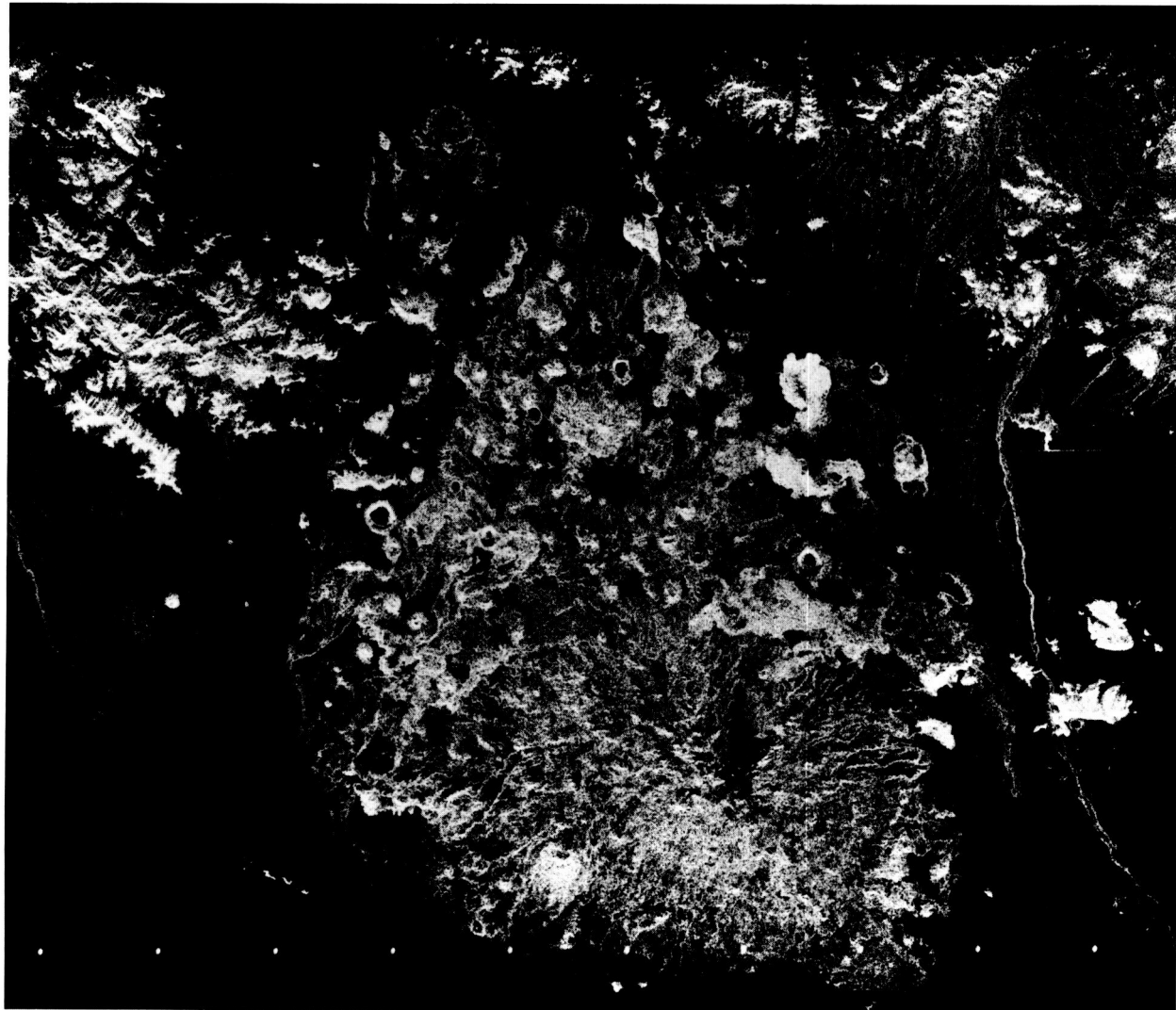


Figure 28. SIR-A radar image of the Pinacate volcanic field, Mexico. Subtle differences in surface roughness appear as brightness differences. Surfaces that are rough at 10 to 40 cm scales appear bright.

units. The MODIS data, which will permit unique mineral identification over large regions, will be used to define and identify large-scale compositional units, and to determine the regional vegetation patterns and cover.

The second phase will involve the acquisition of specific HIRIS and TIMS images. The images will be targeted using the regional framework developed in Phase 1. The TIMS data will be used to determine the composition and distribution of the bedrock and soil units. Ongoing work using TIMS observations has demonstrated that significant improvements in the identification and spatial mapping of geologic units can be achieved with TIMS data, even for relatively well-mapped regions such as the southwestern United States (Kahle and Goetz, 1983).

HIRIS data will be used to determine the abundance of iron-bearing minerals within the different rock units, and to determine the composition of

weathering products. These observations will be used to study weathering rates, ages, and initial composition of exposed rock units. In addition, the HIRIS data will provide an important means of identifying primary deposits and secondary soils derived from volcanic materials. Alteration products produced by fumerolic weathering can be identified using HIRIS, and may provide a means for locating primary vents.

Within the Pinacate region, three major eruptive centers have been tentatively identified (Donnelly, 1974; Lynch, 1981). Using HIRIS and TIMS data, the differences in composition between these major centers and between the individual flows will be determined. Older intrusive and extrusive igneous rocks will be identified, and their relationship to recent activity will be determined.

The SAR data will be used to determine surface roughness. These measurements will be used to differentiate different flows and to determine relative

flow ages based upon the degree of surface mantling (see Figure 28). In addition, the distribution of volcanic ash and cinders will be mapped using SAR roughness measurements, as demonstrated by SIR-A observations of Pinacate (Greeley *et al.*, 1985). These observations will provide clues to the timing and areal extent of maar crater explosive events and the eruption of cinders from the summit and flanks.

The TIMS data will also provide surface texture information due to different emission characteristics of different surfaces. These properties will be used to differentiate flows and will be compared to flow properties, such as length and width, to test models relating flow emplacement to lava viscosity and eruptive rates. Finally, the encroachment of the aeolian sands to the west of Pinacate onto the volcanic shield will be studied to assess the importance of recent surface modification.

Field investigations will play an important role in this study, and will follow the initial, detailed analysis of the Eos data. The Eos perspective will allow the field work to be well focused and efficient. Once significant geologic units and unit boundaries have been identified, these areas will be given specific study. Rock samples will be collected and analyzed to determine their chemistry and age. Using the TIMS and HIRIS images, these specific measurements will be extended to much larger areas, and using MODIS data, the analysis of the HIRIS data can, in turn, be extended regionally.

INTRODUCTION TO LAND PROCESSES

The next four sections of this chapter deal with studies of selected land surface processes. These include soil development, plant productivity, hydrologic processes, and aquatic environments, each of which contains portions of all of the major cycles discussed in Chapter III. Surface processes begin with the weathering of the solid rocks to produce sediments. These, with the aid of biologic activity, develop into soils, which support the growth of higher levels of plant species. Soils act as reservoirs and conduits for all of the constituents in the major cycles and play a fundamental role in determining the rates at which these materials are moved. There is, in turn, a feedback mechanism whereby the development of soils through time is controlled by the presence of water, energy, and organic compounds.

The distribution and composition of soils and rock weathering products also provide direct evidence for the weathering environment at the surface, which is in turn related to the climate and water cycle. Soils provide a major storage and transport medium for water, nutrients, and energy. A significant fraction of the Earth's soils, however, are currently under stress through natural climatic changes or through overuse by man. Because of their im-

tance, understanding the reaction of soils to these stresses is crucial for limiting their deterioration.

The surface of the Earth also contains a tremendous diversity of land and aquatic ecosystems. These systems play important roles in the major water, energy, and biogeochemical cycles operating on the Earth, and support the existence of man on this planet. An understanding of the interplay between these systems, and of man's long-term effects on them, is therefore essential. A particularly important system of land plants are those produced by man for food. Monitoring, management, and control of this system is also important for the short- and long-term management of food supplies and agricultural efficiency.

Other, natural, ecosystems are also of fundamental importance to the balance of life on Earth. These include the tropical rainforests, wetland ecosystems, and arid and polar ecosystems. Many of these systems have received little attention on a global scale, yet they are extremely important parts of the global cycles of energy and matter. Because land processes occur at the surface of the Earth, they are ideal candidates for observation using Eos. Soil composition, soil moisture, climate, plant type and distribution, plant growth patterns and year-to-year variability, and biomass are all parameters that can be determined from Eos. The following sections briefly outline some of this potential.

SOILS

The outermost surface of the solid Earth is made up of material weathered from the rocks of the continental and oceanic crust. This layer of material, usually referred to as sediment by geologists and as soil by biologists, is an interface between the processes of life, hydrology, and climate at the top, and the solid Earth at the base. Soils cover virtually all of the land surface (Figure 29), and are crucial to the processes of life that occur on Earth. Soils also provide reservoirs and conduits for all of the major elements of the Earth's cycles, including those of water, nutrients, and energy. In addition, soils provide direct evidence of the interactions between the surface, the atmosphere, the biosphere, and the hydrosphere. Because they evolve slowly over time, soils may not be in equilibrium with current environmental conditions. Thus, they provide a record of recent changes in climate, and a means for studying how the cycles of nutrients, water, and energy have changed in response to these climate changes. Finally, soils provide the medium for growing man's staple foodstuffs, which makes the loss of soil to natural and man-induced causes a major concern for the long-term habitability of Earth.

Eos observational capabilities are well suited for the study of soils. There are five major factors that control soil development: geologic source material, climate, water abundance, vegetation, and topo-

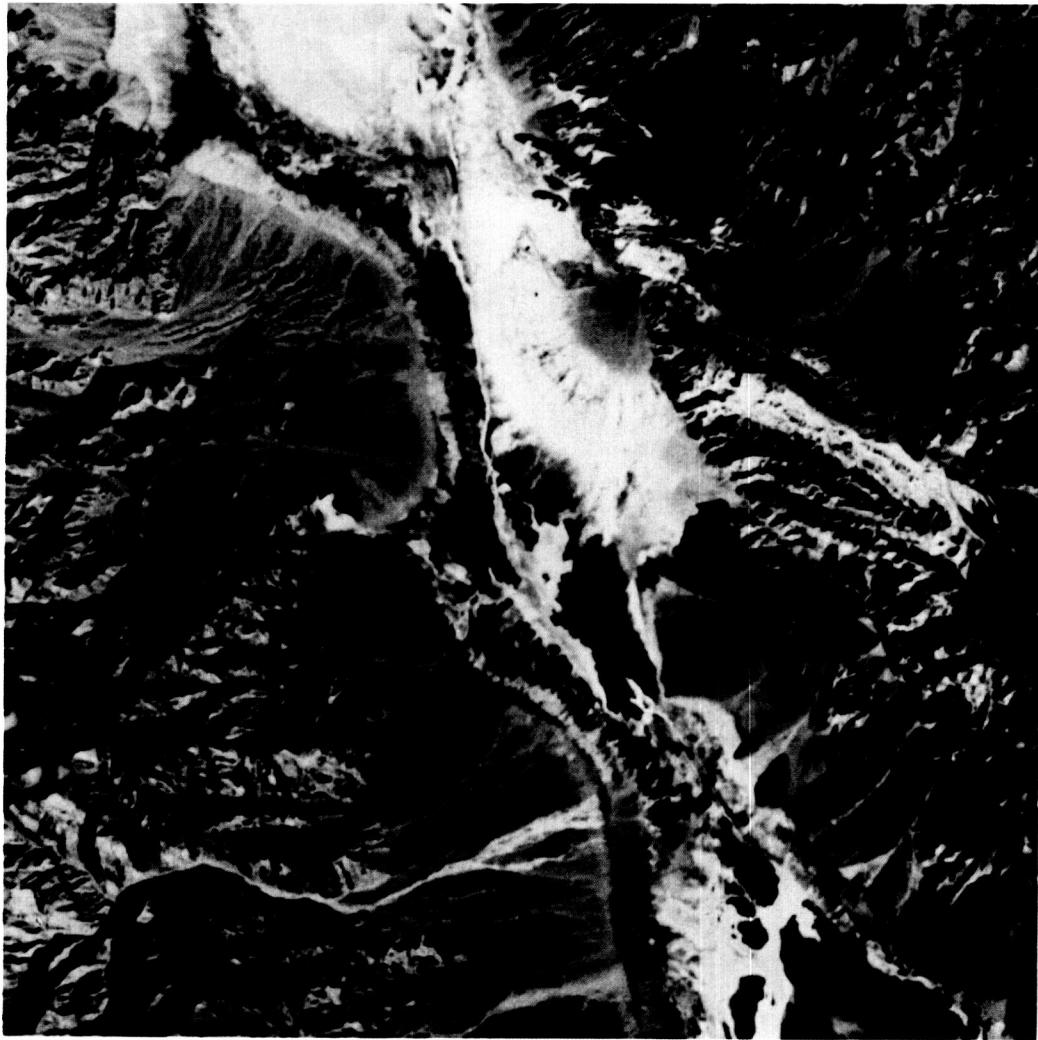


Figure 29. Thematic Mapper image of soils in the Death Valley region, California. This color image shows the variation of soil types as illustrated by surface color differences.

graphy. Each of these factors can be observed and quantified using the suite of Eos instruments. Thus, for the first time on a global scale, the physical characteristics of soils can be directly related to the environmental factors that have led to their development. In addition, changes in soil properties, especially changes due to misuse by humans, occur on time scales that are very appropriate for the time interval over which the Eos platform is designed to operate. Thus, Eos will provide a unique means for quantifying the development of soils on a global scale, for monitoring the parameters that control changes, and for understanding their long-term stability.

A wide range of questions and problems in soil development have particular relevance as man continues to alter and encroach upon natural ecosystems. Among the issues facing soil scientists are: (1) What and where are unstable soil conditions that are subject to rapid changes produced by disturbance?

(2) Are soils a source or sink of carbon, nitrogen, and other nutrients on a global scale? (3) What are the causes of desertification, and how can this process be controlled? (4) What are the long-term effects of agriculture and irrigation on soil chemistry and productivity? and (5) What has been the time evolution of soils, and what can be learned about previous climatic conditions?

All soils, particularly those under stress, are well exposed at the surface. This exposure provides an excellent opportunity to study the factors affecting soil formation (geologic source material, climate, water abundance, vegetation, and topography), each of which is discussed below.

Geological Source Material

Eos will have two sensors, HIRIS and TIMS, that will provide a significant capability for determining soil and rock composition from space. As il-

lustrated in the Continental Geology Section, the HIRIS instrument will provide high spectral resolution images of the surface that will be used to uniquely identify rock and mineral composition (see Figure 25). This instrument is particularly useful for the identification of hydrated minerals, such as clays, which are major constituents of many soils. The TIMS instrument will provide additional information on the primary rock composition, with the capability to distinguish silicate minerals such as quartz, feldspar, and pyroxene (see Figures 26 and 27). Both of these instruments will provide spatial views of the surface, which permit the soil materials to be traced back to their source. These observations will allow the changes in composition and mixing of the parent materials that are produced by weathering and transport to be determined.

Climate

Of the many parameters that determine "climate," rainfall, surface temperature, freeze-thaw cycles, and wind velocity and direction are among the most important for determining soil evolution. Eos will have a number of instruments specifically designed to measure these parameters. TIMS and MODIS will measure the surface temperature, both day and night. These diurnal observations will be used to determine the extent of freezing and the frequency at which the soil is frozen and thawed on a diurnal and seasonal basis. These measurements will also be used to determine the thermal inertia, which relates directly to the particle size and degree of bonding of the soil. Boundary-layer wind velocities for those times of day that are observed by Eos will be determined using a combination of instruments, as described in the previous chapter. These data will provide a limited means of directly determining wind erosion and transport rates, provided that reasonable models can be developed to extrapolate these measurements to surface wind velocity and shear stress. Wind speeds at other times of day will be extrapolated using *in situ* velocity measurements at specific sites, together with observed regional flow patterns.

Rainfall is by far the most difficult climatic parameter to observe from Eos because of the limited time-of-day coverage. Its determination will require additional input from geostationary satellite observations, from *in situ* measurements, and by extrapolation from observed rainfall patterns and Eos observations. Particular care must be paid to rainfall determinations, for in many cases it is the intensity, rather than the total volume, of rain that is the controlling factor in soil erosion.

Water Abundance

The abundance of water plays a major role in determining soil development. As mentioned above,

the rainfall rate has a major effect on soil erosion. In addition, water drainage and retention control the vertical and lateral transport of salts and other ions, and the development of crusts and leached zones. The periodic flooding of low-lying regions introduces fine particles, salts, and nutrients into the soil, which can enhance or reduce its fertility. Finally, a soil's capacity to hold water has a profound influence on the vegetation that it can support.

The primary Eos instrument for studying soil water abundance will be ESTAR, which directly measures soil moisture in the upper few centimeters. Unlike rainfall, which requires instantaneous measurements, the necessary soil moisture observations can be made on time scales of 1 to 2 days. Observations of the time variability of moisture, together with temperature measurements from TIMS and MODIS and selected field observations, will allow the water retention and transport capacities of soils to be determined.

The SAR instrument will also provide a means of studying soil moisture at much higher spatial resolution (30 to 500 m) than from ESTAR (10 km). These observations will allow detailed studies of wetland, flood plain, river channel, and dry lake environments, where soil formation is particularly dynamic.

Vegetation

Vegetation and soil development are intimately related. As soils mature, they can accumulate organic material that changes the soil's fertility and influences the type and abundance of vegetation that it can support. There are also strong interrelationships between soil characteristics and vegetation type. A global determination of this relationship has not been previously possible, nor has a detailed inventory of vegetation and soil types been performed. Using a combination of MODIS and HIRIS data it will be possible to characterize vegetation types into broad categories suitable for comparison with soil composition determined from HIRIS and TIMS. Seasonal and yearly inventories of vegetation type, cover, and health can be made from Eos, and used to monitor changes in soil productivity over long periods.

Topography

The topographic characteristics of landscapes are closely related to soil development in a variety of ways. First, elevation and slope influence the amount of rainfall and the degree of surface runoff. Second, there is a direct tie between morphology and soil evolution because soils develop through the erosion of rock masses. Thus, soils form as terrains become more subdued, and as mountains weather to form peneplains and pediments. Elevation measurements over broad scales will be obtained by ALT, providing

a basis for a global comparison of elevation and soil composition. Local slopes will be determined by stereo imaging using SAR, which will provide input to digital terrain models and models of surface runoff and landform development. Finally, LASA will provide precise elevation and slope determinations for selected regions. SAR will also determine surface roughness at scales of 20 cm and larger, which will be used to estimate surface maturity, soil abundance, and particle size.

The remainder of this section focuses on the question of desertification, and addresses the ways in which specific Eos instruments will contribute to a better understanding of this problem. In particular, the manner in which each of the factors that control soil evolution can be measured from Eos will be discussed.

Desertification

Desertification occurred on the Earth as a natural process long before man began to modify the environment. Throughout the geologic record there is evidence of dramatic changes in environmental conditions and surface morphology. An excellent example is the Colorado plateau, much of which today is covered by pine forests, but in the past was covered by an extensive desert sand sea. Clearly, the "desertification" of this region and its reconversion to a fertile soil were due to natural changes in rainfall, temperature, and wind. Thus, it is of prime importance to understand how natural and man-induced changes affect the environment and to be able to separate these two effects.

The first step toward this understanding will be the development of detailed models that relate soil development and evolution to physical and environmental parameters. Eos will provide the measurements of the physical properties; interpreting these measurements and developing the models will be the challenge faced by scientists over the next 20 years.

Because the details of the processes that produce desertification are poorly understood, a starting point in this investigation will be to first determine the physical properties of the soil and the environment of threatened regions. Soil composition will be determined from HIRIS and TIMS. Soil particle size will be inferred from thermal inertias derived from TIMS and MODIS observations. Surface roughness, rock abundance, and local slope will be derived from SAR data. Together, these parameters will describe the current conditions, which will be monitored for changes with time. In addition, regions under stress will be compared to those in equilibrium with the current environment to determine those parameters that are most subject to disturbances. Climatic conditions determined from Eos sensors and *in situ* observations will also be monitored over time to relate changes in them to changes in soil state.

Through the monitoring of soil properties and environmental conditions by Eos, it will be possible

to determine and monitor global soil conditions and health. An understanding of the stresses to which soils are exposed on a global scale is crucial to any overall understanding of biogeochemical cycles. Clear cutting, salt contamination, and land overuse are human practices producing soil erosion, and in some cases leading to more severe problems of desertification. While these processes will doubtless continue as man attempts to expand his use of the land surface, a careful evaluation of those regions under stress may provide the information needed to contain the deterioration of soils and prevent large-scale destruction of fertile lands.

LAND PLANT PRODUCTIVITY

The study of land vegetation represents a major part of Earth System Science whether one is considering energy, water, or nutrient cycles. Vegetation can affect many factors on the continental to global scale, such as atmospheric CO₂ concentrations, surface albedo, surface sensible and latent heat exchanges, rainfall infiltration, and runoff. Thus, plants have a major impact on inputs to ground water and stream-flow hydrology, water and energy available to the atmosphere, and the cycling of nutrients through the entire Earth system. Furthermore, the vegetation canopy can serve as a sensitive indicator of the state of an ecosystem (NRC, 1985).

Four major goals, which must be met if we are to understand the interactions between terrestrial ecosystems and the atmosphere, oceans, and lithosphere, have been identified by The Land Processes Terrestrial Biology Working Group of the Earth System Science Committee (Moore, 1986):

1. Understand the primary biogeochemical cycles of the planet.
2. Understand the relation between climate and biota.
3. Understand the annual cycle and spatial distribution of primary production and respiration.
4. Understand what controls the spatial distribution of biota over the surface of the Earth.

Many of the large-scale effects of vegetation are considered under the general heading of productivity, where we use the term productivity to mean the accumulation of materials from the atmosphere and the soil into biomass (complex hydrocarbons) through the processes of life. Thus, in our scientific context, productivity refers to the rate at which total biomass is accumulated. In contrast, in agriculture the economic yield is the measure of productivity and depends on the crop. For example, with corn or wheat the grain is of interest and with alfalfa the total above-ground material is important.

Studies of productivity involve considerations of radiant energy from the sun, atmospheric convection, and water and nutrient exchanges with the atmosphere and the soil (see Figure 30). Living vegetation is very dynamic as it senses its environment and adapts to it in ways so subtle that plant scientists are just beginning to appreciate what will be required to fully understand them. Although vegetative production originates in the biochemical factories resident within individual leaves, we are interested in the collective effect of many leaves integrated over some spatial scale that might represent a pixel on a satellite image (Figure 31). Ultimately, we want to integrate these pixels into a global view (Figure 32).

One strength of the Eos approach is that use of space-based platforms offers quantitative observations on scales ranging from 30 m HIRIS and SAR pixels to 500 m MODIS-N pixels with sufficient areal coverage and measurement frequency to interpret observations in regional, continental, and global-scale contexts.

Another strength of the Eos approach is that the simultaneous consideration of all the important aspects of a particular part of the Earth system, using knowledge from all relevant disciplines, allows us to close a relatively general set of equations in a practical way. This in turn permits quantitative predictions of the influence of one part of the system upon the others. For example, models of the terrestrial water budget that do not adequately consider plant productivity and the adaptive character of vegetation lack predictive power. Through use of the Eos inputs to models that characterize vegetation productivity using the results of physiological research, and the hydrologic models discussed in the Blue Planet section of Chapter III, estimates of surface water budgets and plant productivity can be obtained.

The following discussion, which is appropriate for both agricultural and ecological plant types, provides a framework for continental-scale estimates of productivity using appropriate spatial integration.

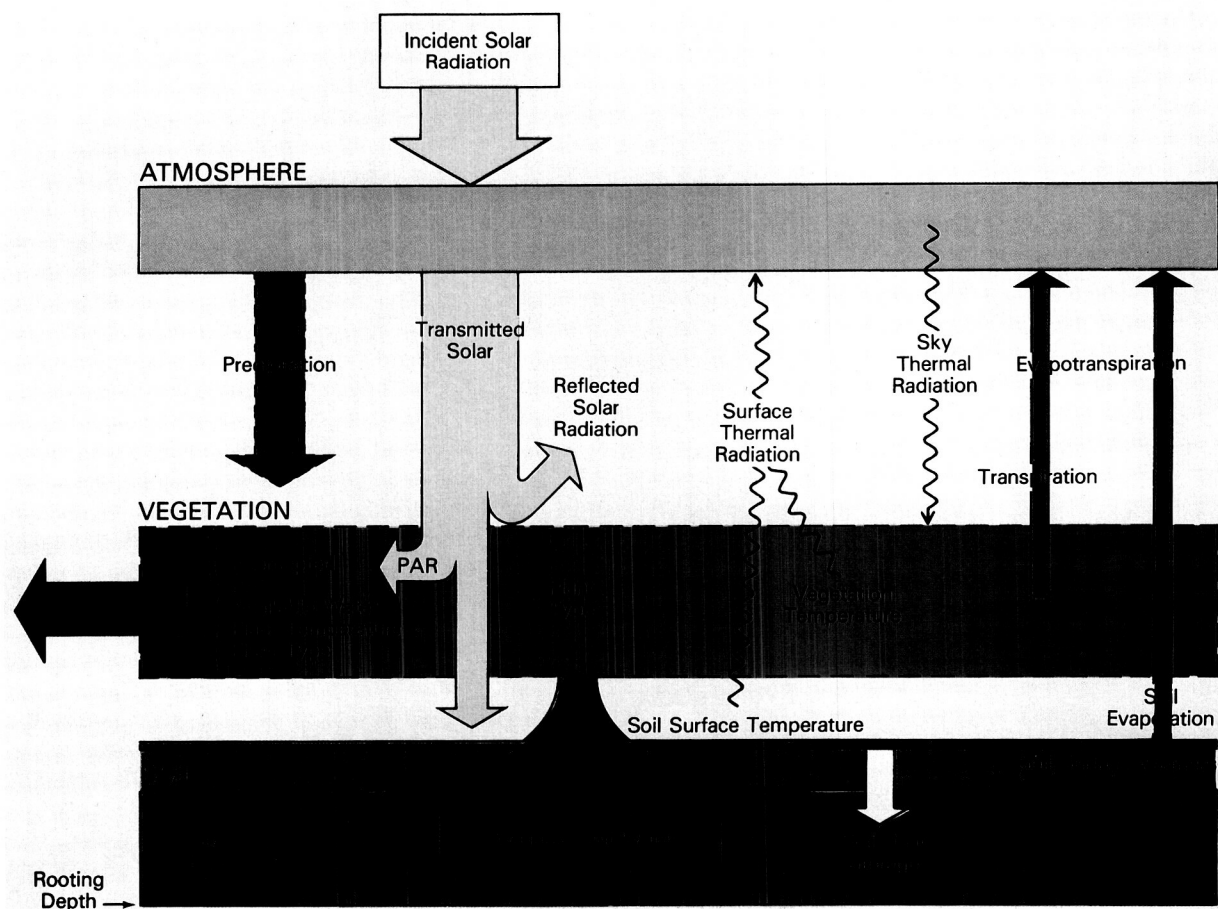


Figure 30. Illustrates the factors that must be measured to estimate large-scale vegetation productivity.



Figure 31. Collective effect of many leaves integrated over some spatial scale that might represent a pixel on a satellite image (courtesy of J. Stubbendick, University of Nebraska).

A Specific Application: Estimating Continental-Scale Vegetation Productivity

As an example of how Eos will be used, the following pages briefly describe a possible strategy for estimating continental-scale vegetation productivity using Eos observations. Continental-scale estimates will be derived from the large-scale integration of satellite observations made at resolutions of 30 m to 1 km. The dynamic character of vegetation, which Figure 32 illustrates, is one feature that can best be captured with satellite observations. The factors shown in Figure 30 represent a reasonable, minimum set of observations for estimation of the productivity of natural and cultivated ecosystems on the continental scale. Essentially we divide this discussion into three parts: radiation absorption and leaf area estimation, plant type and temperature, and available soil water considerations.

The single most useful factor for estimating how the productivity of vegetation can be estimated by remote sensing appears to be the amount of absorbed photosynthetically active radiation (PAR). Predictions are improved with some additional knowledge

of plant type, the amount of vegetation, the temperature, and the amount of available water. The following sections discuss how productivity can be estimated from space-based measurements with considerations of absorbed PAR and vegetation amount, plant type and temperature, and available soil water.

Radiation Absorption and Leaf Area Estimation

The productivity of vegetation depends strongly on accumulated, absorbed, PAR (0.4 to 0.7 μm). Over the past decade plant scientists around the world have studied many kinds of temperate natural and agricultural vegetation, and determined that approximately 2.5 to 3.5 gm of dry matter are accumulated for every megajoule of absorbed PAR (Monteith, 1977), depending on plant type. Estimating absorbed PAR requires both incident PAR and the fraction of PAR absorbed by the vegetation.

Photosynthetically active radiation constitutes about half of the solar radiation incident at the Earth's surface under a wide range of sun angles and sky conditions. Therefore, remote measurements of solar radiation at the surface of the Earth can be translated directly into PAR incident above can-

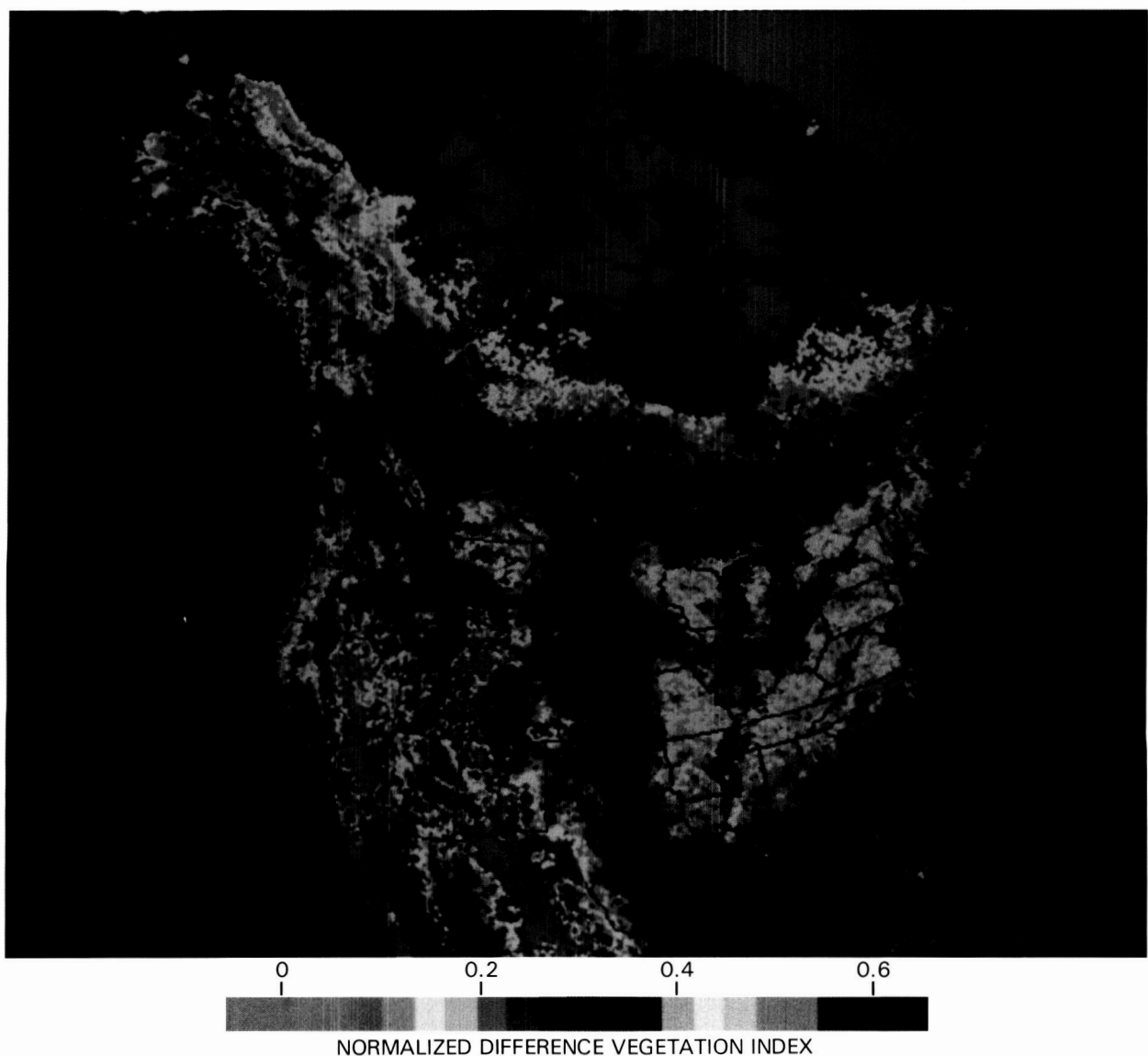


Figure 32. Relative intensity of vegetation over North America using AVHRR data integrated from April to November 1982 (courtesy of C. Tucker, GSFC).

opies. Eos will supply measurements of the atmospheric transmission, which along with geostationary cloud monitoring, will provide frequent measurements of incident PAR reaching the plant canopy.

The fraction of incident PAR absorbed by the canopy can be estimated from satellite measurements. A quantity identified as the normalized difference (ND) is linearly related to absorbed PAR (Figure 33) and given by

$$ND = (N - P)/(N + P) \quad (1)$$

where N refers to the reflected radiance in a near-infrared wave band (0.8 to 1.2 μ m) and P refers to the reflected radiance in the PAR visible wave band (0.4 to 0.7 μ m) (Asrar *et al.*, 1984). The normalized difference varies from near zero (approximately 0.1) with no vegetation to near unity (approximately 0.9) for a full vegetation cover (Asrar *et al.*, 1984).

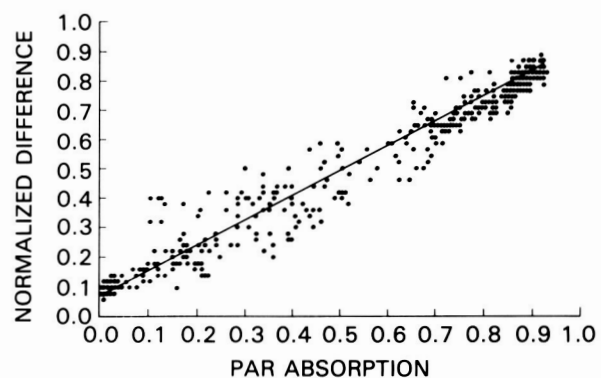


Figure 33. The normalized difference varies from near zero (approximately 0.1) with no vegetation to near unity (approximately 0.9) for a full vegetation cover (Asrar *et al.*, 1984).

no vegetation to near unity (approximately 0.9) for a full vegetation cover (see Figure 33). This variation occurs because both soil and leaves are relatively "dark" in PAR wavelengths, but in the near infrared, leaves scatter strongly and thus appear bright against the darker soil background. The result is that the ND increases with leaf area. Thus measurements of ND can provide estimates of both the amount of leaf area and the fraction of absorbed PAR. Therefore, measurements of daily solar radiation combined with normalized-difference measurements from MODIS, AMRIR, and at high spatial resolution, HIRIS, should provide productivity estimates over a moderate range of environmental conditions and time scales of weeks to months.

The usefulness of the relation between accumulated, absorbed PAR and productivity is enhanced by several factors for longer time scales. First, a correlation usually exists between radiation and other environmental factors that affect productivity, such as temperature. Second, this productivity-light relation is quite conservative because plants adapt to their environment by changing the duration of their various growth periods. Finally, plant productivity per unit of leaf area is relatively stable, so that the accumulated effect of many factors on productivity tends to be reflected in the amount of leaf area, given that the plant has sufficient time to respond (usually weeks to months) and thus maintain some sort of equilibrium with its environment. The effect of nutrient status is implicitly accommodated in the strong feedback between nutrient availability and leaf area.

Although much of the long-term effect on productivity of temperature, water availability, and nutrient availability is accommodated in the relation between productivity and absorbed PAR through leaf-area effects, for time scales less than several weeks, effects of plant type, temperature, and water availability are likely to be important as well.

Plant Type and Temperature Effects

The relationship between productivity, normalized difference, and incident solar radiation depends on plant type for several reasons. First, the relation between normalized difference and absorbed PAR depends on leaf orientation and spatial foliage distributions; to some extent this effect is accommodated by the normalized difference. Leaf orientations vary from mainly vertical in range grasses and crops like wheat to predominantly horizontal in crops such as sunflower. The spatial foliage distribution depends on whether the plants are randomly distributed, oriented in rows, or widely-spaced individual tree crowns.

Second, plant type can affect the conversion factor relating productivity to intercepted PAR and how this factor changes with water availability, temperature, or nutrient status. Third, the amount of fixed carbon used to maintain respiration depends

on plant type. This is especially true for perennial forests, where old trees may respire away a large fraction of the carbon fixed in photosynthesis to maintain their bulk (Waring, 1985). Fourth, the presence of senescent leaves can affect the dependence of dry matter productivity on absorbed PAR and normalized difference (Gallo *et al.*, 1985); plant type, water availability, and temperature can provide information about the growth stage and presence of senescent leaves. Fifth, the rooting depth depends on plant type, so that the size of the reservoir of stored soil water may be related to plant type.

Vegetation type may be distinguished by a time sequence of normalized difference observations (Badhwar *et al.*, 1982). High-resolution spectral measurements in the 0.45 to 2.5 μm wave band from MODIS or HIRIS may be useful in identification of some plant types.

In addition to spectral characteristics, satellite measurements in the 0.8 to 1.0 μm band at three view angles may provide identification of plant type (Goel and Thompson, 1984). Views fore and aft of the spacecraft, and near-nadir can be provided on Eos by MODIS-T or HIRIS. In a midday (within 1 1/2 hours of noon) polar orbit in the 0.8 to 1.0 μm wave band, the effects of the atmosphere are expected to be minor (Simmer and Gerstl, 1985), so that the vegetation is the major factor affecting this signal. Some canopy structural features may be extracted from SAR images using multifrequency-multipolarization data. The SAR will be particularly useful in areas of very large leaf area index, such as tropical rainforests, where optical measurements often saturate.

When temperature stress is present, the task of estimating productivity becomes more difficult. Plant temperature may be measured from space by the thermal channels of MODIS-N, the surface temperature channels of AMSU, and at finer resolution by TIMS. To determine productivity, remote thermal observations can be combined with plant-type information from MODIS, HIRIS, and SAR, and the results of ground-based research on how the productivity of specific plant types responds to temperature. In particular the dependence of plant respiration on temperature and plant type is critical.

Available Soil Water Considerations

Water stress often limits plant growth, and when this occurs water availability may have to be estimated from components of the crop water budget. The most difficult factor to deal with in predictions of plant productivity is available soil moisture. This is true whether one is using satellite observations or *in situ* surface observations. This difficulty arises because evapotranspiration, which is a major factor in determining the available water, is closely coupled to energy, water, and nutrient cycles. Available water is dependent on plant type because of variations in root depth, and because of the effect of a limited amount of water on productivity. To

make matters more complex, precipitation, the most important input to the surface water budget, appears to be difficult to measure on the 1 km spatial scale at the present time whether one uses rain gauges, ground-based radar, or satellite remote sensing.

Transpiration, which is that portion of evapotranspiration that passes through the plant, is only one component of the surface water budget; others are precipitation, drainage, soil water storage, runoff, and evaporation from non-plant surfaces. The Eos strategy for observing these components of the hydrologic cycle has been discussed in Chapter III and in the immediately preceding section of this chapter.

Drainage and runoff components often are small in vegetated areas except during very heavy rains that cause excessive runoff or cause the maximum soil water storage capacity to be exceeded. For the problem under discussion, the key is to determine when water availability is limiting plant productivity. The techniques described elsewhere for estimating soil moisture throughout the vegetative root zone and the rate of transpiration will provide the needed information for calculating productivity if they are applied at spatial scales of roughly 1 km.

An alternative method for estimating the effect of water limitations on productivity uses the ratio of remote observations centered on 1.65 and 1.25 μm wavelength bands (Rock *et al.*, 1985). If this method proves to be robust, then water-limited productivity estimates could be made without estimates of water availability from the water budget. These measurements could be made from MODIS-N. Perhaps the most promising method for measuring the water status of above-ground vegetation is with SAR. Multifrequency-multipolarization data may permit separate measurement of canopy water content, canopy structure, and surface soil water content.

Summary

The concepts outlined above can be used to provide a statistically sound estimate of the productivity of natural and cultivated vegetation on a continental scale from instruments that should be available on Eos and geostationary satellites. This information could provide a much needed terrestrial boundary condition to general circulation models that are being used for predictions of atmospheric CO_2 concentrations. The possibility of monitoring agricultural productivity on a regional scale offers a further benefit.

The use of MODIS and HIRIS to divide vegetation into categories such as coniferous forests, deciduous forests, range land, and several classes of agricultural crops is essential to the success of productivity estimates. The combination of nadir and off-nadir MODIS and HIRIS polar-orbiting measurements providing MODIS coverage every 2 days with half-hourly GOES measurements forms the

heart of the methods discussed here for productivity estimates. Neither polar-orbiting nor geostationary platforms are sufficient by themselves to provide productivity estimates; both are required.

The other instruments required to measure the parameters of the hydrologic cycle may be required on the same spatial scales at the same times. Thus, much of the total Eos payload is required to enable land plant productivity to be determined. The estimates of productivity, from a strategy such as that outlined above, would in turn provide carbon flux boundary conditions for climatic general circulation models for the purpose of predicting the influence of vegetation on climate and CO_2 balance. However, such a strategy could provide productivity estimates on much smaller scales to monitor the impact of natural and man-made disasters on agriculture or forest production; for example, loss of productivity from hail, flood, drought, disease, pest infestations, emissions from industrial sources, or perhaps acid rain.

The application potential of such a high-resolution, global-scale monitoring system will greatly add to our understanding of vegetation and agriculture.

WATER BALANCE DYNAMICS FROM LOCAL TO REGIONAL SCALES

Introduction

Understanding the interrelationship between land surface and atmospheric processes at different spatial and temporal scales is crucial for modeling the global hydrologic cycle. It is also largely an unsolved problem in hydrology.

Over the last 20 years or so, great effort has been spent in developing microscale models of hydrologic processes based on simplified equations of fluid mechanics. Simultaneously, hydrologists dealing with problems at much larger space and time scales (flood flow prediction, water supply, low flow estimation) have developed simple, lumped parameter macroscale models. These models ignore the microscale physics in their derivation and infer the nature of the hydrologic system primarily on the basis of input and output data. Research has not been done into the transition from microscale models to macroscale models with changes in the scale of analysis. Because we have a significant level of understanding with the various microscale elements in the hydrologic cycle, we often assume that these microscale elements and processes can be scaled up to the macroscale level through seemingly plausible causal chains. Unfortunately because of the stochastic variability of hydrologic inputs and system parameters, at some scale or characteristic dimension the mechanistic explanation breaks down (NRC,

1985). Furthermore, the linkage between parameterizations at different scales has not been adequately addressed or answered.

It is now being recognized that advances in the understanding of hydrologic processes will be limited until there is a better understanding of hydrologic scales (NRC, 1985; Beven, 1983). In a significant review of field evidence of the relationship between catchment scales and hydrologic response, Pilgrim *et al.* (1982) concluded: "hydrological relationships between small and large catchments are fundamental to a large range of hydrological works but to date the subject has not been treated in any comprehensive fashion." Dooge (1982), in discussing the application of field-scale data to hydrologic processes at the catchment scale, makes the following assessment: "...in linking phenomena on that scale (field scale of 10 to 100 ha) to the usual scale of catchment analysis (i.e., 100 to 1,000 sq km)...a number of approaches have been tried [but] this problem is largely an unresolved one."

The rest of this section discusses how Eos can be used to investigate hydrologic processes at catchment and regional scales. To understand the specific role of Eos, the hydrologic response at the catchment scale must be understood and a modeling strategy that utilizes Eos data for analyzing catchment-scale processes must be developed.

Hydrologic Response Within A Catchment

For analyzing the hydrologic cycle within a catchment, the boundaries of analysis will be, horizontally, the topographic ridge lines defining the

areal extent of the catchment; as an upper boundary, the land surface, including its vegetation cover; and as the lower boundary, an impervious boundary such that any vertical ground water movement can be ignored. For this system, the inputs will be fluxes across the boundaries: for example, precipitation, solar radiation, wind speed. The response to inputs are system outputs from the catchment and changes in water storage within the catchment. Outputs are streamflows, evaporation fluxes from soil, transpiration from vegetation, and ground water flows across catchment boundaries.

As Figure 34 shows schematically, the hydrologic response within a catchment is controlled by the fluxes of the hydrologic cycle. Figure 34 represents a tremendous aggregation of the processes, which are extremely variable in space and time. Hydrologically, it is convenient to divide the processes into those that dominate during rain events (precipitation inputs, infiltration, runoff production, and streamflow) and those that dominate during inter-storm periods (evaporation, soil moisture redistribution, and base streamflow).

The dynamics of the hydrologic processes are influenced by the spatial and temporal characteristics of the inputs and by the controls exerted by the land surfaces. These controls consist of factors such as soil, vegetation, and topography. Figure 35, which illustrates the variability in saturated soil moisture areas during a rain event, depicts the level of heterogeneity that is typically found within a catchment. The role of topography is clear; vegetation and soils exert an equivalent effect.

Hydrologists have tended not to model hydrologic processes at the detail represented in Figure 35. This is mostly due to the lack of data. The result is

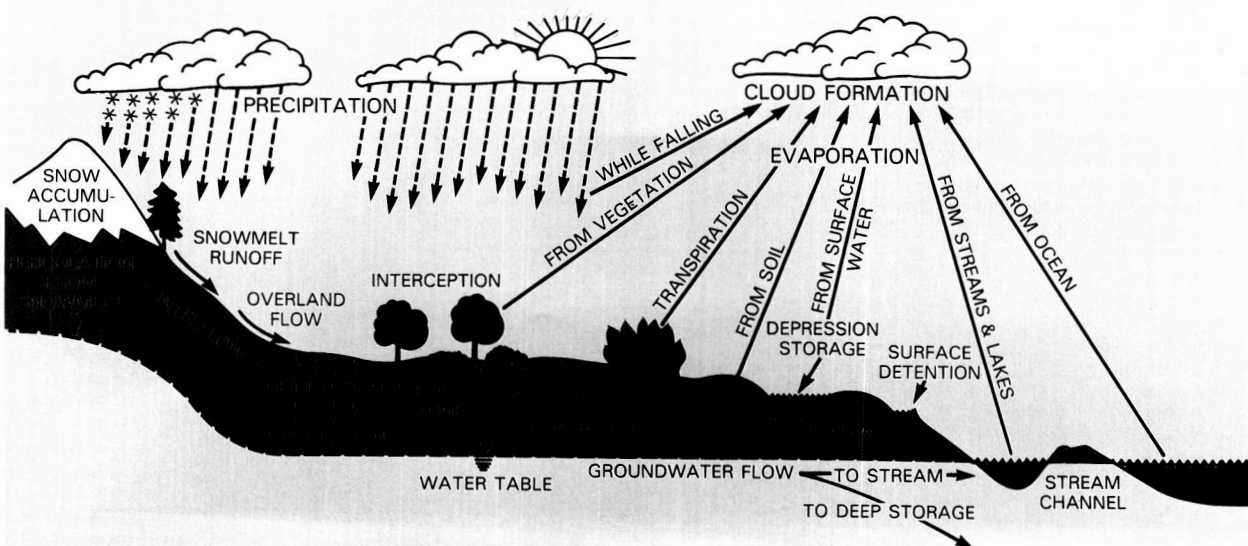


Figure 34. Schematic of the hydrologic cycle.

ORIGINAL PAGE
COLOR PHOTOGRAPH

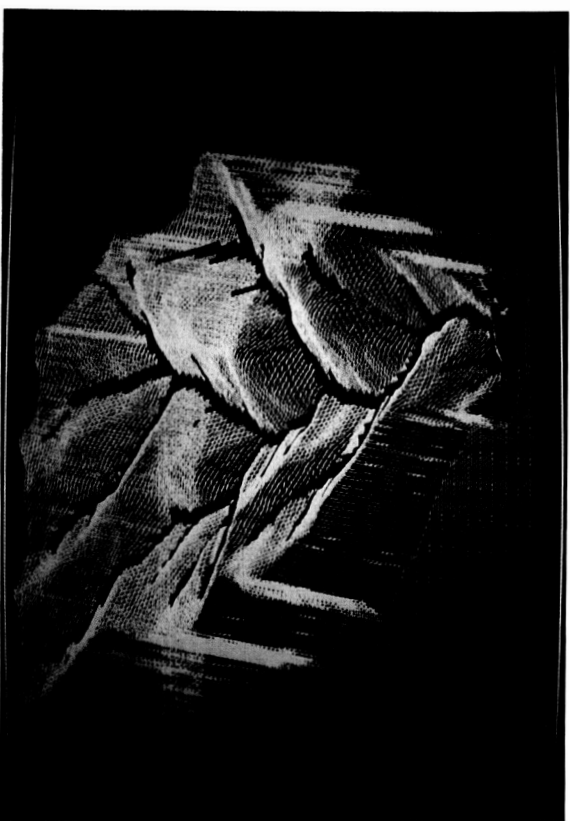
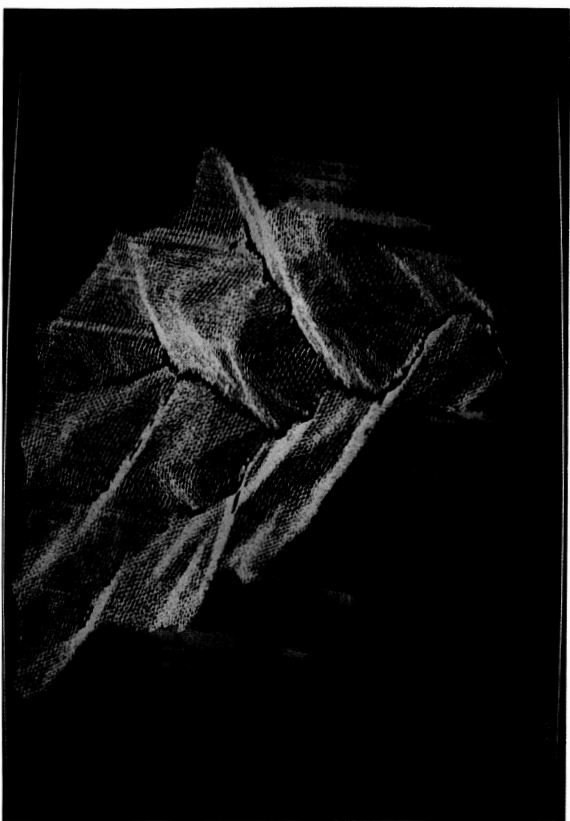
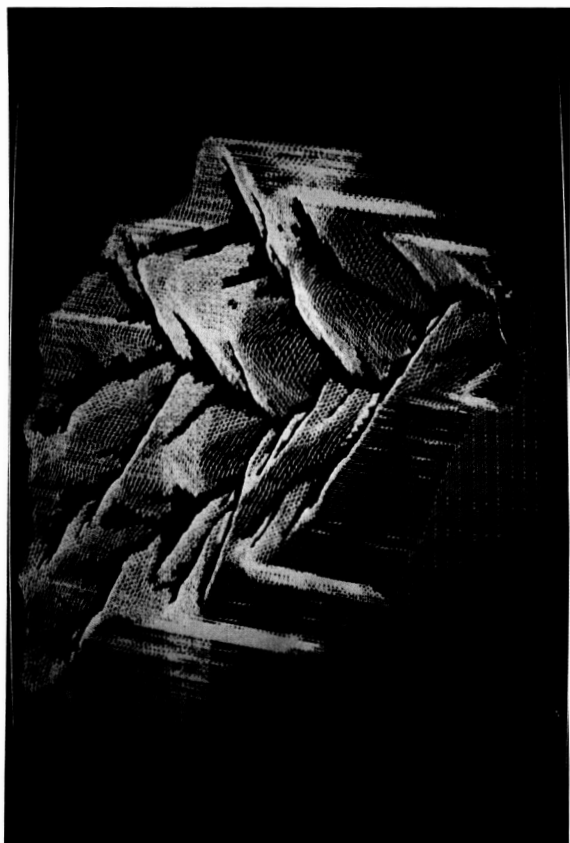
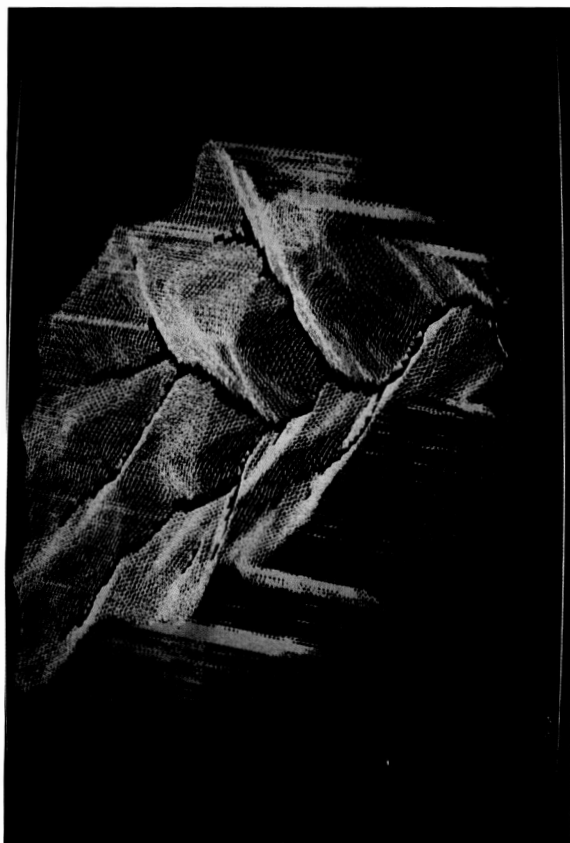


Figure 35. Illustrates the variability in saturated soil moisture areas during a rain event and depicts the level of heterogeneity that is typically found within a catchment.

that hydrologists lack an understanding of the spatial and temporal dynamics of the hydrologic water balance at the local scale, which is necessary to understand the dynamics at catchment and regional scales—the scales required for inputs into global climate models and large-scale meteorological models.

We contend that the problem can only be solved using Eos data in conjunction with field measurements.

How may we solve the hydrologic scale problem? Figure 36 illustrates the analysis. The left portion of the figure depicts the detailed, microscale representation of the hydrologic response illustrated in Figure 35. Temporally- and spatially-varied inputs lead to the distributed response, which can be modelled using a detailed distributed model. A schematic of such a model is given in Figure 37. The right portion of Figure 36 illustrates the typical “lumped” parameter model, where the inputs and parameters have been averaged spatially and accumulated temporally. This results in an averaged catchment response.

The important questions are: (1) What is the relationship between the parameterization of the detailed microscale model and the lumped macroscale model? and (2) What is the relationship between the aggregated outputs of the detailed model and the lumped response? The investigation of these questions requires both a modeling strategy and a measurement strategy.

Modeling Strategy

There are several potential approaches to deriving scale-dependent model equations for water balance dynamics. One reasonable approach would be to divide the analysis into three steps: (1) formulation of a microscale model for energy and moisture balances at the land surfaces; (2) calculation of the sensitivity of the microscale model to those parameters that vary spatially and temporally; and (3) derivation of the regional model by averaging the local model over space and time. Step 3 will assume constant those parameters found to be insensitive in step 2. Step 3 will also require an evaluation of space-time correlations for those parameters found to be sensitive. These correlations could be estimated from remotely sensed data (Zawadzki, 1973), ground measurements (Beven, 1983), or derived from theoretical considerations (Sivapalan and Wood, 1986).

The microscale model would start with the balance equation for energy and water at the land surface. Eagleson (1978) developed a local-scale model for water balance based on water flux models at the land surface. Eagleson's model could serve as a starting point for the averaging described herein. Its disadvantage is the difficulty of incorporating Eos observations within the model structure without additional modeling.

Consider the energy and water balance. The net radiation absorbed at the surface is balanced by three

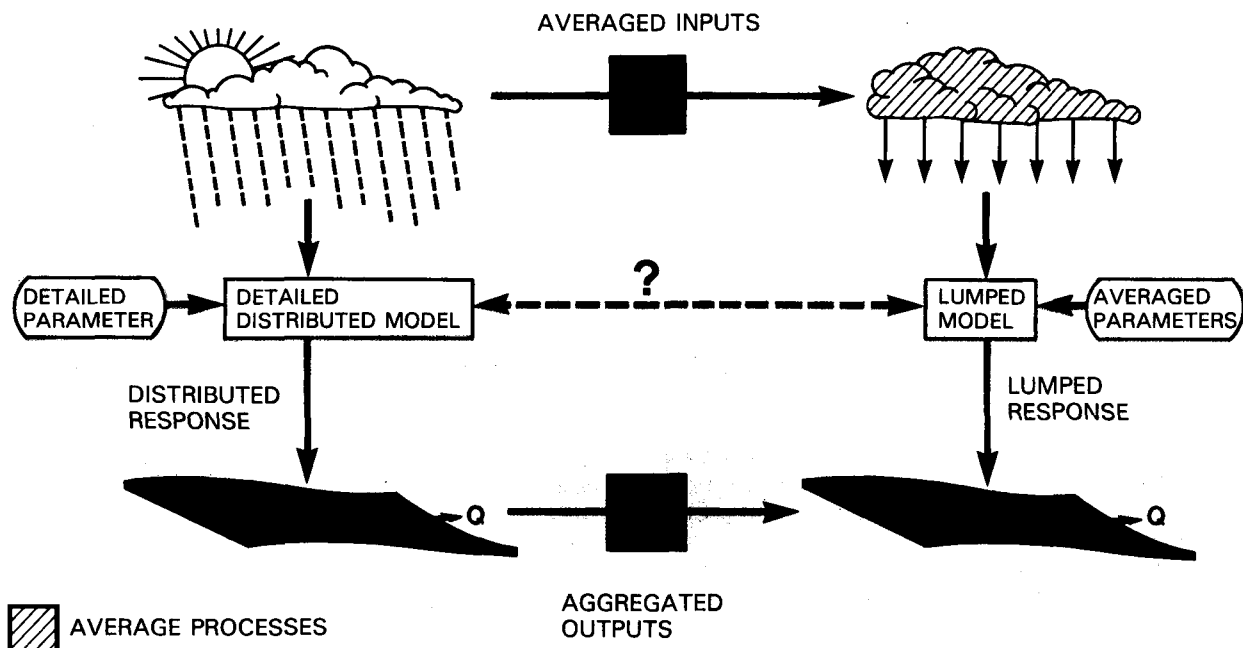


Figure 36. Schematic of modeling hydrologic responses at the catchment scale.

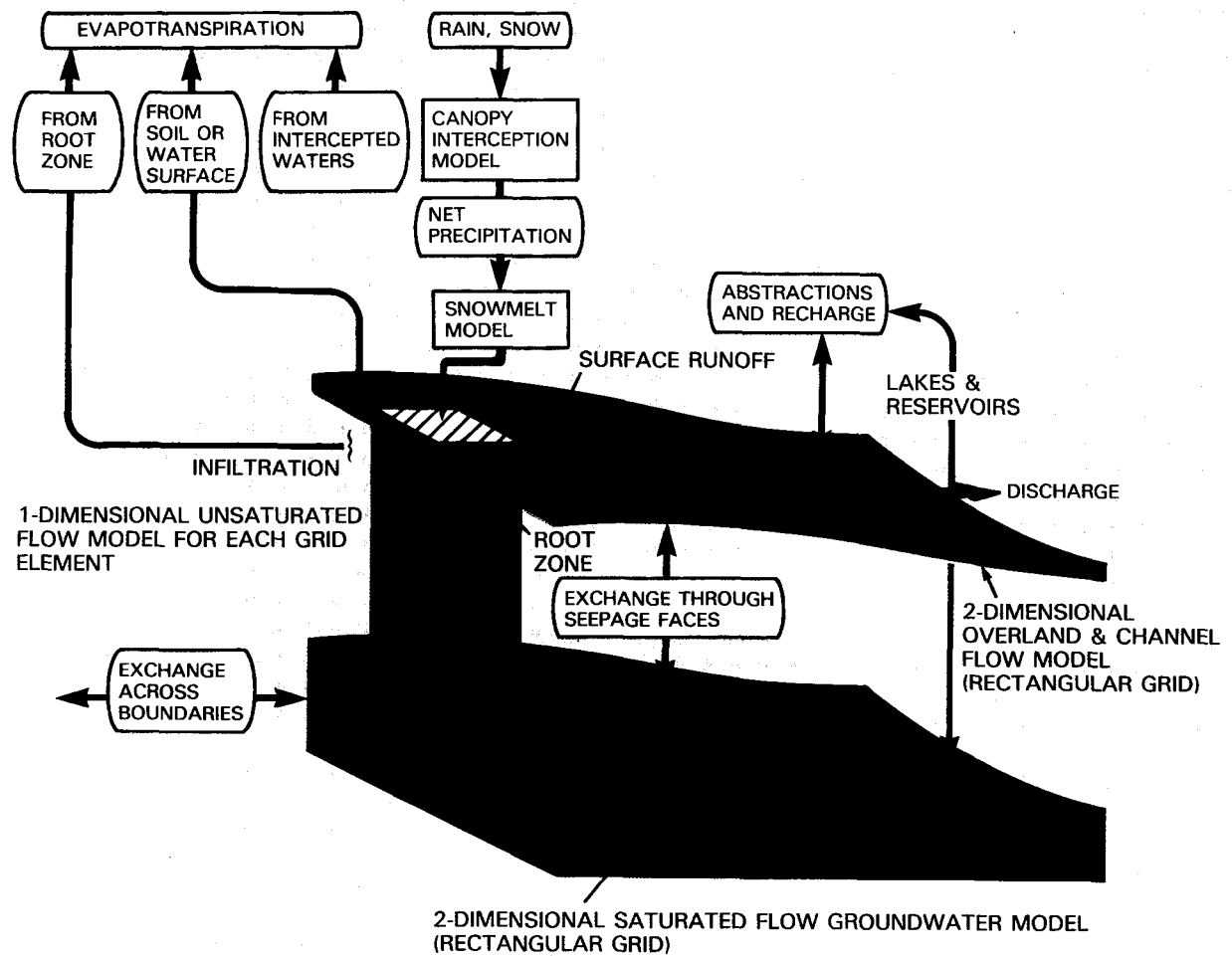


Figure 37. Distributed hydrologic models represent the interactions of numerous processes through conservation equations on a horizontal grid.

energy components: heat flux into the soil, the sensible heat flux from the surface to the atmosphere, and the latent heat flux. For water balance, the major components are precipitation, evaporative flux, total surface and subsurface runoff, and the change in storage as snow, ice, or soil moisture. In principle, the continuity equations for conservation of energy and water are then solvable and coupled through the required equality of the evaporative and latent heat fluxes. Measurement strategies to accomplish this are detailed in Chapter III.

The mass balance for water at the land surface-air interface can be modeled in more detail. One of the most difficult terms is the evaporative flux from soil and vegetation. The evaporation terms can be approached from two directions: by modeling the latent heat flux equations or by modeling the water balance equations when it is not raining and there is no active surface runoff. In the latter case, the move-

ment of water in the soil is dynamically coupled to heat transport. The local change in soil moisture with time depends upon a hydraulic conductivity constant, a moisture diffusion term, and a temperature diffusion term; the latter two are weighted by their respective gradients, i.e., the change in moisture with depth and the change in temperature with depth.

The temperature gradient with depth appears in both the soil moisture equation and the equation for the temperature dynamics at a point in the soil. This term couples soil moisture and temperature. The equations are also coupled through the moisture gradient, since thermal energy is required for the phase change of soil moisture to water vapor. Thus, one has a model of a system where the surface gets heated up, some of this sensible heat conducts into the soil profile, vaporizes water, and diffuses out of the profile into the atmosphere. This results in both a vertical moisture gradient greater than the equilibrium

gradient under gravity alone and a temporal change in soil moisture for any particular depth in the soil column.

The soil column can be viewed as experiencing an evaporative stress whose magnitude varies diurnally due to changes in the radiation/energy balance at the land surface. The soil column will deliver moisture to the surface (i.e., will exfiltrate) at a rate equal to the potential rate that is governed by the evaporative stress, or at a lesser rate if the soil column is unable to deliver water faster. Soon after a precipitation event, evaporation usually occurs at the potential rate. As the soil surface dries out, the delivery of water depends upon the soil hydraulic conductivity term. When the soil begins to dry out (say from 90 percent to 60 percent saturated) the soil conductivity drops by about two orders of magnitude. The relationship between soil suction gradient (constituting one of the forces influencing water movement) and the moisture hydraulic and diffusive properties is soil dependent.

The moisture vapor diffusion coefficient depends on both soil properties and near-surface air properties, the latter being affected mostly through the diffusion coefficient for water vapor, which in itself depends upon surface variables like wind. To model evaporation fluxes from soil surfaces at a point (i.e., not over large spatial scales) requires a set of linked partial differential equations. The change in storage in the soil and how it is distributed, and the evaporation from the soil surface may all be modeled by solving these equations in three dimensions given suitable boundary conditions. This leaves open the question of specifying suitable boundary conditions through measurements. Computationally, solving this problem is probably infeasible at the present time. Nevertheless, advances in parallel and vector processors and in numerical modeling suggest that such computation will become fairly routine in the Eos timeframe.

Measurement Strategy

The parameterization of a microscale model for water balance dynamics is possible today from ground-based observations. Since the microscale model can be parameterized and solved, the sensitivity analysis of step 2 can be carried out. The sensitivity analysis should result in a categorization of the parameters into three groups (Jackson, 1985): (1) variables that were essentially independent of surface type or spatially invariant; (2) variables that are highly dependent on the surface condition; and (3) those that are surface-dependent but time invariant. An example of the first is incoming solar radiation; of the second, reflected solar radiation or infiltration; and of the third, soil properties or surface roughness.

Measurements on the first group can be carried out remotely at low resolution or by ground observa-

tions and averaged over large areas. Measurements on the third group would require intensive short-term, high-resolution remote and ground truth observations. The second group, the surface-dependent variables that show spatial and temporal variation, must be observed remotely with Eos instruments. If the observations can be carried out at resolutions finer than the correlation lengths of the variables, the local-scale model can be solved pixel-by-pixel. For this case, the regional water balance dynamics can be derived directly from the microscale model. If the observations are at resolutions that are too coarse, macroscale models must be developed at the appropriate regional scales.

In modeling water balance dynamics, the evapotranspiration term is most critical for accurate estimation of energy and water flux transfers at the land surface. Modeling approaches for assessing evapotranspiration at regional scales include the work of Rosema *et al.* (1978), Soer (1980), Carlson *et al.* (1981), Gurney and Hall (1983), Camillo *et al.* (1983), and Gurney and Camillo (1984). For the most part, emphasis is placed on using remotely sensed surface temperature. For the work described in the previous section, more ambitious measurements are needed. These measurements are feasible under Eos and are described in the next section.

Data Needs From Eos

Eos instruments are necessary to determine boundary conditions that represent inputs and parameters for the scale-dependent models. Consider the general case of a soil with vegetal cover during an inter-rainstorm period when evapotranspiration components dominate the water and energy balance models. The parameters that must be remotely sensed include land temperature and atmospheric diffusion. Land temperature can be remotely sensed by AVHRR, MODIS, and TIMS (for example) at spatial resolutions from 1 km to 30 m.

The atmospheric diffusion coefficient for water vapor is more complicated and its value will probably be inferred through a model. The diffusion coefficient is a function of air temperature, surface wind, and vegetal canopy characteristics. The air temperature must be modeled based upon data from sounders like HIRS, AMSU, or from VAS on the GOES system along with spot measurements by LASA. Wind measurements require LAWS at about 100 km horizontal resolution, even though a modeling approach based upon horizontal temperature gradients can be made (particularly outside the tropics). A third approach particularly useful in the tropics is utilization of geostationary image data to track clouds and model from cloud velocity to surface wind speed. Vegetation cover and status can be remotely sensed using MODIS and HIRIS, the former at a 500 m resolution and the latter at 30 m. Surface soil moisture at 10 km spatial resolution will

be provided by ESTAR. SAR will provide similar measurements but at 30 to 500 m resolution. These observations can be used to filter the micro-to-macroscale model and to help verify and calibrate the macroscale models.

An alternative route for analyzing the terrestrial water fluxes is to start with a large-scale parameterization model, for example, the potential evapotranspiration model of Penman (1948). Here the potential evapotranspiration is related to the slope of the saturation vapor pressure curve, the net radiation, and the density per unit area and the relative surface soil moisture, which can be observed using ESTAR and SAR.

Further modeling is required to link transpiration from the vegetated areas to depletion of moisture in the soil. Similarly, the estimation of soil moisture profiles from surface moisture is complicated in many climatic areas due to crusting and drying of the soil surface. This drying reduces the hydraulic conductivity so much that delivery of moisture to the surface from the soil column is almost nonexistent. In more humid climates with well-textured soils, this surface drying tends not to occur to the extent described. Thus, the need for *in situ* measurements to augment remotely sensed variables is important.

Similar arguments can be made in examining the energy and moisture balances of snow-covered areas. MODIS, HIRIS, and TIMS may be used to determine snow-covered area, snow-surface temperature, and albedo. SAR and AMSR may be used to determine snow-covered area, snow volume, and snow water equivalent required for input into snow energy and moisture balance models similar to those described above for vegetation-soil interactions.

For daily averaging, the sensible heat flux term can usually be ignored. Net radiation can be easily represented by a balance equation for incoming and outgoing shortwave and longwave radiation. The strategy for obtaining these variables from Eos plus geostationary observations is described in Chapter II.

It is feasible to measure boundary conditions using remotely sensed data and then to model the variables required for estimating potential evapotranspiration. Actual evapotranspiration could be obtained from the potential rate by adjusting the potential by two normalizing constants: the fraction contributed to vegetation that would be related to the vegetation density per unit, and the relative surface soil moisture, which can be observed using ESTAR.

Complicating Factors

As pointed out by Jackson (1985) for the case of estimating regional and local evapotranspiration, there are numerous complicating factors that affect the estimation of water balance dynamics. Two major ones are briefly mentioned here.

- *Temporal Averaging*—Remote sensing will provide instantaneous measurements at varying spatial resolution with approximately 2- to 4-day repeat periods. These data must be utilized in such a way as to maximize their information.
- *Calibration*—Inadequate instrument calibration can cause significant errors in model outputs. Jackson (1985) showed that a 1°C error in surface temperature estimation can lead to a 40 percent error in evapotranspiration estimates.

It is critical that adjoint analysis or sensitivity analysis be performed to evaluate the required accuracy of instruments. This is needed for the design of adequate in-flight calibration procedures.

Concluding Remarks

From this discussion, it is clear that Eos observations will contribute to modeling the terrestrial moisture and energy fluxes. Significant research remains to resolve the inconsistency between the equation scale and the Eos observation scale. We must address questions such as: Are the point process equations correct/relevant/appropriate at the measurement scale of tens of kilometers? We must determine how to spatially average the point equations, over heterogeneous spatial and temporal scales to the measurement scales. And finally, modeling is required to infer the equation parameters from the basic Eos observations, since in many cases direct observation of the equation variables is not possible.

Modeling the terrestrial water balance is thus a feasible but nontrivial problem. Even starting with a large-scale parameterization model for water fluxes will require substantial auxiliary modeling to transfer Eos observations into the required model variables. On the other hand, without the Eos observations, no progress can be made beyond the model formulation stage. Observations, particularly remote sensing from space, are necessary to verify model formulation and supply model inputs over significant geographic areas.

INLAND AQUATIC ENVIRONMENTS

Introduction

Inland aquatic environments consist of rivers, streams, lakes, and wetlands. These environments each play significant roles in global hydrologic and biogeochemical cycles. For example, standing waters such as lakes and wetlands store the freshwater essential to life. Running waters such as rivers and streams, which drain the landscape, are the conduits for most water and solutes passing from the con-

tinents to the oceans. Both running and standing waters are sites of important biogeochemical processes such as the production of methane, nitrous oxide, and carbon dioxide and the fixation of carbon and nitrogen. In contrast to forests and grasslands, the importance of inland waters in global cycles arises more from high rates than from large areas.

Aquatic ecosystems are widely distributed on the continents (Figure 38; Taub, 1984) and often have complex and variable outlines (Figures 39 and 40). Biogeochemical processes active in these waters are strongly influenced by their watersheds and air-sheds and can, in turn, modify their surroundings.

Wetlands border most inland waters. Examples are the broad expanses of floodplain in the Amazon, papyrus swamps in eastern Africa, and bogs in Siberia. These aquatic habitats often consist of a mosaic of open water with plankton and submerged vascular plants, floating macrophytes, and emergent plants that range in height from centimeters to many meters. To illustrate, Figure 41 shows the variety of morphologies represented in one major wetland type, African papyrus swamps. Abrupt changes in size of these and other habitats can be frequent; modifications by human activities can be severe.

Because a rich variety of scientific questions concerning wetlands (Gaudet *et al.*, 1981) are especially well suited to investigation by Eos, wetlands are the focus of this section. The swamps

and floodplains of the tropics will be emphasized because Eos may well be the only way to examine these ecosystems in the repetitive, synoptic manner required for their understanding.

There are major scientific questions concerning the role of tropical wetlands in global biogeochemical cycles of carbon, nitrogen, and sulfur (NRC, 1985; NRC, 1986b). Recent evidence of elevated concentrations of trace gases such as N_2O , CH_4 , CH_3Cl , H_2S , and isoprene over tropical regions may indicate that tropical forests and wetlands are significant sources of these trace gases. Species such as isoprene are involved in atmospheric photochemical reactions, which influence concentrations and perhaps global budgets of tropospheric gases such as CO and O_3 . The concentrations of other gases such as CO_2 and CH_4 are increasing globally (Weiss, 1982; Rasmussen and Khahl, 1981) and may influence the Earth's radiation budget and, consequently, its climate. Therefore, it is essential to understand the factors that determine the fluxes of these gases under both natural and perturbed conditions.

In the following sections, we briefly describe the research required to define the role of tropical wetlands in global biogeochemical cycles and their influence on tropospheric chemistry. This research effort divides into two parts:

1. Determination of the geographic distribution and areal extent of wetlands; and

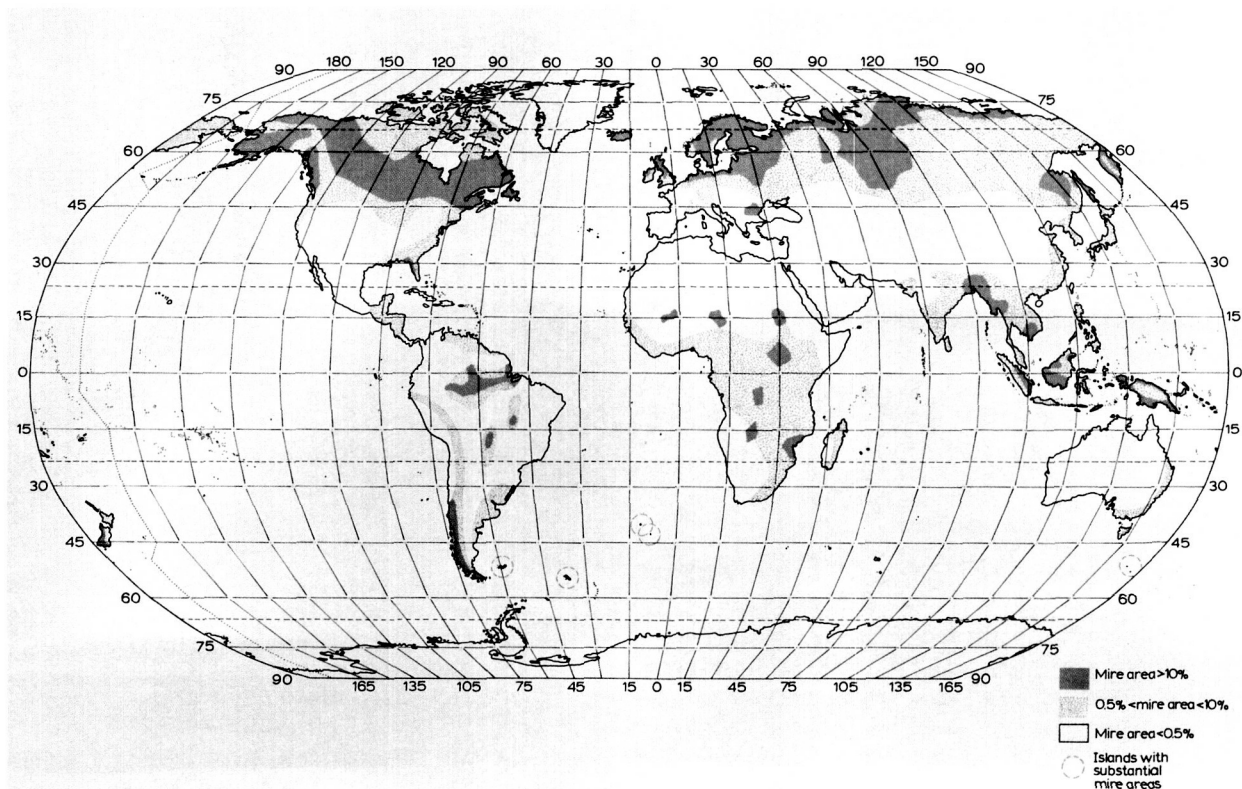


Figure 38. World-wide distribution of mires (from various sources, and approximate only; detailed information is available only for rather limited areas; Gore, 1983).



Figure 39. Map of forested wetlands in Florida prepared by Mark Brown (from Ewel and Odum, 1981).

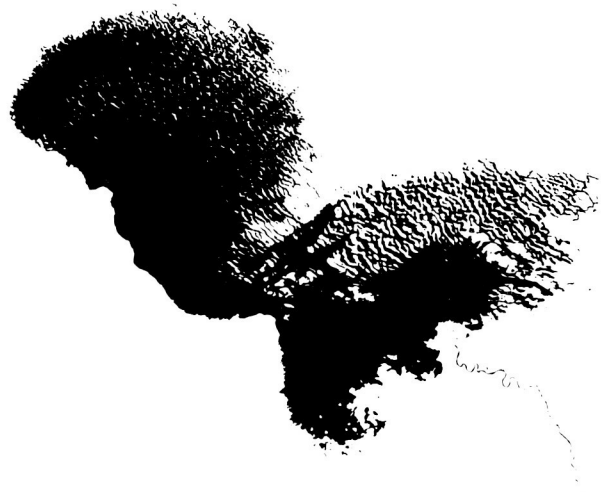


Figure 40. Water surface of Lake Chad (January 1973) from a satellite photograph (from Carmouze *et al.*, 1983).

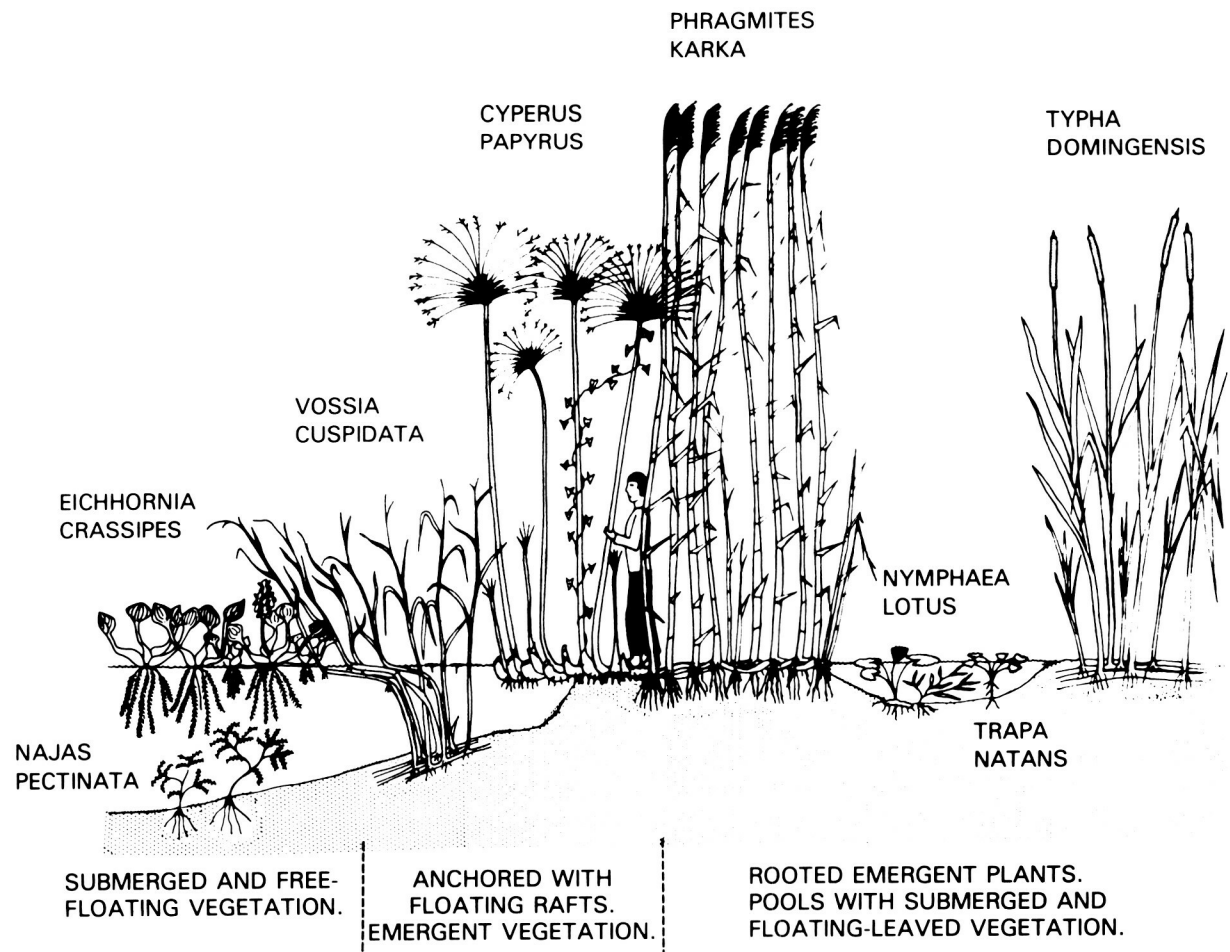


Figure 41. Theoretical compiled transect of vegetation at the fringe of a swamp in the northern Sudd. The person is drawn to give an indication of vertical scale. The horizontal scale is flexible and arbitrary and may represent kilometers (from Denny, 1984).

2. Measurement of the gas exchanges between the wetlands and the atmosphere, adjacent waters, and sediments.

Remote sensing can be directly applied to objective 1. Objective 2 requires a combination of surface and satellite measurements, as well as modeling of the observed processes.

Areal Extent of Wetlands

An inventory of the extent and distribution of wetlands is a critical step in identifying their current and future role in global cycles. At present, coarse resolution inventories for the Earth are available (Matthews and Fung, 1987). The U.S. National Wetlands Inventory is an excellent example of a regional wetland mapping scheme derived in part from aerial photography, but its classification is too detailed for a global inventory. Recent application of Landsat's Thematic Mapper to wetland inventory in North America indicates the major role satellite imagery will play in establishing the extent and distribution of wetlands.

The spatial scale required for a wetland inventory is a critical issue, because wetlands are very heterogeneous and dissected, but can cover vast areas. Therefore, a stratified sampling scheme such as that provided by near simultaneous imagery from MODIS and HIRIS is required. The spectral information provided by MODIS and HIRIS is needed to recognize vegetation types (Tucker *et al.*, 1985; Gross and Klemas, 1985); to apply generalized algorithms for vegetation discrimination will require proper atmospheric correction. The presence of MODIS and HIRIS on the same satellite should substantially improve the possibility of adequate atmospheric correc-

tion. Because radar imagery permits identification of flooded areas, SAR imagery will complement the MODIS and HIRIS. Furthermore, as progress is made in interpretation of SAR signals, discrimination of vegetation types will become increasingly accurate and sensitive (Simonett and Davis, 1984).

An important aspect of mapping and monitoring the areal extent of wetlands is to detect changes: gradual natural and man-related changes, or episodic events with large impacts such as introduction of exotic species, floods, fires, strong winds, insect outbreaks, toxic or nutrient-rich inflows, or abruptly reduced water levels. Complementary application of MODIS, HIRIS, and SAR will be critical for detecting not only changes in areal coverage but also of vegetation type and physiological condition. For example, in many tropical waters introductions of exotic floating macrophytes has caused major ecological problems (Gaudet *et al.*, 1981). Frequent movements of large floating mats is one aspect of such infestations, and these can be readily observed from satellite (Figure 42).

Biogeochemical Processes in Wetlands

Evaluation of biogeochemical processes within wetlands, and exchanges between wetlands and other systems, depends upon identifying characteristics observable by Eos that have well-defined functional connections to these processes and exchanges. The hydrologic regime includes observable characteristics that are linkable to physical, chemical, and biological features associated with biogeochemical processes (Gosselink and Turner, 1978). As shown below, Eos can directly measure the hydrologic regime and the

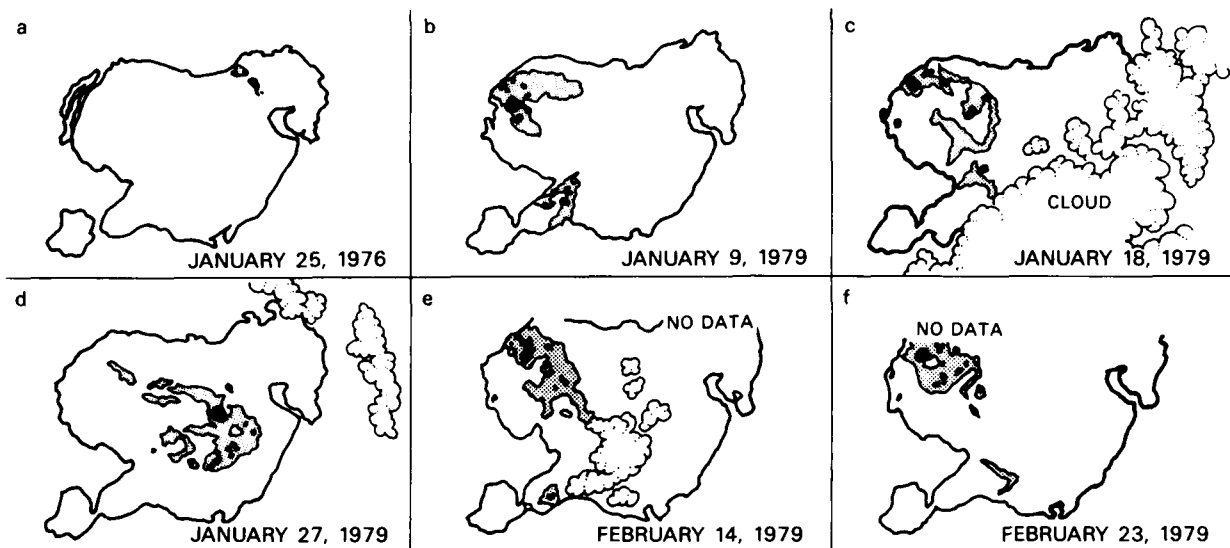


Figure 42. Floating papyrus and *Salvinia* islands, Lake Naivasha, Kenya: a-f shows movements of these aquatic macrophytes mapped with Landsat images (from Gaudet and Falconer).

water turbidity, and indirectly provide estimates of the primary productivity and the gas fluxes—two important biogeochemical processes.

First, SAR observations permit direct determination of the hydrologic regime. The ability of SAR to penetrate clouds and vegetation, its clear detection of calm water typical of wetlands, and its high spatial resolution permit repetitive measurement of flooded areas. The less than total areal coverage of a particular SAR swath should seldom cause serious limitations because water levels vary uniformly over large regions in most wetlands. Furthermore, the changes in shoreline topography are sufficiently slow to permit the compilation of regionally complete maps over a period of months to years. Monitoring shorelines with SAR as water levels vary will permit topographic mapping, a necessary aspect of estimating extent of inundation. Laser altimetry will be useful for reference and intercomparison, although its low repetition rates, restricted number of laser pulses, and inability to penetrate clouds will limit its contribution to topographic mapping for this purpose.

Second, turbidity in wetlands is caused primarily by inorganic sediments transported by inflows or resuspended from the substrata, and organic matter produced locally. The fine spectral resolution provided by HIRIS should permit identification of this suspended material. From their spectral signatures, some suspended minerals can be identified (Goetz and Rock, 1983) and used to trace the origin of the water inflows.

Third, evaluation of primary production and occurrence of plant stress can be obtained by HIRIS observations of the floating and emergent macrophytes (Goetz and Rock, 1983; Hardisky *et al.*, 1984; Gross and Klemas, 1985). The reflectance curve for healthy plants has strong chlorophyll absorption at 480 and 680 nm, weak chlorophyll absorption between 520 and 600 nm, and a sharp rise in reflectance between 680 and 1,000 nm (the red edge). Both the position and slope of the red edge change as the leaf develops; this change permits evaluation of phenology, growth rate, and stress under some circumstances. Fundamental stretching frequencies of organic bonds in the visible and near-infrared, which are observable by HIRIS and are indicative of concentrations of nitrogen, phosphorus, starch, and sugar in leaves, can provide additional data for assessing vascular plant productivity and health (Spanner *et al.*, 1985).

Fourth, estimation of gas fluxes from wetlands to the atmosphere requires combination of several Eos observables. For example, recent measurements of methane fluxes in the floodplain of the Amazon River have identified the hydrologic and biotic conditions associated with very high fluxes (Sebacher *et al.*, 1985). In particular, falling water levels and mats of floating grasses produced the highest fluxes. Extrapolation of these results to the whole Amazon

basin requires integration of data that include patterns of inundation and macrophyte distributions. As an example of the application of Eos to tropical wetlands, an experiment designed to measure methane flux from the Amazon basin is described.

The Amazon is the world's largest river system, draining much of South America and discharging about one fifth of the freshwater reaching the world's oceans. Bordering the Amazon River and its major tributaries is a *circa* 100,000 km² floodplain. The floodplain is a mosaic of open water, flooded forest, and floating meadows that change in area as the rivers rise and fall each year. The dominant seasonal cycle in the central Amazon basin is a 10 m variation in water level, and the floodplain lakes function as capacitors and chemical reaction vessels as they are filled and drained. For much of the year the waters deeper than 3 m and those under floating meadows are anoxic and contain considerable dissolved methane. As the water levels fall and the hydrostatic pressure is reduced, large fluxes of methane bubbles occur (Sebacher *et al.*, 1985).

In mid-1985 NASA conducted coordinated ground and aircraft observations to investigate the role of the Amazon in global biosphere-atmosphere interactions. The Amazon Ground Emissions (AGE) and Amazon Boundary Layer Experiments (ABLE) quantified the emission of key tropospheric gases from Amazon forest soils and canopies and floodplains and examined meteorological transport from ground sources to the atmospheric boundary layer. The results gained from these studies support the global importance of the Amazon basin and strongly indicate the need for synoptic coverage of the whole Amazon and repetitive examination of selected regions. Eos provides the opportunity to conduct such research.

The inputs and resulting physicochemical and biological processes that lead to methane emissions from the Amazon floodplain are diagramed in Figure 43. The factors are: (1) the production of organic carbon by the floating meadows, (2) the formation of anoxic environments where the organic carbon is decomposed, and (3) the vertical entrainment of anoxic water and the decline in water level that release the dissolved methane. The growth of the macrophytes is initiated by the inundation of the floodplain by turbid, nutrient-rich river water.

Satellite-borne sensors on Eos can provide much of the required information. SAR will provide the majority of the information; HIRIS will add complementary data when viewing conditions permit. ADCLS linkages from ground-based stage readers will augment the remotely sensed data. In addition, verification of the functional relations between Eos observables and actual methane fluxes will require field measurements with floating chambers and eddy correlation methods. Remote sensing of methane from Eos may provide the large-scale indication of concentrated sources. This would involve the mea-

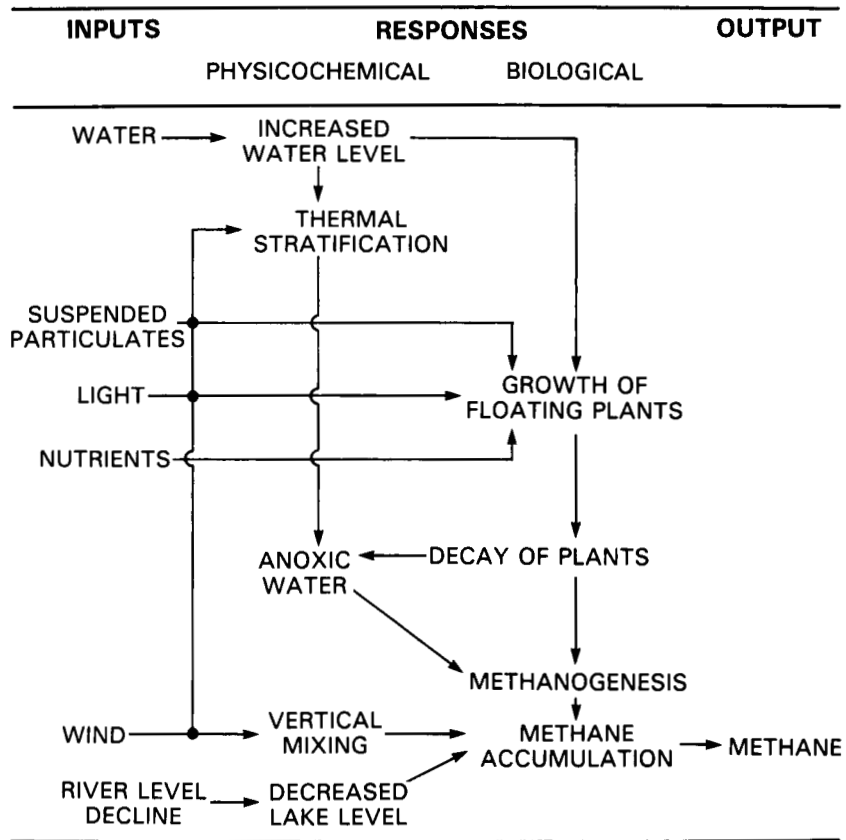


Figure 43. Inputs and resulting physicochemical and biological processes that lead to methane emissions from the Amazon floodplain.

surements of the CR and NCIS instruments. Further aspects of this are discussed in a later section on tropospheric chemistry.

Two sampling designs are appropriate and dictated by the narrow swath widths obtainable with the high spatial resolution needed because of the heterogeneity of the Amazon floodplain. Three areas (each one swath wide) will be examined with biweekly SAR coverage repeated throughout the year to determine growth and decay dynamics of the floating meadows and the extent of inundation. Whenever clouds permit, HIRIS imagery will be obtained for these same swaths to improve characterization of the physiological condition and productivity of the macrophytes. To increase the number of HIRIS scenes will require pointing from all possible orbits with guidance from some sensor about cloud cover. These repetitive applications of SAR and HIRIS will use multiple look angles, wavelengths, and spectral regions and, therefore, generate high data rates. Maximal coverage of floating meadows usually occurs at the onset of the dry season in June. At this time both HIRIS and SAR data will be used to map the areal extent of the communities for the entire basin.

Summary

Wetlands play a major role in global cycles as sites of very high carbon and nitrogen fixation and as sites of gas production. Eos sensors can provide measurements of areal extent of wetlands and of biogeochemical forcing functions such as the hydrologic regime. Such measurements are essential if global estimates of biogeochemical processes associated with wetlands are to be made.

Further evaluation of the seasonal, interannual, and episodic variability of processes such as gas fluxes requires modeling that combines satellite and ground-based measurements.

INTRODUCTION TO OCEANIC PROCESSES

The next four sections demonstrate the use of Eos in the study of selected oceanic problems including biology, dynamics, polar sea ice, and air-sea interaction. The purpose of this introduction is to set these studies in context through a brief description of

the ocean and its importance to the world climate system.

The ocean covers about 75 percent of the Earth's surface area and has a mean depth of 4 km. The ocean circulation is made up of a mixture of time-averaged flows such as mean currents, and a variety of time-dependent flows such as ocean eddies, upwelling, and a large number of wave-like motions. Alternatively, we can think of the ocean circulation as a large Reynolds number turbulent fluid, where the energy of ocean currents is dissipated into cascades of turbulent eddies.

Except in the polar regions, the ocean is warm at the surface, and cold at the abyssal depths. A sharp region of density transition divides the ocean into two parts; a 300 to 1,000 m thick less-dense upper layer, and an approximately 3 km thick dense lower layer. The density transition is called a pycnocline, or if the stratification is caused by temperature only, a thermocline.

The water in each of these layers renews its content of oxygen and other atmospheric gases through periodic contact with the atmosphere. Radiocarbon observations show that the water residence time of the two layers is very different—of order 10 years for the upper layer and 1,000 years for the lower. Because of these profoundly different time scales, the two layers play distinct but important roles in ocean circulation. In each layer, the atmospheric gas content is renewed through equilibration with the atmosphere at the surface. In certain areas, surface processes also increase the water density. Evaporation accomplishes this in the subtropics, while cooling is responsible in the subpolar oceans. For each layer, this density increase causes the water to sink into the layer interior, following which the water moves laterally, then returns to the surface through upwelling.

For the upper layer, this initial sinking or subduction is enhanced by a wind-driven surface convergence at mid-latitudes, so that the upper layer subduction primarily occurs in the mid-latitude gyres, such as the Gulf Stream system in the North Atlantic. Other similar systems lie between 15° and 45° latitude north and south. The return upwelling occurs along the eastern oceanic boundaries, which are the continental west coasts, and in the equatorial region between 15° north and south. The cycle or residence time for this process has been measured through radiocarbon techniques, which suggest that the residence time of water in the upper layer is of order 10 years.

Because this decadal time scale is comparable to the scale at which carbon dioxide is being added to the atmosphere, the upper layer may play a major role in the removal and storage of atmospheric carbon dioxide. In this cycle, the surface waters equilibrate with the carbon dioxide in the atmosphere. Because of the large surface area involved, a

significant portion of the added carbon dioxide is absorbed in the upper ocean. The waters then sink due to the combination of the wind-forced downwelling and increased density. When these waters return to the surface again in 10 to 20 years, the water re-equilibrates with the now higher atmospheric carbon dioxide concentration, removing another fraction of the atmospheric load, and so forth.

For the lower abyssal layer, evidence from radiocarbon measurements suggests that the residence time is of order 500 to 1,000 years. The atmospheric gas content of this deep water is renewed at a few small subpolar geographic areas, where extreme cooling makes the surface water dense enough to penetrate the pycnocline. These bottom-water renewal regions include the Norwegian/Greenland Seas in the North Atlantic, and the Weddell Sea of the Antarctic Ocean. The sinking of surface water in these regions renews the oxygen of and cools the bottom water. Once this water sinks, it circulates slowly throughout the world ocean, then upwells back to the surface, providing the 500- to 1,000-year cycling time. Because the chemical equilibration time of CO₂ between the atmosphere and the surface mixed layer is of order 1 year, while the cooling time for this water is of order 1 month, the abyssal circulation may not be as important to the removal of atmospheric CO₂ as the upper layer circulation. Thus the ventilation of the abyssal ocean has an unknown but possibly significant impact on the cycling and storage of carbon dioxide.

The ocean is also important in the generation of weather and climate. Heat, water vapor, and momentum are exchanged across the air-sea interface. Further, as events like the 1983 El Niño show, changes in the circulation of the equatorial Pacific are associated with large-scale changes in planetary weather. The large surface area of the ocean and sparse number of island and shipboard meteorological observations make satellite data essential for investigation of these processes.

The ocean moderates changes in the Earth's climate because of the great mass of the ocean and its large heat capacity relative to air. Climate models show that the decadal circulation of the upper ocean layer also removes heat from the atmosphere and thus slows the rate of long-term atmospheric warming. The ocean current systems are also important to world climate studies. Through current systems such as the Gulf Stream and the Kuroshio, the oceans transport heat meridionally. For example, in the northern hemisphere between 0° and 30°, these two currents carry the same amount of heat northward as the atmosphere.

In the polar regions, heat is also transported by the movement of ice. In both hemispheres, ice is produced at high latitudes, then exported to lower latitudes where it melts in the surrounding warm ocean. In the North Atlantic, the East Greenland drift stream exports about 3,000 km³ of ice per year

toward the equator. The export and melting of this ice, and of the more diffuse Antarctic ice edge, warms the polar regions and cools the temperate latitudes. To understand the oceanic contribution to the global heat balance, the exchanges and transports of heat in both the temperate and polar oceans must be observed at monthly intervals for at least a decade to determine interannual variations.

In the polar regions, the formation and growth of sea ice affects the local heat balance. Sea ice grows through a change of phase. In winter, heat is released to the atmosphere through freezing, and in summer, heat is absorbed through melting. This release and absorption moderates the seasonal temperature extremes. The sea ice albedo is also important. Since sea ice reflects about seven times more energy than open water reflects, during the polar summer the area covered by sea ice reduces the solar heating of the Earth's surface. The reflection of this energy by increased or decreased areas of sea ice associated with colder or warmer climates plays an important role in models of future climate.

Finally, the ocean supports an important biological community. The optical properties of seawater restrict the primary biological productivity to the top 10 to 120 m, but this is the basis of virtually the entire marine food chain. Some of the plankton species form carbon-containing skeletons, which fall through the water column after the organisms die. This results in rapid downward transport of carbon into the deep marine sediments; thus bioproductivity plays a possibly critical role in the global carbon cycle.

Satellites provide a way to observe ocean dynamics and biological productivity. For biological oceanographers, the important wavelengths of electromagnetic radiation lie in the visible, which are the only wavelengths for which seawater is not opaque. In the visible, sunlight produces photosynthesis in the upper 5 to 120 m, and backscatters radiation to satellite sensors. Roughly speaking, when the ocean is a biological desert it appears blue, while oceanic regions of biological productivity contain an abundance of pigments that make the water appear green. Studies of ocean color at specific narrow-band wavelengths permit determination of the oceanic primary productivity.

For physical oceanographers, the critical frequencies occur where the ocean is opaque to radiation. This permits determination of many ocean surface processes. For example, from wavelength bands in the thermal infrared, the ocean surface temperature can be measured. At microwave frequencies, a variety of active and passive instruments, such as scatterometers, altimeters, imaging radars, and passive microwave radiometers, permit determination of surface processes such as the ocean dynamic height associated with geostrophic current systems, surface temperature, wind speed and direction, significant wave heights, and open ocean tides. In the

polar regions, these instruments provide estimates of areal ice extent, some delineation of sea ice types, indications of sea ice motion, and information on iceberg size and position.

Satellite instruments provide a good description of ocean surface conditions. To completely characterize the ocean, however, we also need to determine its interior circulation. The data relay and positioning capabilities provided by satellites contribute to the determination of the interior ocean properties. For example, the position determination systems permit direct measurement of ocean currents through use of satellite-tracked buoys, and the data relay allows for the transmission of data from arrays of moored current meters. Similar buoys collect weather and current meter data from polar sea ice.

In summary, satellite observations permit direct determination of ocean biological properties in the euphotic zone and measure certain surface properties of importance to physical oceanographers. Through the relay of data from sensors deployed throughout the ocean depths, the satellites help provide a view of the ocean interior. As the following four sections show, satellite observations, in combination with measurements from buoys, ships, and aircraft, strongly contribute to our understanding of global oceanic processes.

OCEAN BIOLOGY

One of the central questions in biological oceanography is the role of primary production in the global carbon cycle and the processes that are responsible for fluctuations in production. In particular, we need to characterize the mean and fluctuating components of primary production in the world ocean and the final fate of this production (NRC, 1984a; 1985). Although several maps of global primary production have been produced in the past, these have been composites of ship measurements that were collected over a period of many years (Platt and Subba Rao, 1975; Koblenz-Mishke *et al.*, 1970). For ecological processes it is necessary to have an understanding of the patterns of temporal and spatial variability. This variability is primarily forced by physical processes such as mixing, solar radiation, and advection (Denman and Powell, 1984).

There are other equally important processes in biological oceanography; larval recruitment, zooplankton production and dynamics, and large-scale changes in plankton community composition are some examples. However, primary production is amenable to remote observation from space, thus allowing global, quasi-synoptic measurements. Primary production is one of the intermediaries between the dissolved and particulate pools of carbon, particularly the conversion of dissolved inorganic carbon to particulate organic carbon. The final fates of

these materials are important to the potential long-term storage of carbon in the deep sediments (Eppley and Peterson, 1979). Figure 44 is a schematic of primary production and some of the key biological and physical processes that influence its variability. Variations occur on a broad range of time and space scales.

This section will explore one particular process and consider how we will use the information generated by Eos to study this process. We will discuss the interannual variability in primary production in the California Current System in response to large-scale changes in atmospheric and ocean circulation forcing, such as El Niño type events (McGowan, 1983). The characteristic time and space scales of the problem will determine which processes are important (Mackas *et al.*, 1985; Denman and Powell, 1984). Processes on continental margins may be particularly important to the global carbon cycle despite their small areal extent. It is thought that up to 50 percent of the organic carbon that is buried in deep sediments is produced on the margins.

The main source of historical *in situ* data from the California Current domain comes from the California Cooperative Oceanic Fisheries Investiga-

tions (CalCOFI), which has been making regular measurements of biological, chemical, and physical properties for the last 40 years (Hickey, 1979). The resulting time series show considerable variability at annual and longer time scales, as well as at corresponding large spatial scales (> 200 km). For example, patterns of zooplankton biomass appear to be related to the strength of southward flow of relatively nutrient-rich subarctic water (Chelton *et al.*, 1982). However, there have been only a few direct measurements of primary production, and the link between zooplankton (or secondary production) and nutrient concentrations was based on inferred primary production (Bernal and McGowan, 1981). In addition, the CalCOFI sampling grid is too coarse for resolving mesoscale processes such as upwelling and coastal jets that may play an important role in the biological and physical dynamics of the California Current System. Figure 45 shows a monthly mean of phytoplankton pigment concentrations derived from satellite data. One can easily see the variety of patterns present in the California Current.

Figure 46 shows a schematic of the key biological and physical processes and how they may affect interannual variations in primary production.

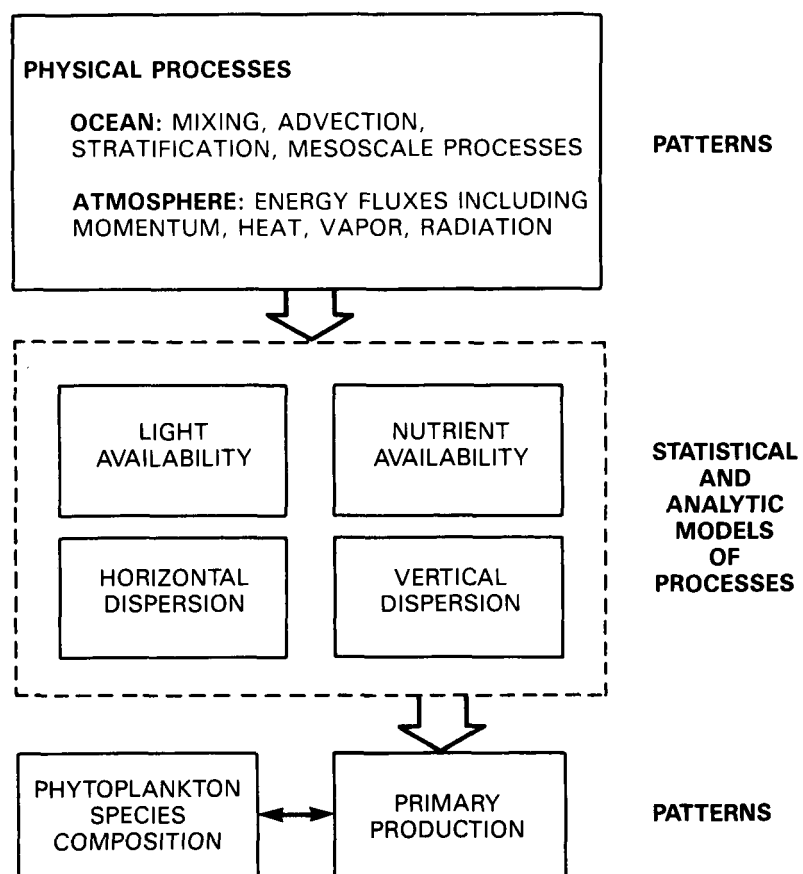


Figure 44. Key biological and physical processes influencing primary production.

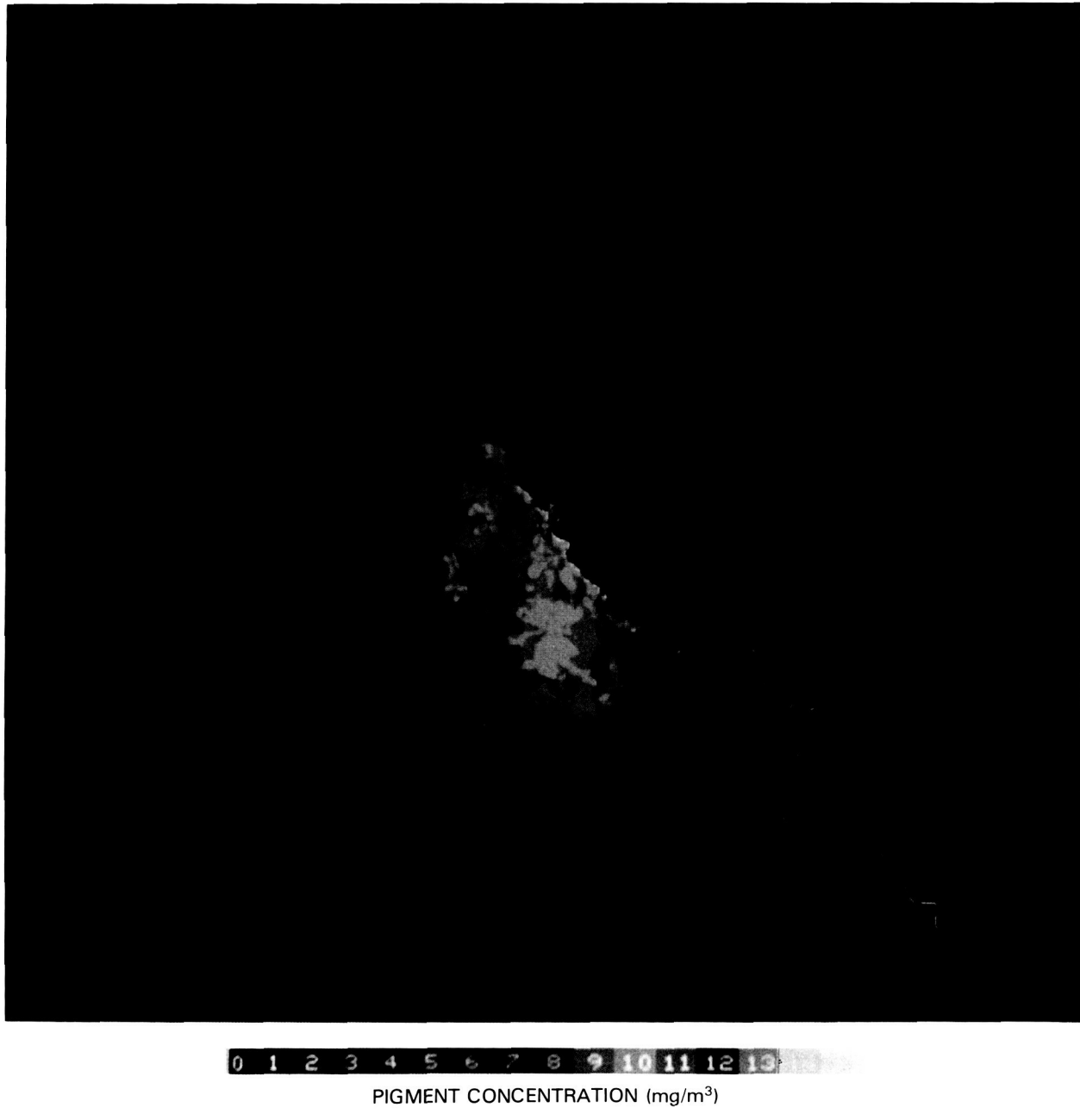


Figure 45. Mean near-surface phytoplankton pigment concentrations obtained from 13 CZCS images during a 25-day period, May 22 to June 16, 1981.

Our understanding of all the key processes and their interrelationships is not as complete as this figure indicates, but it does serve well as an initial framework. Starting with the atmospheric component of this system, we expect that the pattern of the large-scale surface wind field on a 2° by 2° grid on a monthly basis for the North Pacific basin, as well as the equatorial region, will be required. Cloud cover maps will provide basic information in the determination of the net shortwave and longwave radiation reaching the sea surface. Similar maps of sur-

face air temperature and humidity would play an additional role in the estimation of surface energy fluxes. These techniques are described in Chapter II.

These patterns of atmospheric forcing will be important to the patterns of primary production. There is evidence that El Niño events in the eastern tropical Pacific can propagate up the west coast of North America, significantly affecting the physical regime and, hence, biological production in the California Current System (Chelton *et al.*, 1982). It has been hypothesized that similar large-scale pat-

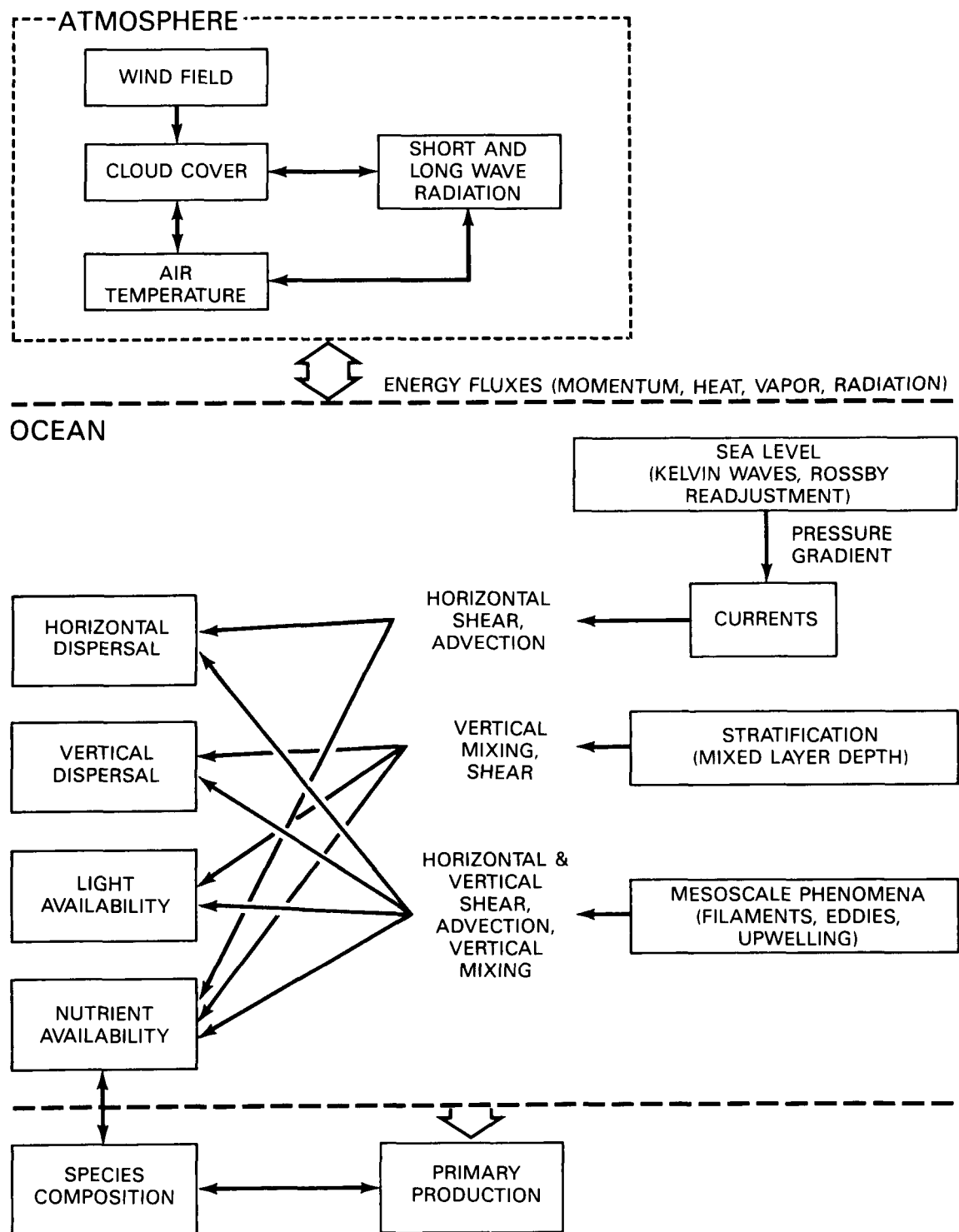


Figure 46. Key biological and physical processes affecting interannual variations in primary production.

terns in the North Pacific have similar "teleconnections" (relationships between distant areas). The connections between the atmospheric and oceanic systems are not completely understood, but the most important are fluxes of momentum, heat, and radiation (Chelton and Davis, 1982).

A study of interannual variability in the California Current will examine the basin-scale patterns of these processes and address their relationship to specific processes occurring in a much smaller area. We will assume that these large-scale patterns are taken as inputs to our system; we need not understand the details of the interactions at these large scales. Instead, our study will focus on the detailed response of physical and biological processes on a current system scale, rather than on an entire basin.

There are several physical patterns that are of importance, as shown in Figure 46. Changes in sea level occur in response to a variety of factors; we are interested primarily in changes due to processes such as Kelvin waves and other low-frequency phenomena. Obviously, sea level itself is not particularly important; rather it strongly influences surface and subsurface currents by altering the horizontal pressure gradient field. For example, relaxation of the equatorial trade winds releases a Kelvin wave that propagates eastward along the equator (NRC, 1982; 1983). When the wave reaches the west coast of South America, it changes the physical regime sufficiently to reduce significantly the strength of coastal upwelling (Chelton and Davis, 1982; Chelton *et al.*, 1982; Enfield and Allen, 1980).

Another physical pattern of interest is seasonal stratification, particularly as it relates to the depth of the seasonal mixed layer. Mixed-layer depth is closely related to surface energy fluxes as well as to subsurface mixing processes (Niiler and Kraus, 1977).

The last physical pattern of interest concerns the large class of mesoscale phenomena. We are more interested in the annual "regime" of mesoscale processes than in individual events. Several mesoscale phenomena are important: upwelling (both coastal and wind stress curl-induced; Chelton, 1982), eddies, and jets (or filaments). Upwelling events are characterized by strong turbulence and generally enhanced nutrient levels (Brink *et al.*, 1981). These events tend to be episodic, lasting 3 to 5 days. The timing, persistence, and strength of upwelling varies considerably in the California Current domain, in large part due to the spatial and temporal variations of the wind field (Huyer, 1983). Mesoscale eddies are common throughout the current system and may significantly affect the circulation of the current (Mooers and Robinson, 1984). Although the amount of eddy kinetic energy is generally much smaller than in western boundary currents (e.g., the Gulf Stream), there are indications from previous work with satellite imagery that such eddies are the dominant form of near-surface horizontal transport (Bernstein, 1983). Finally, filaments are a relatively new dis-

covery. These large features may transport significant amounts of heat, momentum, and materials (such as nutrients and phytoplankton) far offshore into the open ocean region (Davis, 1985a; Flament *et al.*, 1985; Rienecker *et al.*, 1985). Although the dynamics of these features is poorly understood at present, they seem to be driven in large part by the wind field and the horizontal pressure gradient (Davis, 1985b). All of these mesoscale processes vary significantly from year to year as the atmospheric forcing changes.

To understand the response of primary production to these physical processes, we must combine remote observations of these patterns with models and *in situ* data to develop information on four key processes: light availability, nutrient availability, horizontal dispersal, and vertical dispersal. Light availability will be a function of the amount of short-wave solar radiation reaching the sea surface as well as the effective amount of light received by a phytoplankton during vertical mixing (Denman and Gargett, 1983). Nutrient availability will depend on the amount of horizontal transport of high-nutrient waters (Haury and Schulenberger, 1982), the amount of vertical mixing (Klein and Coste, 1984), and the amount of upwelling (Jones *et al.*, 1983) (ignoring for the moment various biological processes such as recycling). Horizontal dispersal will depend on the advective effects of currents and filaments as well as horizontal diffusion due to current shear and mesoscale eddies (Angel and Fasham, 1983). Vertical dispersal will depend on the strength of vertical mixing and stratification as well as upwelling (in some instances).

Note that vertical mixing is one area where biological processes can affect physical processes through the modulation of the sunlight attenuation depth with changes in phytoplankton biomass. It has been shown that estimates of mixing are sensitive to estimates of light attenuation and that variations in light attenuation are largely the result of changes in phytoplankton biomass (Denman, 1973; Smith and Baker, 1978).

The biological state variables of interest are phytoplankton biomass, chlorophyll fluorescence, and phytoplankton pigment groups. Patterns of biomass and fluorescence will be used to derive estimates of primary productivity. Patterns of pigment groups will allow further delineation of the phytoplankton community into some functional group classes (e.g., cyanobacteria; Carder and Steward, 1985). Some of this information could be used in later studies of the ultimate fates of organically fixed carbon.

This study is statistical in nature, involving analysis of a large set of data collected over a long time period. As some of the processes causing interannual variability occur fairly irregularly (e.g., El Niño events), the study data set will, by necessity, involve data from the pre-Eos timeframe (Chelton *et*

al., 1982). Statistical comparisons of the biological and physical data sets will allow us to refine our model and improve our understanding of the causes of variability.

We must have access to a variety of Eos data sets covering a relatively large area of the world ocean and encompassing a long time period. Advances in our understanding of these processes will only occur if we have access to the long time series of data collected by (or made available through) Eos. The surface wind field data set need only consist of weekly averages on 2° by 2° grid for the open ocean; 50 km maps will be needed for the California Current domain. We will need primarily vector wind stress data from the scatterometer, although wind speed data from the altimeter and AMSR may also be useful. Data on cloud cover will come primarily from the visible/IR sensors on geostationary satellites such as GOES, although MODIS may also play a secondary role in these measurements. When combined with standard calculations of available sunlight as a function of season and latitude, we should be able to estimate incoming shortwave solar radiation on a similar grid as the wind measurements. Estimates of surface air temperature and humidity will be more difficult, but perhaps microwave and lidar techniques may be sufficiently accurate. These antecedent patterns, along with the cloud and wind fields, will be necessary for estimating longwave radiation and latent heat transport between the atmosphere and ocean. Data from MODIS (sea surface temperature), AMSR (water vapor concentration), the NOAA atmospheric sounders, and LASA (water vapor and surface temperature of the air) would be used in estimating moisture and heat flux between the ocean and atmosphere. Patterns of mesoscale variability would be derived from MODIS visible and infrared data, as well as from altimeter data. We will need these measurements over the study domain on a weekly basis on a 10 to 50 km grid. As described earlier, we are interested in the annual regime of these processes rather than in specific events.

Phytoplankton biomass and fluorescence will be derived from MODIS data. Primary production will be derived from these patterns using models developed from *in situ* measurements. Phytoplankton pigment groups will also be measured by MODIS. We will need these maps for the California Current domain on a weekly basis, at resolutions of about 10 km.

Although we will have preliminary models of how the various physical processes affect light and nutrient availability, and horizontal and vertical dispersal based on historical *in situ* measurements, we will need to make statistical comparisons of the patterns of physical and biological processes from several years' worth of data to test and refine these models. For example, intensity of coastal upwelling may not be closely related to the local wind field

because it is more strongly influenced by large-scale patterns in the wind field over the North Pacific (Chelton, 1982). Statistical comparisons should help delineate such relationships.

Although we have presented the study plan as something that is relatively straightforward, there is no doubt that this is an optimistic assumption. This program will require a variety of studies in order to delineate and parameterize many of the key processes. Many of these studies can begin now, while others must wait until the Eos era. While we cannot explore these studies in great detail, there is no doubt of their importance for this example study. One of the key studies will be the estimation of primary productivity from MODIS data. These estimates may rely on models (both statistical and analytical) using data on phytoplankton biomass and environmental processes such as daylength (Eppley *et al.*, 1985a). Measurements of phytoplankton fluorescence from MODIS will improve these productivity estimates. However, a cautionary note is required; as a significant fraction of the water column productivity cannot be sampled remotely from space (Hayward and Venrick, 1982). MODIS observations of the near surface water must be extrapolated to obtain the integrated water column biomass and/or productivity. Previous estimates of water column productivity using surface biomass measurements have met with only limited success (Eppley *et al.*, 1987).

Similar studies are needed in physical oceanography and meteorology. In particular, we need process studies to link satellite-measured variables and the processes of interest. For example, estimates of mixed-layer depth will be essential to this study but cannot be observed directly by satellites. These estimates will be derived from models using information on heat, momentum, and vapor flux through the air-sea interface (Davis *et al.*, 1981). Models estimating vertical and horizontal mixing will also be required.

This example study will impose some requirements on the Eos data and information system; in particular, the need for access to large volumes of data (particularly image-type data) from a variety of sensors from multiyear time series. Comparisons of these data sets will require that we have appropriate techniques for overlaying variables that have been derived from sensors that may have significantly different sampling patterns. For example, comparisons between the nadir-looking altimeter and the swath-wide MODIS will require particular care. Such overlay techniques must accurately retain the basic statistics of the data sets, as this is primarily a statistical study (Freilich and Chelton, 1986).

A difficult aspect of this study will be coping with the various sampling patterns of the Eos instruments. Data from the active and passive microwave sensors (assuming that they are always functioning and the data are retained and accessible) should be relatively straightforward to incorporate

into statistical models. Because clouds will obscure varying portions of the ocean surface, the more difficult data sets will be the visible and infrared images. Gaps in these data sets are not distributed uniformly in time and space, and this can lead to a significant bias in the data set (Abbott and Zion, 1987). For example, some areas near the coast are frequently cloudy, apparently as a result of the local wind field. Figure 47 shows the distribution of usable data from a set of 13 CZCS images during a 1-month period in late spring 1981. Similar gaps can occur in the temporal dimension as particular meteorological condi-

tions tend to be associated with clear skies. Obviously, such sampling can lead to a biased data set. Reduction in the amount of available data also may make observations of some phenomena, nearly impossible. For example, the spring bloom on the continental shelf often occurs over a 10-day time period. It is quite possible for no useful visible imagery to be acquired during such an event. This problem is particularly acute in studies of mesoscale biological and physical phenomena, where the relevant time scales are often in the 3- to 5-day range. However, sampling by ships also has inherent biases and is far more

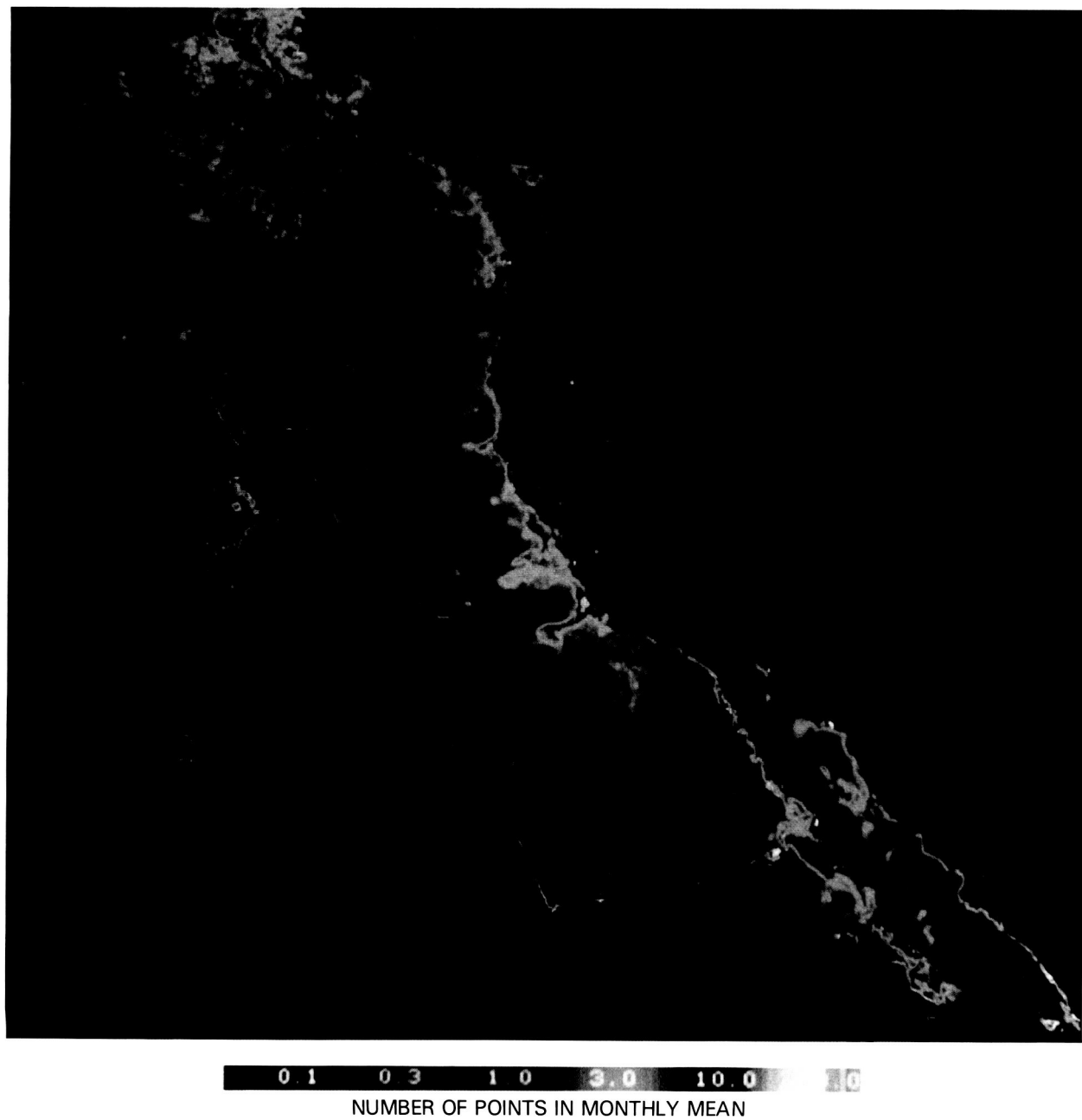


Figure 47. Distribution of useful ocean data during June 1981.

prone to undersampling. Such phenomena will require a complete sampling strategy consisting of observations at a wide range of scales. Satellite data are just one component, albeit an important one.

In any study of interannual variability, we must have access to long time series in order to resolve statistically the long-period fluctuations. This is one of the key components of this study; the Eos data and information system must provide access to these historical data sets along with data from current Eos sensors. In addition, we need to be able to separate naturally-occurring variability from variations in instrument calibration and data processing. Many of the changes have a small signal; it is essential that they not be masked by processing and instrument variability (Bernstein and Chelton, 1985).

This science scenario is one where our understanding of the key processes and their interrelationships is vague at best. We will need access to large volumes of data in order to develop the basic patterns (both in time and space) of what we think are the key variables. We will perform various statistical analyses to test our initial assumptions of the relationships, as well as to elucidate new relationships. It has only been recently demonstrated that zooplankton biomass in the California Current responds to changes in atmospheric forcing in the equatorial Pacific. However, even this relationship does not explain all of the observed variability, and does not make the connection between primary production and this physical forcing. We expect that access to these long time series of basin-scale patterns will reveal many new teleconnections and help explain more of the observed biological changes.

OCEANIC MESOSCALE VARIABILITY

Introduction

For centuries, the oceans were assumed to be dominated by steady, slow-moving currents that stirred and recirculated waters in a given basin. Since the 1930s, increasing scientific evidence suggests that oceanic flow fields are extremely variable. Ocean currents and their associated fields of temperature, pressure, and density vary temporally and spatially over the entire globe. This energetic variability is collectively referred to as oceanic mesoscale variability or the oceanic eddy field.

The mesoscale motions in the ocean are the marine equivalent of atmospheric weather; in essence, they are synonymous with the meteorologist's synoptic-scale storms (Duing, 1978). Mesoscale variability includes the meandering of major ocean currents, such as the oscillations of the Antarctic Circumpolar Current shown in Figure 48; the formation of intense jets or filaments in the Califor-

nia Current shown in Figure 49; ring currents that evolve from the meanders and jets shown in Figure 50; complex structures resulting from the interleaving of water masses such as the density fronts over the Mid-Atlantic Ridge shown in Figure 51; and many classes of large-scale planetary wave phenomena (Robinson, 1983).

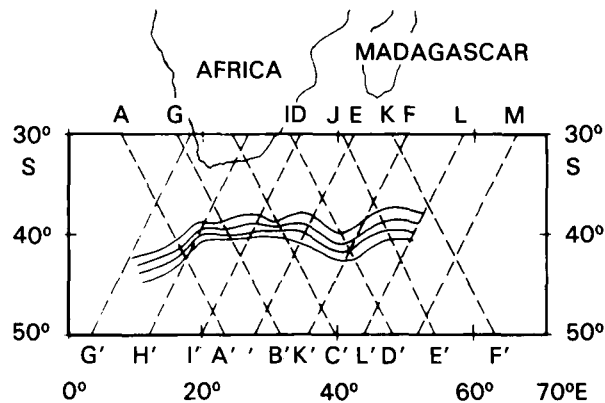


Figure 48. Reduced Seasat altimeter data depicting meanders in the Antarctic Circumpolar Current induced by topographic effects of the Mid-Atlantic and Southwest Indian Ridges (after Colton and Chase, 1983).

The oceanic mesoscale variability consists of structures with length scales ranging from tens of kilometers up to a few hundred kilometers and characteristic time scales ranging from a few days up to approximately a year. Vertical scales of these structures can extend to the full ocean depth, although no simple characterization describes ocean eddies. The eddies are time-dependent and are influenced by topographic features and the presence of strong ocean currents (Schmitz *et al.*, 1983).

A dominant feature of the oceanic mesoscale variability is its horizontal inhomogeneity. The eddies are distributed unevenly with energy levels and dominant space and time scales changing dramatically from one locale to another. However, the patterns observed in maps of eddy kinetic energy suggest that the mesoscale variability is closely tied to the general circulation of the ocean. As an example, consider the mesoscale surface height variability, as determined by the Seasat altimeter, shown in Figure 52 (Cheney *et al.*, 1983). The highest values of eddy height (and eddy kinetic energy) variability occur in the mid-latitudes and are most frequently associated with western boundary currents. Interior gyre regions have a broad pool of nearly constant eddy kinetic energy. Increased activity associated with eastern boundary currents, equatorial currents, and the Antarctic Circumpolar Current produces higher kinetic energy in those regions. The geographical correlation of high eddy kinetic energy with major current sys-

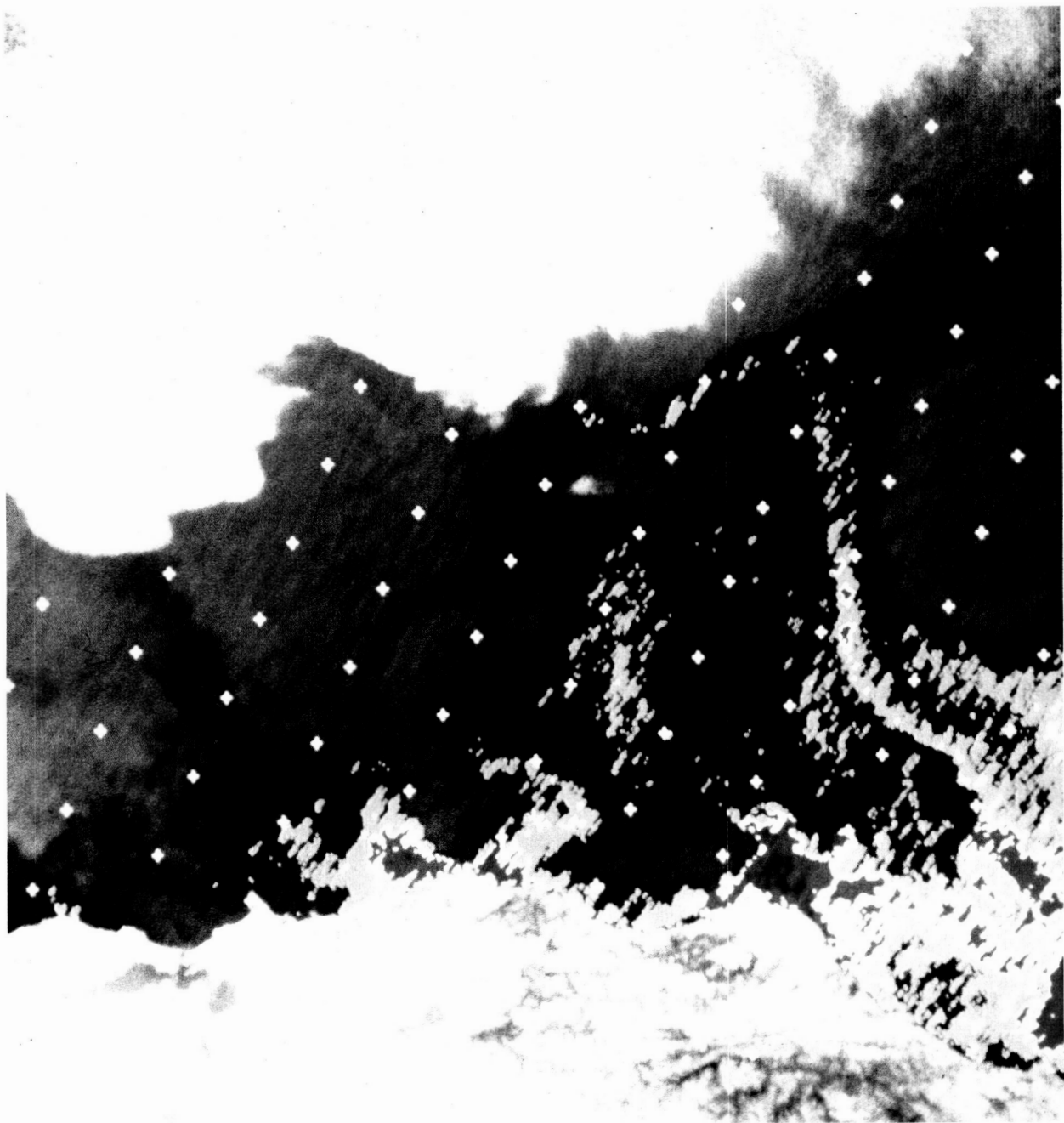


Figure 49. AVHRR image of filaments (also referred to as jets or squirts) associated with the California Current (courtesy of Kelly G. Luetkemeyer).

tems is both convincing and dramatic. Thus, it appears that the mesoscale variability and general circulation are coupled and must be addressed jointly rather than separately.

Importance of the Oceanic Mesoscale

The oceanic mesoscale variability has a profound impact on many scientific research questions. For example, consider the processes through which passive tracers (dissolved substances or suspended

particulates) are distributed and dispersed by the oceans. These substances include naturally occurring and anthropogenic chemicals and nutrients, while the particulates include both waste materials and marine organisms and detritus. In the mid-ocean, mesoscale eddies are particularly important in the dispersal and redistribution of the substances and particulates (c.f. Haidvogel *et al.*, 1983).

Since mesoscale variability occurs on a variety of space and time scales and with significant geographical variation, its associated transport effects

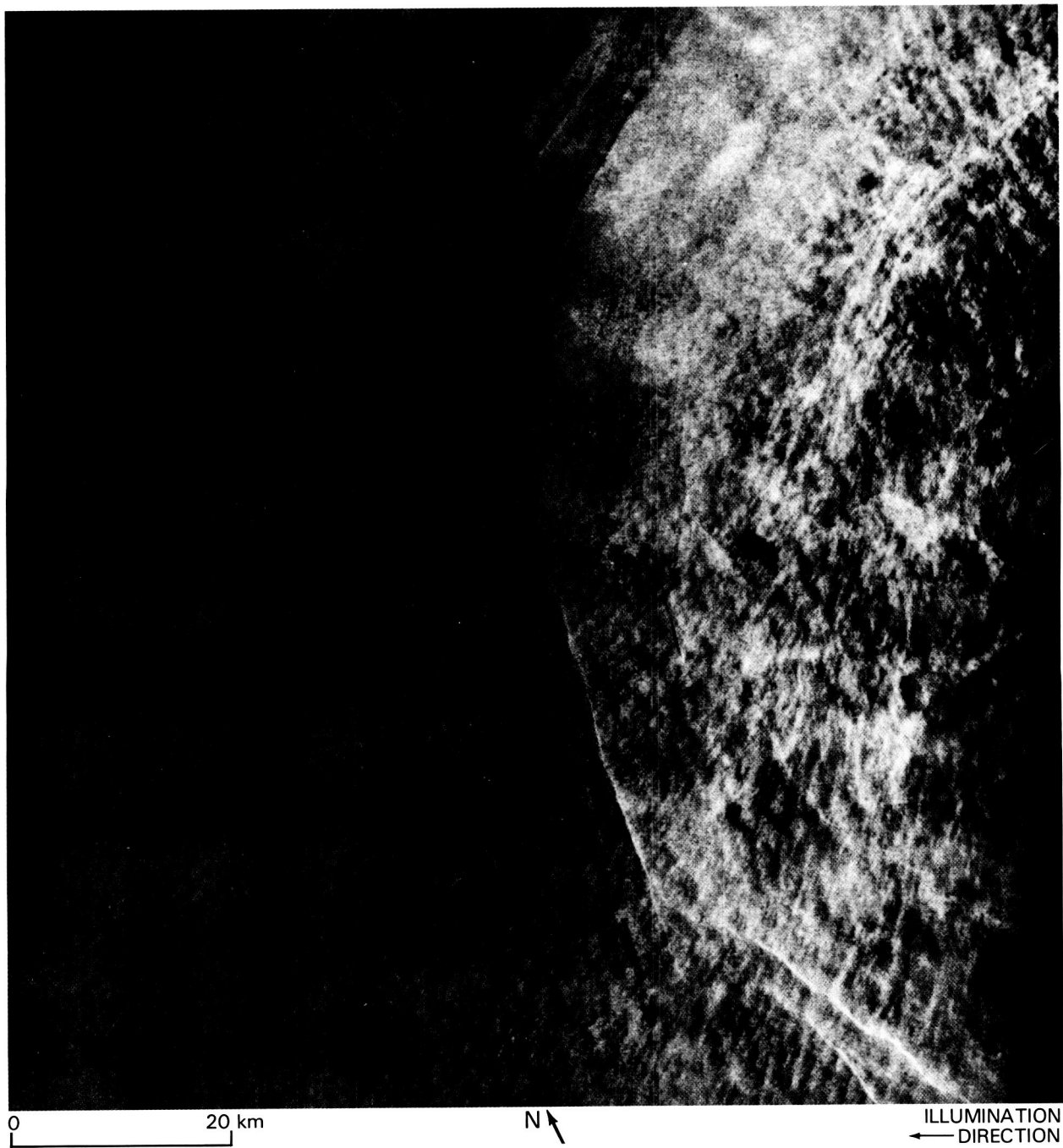


Figure 50. A SAR image of a warm-core ring located about 100 km southeast of Delaware Bay (from Fu and Holt, 1982).

can be quite diverse. Initially, substances released into the ocean may disperse locally according to classical diffusion (c.f. Csanady, 1973). In time though, they will diffuse until they reach a scale of the order of the Rossby radius of deformation, which is a length scale relating the vertical stiffness of the fluid due to stratification and the effect of the rotation of the Earth. At these scales and larger, the mesoscale eddy transport processes of stirring and mixing become important. Stirring forms long, in-

tertwined filaments, where mixing is enhanced to produce locally homogeneous distributions.

These mesoscale eddy processes may significantly affect biological productivity in many areas of the globe, through the transport of nutrients and organisms (Yentsch, 1980; Angel and Fasham, 1983; Denman and Powell, 1984). Similarly, the oceanic eddy transport must be considered in the selection of disposal sites for anthropogenic wastes, particularly toxins in high-level nuclear materials (Goldberg,

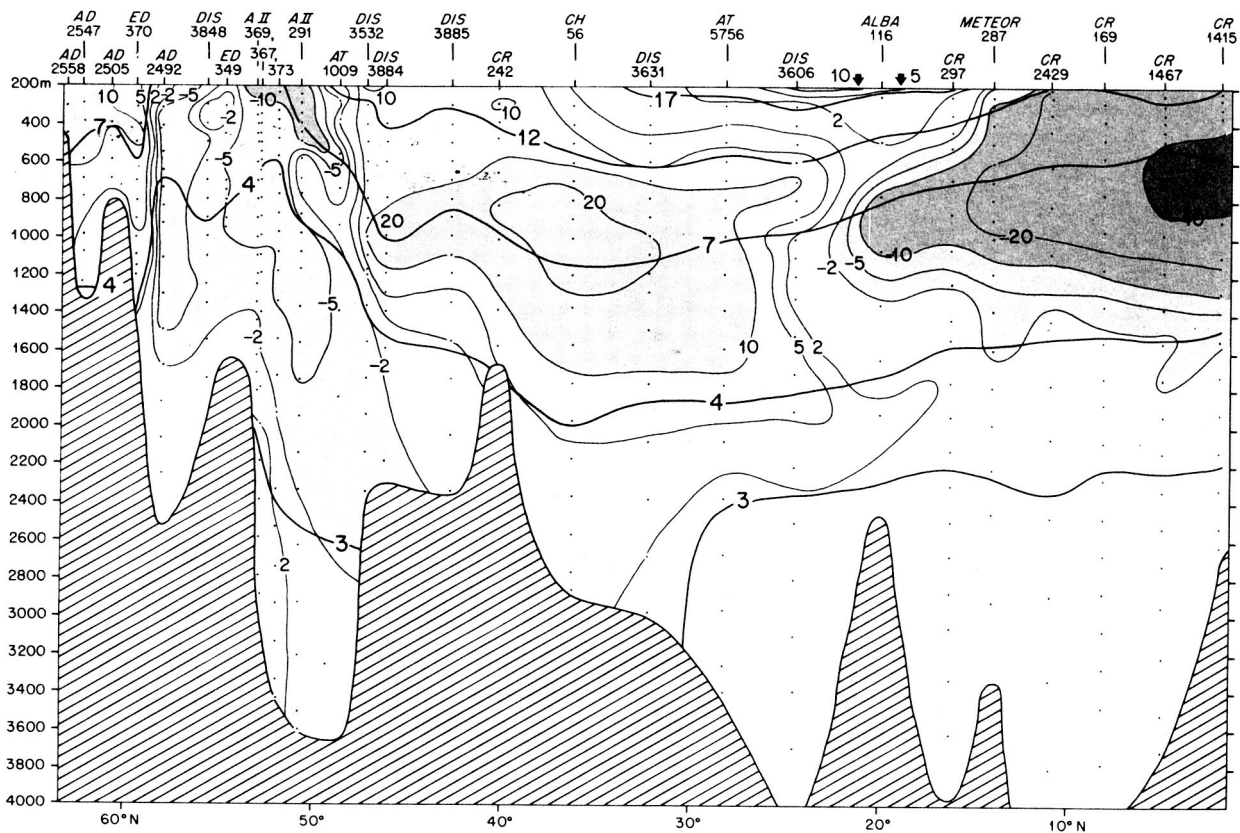


Figure 51. Interleaved water masses forming complex density fronts along the Mid-Atlantic Ridge (from Worthington, 1976).

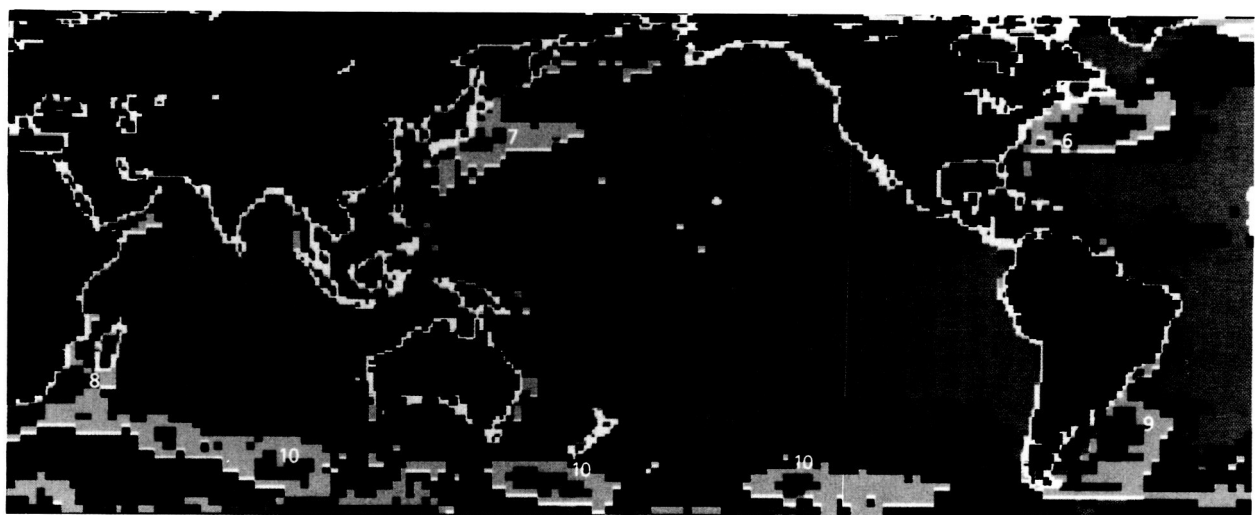


Figure 52. Mesoscale sea surface height variability based on Seasat altimetric data (from Cheney *et al.*, 1982).

1979; Marietta and Robinson, 1980). The oceanic mesoscale variability can affect global climate in two ways. The transport of heat and momentum by mesoscale phenomena plays an important role in air-sea interaction (Katsaros, 1980; Gill, 1983; Charnock and Pollard, 1983). Changes in ocean heat transport and exchange of heat with the atmosphere due to mesoscale eddy effects can have a direct impact on climate, but indirect effects can occur through changes in ocean circulation and air-sea exchange rates. For example, the ocean may be a reservoir for carbon dioxide and changes in the air-sea exchange of carbon dioxide clearly have a significant impact on any possible greenhouse effect for the Earth (NRC, 1979; 1985; Broecker and Takahashi, 1984).

Mesoscale Observational Techniques

Seasat, launched in 1978, opened a new era in oceanographic research, an era where marine scientists could contemplate performing meso- to large-scale experiments aided by the near synoptic remote sensing capabilities of artificial Earth-orbiting satellites (Wilson, 1981). Since then, three significant uses for satellite capabilities have emerged in oceanographic research: (1) the actual research use of satellite remote sensing data within an experiment; (2) the use of data collection and location systems on the satellites for *in situ* observations; and (3) the use of synoptic satellite observations to optimize research observations, such as planning ship station locations based upon satellite sea surface temperature images.

The pertinent measurements of mesoscale eddies from the remote sensing instrumentation proposed for Eos will be: sea level elevation from the altimeter (ALT), sea surface temperature from the radiometer (AMSR) and spectrometers (MODIS and TIMS), areal extent of the eddies from repeated passes of the altimeter (ALT) and from the imaging spectrometers (MODIS and HIRIS), interfacial heat flux inferred from the radiometer (AMSR) and the sounder (AMSU) data, the velocity field of the eddy inferred from the altimeter (ALT) assuming geostrophy and from repeated imagery of temperature (AMSR) or passive tracers such as chlorophyll (MODIS), horizontal filament structure and entrainment from the synthetic aperture radar (SAR), and chlorophyll and suspended particulate content from the spectrometers (MODIS and HIRIS). While the list of information available is extensive, the ocean is a four-dimensional domain and satellite remote sensing data provide information in only three dimensions, two horizontal dimensions and the time domain. To obtain information (e.g., temperature, density, and velocity) in the third spatial dimension, Eos will carry an advanced data collection and location system (ADCLS). Through this system, *in situ* data matched in time and space to the remote sensing data can be obtained.

An Approach to Mesoscale Experimentation

A new research methodology is emerging in oceanography, reflecting the model-building approaches used in the dynamical meteorological community during the last two decades. Success with this methodology requires acquiring sufficient information in all three spatial dimensions over time to provide updates for analysis and modeling. It requires an oceanic equivalent of the atmospheric observing system.

The approach itself represents a radical departure from the data-limited manner in which ocean dynamics research has traditionally been pursued. If satellite oceanographic data is acquired quickly, processed with powerful new computing facilities, and disseminated rapidly, it can bring new insights to our understanding of the oceanic mesoscale, insights that are not possible from traditional oceanographic experimentation.

Based upon sampling theory, the description of a mesoscale field cannot be totally separated from a similar portrayal of the mean field. In order to specify the time-dependent field at a given location, it is also necessary (by definition) to determine the temporal mean (i.e., time average) as well. Spatially, the same scales are relevant for either the time-dependent or mean fields; both are within the orbital-scenario sampling envelopes under consideration for Eos (Chase *et al.*, 1987). To determine a given mesoscale field, the temporal average either must be determined in advance or extracted from the measured variability during the experiment. In this scenario, we assume that statistically independent baseline (mean) fields have already been derived (e.g., from TOPEX, NOAA/Polar Orbiters, Nimbus-7 CZCS, *in situ* instruments) and are resident in Eos-accessible archives. We further assume that baseline statistics have been obtained for all pertinent fields. Attention is then focused on utilizing Eos to perform a case history of the genesis and evolution of a particular mesoscale structure, a warm-core ring.

A Warm-Core Ring Case History Experiment

Western continental slope waters are dominated by complex mixing processes arising from their interaction with both shelf and boundary current regimes. Much of the variability found in slope water regimes results from well-organized, mesoscale features known as warm-core or anticyclonic rings.

Warm-core rings are injected into slope water regimes from unstable meanders in the western boundary currents. A typical newly formed ring is near-circular in the horizontal plane with a diameter of 100 to 200 km. Isothermal and isohaline surfaces

slope downward toward the ring center, reflecting the ring's characteristic warm core of waters from the subtropical gyre interior. Penetration depths for the core are typically on the order of 1,000 m.

A ring is characterized by strong currents at the periphery, ranging from about 40 cm per second at mid-depth to over 100 cm per second at the surface. The detailed trajectories of spawned rings are erratic, but on average they drift to the west or southwest in the northern hemisphere, eventually being re-trained in the gyre-scale circulation. Translational velocities for established warm-core rings are of the order of a few centimeters per second and are a key factor in determining the life-cycle duration of the feature. During their lifetimes (which can last from a few months to a year) rings continually interact with their surrounding environment. They impinge upon continental rises and slopes; entrain shelf water into their surface circulation; exchange mass, momentum, chemicals (nutrients), and organisms with the slope water regime; continuously affect the overlying atmosphere; and modify the mean or ambient characteristics of air-sea exchanges at a given geographic locale.

Since we assume that all necessary baseline statistics have been obtained, the purpose of this experiment is to determine, in detail, the genesis, evolution, and decay of a specific anticyclonic ring, providing a means to convert pattern to process-based knowledge for one class of mesoscale phenomena.

After site selection, we begin by acquiring, reducing, and analyzing MODIS and AMSR data (see Figure 53) to detect the first signs of ring spawning. From these data, we note the length scales (amplitudes and wavelengths) of western boundary current meanders, which can be used in modeling the instability process that produces rings. Based upon a simple baroclinic instability model, we believe that a new ring is about to form. Consequently, acquisition and analysis of altimeter data are initiated to determine the geostrophic velocity of the boundary current (Figure 54), which is also the initial velocity of the ring, once formed.

In time, the candidate meander pinches off, forming a ring. MODIS, AMSR, and ALT data are used to characterize the areal extent, temperature, velocity, and trajectory of the ring. SCATT data are used to assess the effects of wind stress forcing on ring trajectory and speed, while both pressure-gradient-controlled shelf circulation and geostrophic gyre-scale forcing are examined with the aid of ALT. In time, these data provide—when used in eddy-resolving numerical models—a quantitative picture of the evolution and eventual decay of the ring. Fine-scale structure entrainment estimates can be obtained from SAR (Figure 51) and HIRIS, bioproductivity estimates can be derived from MODIS and HIRIS, and surface fluxes can be calculated from a combination of AMSR and AMSU data.

To determine the subsurface structure and dynamics of the ring, we initiate a field experiment, seeding the ring with air-deployable, satellite-linked Lagrangian drifters. These drifters cycle between isopycnal surfaces, charting out the internal temperature structure as a function of time. Further, they provide us with a time-based history of interior fields from which internal dynamics can be investigated. Based upon *in situ* data uplinked through the ADCLS, we find a peculiar internal toroidal structure. Since this structure may play a significant role in ring dynamics, a second aircraft sortie is launched to survey the ring with expendable bathythermographs. The complete *in situ* data set thus obtained is composited with remote sensing data to produce a three-dimensional “snapshot” of the ring (see Figure 55).

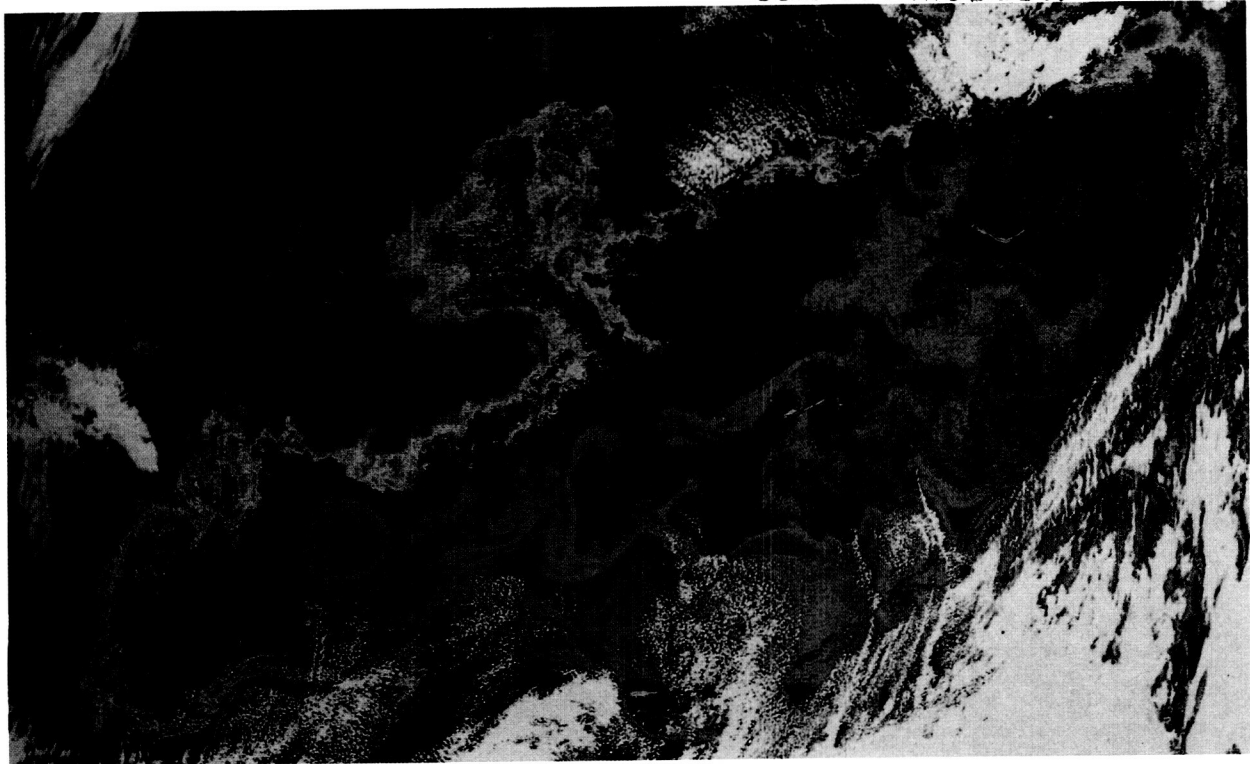
The detailed structure that we now have (see Figure 55) shows us the effects of horizontal entrainment as a function of depth. We see that the internal toroid is not in the horizontal plane but rather tilted against the normal to the local vertical, penetrating the surface and explaining the warm pool on the eastern (right) side of the ring at the surface. Further, the internal thermal field (and its associated jet) appear intensified on the eastern side of the ring and less evident to the west (left side). The staircase structure along the base of the lens suggests that entrainment and mixing are occurring at the margins. Cloud cover and thermal gradients (from ocean to atmosphere) indicate that the ring is dissipating significant quantities of heat from its interior to the atmosphere. These fluxes are a significant alteration of the ambient fluxes for this geographic location compared with those found a short distance from the ring.

While interesting and enlightening, this case history is not sufficient to understand the genesis, evolution and dissipation of warm-core rings. Many rings need to be observed to understand the physical processes at work during the life cycle of a ring. This experimental scenario is limited in time and space, but the full understanding of the dynamics of mesoscale eddies will require the long time series and global data sets of many remotely sensed physical, chemical, and biological fields to be obtained with the Earth Observing System.

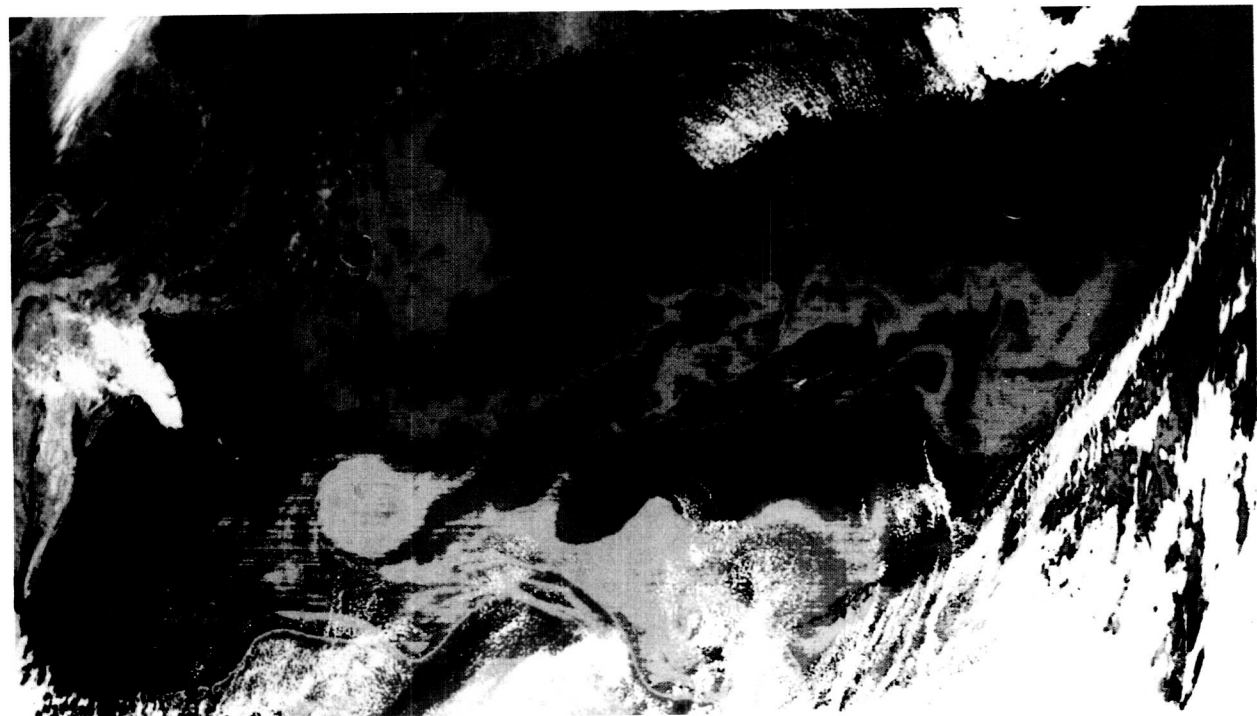
SEA-ICE DYNAMICS

Introduction

Sea ice covers about 10 percent of the surface of the world ocean. The extent of this ice cover increases and decreases throughout the year in response to seasonal changes in atmospheric temperature and winds. Over a polar winter, undeformed sea ice grows to a thickness of 1 to 3 m. As the ice grows, it rejects salt to the underlying ocean, so that



(a)



(b)

Figure 53. CZCS image of the Western North Atlantic showing the Gulf Stream system, spin-off eddies (warm and cold core rings), meanders, entrainment, and the Labrador Current. Panel (a) phytoplankton pigments, panel (b) surface temperature distribution (from Oceanography from Space, 1984).

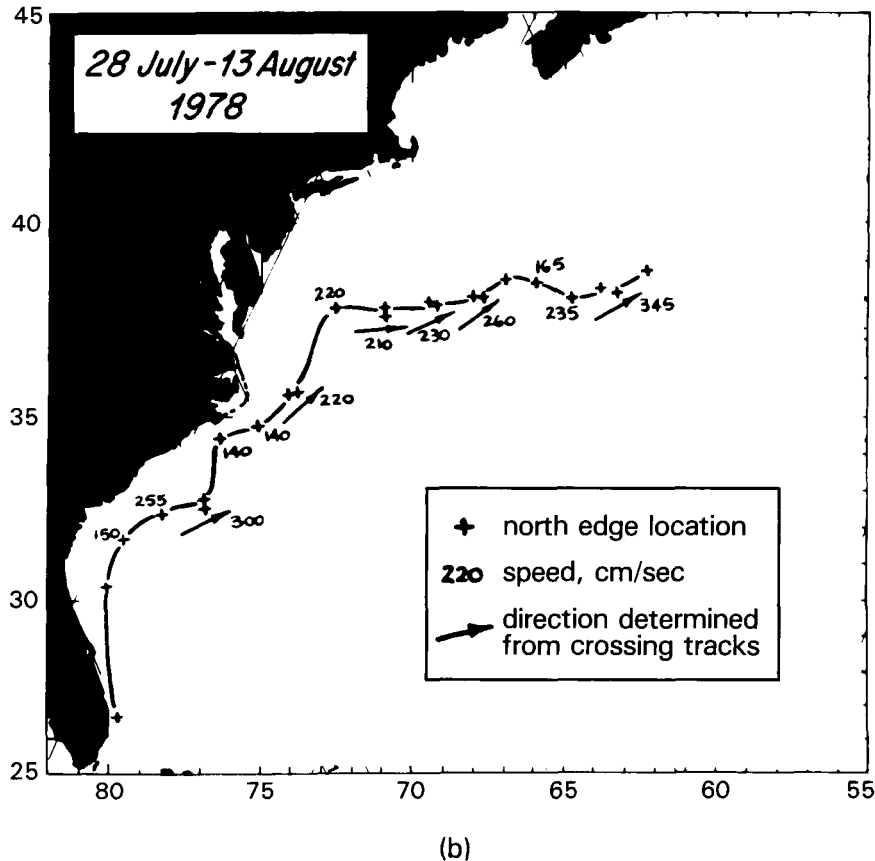
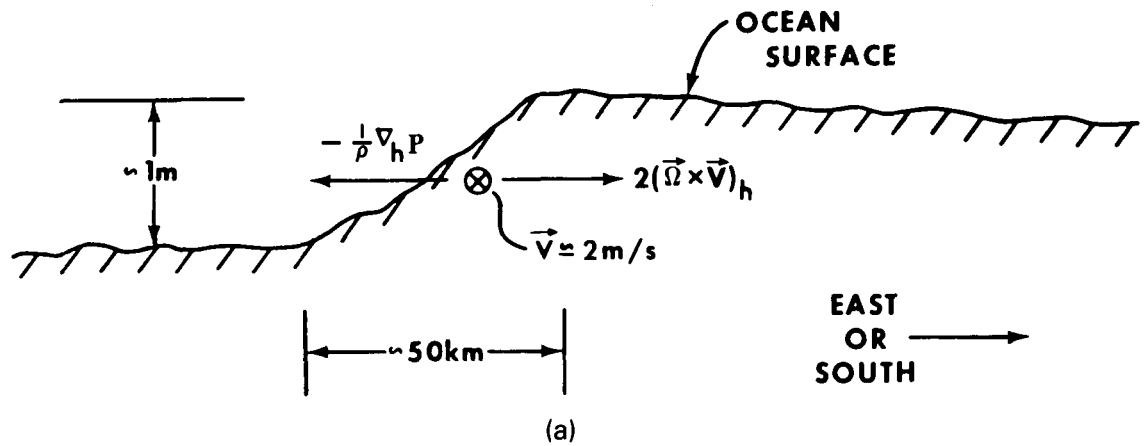


Figure 54. Geostrophic surface velocity derived of spaceborne altimetric measurements. (a) The calculation of surface geostrophic velocity; (b) surface geostrophic velocities of the Gulf Stream derived from 17 days of Seasat altimetric measurements.

in certain areas of the polar ocean there is a downward flux of cold, saline, oxygen-rich water to the deep ocean.

Because sea ice forms an insulating layer between the atmosphere and ocean, there is 5 to 10 times more heat flux from an open-water area than from the same area of solid pack. Therefore, open-water regions within the pack are very important to the flux of salt and heat to the underlying ocean.

Because the solubility of oxygen increases as the water temperature decreases, the downwelling of cold surface water in the polar regions provides much of the bottom-water renewal for the world ocean. This is particularly significant in the Weddell Sea region of the Antarctic Ocean.

In this subsection, we first discuss the atmospheric and oceanic forces that contribute to the growth and deformation of sea ice. We then discuss

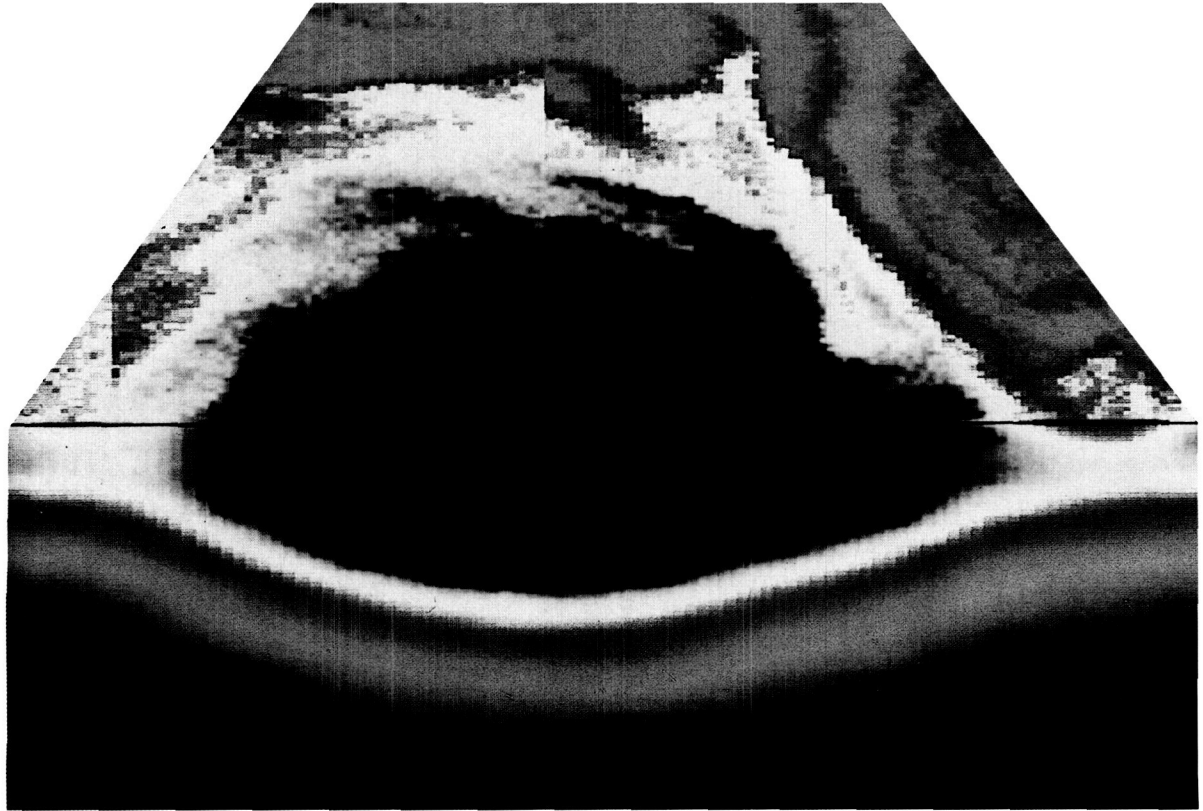


Figure 55. Three-dimensional composite image of a Gulf Stream warm-core ring in the Western North Atlantic from AVHRR and expendable bathythermograph profile data (image courtesy of Kelly G. Luetkemeyer).

the physics of large, semi-permanent areas of open water within the polar pack, called polynyas, with specific reference to the 10^5 km^2 -sized Antarctic Weddell Sea polynya. We spend the rest of the chapter on the Weddell polynya, beginning with a discussion of its discovery by passive microwave satellite observations in the 1970s, and continuing with the additional satellite, theoretical, and oceanographic studies. The theoretical studies show that the oceanographic importance of the polynya may be that the heat and salt fluxes from the open water contribute to the Antarctic bottom-water formation. For contrast with the satellite observations, we also describe the one oceanographic attempt to study the polynya, namely the joint U.S.-U.S.S.R. 1981 expedition on the MIKHAIL SOMOV, which arrived at the ice during a year in which the polynya did not form. Finally, we describe a hypothetical investigation of the polynya using the Eos instruments and data system.

To begin with a discussion of the sea ice dynamical system, Figure 56 shows a box model of the general winter sea ice behavior and its interactions with the atmosphere and ocean. Examination of the figure shows that the sea ice forms an interac-

tive buffer between the ocean and atmosphere. The atmosphere extracts heat from and generates a wind stress on the ocean surface. The heat flux causes ice growth, and the wind stress causes a differential ice motion. Simultaneously, there are additional fluxes of heat and momentum from the ocean interior. The balance between these dynamic and thermodynamic fluxes yields phenomena ranging from pressure ridge formation at one extreme, to the formation of large polynyas.

Figure 57 shows a block diagram of the polynya dynamics and thermodynamics. The polynyas remain open either by the mechanical removal of ice by winds, or because a strong oceanic heat flux prevents ice formation. Because polynyas are generally ice-free, the strong fluxes of heat and moisture to the atmosphere, as well as the mechanical removal of desalinated ice, lead to a strong convective flux of cold, salty, oxygenated water into the ocean interior.

There are many polynyas in the Arctic and Antarctic. Examples in the Arctic include the North Water in Baffin Bay, the polynyas adjacent to Novaya Zemlya and Franz Josef Land in the Barents Sea, and the open-water region north of Svalbard in the North Atlantic. Of these, the Svalbard and

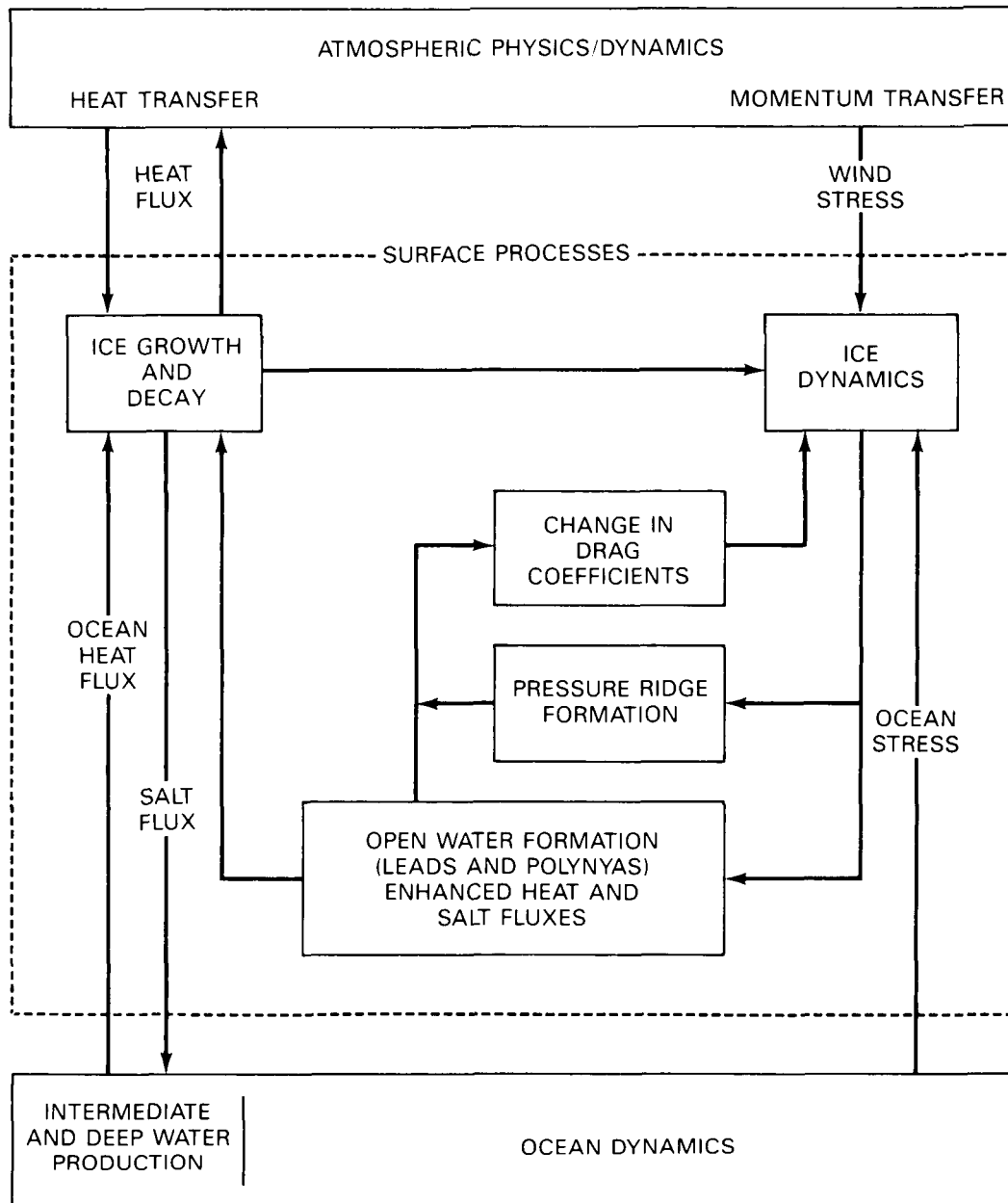


Figure 56. A system model for winter sea-ice behavior.

Barents Sea polynyas are suspected to play an important role in the conversion of the North Atlantic water into Arctic Ocean deep water. In the Antarctic, polynyas form adjacent to the Drygalski Ice Tongue in the Ross Sea, along the Wilkes Land/Adelie Coasts, and in the Weddell Sea. Of all these polynyas, the Weddell polynya is both the largest, with an area equal to the State of Pennsylvania, and the most inaccessible; oceanographers also suspect that it makes a major contribution to formation of Antarctic deep and bottom water.

Background

The Weddell polynya is of particular interest to the Eos program because it was discovered from data taken by the 19 GHz Electronically Scanned Microwave Radiometer (ESMR) on the 1972-launched Nimbus-5 spacecraft. From Carsey's (1980) analysis (see Figure 58) for 1974 the imagery shows the presence of a large region of open water within the Weddell Sea pack ice. During August 1974 for example, the open-water region was approximately rec-

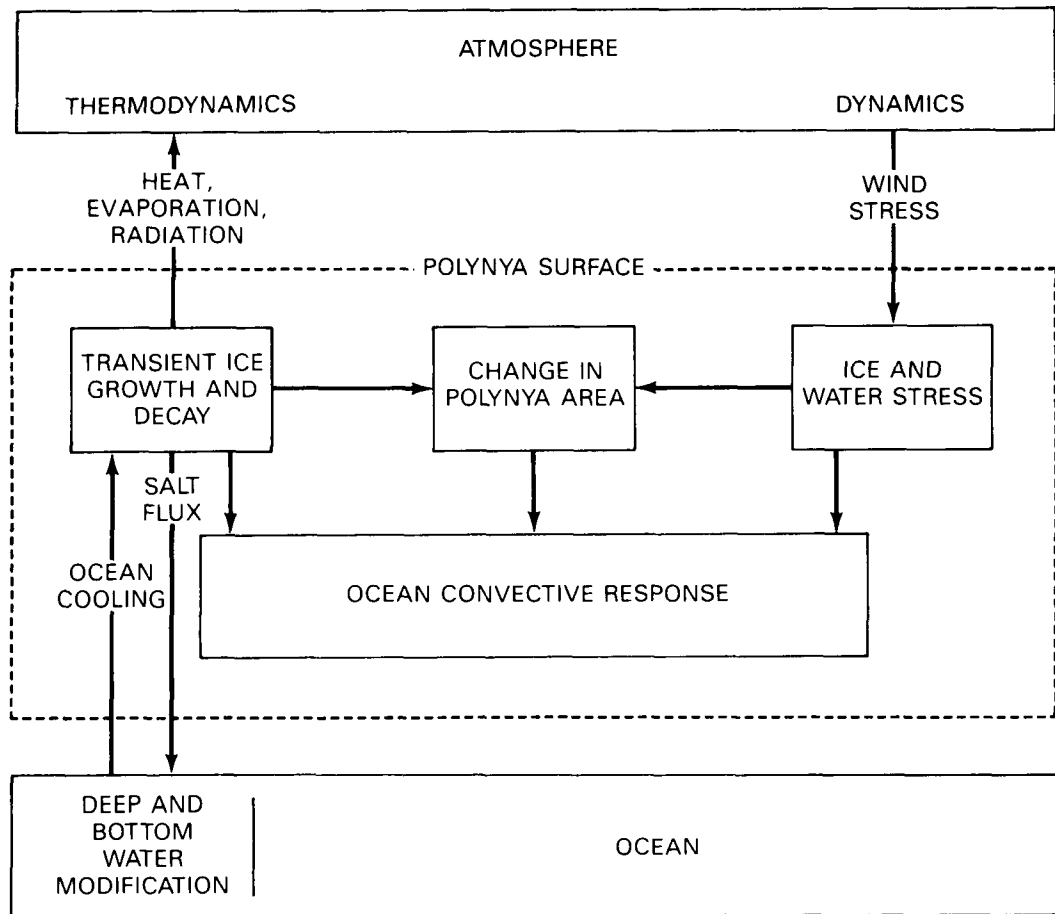


Figure 57. Specific polynya processes.

tangular and measured 300 km \times 1,100 km. Sequential images of the polynya over a 7-year period (Martinson *et al.*, 1981) show that the polynya occurred throughout the winter in 1974, 1975, and 1976; occurred briefly in 1973 and 1977; not at all in 1978; and briefly in 1979.

Martinson *et al.* (1981) and Gordon, (1982) summarize the theoretical and oceanographic work in the polynya region. Examination of the weather data suggests that a large oceanic heat flux, rather than mechanical ice removal, keeps the polynya ice-free. The theoretical analysis of the few summer oceanographic transects suggests that heat transfer within the polynya occurs in the form of a few eddies, called chimneys, which measure about 30 km in diameter and through which most of the heat transfer takes place. The models further suggest that the heat transfer takes place through a cyclic overturning in which thin ice occasionally covers the polynya surface.

Because of the interest in the polynya, beginning in 1979, Arnold Gordon of the Lamont-Doherty Observatory and E.I. Sarukhanyan of the Arctic and Antarctic Research Institute in Leningrad began

planning a joint U.S.-U.S.S.R. polynya expedition. The experiment, called WEPOLEX-81 (Weddell Polynya Experiment), was scheduled for the fall of 1981. After considerable planning and the additional encouragement of satellite observations of a small polynya during 1980, the cruise began when the Soviet icebreaker MIKHAIL SOMOV left Leningrad in early September 1981 for Antarctica. In early October, the SOMOV arrived in Montevideo to pick up the U.S. scientists, then left Montevideo for the ice on October 9. The SOMOV entered the ice near the anticipated location of the polynya on October 20. Unfortunately, as satellite observations later verified, no polynya occurred in 1981, so the SOMOV departed the ice on November 25 without the desired oceanographic and heat flux observations (Gordon, 1982).

This 2- to 3-year planning cycle for the SOMOV cruise is typical of oceanographic research; this brief description of the expedition points out the difficulties in the oceanographic study of transient phenomena. Because of these difficulties, we next describe a hypothetical Eos study of the polynya.

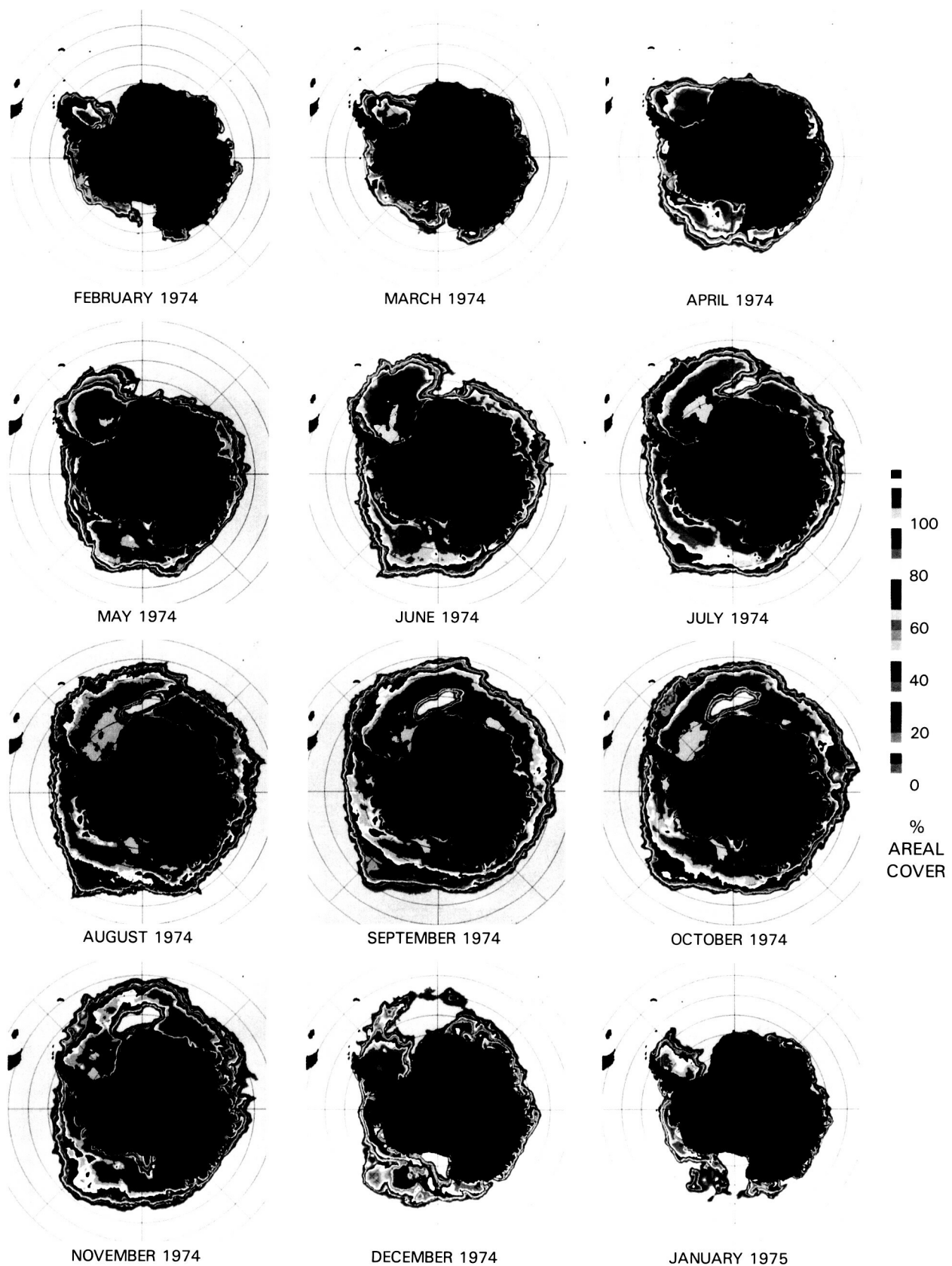


Figure 58. Passive microwave satellite images for 1974 of the Antarctic ice cover (courtesy of Frank Carsey).

The Satellite Study

Let us focus on a single scientific experiment designed to describe the polynya behavior from satellite observations. To model the polynya behavior, we need the following measurements:

- The polynya area, the ocean wave field, and the nature of the thin ice cover within the polynya;
- The wind field over the polynya and surrounding pack;
- The motion and deformation of the thick sea ice surrounding the polynya;
- Evidence for the occurrence of convection within the polynya; and
- The heat flux and if possible the moisture flux from the polynya to the atmosphere.

Given these necessary measurements, how could we use the proposed Eos instrument package to examine the polynya processes?

The Specific Experiment

Imagine that we are at the beginning of the austral winter in April-May, with the Eos system up and working. We also have a program to instrument the ice pack surface with a number of air-dropped ADCLS buoys that report position, surface temperature, and pressure.

Step 1—We begin our study with the examination of selected MODIS and AMSR channels. We use MODIS to search for cloud-free images of the Weddell Sea, and the passive microwave data to derive sea ice concentrations for the entire Weddell Sea. We also examine the related weather observations as taken by AMSU and HIRIS, and the atmospheric surface pressure charts as improved from the ADCLS buoy pressure data.

Step 2—If we observe the formation of a polynya, we call for the following instrument sequence within the much smaller polynya area:

- **SAR Imagery**—The computer simulation of the Eos instruments and orbits shows that SAR observes the polynya twice a day at approximately 12-hour intervals. This regular sampling of the polynya will allow us to see convective features with time scales greater than 12 hours. We will, therefore, use the high-resolution radar imagery to tell us if and what kind of ice formation occurs in the polynya. The SAR should also show if long-period surface waves occur. Previous work shows that ice formation in a wave field occurs in the form of small millimeter-scale crystals called frazil ice, which are herded into

long streaks parallel to the wind by a Langmuir circulation. Because our experience with Seasat shows that this circulation is visible from satellite, it should also be observable by Eos. Our first cut at the problem, then, will be to see if any ice growth occurs in the polynya, or if the oceanic heat flux keeps the polynya ice-free.

- **Scatterometer Observations**—We want to know how surface winds affect the polynya. For example: does ice grow in the presence or absence of winds? Do the polynya boundaries melt as the winds advect them into the region, or do the polynya boundaries alter? To answer these questions, we need direct surface-wind measurements. Because the scatterometer Doppler cell measures about 70 km \times 50 km, given the polynya size, we should acquire several direct surface-wind observations from the polynya. In order to ensure that the polynya is ice-free, we would like these measurements to be simultaneous with the SAR coverage. For this case, the computer simulation shows that if the two instruments are on the same satellite, the broad scatterometer swath always overlaps the SAR swath; if the instruments are on different satellites, the scatterometer frequently overlaps the SAR.

Step 3—Because the polynya consists of warm water exposed to cold air, low clouds or fog are likely to cover the polynya. If however, the MODIS observations show that there are periods when the polynya is cloud-free, we will also call for a HIRIS and TIMS examination of the polynya in an attempt to observe the temperature structure of any possible convection.

Step 4—Finally, we will take altimeter and possibly LASA observations over the polynya to measure the ice or water surface roughness.

We anticipate that the first high-resolution examination of the polynya would last for 1 week, or alternatively through one weather cycle, after which we would stop the high-resolution measurements and do a preliminary data analysis.

Data Analysis

From the surface temperature, wind field, and the radiative losses from the polynya, we will estimate the heat and moisture flux from the polynya. From the sequential SAR images, we will search for evidence of deep convection in patterns on the ocean surface, which theoretically may occur either in the proposed chimneys or in alternative patterns such as Benard cells or rolls. We will use the fluxes and form of the convection to model the salt and heat flux to the interior. We will continue the

passive microwave observations throughout the austral winter, and plan on repeating the high-resolution observations for about 1-week periods through each of the months that the polynya is active.

In summary, the initial goal will be to work with a relatively small amount of data to see what goes on in the polynya; our purpose is to understand the physical processes, and to develop a physical model of the polynya. Our eventual goal is to find out if the polynya serves as a source of bottom water, and to estimate the magnitude of this source.

AIR-SEA INTERACTIONS

Introduction

During the past decade, scientists have discovered that sea surface temperature changes of order 1°C in the equatorial Pacific Ocean are associated with major global changes in atmospheric patterns of rain, storm tracks, and drought. Further, ocean cruise results show that these surface temperature changes occur throughout the oceanic surface mixed layer, and thus correspond to large changes in heat storage. Because the source of this stored heat is the sun and the atmosphere, the rates at which energy is added or subtracted from the ocean are determined by small-scale flux processes at the air-sea interface. Our purpose in this section is to examine how the Eos measurements of the processes that transfer heat, water vapor, and momentum between the atmosphere and the ocean will contribute to air-sea interaction studies.

As the Blue Planet section in Chapter III describes, air-sea interaction processes couple the atmosphere and ocean (Figure 15). This coupling determines the state and evolution of the atmosphere-ocean system. In this section, we apply the results of the Eos measurement techniques described in the Blue Planet section to the specific problem of determining the interaction between the atmosphere and the equatorial ocean.

The oceanic storage and release of heat occur through the transfer of radiation and latent and sensible heat at the interface. This transfer plays a major role in the maintenance and moderation of the global climate. At the large scale, the effect of these small-scale transport mechanisms on the ocean is as follows. Because the earth is spherical and has an inclined axis, solar heating has a strong seasonal variation as well as being much stronger at the equator than at the poles. However, the past few decades of oceanic observations show that the average ocean temperature has remained constant, so that the ocean assists the atmosphere in transporting the surplus of energy received at low latitudes to energy-deficit regions at high latitudes. Because an ocean basin can absorb an excess of heat at one season,

transport it to a different location, then give it back to the atmosphere at a different season, this transport of energy does not occur uniformly in time or space.

To understand the changes in the global climate and hydrologic cycle, we need to measure and understand the ocean basin-scale fluxes of heat, water vapor, and momentum. Of particular importance to climatologists are several areas of large spatial-scale inhomogeneities in seasonal oceanic heating of the lower atmosphere. As Niiler (1981) describes, the most important of these regions to world climate is the central equatorial Pacific Ocean. The anomaly pattern in this region, called "El Niño," consists of a large-scale ocean surface warming, and a change in the global atmospheric pattern called the Southern Oscillation. Because of the global importance of El Niño, we will concentrate on its description and specific observational requirements.

In the next decade, an international research program called Tropical Ocean and Global Atmosphere (TOGA) has as its goal to understand the coupling between the equatorial Pacific and the global atmosphere associated with El Niño. Specifically, TOGA hopes to accomplish the following (NASA Ocean Energy Fluxes, 1985):

- To determine the extent to which the time-dependent behavior of the tropical oceans and global atmosphere system is predictable on monthly to yearly time scales;
- To study the feasibility of modeling this coupled ocean-atmosphere system for prediction purposes;
- To provide the scientific background for the design of an observation and data transmission system for operational prediction, if this capability is demonstrated by coupled ocean-atmosphere models.

In this section, we describe the phenomenon of El Niño and the magnitude of the changes in the observed fluxes and sea surface temperature associated with it. We then describe the present and future monitoring programs that will allow prediction of the onset of El Niño and of other ocean phenomena associated with climate change. As background for this discussion, the Blue Planet section describes the processes that transfer heat, water vapor, and momentum between the ocean and atmosphere.

The El Niño

The recent interest in studies of the equatorial Pacific is due to the exceptionally strong 1982 to 1983 El Niño. By some estimates, this climate anomaly, associated with a surface temperature change of about 1°C, caused 1,000 deaths, as well as severe economic

damage in Australia, Asia, South America, and Africa. The heating of the equatorial Pacific that occurred at this time was associated with modifications in weather and rainfall around the world. For example, severe droughts occurred in Australia, Indonesia, and South Africa. Torrential rains caused severe flooding along the South American coast. The California coast also suffered heavy rainfall, and the fisheries off Ecuador and Peru were destroyed by the lack of upwelling.

Under regular conditions in the equatorial Pacific, the winds blow steadily across the Pacific from east to west, pushing the warm surface waters before them. This oceanic circulation produces strong cold-water upwelling along the coast of Ecuador and Peru, and intense convection at the Asian side of the Pacific produces heavy rainfall in Australia and southeast Asia. During the anomalous El Niño years, conditions change in both the atmosphere and ocean; the ocean surface temperature warms, the easterly winds weaken, the South American upwelling does not occur, and drought occurs in Australia and southeast Asia, with additional modifications to global rainfall and storm patterns.

Figure 59 shows the distribution of a composite SST anomaly at the height of the El Niño. There is a warm lens of water spreading westward from the South American coast along the equator, with a temperature anomaly maximum of about 1.5°C . Figure 60 shows the corresponding heat flux anomalies; the magnitude is about 100 W m^{-2} . Although both of these maximum signatures can be identified by satellite, our goal with Eos is to identify the much smaller precursor signatures, and to follow their evolution.

To study the onset of El Niño, Liu (1985) shows that we need improved monthly averages of the heat

fluxes at a 2° spatial scale (about 200 km). As discussed in the Blue Planet (Chapter III), the critical variables are sea surface temperature (SST), the specific humidity, the surface wind speed, and the radiation balance. Of these parameters, the largest source of variability in the equatorial Pacific comes from the radiation balance and the evaporative heat loss. Of these two, the most difficult to determine is the evaporative heat loss, because it cannot at this time be determined from a single satellite measurement. Following Liu and the NASA Ocean Energy Fluxes Study (1985), to predict an El Niño, the root-mean-square (rms) accuracies of our variables must be as follows: winds to 1 m s^{-1} , heat fluxes to 20 to 40 W m^{-2} , and SST to 0.3°C .

Present Measurement Techniques

To determine the heat, moisture, and momentum flux to and from the ocean, we need to measure the following quantities. For the radiative fluxes, we need the solar flux, the cloud distribution, and the sea surface temperature. For the sensible, latent, and momentum fluxes, we need the wind speed and direction, the sea state, and the vertical boundary layer stability. The stability requires knowledge of the air temperature at some fixed height above the sea surface, the SST, and the specific atmospheric humidity. For completeness, we also require precipitation rates.

Radiation

The radiation balance at the sea surface is a strong function of the cloud cover. For the short-wave radiation, daily averages are currently provided from the geostationary satellites with an accuracy of about 10 W m^{-2} , with improved accuracies over

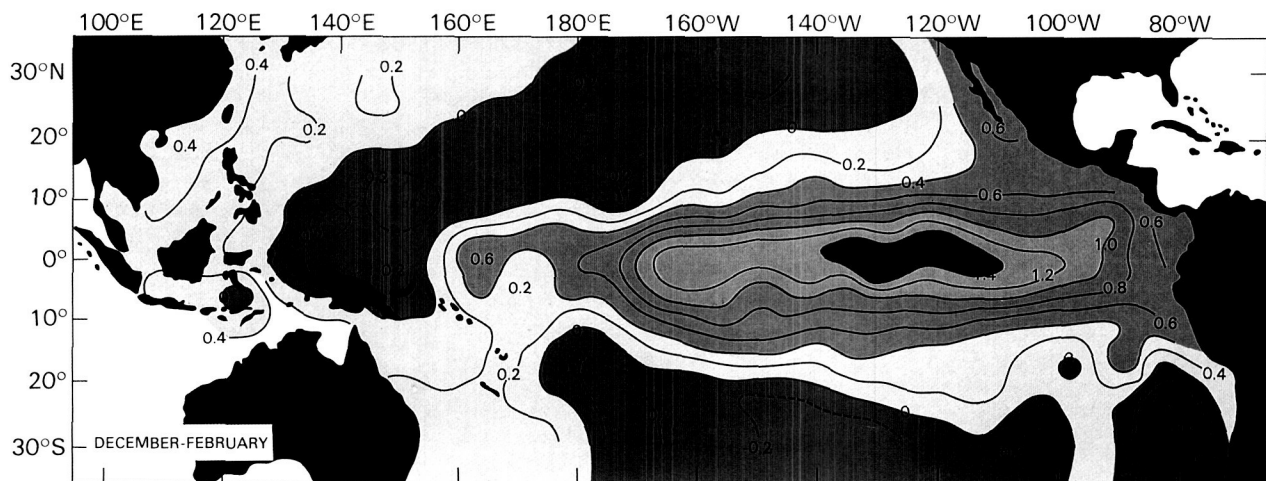


Figure 59. Contours of the composite SST anomaly taken from ship track data and generated by the six El Niños between 1949 and 1981. The "H" and "L" stand for highs and lows in the temperatures (adapted from Rasmusson and Carpenter, 1982).

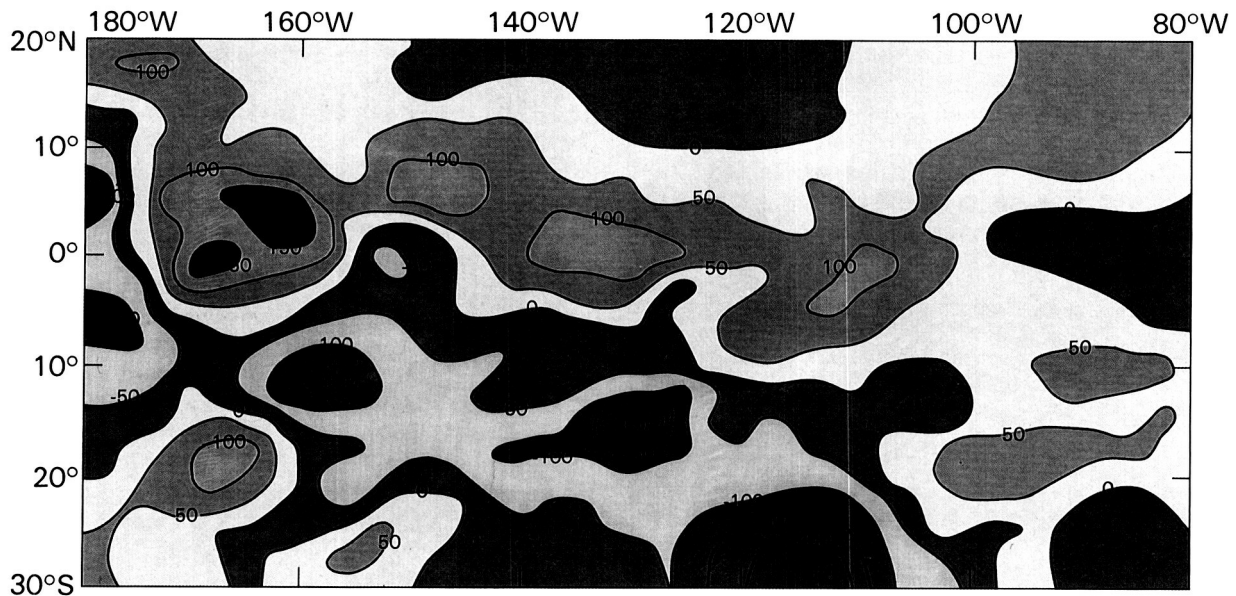


Figure 60. The latent plus sensible ocean heat flux difference between December 1972 El Niño and December 1973 non-El Niño. Along the equator the ocean is cooled more and the atmosphere is heated more in December 1972 than in December 1973. Contours are in watts per square meter; positive numbers (shaded areas) mean a flux from the ocean to the atmosphere (adapted from NASA Ocean Energy Fluxes, 1985).

monthly time scales. In the near future, the International Satellite Cloud Climatology Project (WCRP, 1985) will facilitate the computation of shortwave radiation. For the net longwave radiation, which is a function of cloud cover, atmospheric water vapor content, and sea surface temperature, the validation of existing models requires further work.

For the equatorial Pacific, the long-wave radiation makes a small contribution to the total heat flux (10 to 20 W m^{-2}) over most of the area of interest. This may not be the case, however, in the eastern Pacific near the South American coast, where stratus clouds often prevail over cold upwelling regions. Low stratus clouds increase the downwelling longwave radiation flux in comparison with clear air conditions, and cold upwelled waters induce large air-sea temperature differences, which also enhance the sensible heat flux from the ocean surface. To obtain the radiation balance, the dependence of the downwelling longwave radiation on the cloud cover must therefore be determined to the accuracy of the shortwave determination.

Surface Winds

Currently, surface winds are either measured directly from shipboard observations or are inferred from cloud displacement vectors operationally produced from geosynchronous satellite imagery. The disadvantages of these techniques is that shipboard winds are only available along the major shipping routes, and the cloud displacement winds represent winds only at cloud level. Cloud displacement winds

are also not available in areas where high clouds obscure low clouds or where there are no clouds. As the review in WCRP (1984a) shows, wind speeds can also be measured by microwave radiometers and altimeters; however, these techniques measure only wind speed, and not direction. The best method for measuring both wind speed and direction appears to be the scatterometer.

Analysis of the 3 months of data from the Seasat scatterometer showed that the global wind fields could be derived with higher resolution and better accuracy than was possible with either shipboard or cloud-tracking observations. The wind stress can then be derived from the wind vectors using conventional bulk formulas or directly from the radar backscatter.

The next NASA scatterometer is scheduled to be flown in the early 1990s. It is designed to measure wind vectors with 50 km resolution, 2 m/s (rms) or 10 percent accuracy in wind speed, and 20 percent (rms) accuracy in direction, for wind speeds ranging from 3 to 30 m/s. Further improved scatterometer technology is being developed and should be ready by the time of Eos, but until these instruments are developed and flown, it will be difficult to obtain the global wind flux.

Moisture Flux

The Blue Planet section in Chapter III describes the techniques for estimation of the moisture flux from shipboard weather observations and from satellite techniques. For the analogous monthly

mean latent heat flux, Liu (1985) found that the values derived from satellite radiometer measurements fall within 30 W m^{-2} of the latent heat fluxes derived from ship reports. To illustrate the relative accuracy of the SMMR algorithm, Figure 61 shows the variation of the latent heat flux with latitude, as derived from ship reports and from SMMR. Comparison of the curves shows that the two derivations yield equivalent results.

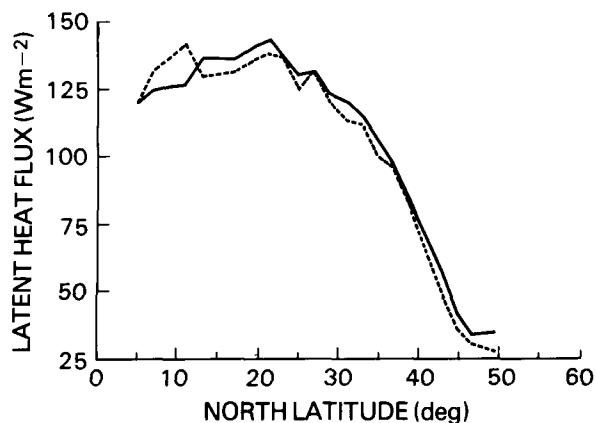


Figure 61. The zonal mean latent heat flux for the northern hemisphere calculated from coincident ship reports and the Nimbus-7 SMMR for the year 1982. The dashed curve is from ship reports; the solid curve is from SMMR data (courtesy of T. Liu).

To illustrate the utility of the present SMMR observations, and to show the difference between a "normal" and an El Niño period, Figures 62 and 63 show the distribution in the equatorial Pacific of SST, wind speed, precipitable water, and latent heat flux for both a normal and an El Niño period. On these figures, the land is grey, and black is missing data.

To examine first the "normal year," Figure 62 shows the combined monthly averages for January 1980 and 1981 of the SST, surface wind speed, precipitable water, and the latent heat flux derived from these three parameters. In this normal period, the distributions of these four parameters are closely related. The SST shows that along the equator and away from the coasts where the SST algorithm breaks down, there is a cold tongue extending from the South American coast that interrupts the warm-water belt of the tropical Pacific. Because of convective lifting of the air and surface evaporation, the regions of large atmospheric water vapor overlie the warm surface water. In contrast, the air over the cold tongue is a region of low atmospheric water vapor. Because of this surface convergence and the rising air, low wind speeds occur in these same regions. Finally, the latent heat flux is approximately proportional to the wind speed.

Later in 1982, one of the most intense El Niño/Southern Oscillation episodes began. Figure 63, which gives the analogous distributions for January 1983, shows the changes that have taken place at the height of El Niño. The SST shows that the cold tongue along the equator has vanished, due to the disappearance of coastal upwelling, and that the entire Pacific is warmer. Examination of the winds shows a strengthening of the trade winds north of the equator and a weakening of the winds to the south. Atmospheric convection above the warm water yields a region of large water-vapor content that extends all along the equator. Physically, surface observations showed that this change in the water vapor distribution led to large rainfall and flooding in certain of the equatorial islands. Finally, the latent heat flux pattern is strongly altered, with the largest fluxes now lying entirely north of the equator. The change in these fluxes is dominated by the change in the surface wind patterns.

Sea Surface Temperature

Sea surface temperature can be measured by infrared and microwave radiometers and by atmospheric sounders. Various techniques were recently evaluated in a series of NASA Sea Surface Temperature Workshops; the results are summarized in a special issue of the *Journal of Geophysical Research* (Vol. 90, No. C6, 1985).

To illustrate the problems and potential of different SST measurement techniques, Figure 64 shows the SST anomalies derived in four different ways for November 1979 (from Hilland *et al.*, 1985). In each case, the measurement rms accuracy is about 1°C . The top figure shows the surface ship data, where black indicates no data. The figure shows that ship data are only available along major shipping routes, such as the great circle routes between the United States west coast and Asia, and the tanker routes around the tip of South Africa. The figure also shows that there are very few data from the critical region of the eastern Pacific.

The second figure shows SSTs derived from the infrared AVHRR instrument. This high-resolution SST instrument cannot see through clouds. The missing data points along the equator show the location of the cloud bands that lie in the equatorial convergence. The figure shows that even for a 1-month average, there are large areas of missing data in the western tropical Pacific due to clouds.

The third figure shows the SST derived from the TOVS (Tiros Operational Vertical Sounder), which uses a combination of infrared and microwave observations to determine SST. The fourth figure shows the SMMR SSTs at a 150 km resolution, where the SMMR data was only processed for the Pacific. The gaps in the SMMR temperatures near land are caused by side-lobe contamination, which, as the figure shows, causes data gaps in the tropical Pacific. It would appear from this figure that the hybrid in-

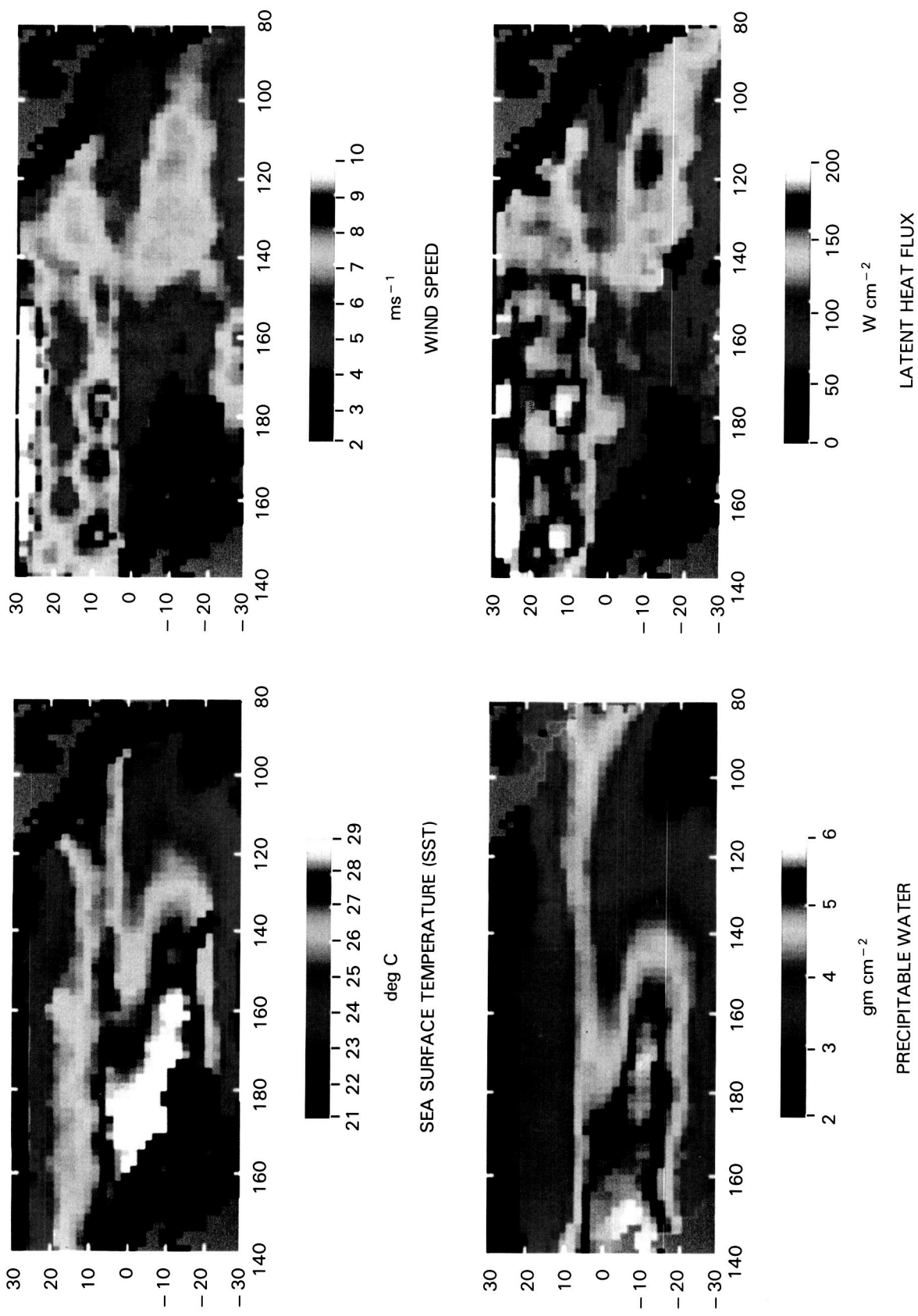


Figure 62. The combined monthly averages for January 1980 and 1981 of SST, wind speed, precipitable water, and latent heat flux (courtesy of T. Liu).

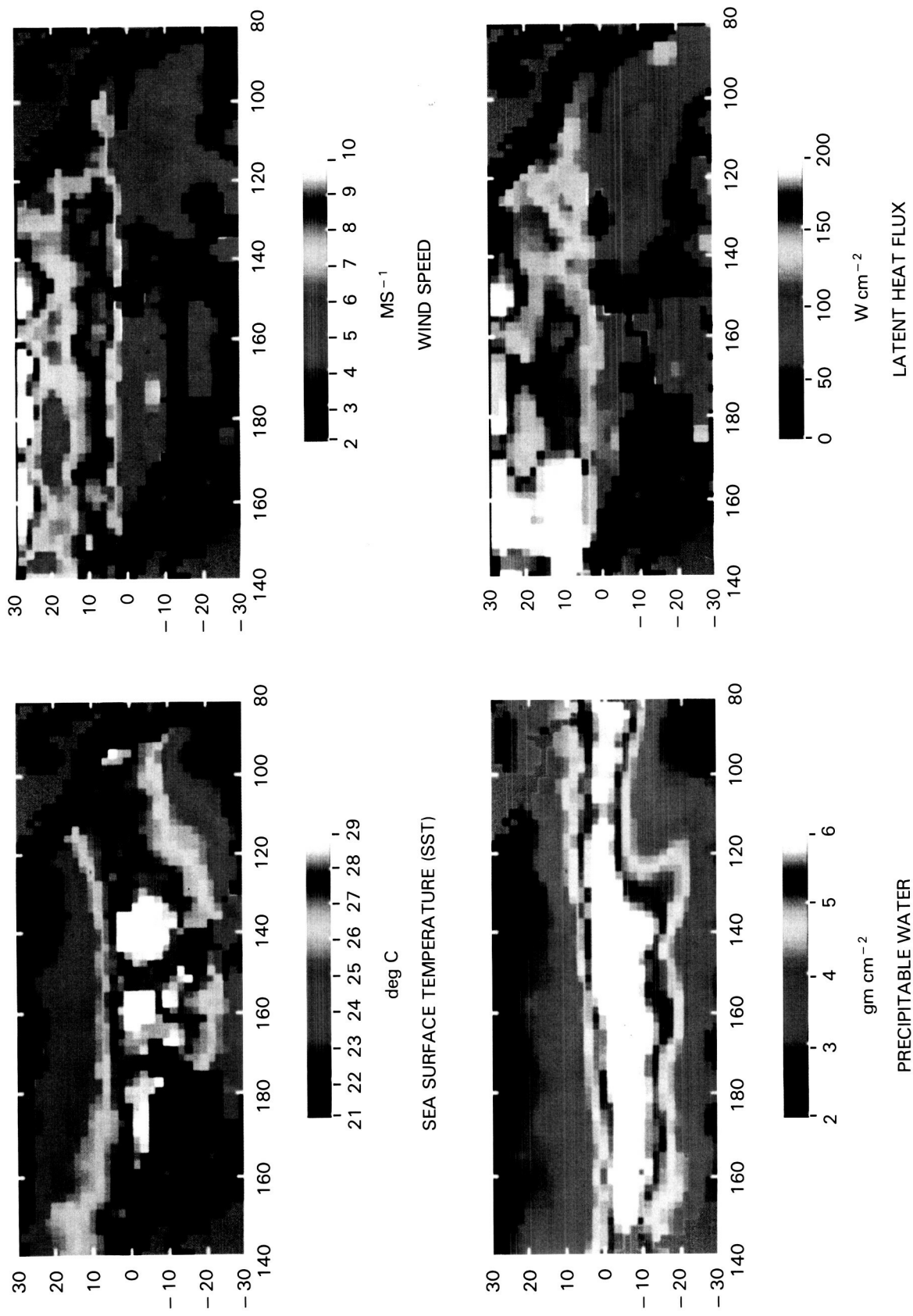


Figure 63. The combined monthly averages for January 1983 of SST, wind speed, precipitable water, and latent heat flux (courtesy of T. Liu).

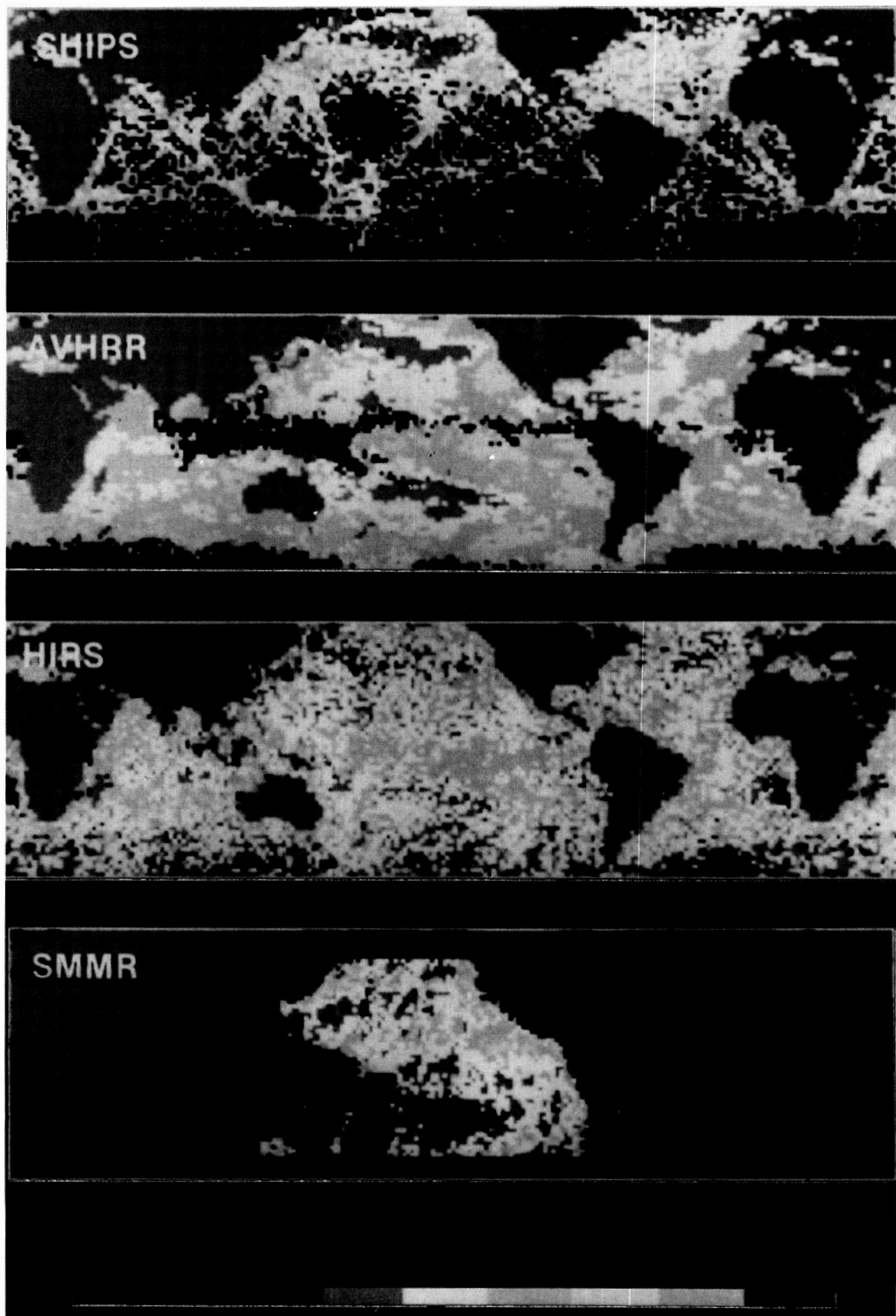


Figure 64. Anomalies in sea surface temperature observed in four different ways for November 1979. The figure shows SST anomalies as determined from ships, AVHRR, HIRS, and SMMR, where the SMMR coverage is restricted to the Pacific (from Hilland *et al.*, 1985).

framed passive microwave TOVS may be the most suitable instrument for climate studies in the tropical Pacific.

To summarize the above discussion, our major needs are for measurement of cloudiness and its impact on the downwelled longwave radiation, and for an improved measurement of the latent heat flux in time and in accuracy. We also need improved measurements of the rain rate, and for prediction purposes, improved surface wind and SST observations.

The many measurements required to determine the total heat flux necessitate a synergistic approach. The TOGA Heat Exchange Project (Liu and Niiler, 1985) is an example of such an approach. It is an attempt to determine the total heat flux over the tropical Pacific using a number of existing space-borne sensors. In TOGA, the expertise of a number of investigators is pooled together with a validation and data management program into a coherent plan. This pre-Eos exercise should also serve as a model for future Eos work.

The Role of Eos

In the air-sea interaction studies of the future, Eos will provide the following:

- Every other day coverage of the tropical and temperate oceans;
- The desired measurements of wind speed, specific humidity, and air and sea temperatures to an accuracy sufficient for prediction of climate change;
- Better measurements of precipitation through the Eos AMSR and TREM; and
- Timely access to the flux data base through the Eos data and information system.

As discussed both in this section and in the Blue Planet section, the present spaceborne sensors and remote sensing techniques provide useful estimates of ocean-atmosphere exchanges of momentum, heat, and moisture only in certain regions and at specific time scales. New sensors and improved techniques developed for Eos will fill the gaps. Eos will also provide the first opportunity to monitor comprehensively the coupled atmosphere and upper-ocean heat budget.

Measurement of the Rain Rate

The TREM, which is an essential part of the total Eos strategy, should provide validated measurements of the tropical rain rate. These data, combined with the supplementary measurements from the geosynchronous satellites, will yield an estimate of the precipitation component of the freshwater budget, as well as provide the data

necessary to calculate the diabatic atmospheric heating.

SST and Wind Retrievals

The advanced imaging spectrometers MODIS and TIMS will provide better accuracy, precision, and spatial resolution in the measurement of sea surface temperature. Also, the improved scatterometer design by the time of Eos or the deployment of multiple instruments should eliminate the problems due to the limited swath and the nadir gap of the present scatterometers. The combination of wind stress and SST measurements should make possible estimates of surface currents, mixed-layer depth, and the entrainment rate. Determination of momentum and heat flux to compatible temporal and spatial scales will facilitate the study of upper ocean heat budget.

Use of Data Collection Buoys

The upper ocean thermal structure description requires subsurface data not directly obtainable from space. However, the ADCLS on the initial polar platforms will be essential for the acquisition of these data. As discussed above, the routine collection of climate data by ships will not provide an adequate sampling over large parts of the Pacific, so that large regions of sparse sampling will need to be filled. This will require deployment of a number of moored arrays and drifting instrument systems, and the data from these will be relayed through ADCLS.

Better Data Transmission and Management

The study of ocean-atmosphere interaction and coupled upper-ocean and atmosphere heat budget require processing and merging of large volumes of spaceborne and *in situ* data. Eos will provide efficient collection, transmission, and archiving of these data. In summary, the Eos spaceborne measurements combined with the ADCLS and other surface measurements will provide a greatly enhanced data base for the determination of global air-sea interactions.

INTRODUCTION TO ATMOSPHERIC PROCESSES

The final four sections of this chapter deal with studies of atmospheric processes. They include studies of the chemistry and dynamics of the troposphere, the stratospheric ozone layer, and the mesosphere, or those regions of the atmosphere between the Earth's surface and a height of about 90 km. Conditions vary greatly over this large altitude range, in which the pressure and density both decrease by six orders of magnitude. Some basic conditions are the same, however. The atmosphere is

overwhelmingly composed of neutral molecules, and the major species are uniformly mixed.

For many purposes it is necessary to take account of the differences. A traditional approach is to divide the atmosphere according to the mean temperature structure, as illustrated in Figure 65. That ap-

proach will be followed here, but it should not obscure the fundamental unity of the atmosphere, or cause the strong coupling among atmospheric regions to be overlooked.

The troposphere, the lowest 8 to 16 km of the atmosphere, is a region in which the temperature

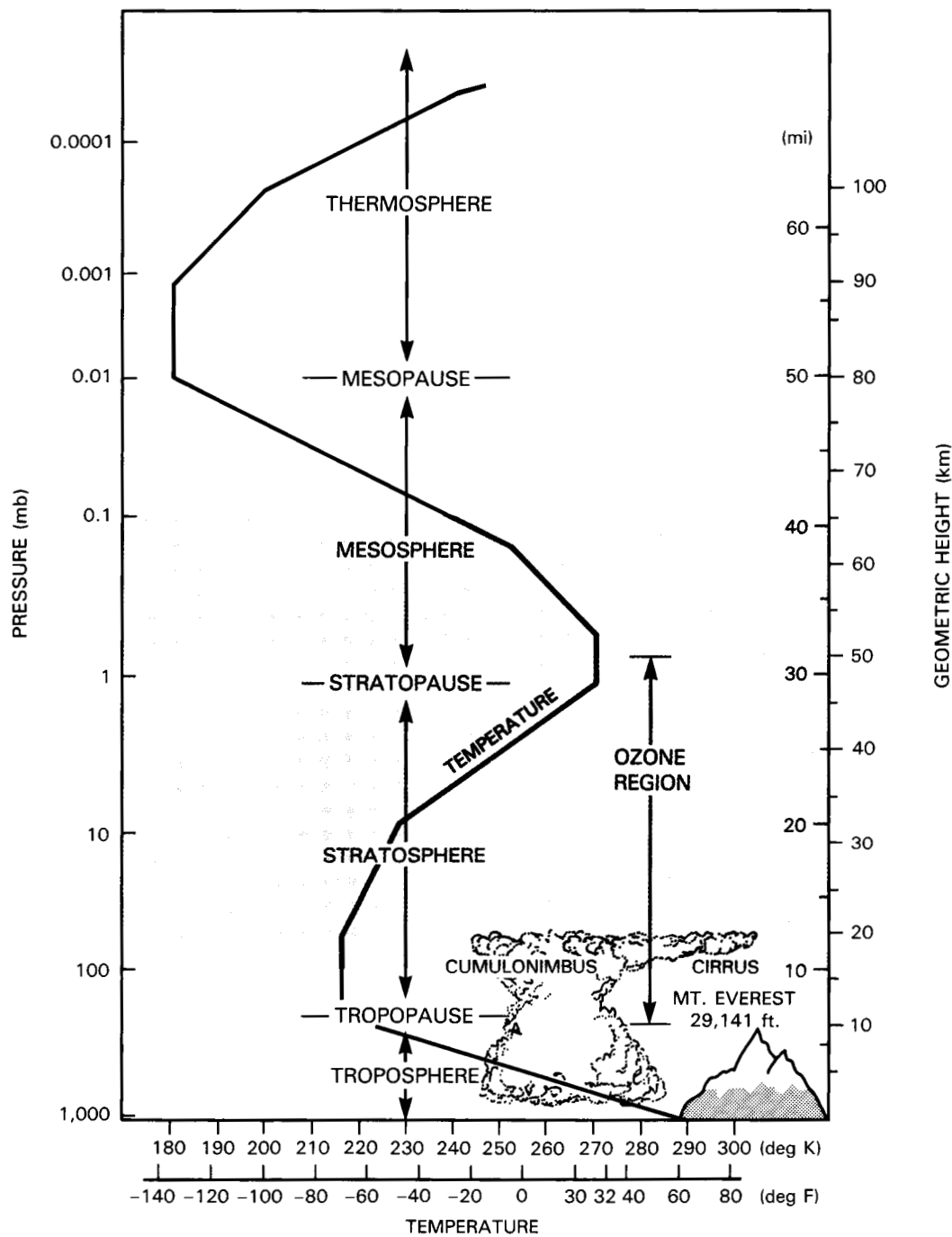


Figure 65. Plot of vertical temperature distribution in Earth's atmosphere from surface to 100 km altitude, giving the nomenclature of atmospheric regions. For comparison, the heights of high clouds and Mt. Everest are also shown.

decreases rapidly with altitude, and the vertical temperature gradient is close to convective instability. The major heat source for the lower atmosphere is the absorption of visible light from the sun at the Earth's surface. This heat is then transferred to the atmosphere by a variety of processes. While horizontal motions of planetary scale are important, vertical mixing and small-scale motions also play essential roles in the dynamics of the troposphere. Most clouds are found here, although vigorous convective systems can push through the upper boundary—the tropopause—and reach the lower stratosphere. This is also the region in immediate contact with the biosphere. In particular, it is the region in which we live, and into which the gaseous by-products of our activities are released.

The stratosphere stretches from the tropopause, which in mid-latitudes is about 11 km high, to the stratopause, a region of temperature maximum at an altitude of about 48 km. Between these levels the temperatures are either constant or increase with altitude, which makes the stratosphere dynamically stable against convective overturning, and favors the occurrence of large-scale circulation systems. It is also the region in which photodissociation of molecular oxygen leads to ozone formation, and in which a large number of natural and anthropogenic species catalyze ozone destruction. The ozone layer is of critical importance because it shields the Earth's surface, and in particular its nucleic acid-based life, from destructive ultraviolet solar radiation.

Chemical, dynamical, and radiative processes are closely coupled in the stratosphere. This region is also strongly linked to the troposphere by dynamical effects, radiative exchange, and by the exchange of chemical constituents. In general, the net effect is for the stratosphere to receive insoluble substances from the troposphere, and return soluble compounds to it. In the stratosphere ultraviolet light photodissociates most of the long-lived chemical products of man and the biosphere.

From the stratopause, the mesosphere extends up to the mesopause at 80 to 90 km. Over this altitude range the temperature decreases with altitude, but not so rapidly that it is near a state of convective instability. Here polyatomic molecules are for the most part dissociated by the strong solar UV, and ozone chemistry is controlled by hydrogen and oxygen reactions. The dynamics are for the most part dominated by energy and momentum propagating up from below, although at times there are effects driven from the overlying thermosphere.

The mesopause can be thought of as an approximate boundary between the underlying atmospheric regimes that are dominated by processes resulting from the absorption of solar radiation with wavelengths greater than 120 nm (Ly α) by the Earth's surface and lower atmosphere on the one hand, and the overlying upper atmosphere that is dominated by solar wavelengths shorter than Ly α , and the solar

wind interaction with the earth's magnetic field on the other.

Probably no discipline has benefitted more from satellite data than atmospheric science. The first TIROS spacecraft in the early 1960s provided pictures of cloud systems that gave a completely new perspective on the ways in which motions on different scales were organized. The first remote sounders on Nimbus-3 in 1969 provided quantitative temperature profiles up to an altitude of 30 km, the ceiling of conventional balloon-borne meteorological observations. For the first time satellites filled in the enormous data voids over oceans and in the Southern Hemisphere. Subsequent advances have improved the accuracy, vertical resolution, and ability to penetrate clouds for tropospheric sounding. Other developments have extended observations up to 90 km, greatly increased the vertical resolution of these observations by scanning the Earth's limb, and determined the distribution of ozone and a large number of the chemical species with which it interacts.

These advances have solved some problems, led to rapid progress in many other areas, and extended our knowledge to the point where our framework has changed and new questions have been raised.

In the following four sections, a few current problems in the atmosphere below the mesopause are described. Some of the ways in which measurements from Eos sensors will be used to address them are outlined. The reader should bear in mind that these are only examples from a complex set of questions, and that they underestimate the possibilities and needs for interdisciplinary investigations.

USE OF Eos FOR STUDIES OF ATMOSPHERIC PHYSICS AND DYNAMICS

Introduction: Benefits and Requirements for Advancement

Anticipated developments in satellite-borne remote sensing and in computational power will soon allow scientists to observe, predict, and understand atmospheric behavior to levels of detail and sophistication unimaginable a mere decade ago. The gains from this potential for gathering atmospheric information and creating a physically consistent spatial and temporal data base are probably beyond our current enthusiastic expectations. As we observe and comprehend more of the fundamental physical processes and incorporate their effects in models of atmospheric behavior, weather and climate prediction skills will improve. The nature of atmospheric circulation is thought to limit deterministic forecasts to about 2 weeks. The more comprehensive data sets available from Eos and improved geostationary satellites will extend our deterministic prediction

capabilities toward that perceived limit. They will greatly improve our ability to predict trends on seasonal and longer climatic scales, for specific regions of interest as well as for the entire globe. They will also clarify the mechanisms by which the atmosphere is coupled to the Earth system, and the details of its role in that system.

The key concept for these advances is that the atmosphere is not isolated from its geophysical environment. Fluxes from the surface of energy, momentum, moisture, and CO₂ (and possibly other trace gases) are required for boundary and initial conditions for climate modeling, numerical weather prediction, and diagnostic studies of atmospheric behavior. While these fluxes force the motions of the free atmosphere above the boundary layer, there is a dynamic coupling between the atmosphere and the Earth's surface through the atmospheric boundary layer. The atmosphere exchanges momentum with both the oceans and the land. The most important surface-to-atmosphere coupling is through the fluxes of moisture. This is because the latent heat released during condensation is an important energy source for atmospheric motions and because the input of water to the atmosphere ultimately determines how much water vapor is available for cloud formation and precipitation. Advances in the determination of surface fluxes as well as of the free atmosphere winds (especially tropical winds) will improve our understanding and prediction of atmospheric behavior.

The Earth Observing System will help form the foundation for these advances by providing detailed simultaneous data sets from the entire physical system—the atmosphere and the underlying land and ocean surfaces. These data will permit the development of new insights into physical processes, thereby improving the quality of the models, and will provide more detailed data as input to models. The principal scientific goals for the improved understanding of atmospheric physics and dynamics are well stated in the recent National Research Council publication of the Space Science Board's Committee on Earth Sciences (CES) (NRC, 1985). In summary, it recommends detailed understanding of physical processes and feedback effects that will allow an understanding of the coupled climate system and eventually lead to improved predictions of weather and climate.

Specifically, the CES states that the primary scientific objectives in observing lower atmospheric processes over the next 10 to 15 years in order of priority are as follows:

1. (a) To obtain global data for the internal- and boundary-forcing processes that maintain the atmospheric circulation. The required data sets are (i) surface wind, atmospheric temperature and humidity, wind stress over the oceans, and land and sea surface temperature; (ii) precipitation, and closely-related surface characteristics including soil moisture, snow and ice

cover, and vegetative biomass; (iii) surface radiation and albedo, radiation at the top of the atmosphere; and (iv) cloud characteristics including type, amount, height, temperature, liquid water content, and radiative properties.

- (b) To obtain temporally-continuous global data sets of sufficient spatial density and accuracy to determine the large-scale structure of the troposphere. The required data sets are for (i) wind, temperature, and moisture in the free atmosphere; and (ii) surface pressure.

2. To obtain special high-resolution data sets to answer fundamental scientific questions concerning the generation, maintenance, propagation, and decay of mesoscale atmospheric phenomena. The required data sets are for (i) wind, temperature, and moisture in the free atmosphere; (ii) surface wind, humidity, air temperature, and temperature of the underlying surface; (iii) precipitation, soil moisture, snow and ice cover, and vegetative biomass; (iv) type, amount, height, temperature, and liquid water content of clouds.

While certain of these observables are available from surface-based sensors, the only reasonable way to accomplish these objectives is to obtain simultaneous observations over the various regions of the globe from orbiting space platforms.

Major Scientific Issues to be Addressed

It is clear from our present knowledge of the Earth system that the atmosphere plays a key role in the interaction between the various components. It is primarily in the atmosphere, for example, that solar heating is converted to kinetic energy. It is the atmosphere that carries water from the oceans to the lands, as well as determining (through its composition) the temperature of that part of the planetary surface on which we live.

The prediction of atmospheric behavior on the time scales of days and weeks has obvious economic importance as well as great scientific interest. The predictability of the atmosphere is limited by its intrinsic nature as a nonlinear dynamical system. Current prediction capabilities are further constrained by the accuracy and coverage of measurements and computational limitations on models. One implication of the fact that large-scale motions of the atmosphere can be considered to be "approximately" two dimensional is that skill in deterministic prediction cannot extend beyond 2 to 3 weeks. Current modeling skills, however, are not yet reaching this upper limit. The primary reasons for this are:

- Imperfect modeling of the interaction with the planet's surface;

- Data sparse regions in which crucial observations are lacking, the most important example being tropical winds; and
- The broad range of spatial scales that are important.

Processes occurring on cumulus cloud scales (a few meters) are important for the prediction of planetary-scale motions. While these processes can be parameterized with some accuracy, processes occurring on the mesoscale (100 km) cannot be parameterized with current knowledge. Explicit modeling of planetary scale and mesoscale is just beginning to become possible with current supercomputers.

The Earth Observing System is designed to be a major means through which the above difficulties can be overcome. Areas of major emphasis in improving our understanding of physical processes include:

- The interaction of large-scale, quasi-two-dimensional motions with mesoscale three-dimensional scales of motion
- The interaction of all scales of motion with energy released in the precipitation process
- The interaction of orography with large-scale motions
- The interaction of the oceans with the atmosphere
- The interaction of soil and vegetative processes with the atmosphere
- The interactions of ice-cap and ice-field processes with the atmosphere
- The role of longwave and shortwave radiation in energy transfer, especially as modulated by clouds

A Representative Eos Investigation

Precipitation and the Dynamical Implications of Moist Atmospheric Processes

Observations required by a number of Earth science disciplines can be brought to bear on problems particular to atmospheric sciences. Gradients in atmospheric heating are the principal forces for all scales of motion, the sun serving as the ultimate source of this energy input. The pathway by which this energy reaches the atmosphere is largely indirect, since most of the non-reflected solar energy warms the Earth's surface, which in turn exchanges heat, moisture, and momentum with the overlying atmosphere. Latent heat release accompanying the formation of precipitation is a major mechanism by which solar energy is ultimately realized as a source of atmospheric internal and kinetic energy. Our current ability to quantify this intricate but important linkage between solar heating, atmospheric dynamical processes, and the hydrologic cycle is limited at best.

A strategy for obtaining a more thorough understanding of the relationships between the cycling of moisture and atmospheric dynamics will involve several components. First, Eos sensors will provide a more complete portrayal of moisture in the atmosphere. These observations include vertical distributions and transports of water vapor, liquid water, and ice, and sources and sinks of atmospheric water via precipitation and evapotranspiration. These observations will then be quantitatively analyzed for use in conceptual, analytical, and numerical models. One example of such an analysis will address the question of what dynamical and microphysical processes are involved as middle latitude waves tap subtropical low-level moisture, transport it poleward, and organize it into precipitating cyclonic cloud bands. New conceptual understanding will be used to guide resynthesis of Eos data. This will permit consideration of more subtle fundamental questions. For example, problems of complex transient behavior and interaction between the atmospheric moisture cycle and other physical systems could be considered. Numerical models might address such questions as how loss of vegetative biomass and its attendant evapotranspiration could affect rainfall patterns and the three-dimensional structure of tropospheric heating.

Eos sensors will provide the basis for an augmented observing capability now largely dependent on conventional observations. Global observations of atmospheric moisture will depend upon blending vertical profiles and bulk estimates from AMSU, AMSR, MODIS-N, HIRS, and LASA. Microwave measurements will be crucial in sounding temperature and water vapor in cloudy regions, while HIRS and LASA will provide critical information on the vertical structure of moisture in clear areas. Fluxes of moisture from the oceans and land will be estimated using techniques based on MODIS-N, AMSR, ESTAR, SCATT, and other sensors as described in the Blue Planet section of Chapter III. Precipitation estimates will be obtained by combining data from a number of sources (see the description of the Eos precipitation measurement strategy outlined in Chapter III). Crucial to estimates of moisture transport will be direct wind measurements from LAWS and SCATT. Winds diagnosed from atmospheric mass structure will also be required, particularly in cloudy regions, but will remain of little use in the tropics. Moisture and cloud-drift winds from GOES will contribute high time-resolution information, but only at a few vertical levels (see Figure 66).

A major challenge to be faced is blending or assimilating a variety of observations with wide variations in accuracy, observational density, and sampling strategy into a dynamically consistent analysis. Numerical models run in assimilation mode will likely be the tool used to synthesize observations into analyses that retain maximum information con-

tent and minimize weaknesses in observational capabilities. The following is a specific step-by-step discussion illustrating how satellite and conventional data might be used with modeling experiments for precipitation estimation/prediction.

1. Collect available conventional atmospheric data to form a data set for analysis and/or entry into a computer model as an initialization data base (see Figure 67).
2. Use the satellite-derived temperature and moisture profiles to augment the horizontally and temporally coarse-resolution conventional data base with frequent, fine horizontal-scale observations for analysis and assimilation into the computer model initialization data base.
3. Use actual stereo perspective techniques or CO₂ slicing algorithm with two images from synchronized geostationary satellites calibrated with LASA measurements of cloud-top heights to derive a cloud height field from which to assign accurate heights for wind vectors derived from cloud motions or water vapor motions (see Figure 68).
4. Estimate cirrus emissivity, by comparing cloud heights estimated from IR brightness temperatures with actual heights obtained via stereo techniques (see Figure 69).

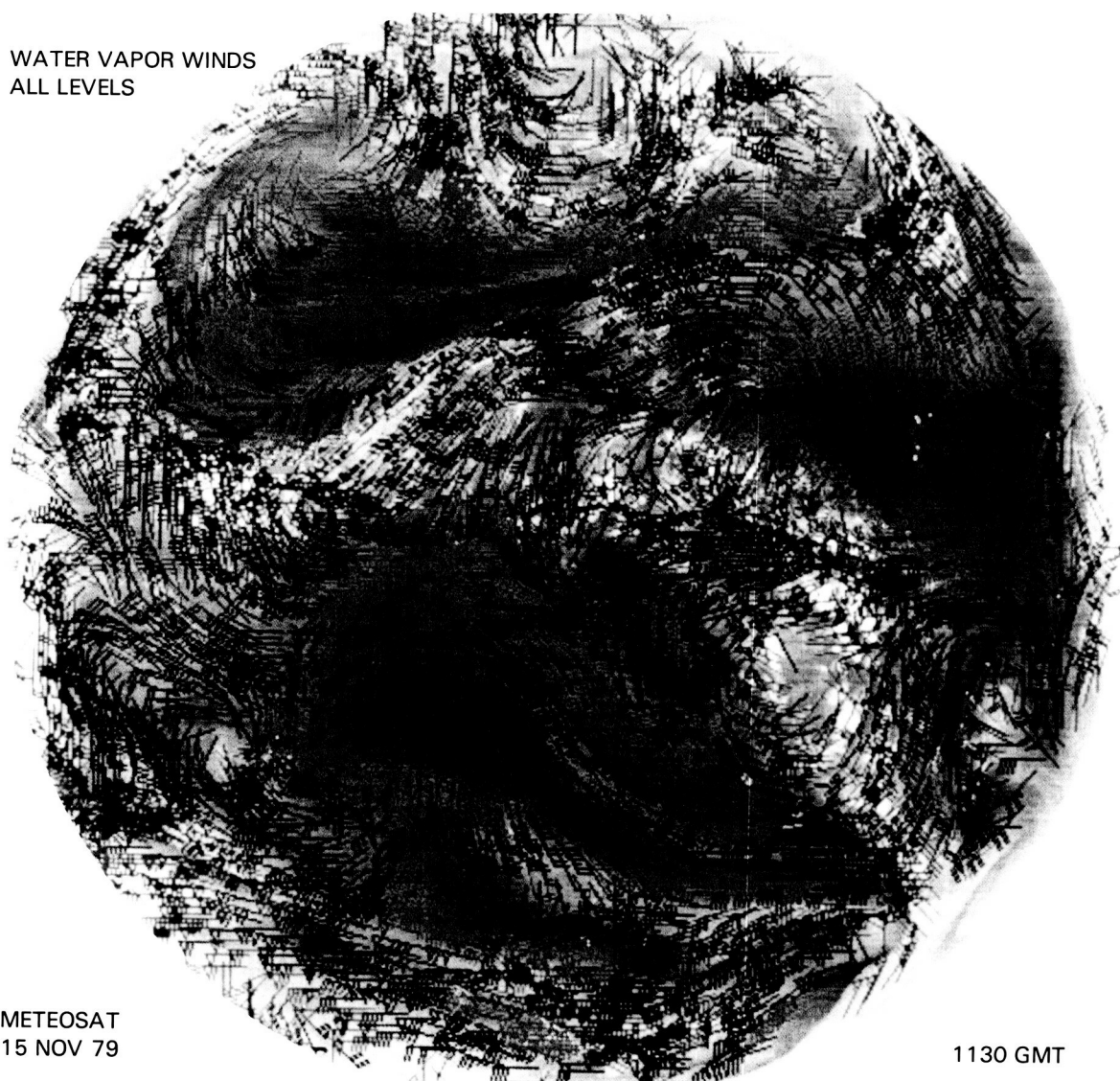


Figure 66. Atmospheric "winds" derived from water vapor motions observed in Meteosat-I 6.7 μ m radiance imagery. Color codes denote pressure altitude of the "wind" bars. Red = 100 to 250 mb; Blue = 251 to 350 mb; Green = 351 to 450 mb.

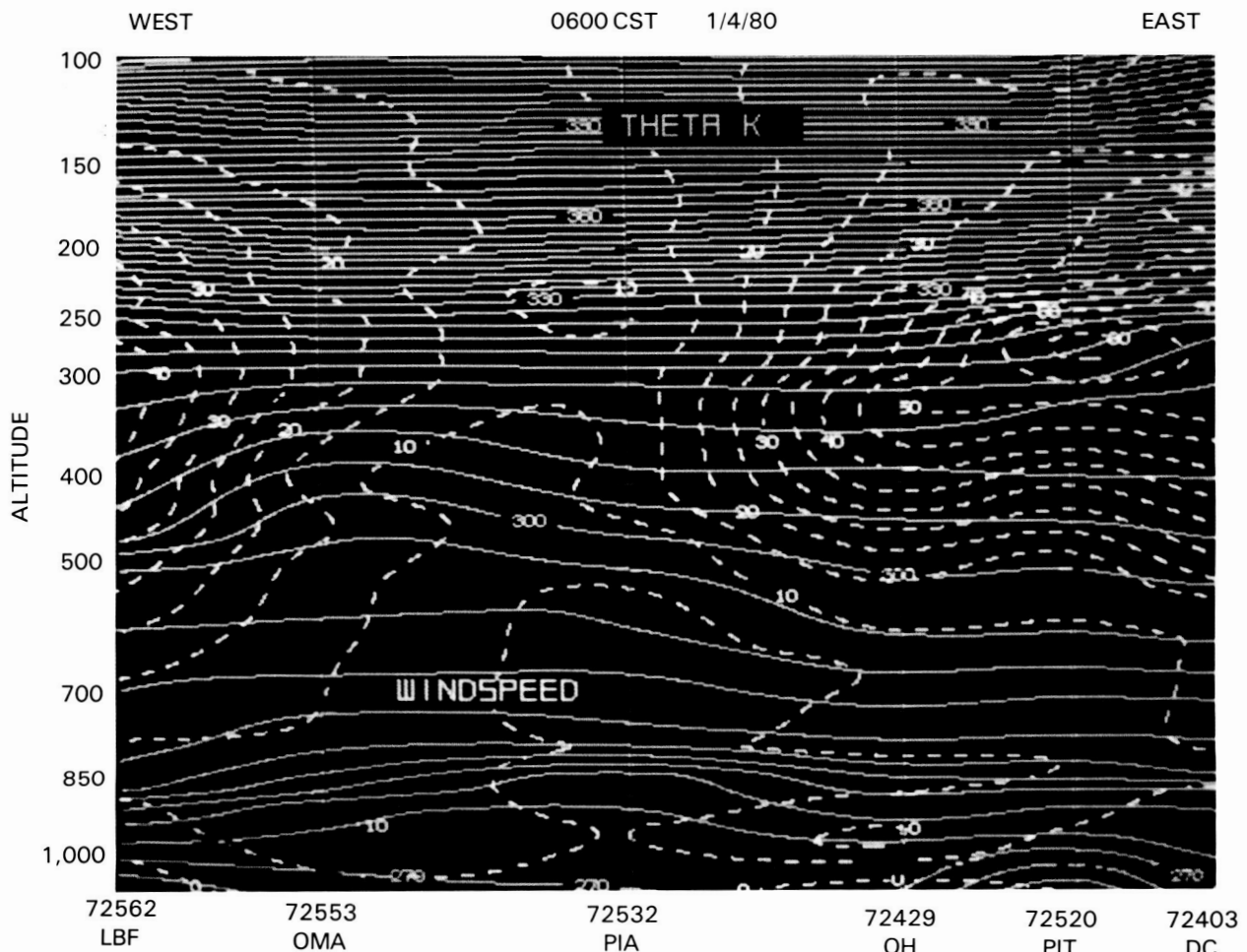


Figure 67. Example of machine-plotted vertical cross-section of potential temperatures and wind speed derived from conventional radiosonde data.

5. Use data from AVHRR, MODIS, and other sensors to estimate atmospheric lower boundary heat and moisture fluxes via estimations of sea surface temperatures, land temperatures, and vegetative indices, as shown in Figures 70 and 71.
6. Incorporate into the data base an estimate of precipitation from AMSR and MODIS-N and other sources (Figure 72).
7. Incorporate into the data base three-dimensional wind fields obtained from LAWS.
8. Integrate all available satellite and conventional data into a four-dimensional Earth-located data base for multipurpose display and model assimilation purposes as shown in Figure 73.
9. Undertake high-resolution studies of particular convective systems at different latitudes, seasons, and times of day to develop catalogs of appropriate model parameters for full dynamical modeling.
10. Run numerical model calculations with outputs keyed to the determination of precipitation rate and total amount.
11. Verify using accurate radar near land and extrapolated to ocean areas with passive microwave observations from AMSR.

TROPOSPHERIC CHEMISTRY

The Earth's atmosphere is unique because many of its reactive components are products of biological activity on the surface and in the ocean. The lower part of the atmosphere, the troposphere, is a globally pervasive fluid medium that has complex dynamical and chemical behavior. The troposphere interacts with the land, ocean, and their biota, and serves as the principal link among them. These interactions center on the ability of the troposphere to readily exchange sensible heat, momentum, radiation, water, trace chemicals, and aerosols with the Earth's surface. These properties or materials are transported over regional and global scales, as well as vertically across the tropopause. All of the above quantities are



Figure 68. Example of cloud wind vector height assignment made by stereo height determination (red: 0 to 5 km; yellow: 5 to 10 km; blue >10 km).

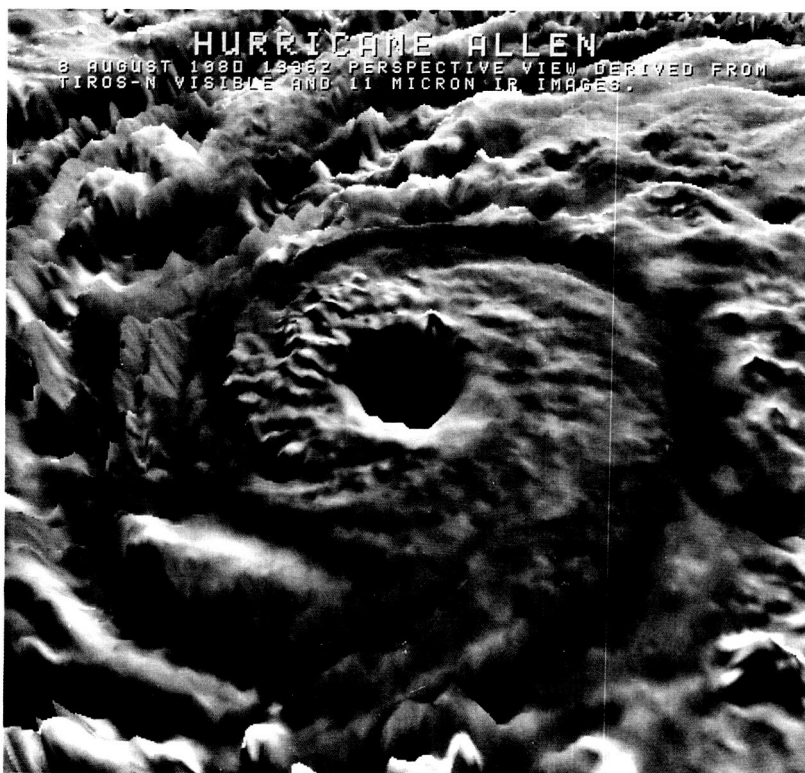


Figure 69. Cloud-top surface derived from observed high-resolution (AVHRR) IR image with the assumption of cloud-top cirrus emissivity equal to unity.

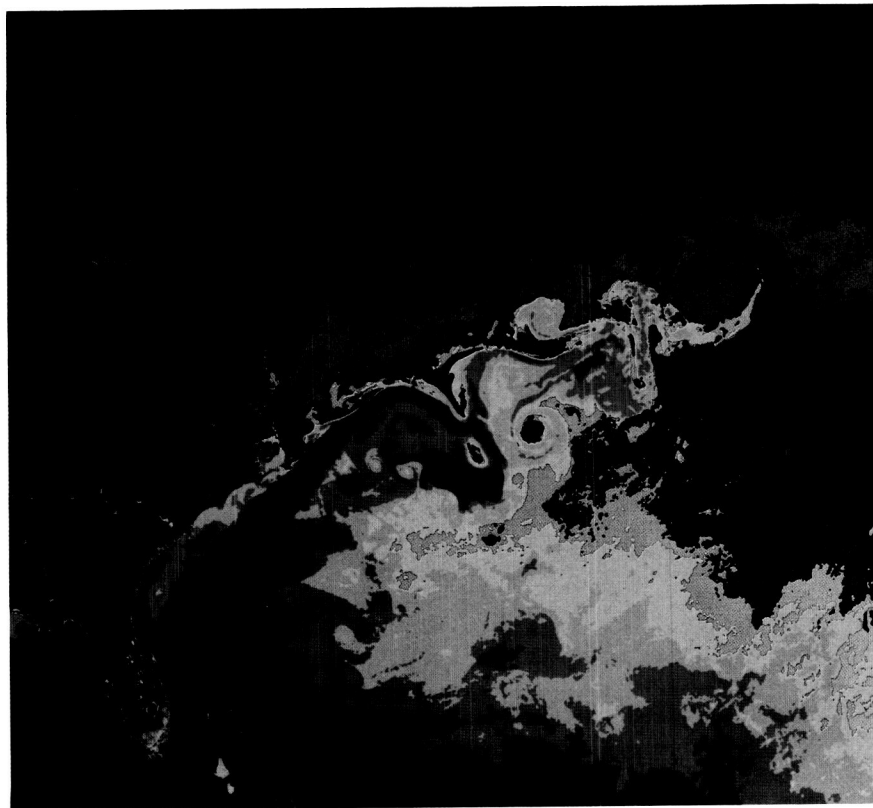


Figure 70. Example of sea surface temperature obtainable by multiview, cloud-elimination algorithm process to be used as a refined boundary heat flux pattern for atmosphere model calculations.

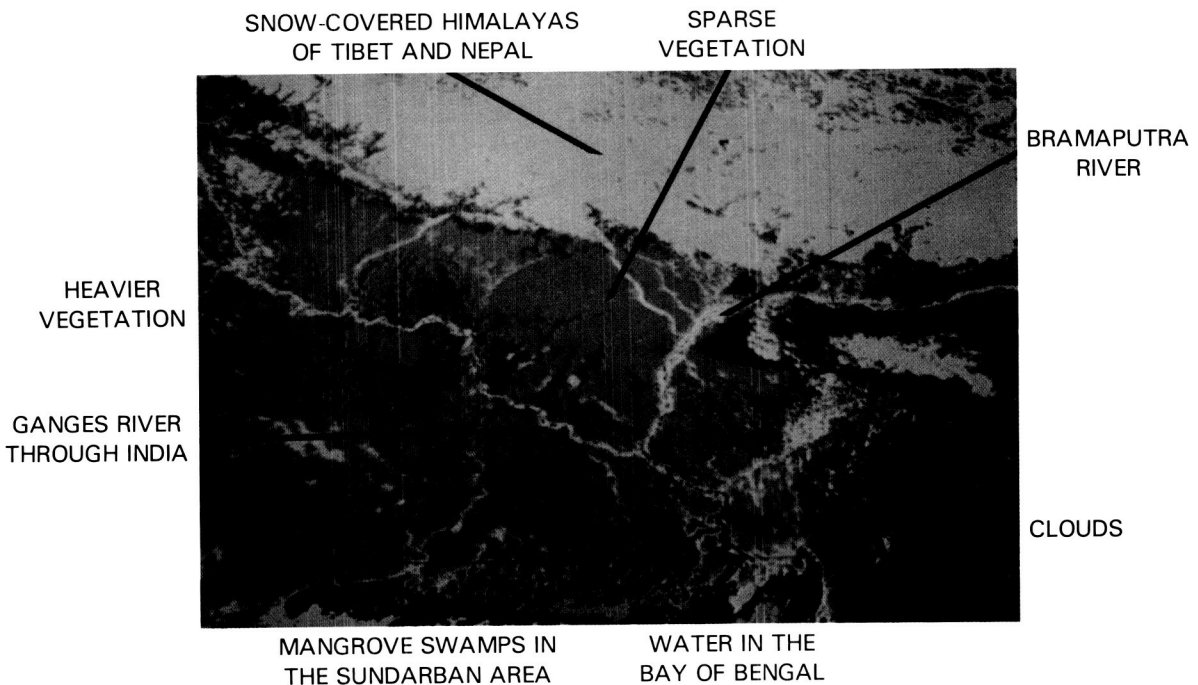
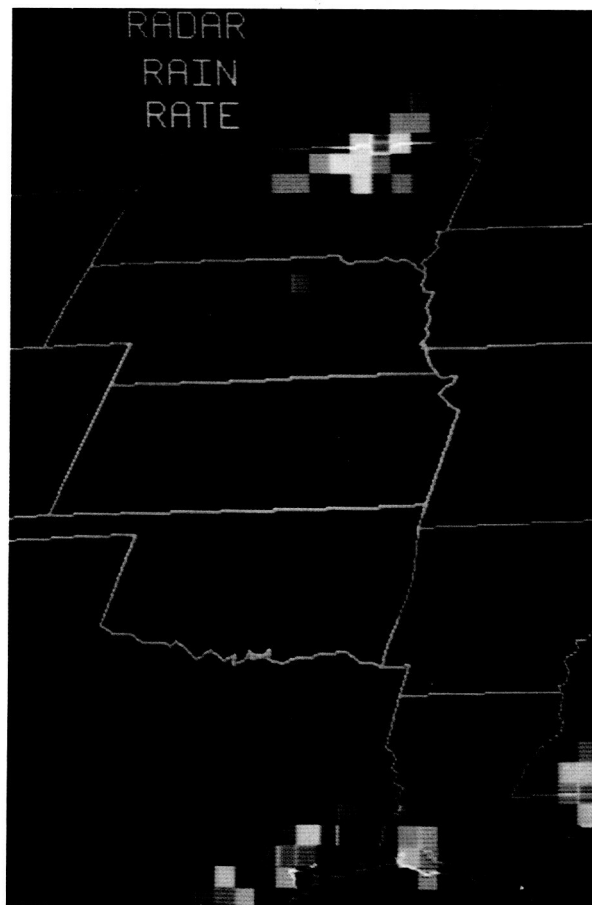
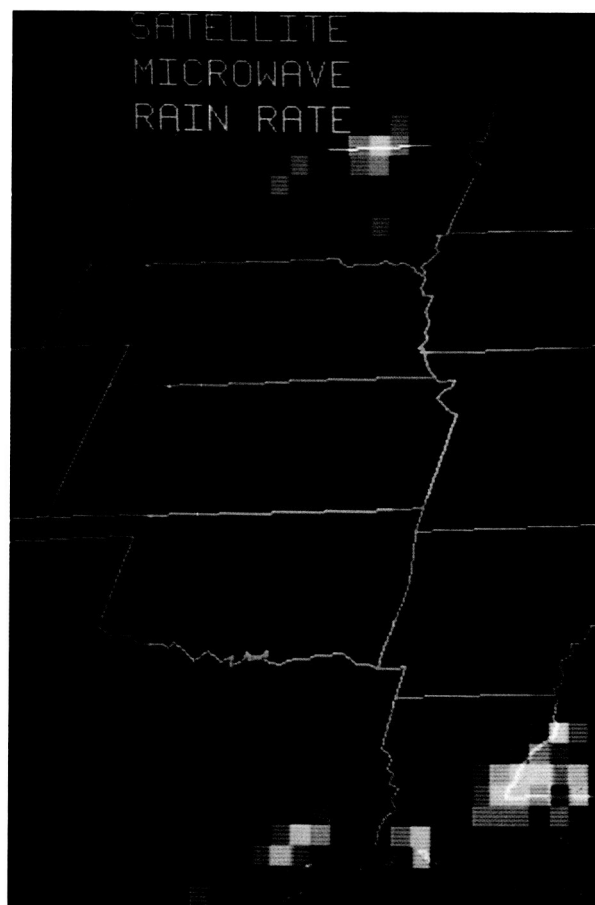


Figure 71. Example of vegetative index obtainable from an algorithm using a pair of high-resolution AVHRR bands in the visible and near-IR and providing information concerning vegetation coverage for an estimate of available moisture flux into the atmospheric boundary layer.



(a)



(b)

Figure 72. Comparison of heavy rain estimates from SMMR on Nimbus-7 and ground-based radar.

of fundamental importance to the chemistry of the troposphere. The overall troposphere-land-ocean-biota system possesses complex feedbacks that defy easy and immediate analysis and hamper present attempts to readily predict its future evolution.

The troposphere constitutes a vital medium for the completion of major biogeochemical cycles essential to life. Together with water and oxygen, four classes of chemical compounds—those containing carbon, nitrogen, sulfur, and halogens—are of special interest in tropospheric chemistry. Several important National Academy reports (NRC, 1984a; 1985) have been published over the past four years focusing on the current status of tropospheric chemistry and future research needs. The objectives stated there for a global tropospheric chemistry program are:

- To understand the basic chemical cycles in the troposphere through field investigations, theory aided by numerical modeling, and laboratory studies;

- To predict tropospheric responses and consequences of natural and man-induced perturbations to these atmospheric chemical cycles; and
- To provide the fundamental information required for the effective future management of the atmospheric component of the global life support system.

The importance of atmospheric chemical and physical processes to the planetary life support system has been brought into sharp focus in recent years, not only by fundamental research discoveries, but also by a recurring sequence of problem identification and response (e.g., photochemical smog, acid rain, ozone depletion, etc.). In addition, perturbations to the chemical composition of the atmosphere have important implications for global climate. The identification of such problems and questions can be expected to increase in frequency and variety during the next few decades. Attempts to

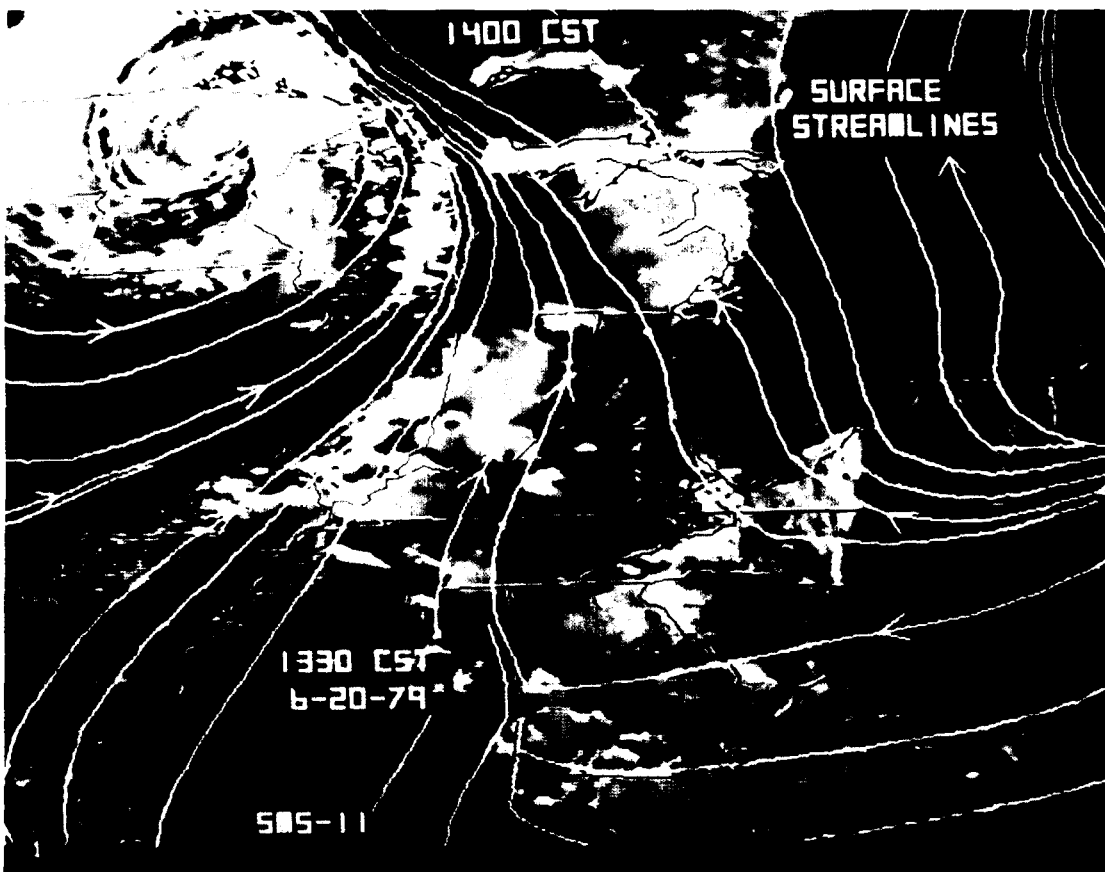


Figure 73. Example of a combined data product from a four-dimensional data base (fourth dimension is time) showing super-position of wind streamlines calculated from reported surface observations of a visible-band cloud image.

answer basic questions about these potentially important societal issues have been frustrated by the lack of knowledge of the tropospheric chemical system.

For instance, the troposphere can act as a "chemical filter" for numerous trace gases that are emitted at the Earth's surface and are transported into the stratosphere or back to the surface. The hydroxyl radical OH plays a central role in the oxidation of these trace gases (see Figure 74). The tropospheric abundance of OH is therefore a key question since it largely determines the "oxidation potential" of the troposphere and thus the lifetimes for many key species of the biogeochemical cycles that are essential to life.

Few reliable measurements of hydroxyl (OH) radicals have been made so far, primarily because of the difficulties in measuring its low atmospheric concentration, which is thought to be of the order of 10^5 to 10^7 molecules per cm^3 . These few measurements are insufficient to test photochemical theories. Indirect methods have been used, however, to test current models of tropospheric chemistry, and for the estimation of average OH concentrations. These methods rely upon mass balance when various pro-

duction and destruction mechanisms are considered, and they provide a globally averaged estimate for OH. Effective utilization of this approach for determination of OH requires that a destroying species satisfy a number of conditions: (1) Its atmospheric abundance in time and space must be defined accurately; (2) It must be known that removal occurs predominantly by reaction with OH and the rate constant must be determined accurately; and (3) The source magnitude and distribution in time and space must be known accurately.

Odd-hydrogen radicals (primarily OH and HO_2) are produced when ozone (O_3) is photolysed, producing excited oxygen atoms that subsequently dissociate water molecules to create OH radicals. Water vapor and ozone have reasonably steady tropospheric distributions for which average observations exist. In addition, the partitioning between OH and HO_2 can be estimated, allowing OH production rates to be calculated.

The reactions of OH with carbon monoxide (CO) and methane (CH_4) account for about 97 percent of the total tropospheric destruction of OH, and thus control its global concentration. More specifically, for noontime ground-level conditions at 45°N ,

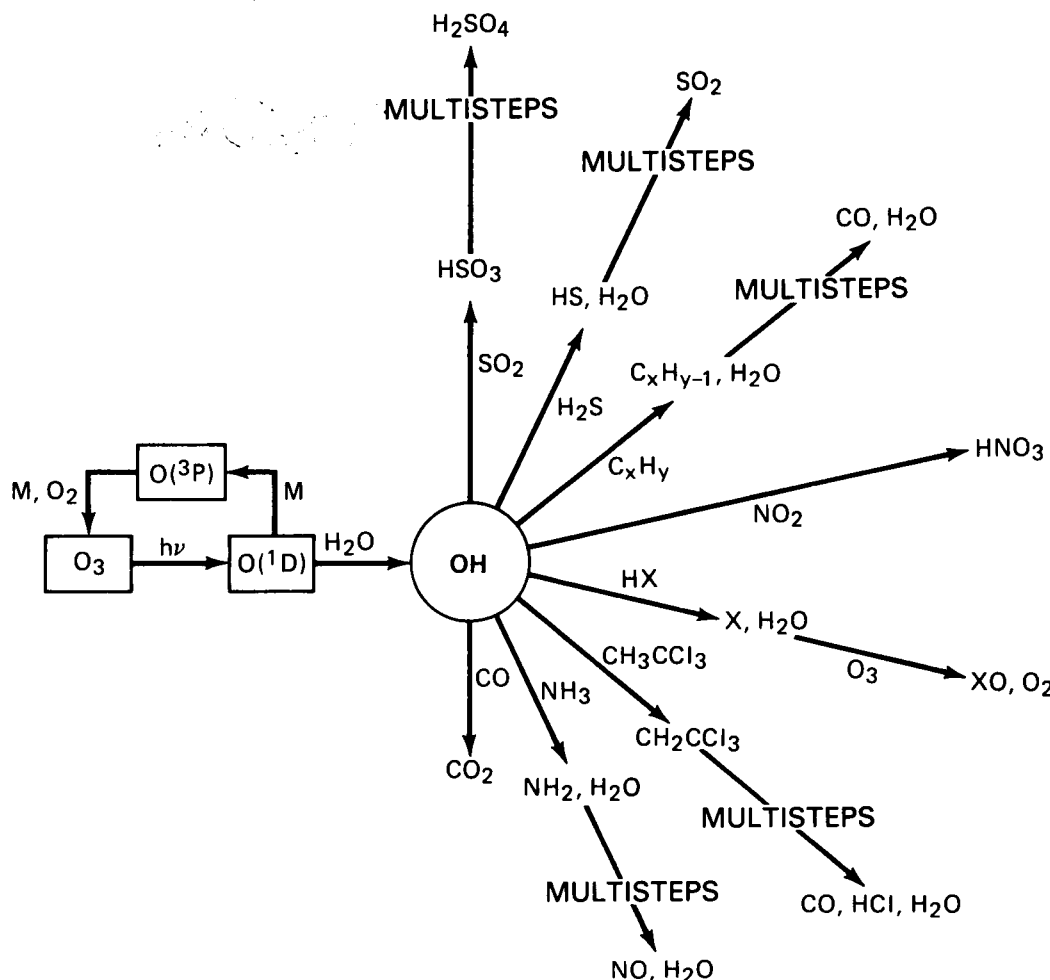


Figure 74. The central role of OH in the oxidation of tropospheric trace gases.

theory predicts that carbon monoxide alone accounts for over 80 percent of the total destruction of OH. Therefore, the measurement of the global distribution and trend of carbon monoxide can serve as a relatively accurate indicator for assessing the hydroxyl concentration and through it the oxidation state of the troposphere.

There are strong indications that the amount of CO in the atmosphere has increased—and may still be increasing—in the troposphere. A large source of carbon monoxide is fossil fuel combustion. The methane oxidation chain also leads to photochemical production of carbon monoxide, and the atmospheric concentration of methane is also rising. In addition to fossil fuel and biomass combustion, and methane oxidation, there are many other natural and man-made sources for carbon monoxide.

In general, the global atmospheric concentration fields of trace gases such as carbon monoxide have not been measured. They cannot be determined from ground-based measurements alone, because of high temporal and spatial variation. For carbon monoxide, a viable approach is to observe the global

concentration field from Eos. Flights of the MAPS on the Space Shuttle have demonstrated this capability (Figure 75). Remote sensing of global tropospheric carbon monoxide will be supplemented with *in situ* measurements at a few strategically located ground stations, where high precision and accuracy can be achieved for detecting temporal trends in carbon monoxide. Upward trends of around 1 percent per year have been measured, but the geographic extent over which these changes in ambient carbon monoxide concentrations have occurred is unknown. Other key species in tropospheric chemistry include ozone and methane. Both are candidates for remote detection by Eos as soon as the sensor technology becomes available. However, carbon monoxide alone will provide much useful information for tropospheric chemistry, and the CR is included in the Eos payload for precisely this reason. It is anticipated that the CR will map the global tropospheric carbon monoxide concentration in three or more vertical layers.

The Eos-recommended payload also includes advanced passive and active remote sensing systems

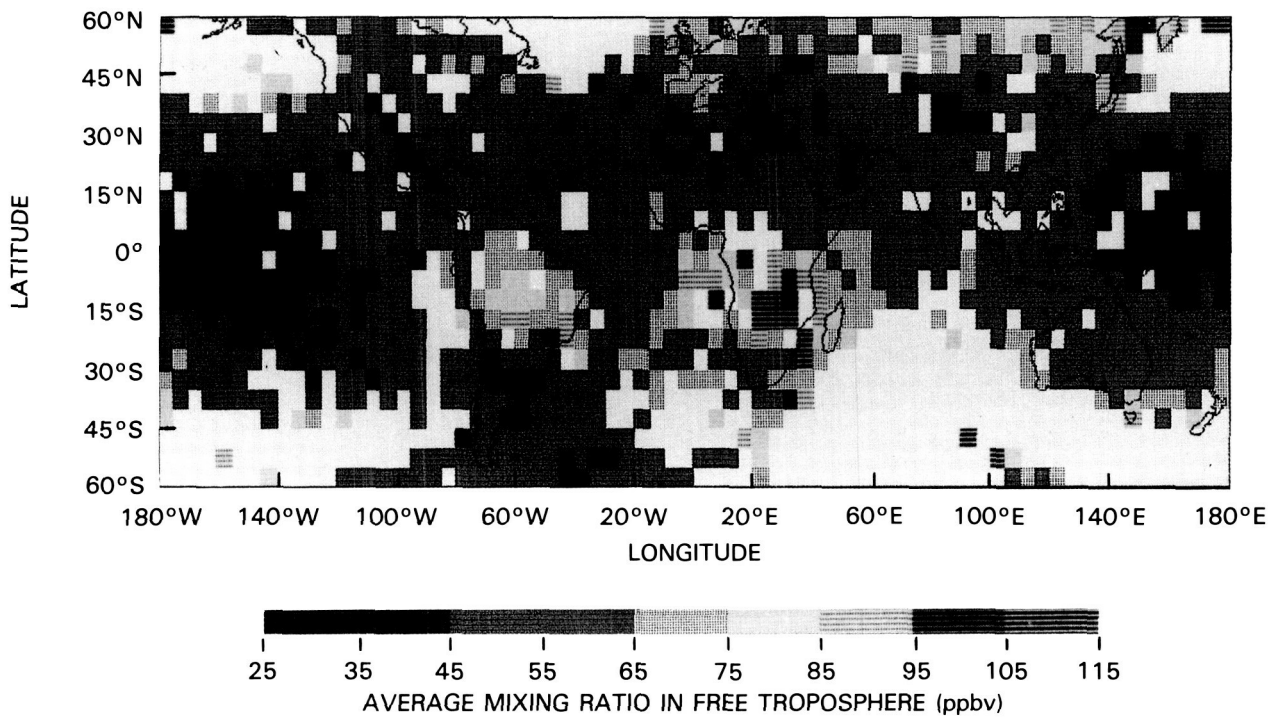


Figure 75. Carbon monoxide mixing ratio in the upper troposphere derived from measurements by the MAPS on the Space Shuttle (H. Reichle, private communication).

such as NCIS and LASA, which offer the promise of measurements of column densities or concentration profiles of CH_4 , O_3 , and other tropospheric trace constituents.

The global methane concentration appears to be less variable because of its longer tropospheric residence time, and hence the concentration levels obtained from *in situ* measurements contribute only small uncertainty to the derived OH concentration.

While it will be significant progress to have these initial estimates of the globally-averaged OH concentration, it nevertheless constitutes just the first phase of a more ambitious measurement program. The next and more complex phase would incorporate information from other Eos sensors leading to a more completely defined system with improved spatial and temporal resolution, and would involve the application of a simplified Global Circulation Model (GCM) with a chemical transformation module for predicting the OH concentration field around the globe. Conventional data such as temperature, pressure, wind, and water vapor will be augmented with satellite-observed winds (as discussed in the atmospheric dynamics section) and planetary boundary layer heights, and water vapor and ozone column contents and profiles from LASA. Present data voids in the tropics, oceans, and southern hemisphere can be filled by Eos data, and this will allow more stringent tests of the dynamics and transport predictions of GCMs.

With the tropospheric distribution of carbon monoxide and ozone obtained from remote sensing

efforts, we will be able to map the oxidation state of the troposphere with a resolution and level of confidence never before obtained. This is important since, if the efficiency of the tropospheric chemical filter changes temporally or geographically because of changes in its oxidation potential, then more or less of a particular trace substance (for example methane, higher hydrocarbons, or chlorofluorocarbons containing hydrogen atoms) will leak into the stratosphere. This can have a profound impact on stratospheric chemistry, or on surface climate if the trace gas under question is radiatively active.

The fate of carbon monoxide, remotely detected from space, in conjunction with a few other critical meteorological and chemical parameters, is crucial to our understanding of the chemical reaction sequences that occur in the entire troposphere and govern most of the biogeochemical trace gases.

MIDDLE ATMOSPHERIC OZONE

The stratosphere and mesosphere are of critical importance to life on Earth because these regions of the atmosphere contain the layer of ozone that screens the Earth's surface from biologically harmful ultraviolet radiation. Ozone also plays a major role in the Earth's radiative balance, and in the influence of the stratosphere on climate at the Earth's surface.

The biological relevance of the ozone amount derives from observations and calculations showing that a 1 percent decrease in the column of ozone overhead results in a 2 percent increase at the Earth's

surface in the intensity of ultraviolet radiation capable of damaging DNA molecules. Because these molecules are critical to living organisms, this radiation is potentially harmful to all terrestrial and surface aquatic life. Human skin cancers have been the subject of greatest concern to date, but grazing animals, some field crops, and other biota are also likely to be adversely affected.

Clearly there are compelling practical reasons for improving our understanding of the processes occurring in the stratosphere and mesosphere. In addition there are intellectual challenges to understanding this system, which is characterized by tight coupling among the radiative, chemical, and dynamical processes, and by significant links to the troposphere and thermosphere through the exchanges of mass, chemical species, momentum, and radiation.

These are illustrated schematically in Figure 76. Here the upward propagation of dynamical influences, such as planetary waves (with longitudinal wavelengths greater than about 5,000 km) or gravity waves (with wavelengths less than about 1,500 km) drives motions in the stratosphere that transport heat and trace species, including families of compounds that are carried into the stratosphere from the troposphere. At the same time, solar ultraviolet radiation is creating ozone, and differentially heating the atmosphere, further modifying the winds. The photolysis of the trace species containing nitrogen, hydrogen, or chlorine produces molecules of NO_x, HO_x, and ClO_x, respectively, with unpaired electrons that are very reactive and are capable of catalytically destroying ozone and altering its distribution.

Examples of some of these interactions can be seen in results from the LIMS experiment (Gille and Russell, 1984). Figure 77 shows the ozone distribution during a major stratospheric disturbance that is forced by upward-propagating planetary waves. On the 10 mb surface (approximately 30 km altitude) the region of low ozone (blue) has been forced off the pole by the air motions bringing ozone-rich air from the Caribbean across Europe to Siberia and (with lower concentration) right across the pole. The same effects can be seen for nitric acid in Figure 78, at about 24 km altitude, where air with low tropical mixing ratios is being carried northward and over the pole.

These demonstrate the effects of the troposphere and dynamics in modifying the distribution of two trace species. Clearly, these will lead to changes in the chemical interactions between NO_x and ozone, and on the radiative heating by ozone, which will alter the wind distribution later.

In addition, over the last 15 years, research on the chemistry of the middle atmosphere has shown that the ozone concentration, which is a few parts per million, is controlled by chemical radicals that are present in concentrations that do not exceed the parts per billion range. These trace species are ex-

tremely important because each radical can destroy tens of thousands of ozone molecules. The detailed quantitative interrelations are complex and multidimensional, requiring coupled chemical-dynamical-radiative models for their explanation.

The amount and distribution of ozone depends on a large number of such interrelated processes. Natural variations and human activities are capable of influencing the balance among these mechanisms in numerous ways. Further, the extent of these effects may be a very non-linear function of the inputs. Among the potential natural causes of ozone variations are changes in the concentrations of methane and nitrous oxide (such as their recently observed increases), changes in solar ultraviolet flux, and possible increases in the biological emission of chlorine compounds.

However, most concern has focused on the results of several human activities. Foremost among these is the release of relatively inert chlorine compounds into the atmosphere. When these reach the stratosphere, they are photodissociated, and the resulting ClO_x are very effective in destroying ozone. Similarly, both the increased use of fertilizers and high-altitude aircraft flight results in the release of nitrogen compounds, which results in increased NO_x and enhanced catalytic ozone destruction. However, these nitrogen species also bind active chlorine in temporarily inactive forms, thus mitigating the effects of the chlorine.

The long-term increase in carbon dioxide, due to the burning of fossil fuels and clearing of forests, is also predicted to affect the abundance of ozone. Calculations indicate that this will lead to a temperature decrease in the stratosphere, in addition to the warming at the Earth's surface. The stratospheric cooling affects the ozone concentration because many of the reactions controlling ozone production and destruction are temperature sensitive.

Ozone and stratospheric aerosols play a role in the radiative energy balance at the Earth's surface. The latter appear to be formed by the oxidation of sulfur compounds, such as SO₂ and COS, that are transported up from the troposphere, although there is much that is not understood about the sulfur cycle. Aerosols act to reflect and absorb both incoming solar radiation and thermal radiation from below. These two effects are in opposition and the net result depends on the specific conditions. Ozone in the upper troposphere may have a significant stratospheric source and acts as a greenhouse gas.

Finally, ozone is the principal source of heating in the middle atmosphere, and is responsible for the warm stratopause. A change in its amount and distribution would lead to changes in the temperature structure of the middle atmosphere, and in its static stability. In turn, this may affect the dynamical coupling between the lower and middle atmospheres and the climatology of tropospheric weather.

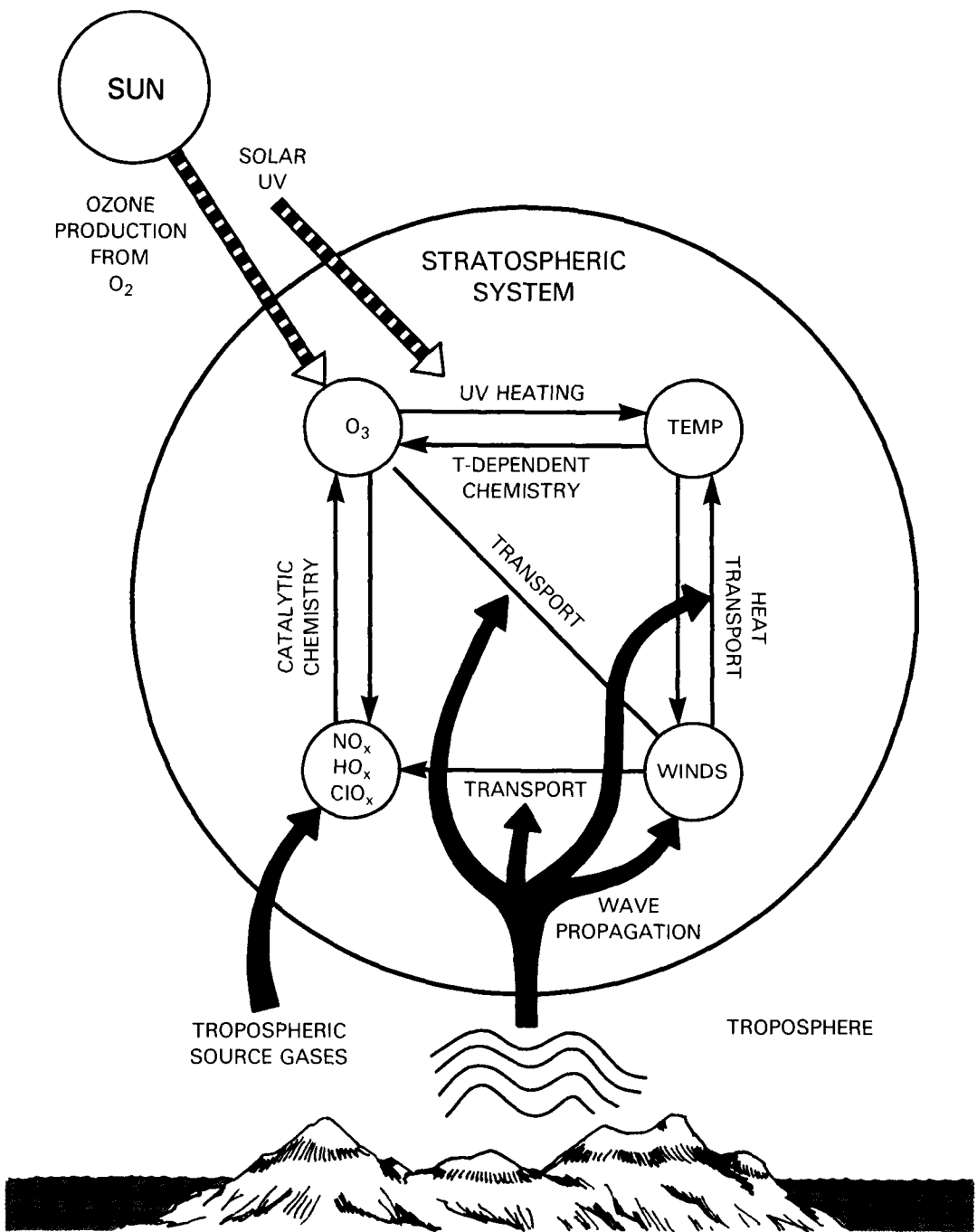


Figure 76. The stratosphere and mesosphere are complex atmospheric regions where radiative, chemical, and dynamical processes play significant roles. These processes are driven from below by the addition of various sources of energy and trace gases, and from above by solar radiation, particles, and trace species.

The scientific goals of studies of the stratosphere and mesosphere for the next 15 years have been described by the Committee on Earth Science of the Space Science Board (NRC, 1985). These are:

- To understand quantitatively the radiative, chemical and dynamical processes and their

couplings, which determine the structure, circulation and distribution of ozone and trace constituents in the middle atmosphere; and

- To use this knowledge as the basis for understanding observed changes in the ozone distribution, and for predicting the impact of

anthropogenic chemical perturbations of the middle atmosphere on the ozone layer and on the meteorology and climatology of the troposphere.

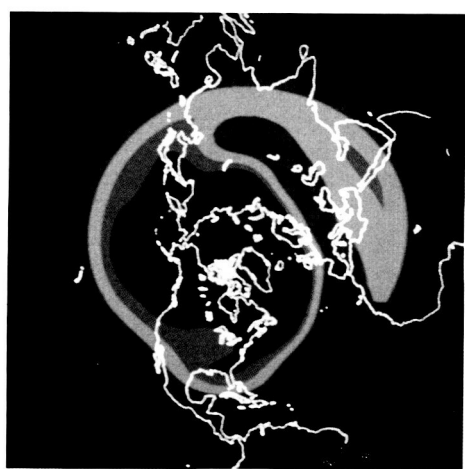


Figure 77. Shows the ozone distribution during a major stratospheric disturbance forced by planetary waves propagating up from below.

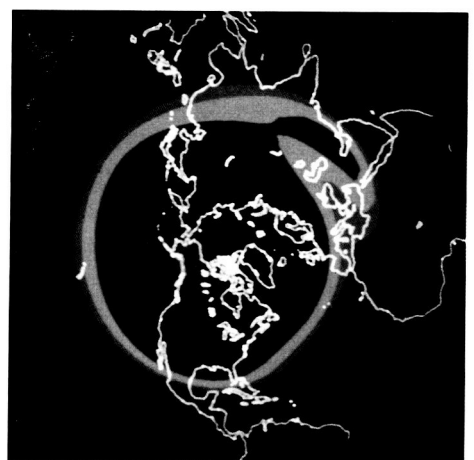


Figure 78. Shows the nitric acid distribution during a major stratospheric disturbance forced by upward propagating planetary waves.

The first is built on the concept of obtaining detailed measurements of the interacting elements of the system, to check the understanding of the basic processes. It is anticipated that the UARS will make major advances in this direction, but that new questions will emerge to join older ones that will not be completely resolved by this mission. Subsequently, it will be possible to identify the reasons for any observed changes in ozone or aerosol opacity.

The strategy that has evolved to deal with this complex system is to use a range of models to study different aspects of its behavior. A large number have been developed over the past several years, treating variations in one, two, and three spatial dimensions. Within these types, there are those that attempt to isolate and understand the most important processes taking place (mechanistic models), and those that aim to simulate the detailed behavior of the atmosphere. Ongoing work is aimed at improving the accuracy with which the various processes are treated in these models. They can then be used to predict the future consequences of various perturbation scenarios with greater confidence.

Even with the best of models, however, nature surprises us by displaying phenomena that have not been predicted by the models and are not readily explained by them. It is important that such occurrences be exploited to improve our understanding and our models. Implicit in such investigations is the accurate measurement of the phenomenon and the variables that are responsible. A particularly timely example of such a phenomenon is the recently discovered "hole" in the ozone over Antarctica. The first evidence for this deep local minimum in ozone column abundance came from ground-based measurements during October above the Halley Bay base of the British Antarctic Survey. These showed that after a 20-year period in which there were no systematic changes, a large and continuous decrease took place from the mid-1970s to 1984. A subsequent review of satellite data has confirmed the decrease and provided additional information. Maps of total ozone obtained by the Total Ozone Mapping Spectrometer (TOMS) are shown in Figures 79a and 79b for October 5 of the years 1979 to 1986. They show a large asymmetric region of low ozone around the South Pole. The striking feature is that the minimum total ozone amount decreased sharply from 1979 to 1986, reaching values less than 150 Dobson Units ($1 \text{ DU} = 10^3 \text{ atm cm}$), compared to earlier values of 250 to 350 DU. In addition, the area of low values has expanded. The irregular rotation of the low ozone region about the pole has not changed over the last several years, but the amount of ozone has dropped steadily to the lowest values ever seen.

Several mechanisms and theories have been propounded to explain these facts, but none has been corroborated at this time. The problem is complicated by the physical and logistical difficulties of making observations in Antarctica. Here we describe

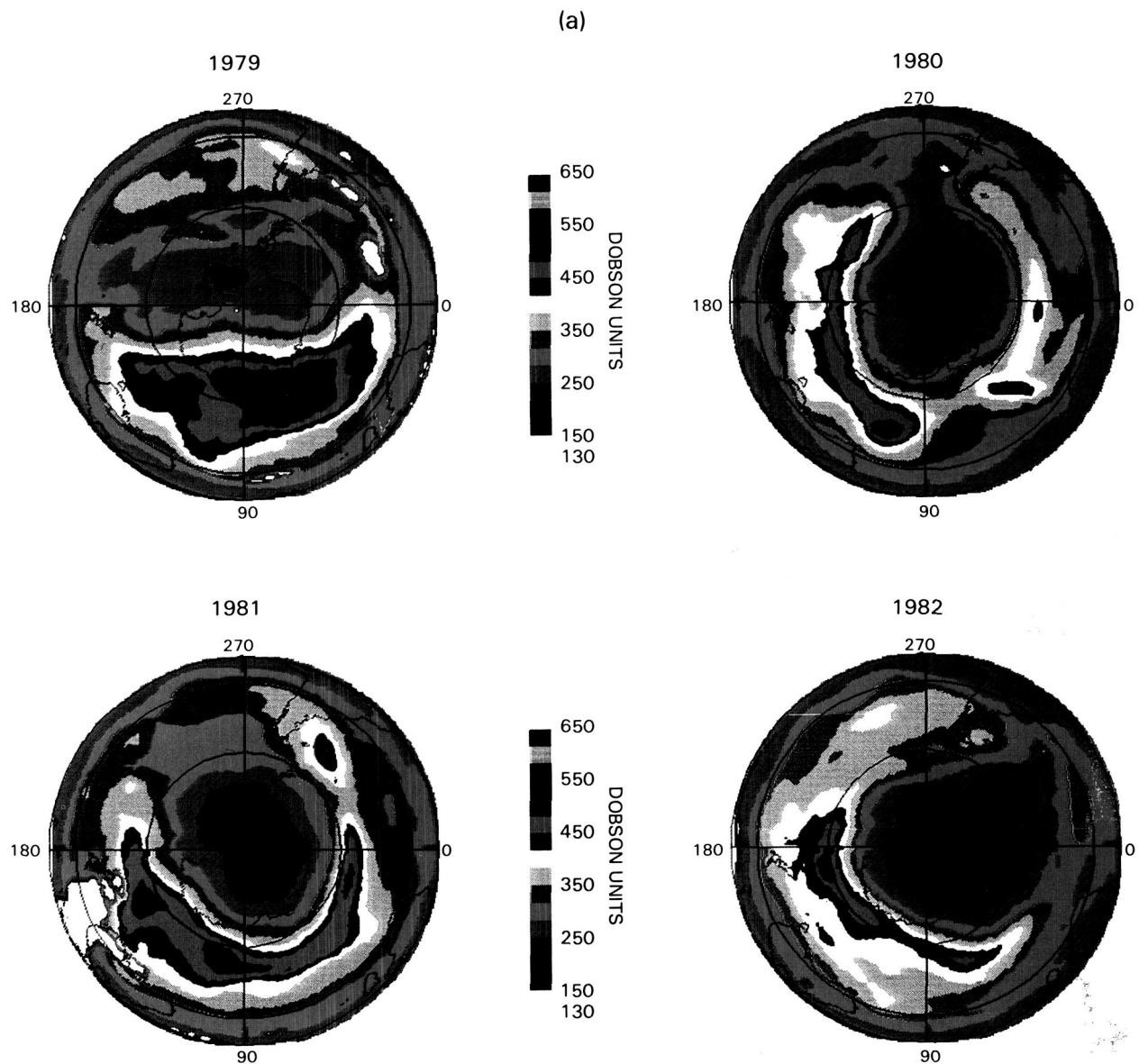


Figure 79. Maps of total ozone for October 3 of the years (a) 1979 to 1982 (above) and (b) 1983 to 1986 (facing page) obtained by TOMS flown on Nimbus-7 satellite.

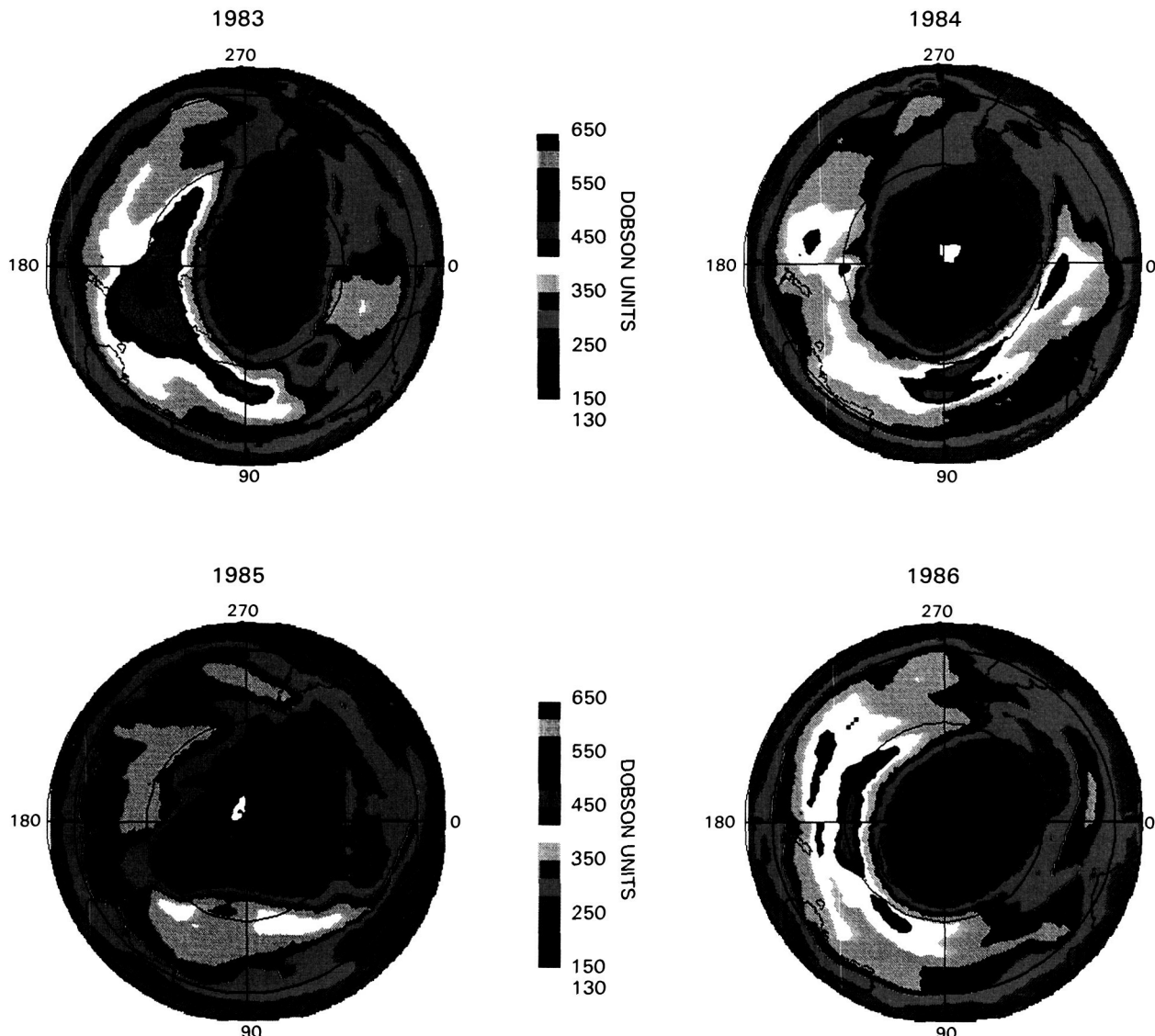
how such an investigation could be carried out if Eos were operational at this time.

In order to define the nature of the effect, measurements of the ozone profiles from the upper troposphere to the stratopause are needed during polar night. These could be obtained with the IR-RAD, GOMR, and/or the Cryogenic Interferometer Spectrometer (CIS). Derivation of ozone distributions will require determination of the temperature in the same regions, which can be derived from the same instruments. The temperature is also needed to help interpret the chemical and dynamical effects taking place. These instruments could also provide the distributions of the nitrogen species, N_2O , NO ,

NO_2 , and HNO_3 , which are believed to be involved in the control of the ozone balance in the unperturbed stratosphere, and are central to the theory that the ozone depletion is due to greatly increased destruction by NO_x .

It has also been suggested that the Antarctic reduction is due to the action of chlorine-containing species. The most reactive of these is ClO , which can be measured with the MLS. The other major chemical family that interacts in the ozone chemistry is that of hydrogen. The SUB-MM will provide measurements of at least OH , which will allow changes in the concentration of this chemical group to be inferred. The solar UV irradiance is another variable that

(b)



needs to be monitored, since it drives the photochemistry. The measurements are required both to assess solar effects and to remove them from the other measured quantities. They will be obtained with the SUSIM.

There are also indications that the changes are strongly influenced and perhaps controlled by dynamical factors that have their origins in the troposphere. Long-term changes of tropospheric climate would thus induce long-term trends in stratospheric ozone. This is potentially important because it suggests a tight linkage between the problems of ozone reduction and climate.

Polar stratospheric clouds are another atmospheric feature for which a role has been suggested. They are a thin veil of clouds that appear in the winter lower stratosphere when the temperature becomes sufficiently low. The occurrence, coverage, and vertical extent of these can be determined with

the LASA and/or LAWS instruments. Finally, the direct observation of winds by F/P INT and LAWS will allow the evaluation of the transports of all the species mentioned above.

Clearly, such a suite of measurements would go a very long way to define the phenomenon. While it is possible that these data would not uniquely determine the cause, they would provide very stringent constraints on the possible explanations that could be incorporated in predictive models.

Even in the absence of an unexpected phenomenon such as the Antarctic ozone "hole," Eos measurements will ensure that our understanding of the underlying processes is adequate, and serve as a check on the accuracy of predictive models. They will be critical for providing evidence of long-term changes, showing their causes, and pointing the way toward actions that may be required to protect this fragile part of our environment.

MESOSPHERIC DYNAMICS AND CHEMISTRY

The mesosphere is the highest region of the neutral atmosphere. Much of the extreme ultraviolet sunlight is absorbed in this layer. The processes that occur where these high energies are absorbed naturally lead to very non-thermal chemical reaction chains. The study of this region centers on understanding these processes and on quantifying the factors that control mesospheric chemistry and dynamics.

The first models of the mesosphere were based on purely chemical reaction processes and yielded approximate simulations of the present state of the mesosphere. However, it has become obvious that prediction requires knowledge of the variation of all of the factors that characterize these early models. These factors—the winds, turbulence, and the thermal state—respond in a complex feedback system that must be understood if we are to generate a useful prediction model of this transition region. A schematic of the factors and relationships that occur in the mesosphere is similar to that presented in Figure 76, but there are notable differences. The more energetic UV radiation photolyses almost all the polyatomic species present at lower altitudes, resulting in simple chemistry involving primarily ozone, atomic oxygen, and reactive hydrogen compounds with unpaired electrons, referred to as HOx. It has recently been recognized that gravity waves originating in the troposphere are extremely important in driving the mesospheric circulation.

The Eos will allow us to systematically examine this system by providing diagnostic glimpses of the state variables and of the rates at which processes occur within the system. The study of the mesospheric system will, of course, be broken into many individual subproblems, but out of these fragmentary submodels will evolve an overall understanding of the system as a whole. To illustrate the contribution of Eos, we examine a single subproblem, that of the influence of gravity waves and the nonlinear wave-breaking process on the upper atmosphere.

Gravity Waves and the Mesosphere

It has long been known that gravity waves play an important role in the local fluctuations in density at mesospheric altitudes. These in turn are manifested in wave-like structures in airglow emissions and noctilucent clouds. Indeed, such structures reveal important information regarding the horizontal wave-lengths and occurrence frequencies of the waves.

Recently, however, the study of mesospheric gravity waves has assumed much greater emphasis because of the realization that these waves probably play a predominant role in the basic transport phenomena at these altitudes. In particular, theoretical studies have suggested that breaking mesospheric gravity waves are responsible for

depositing much of the momentum needed to balance the Coriolis forces on the mean meridional circulation in the mesosphere, and for the turbulent eddy diffusion in this region. Theoretical studies of the chemical and dynamical structure of the mesosphere that explicitly include the upward propagation and dissipation of gravity waves have been successful in explaining a number of observed variations in composition and in dynamics of the mesosphere that were previously unexplained. For example, the cold summer mesopause temperatures at high latitudes are consistent with models that include gravity wave processes. The observed spring maximum in 5577 Å emission is simulated in such models as a direct result of seasonal variations of the intensity of turbulent mixing in the upper mesosphere due to breaking gravity waves. The spring/fall maximum observed in ozone near 80 km also appears to result from the seasonal variability in mesospheric transport due to breaking gravity waves. While a remarkable number of chemical and dynamical observations in the mesosphere and lower thermosphere appear consistent with theoretical models that consider the effects of these waves, a fuller understanding and meaningful test of the theory requires further observations; in particular, simultaneous global-scale observations of several parameters would enable some critical concepts to be tested.

The characteristics of gravity waves that break at mesospheric altitudes, and the amount of turbulent mixing generated by the breaking waves, depend critically on the zonal winds of the stratosphere and lower mesosphere (through which they must propagate). Under certain conditions, the stratospheric winds block upward propagating waves from reaching the mesosphere, and the waves are absorbed. The horizontal wavelengths of the waves are also of extreme importance in the transport properties induced by these waves.

Nadir imaging of airglow features such as the green line or the OH Meinel bands could be used to derive horizontal wavelengths, and perhaps even phase speeds of the waves, on global scales. Simultaneous direct measurements of the zonal and meridional winds in the underlying stratosphere and lower mesosphere would critically test the theory of wave propagation. Such measurements should be accompanied by observations of chemical tracers that are sensitive to the transport induced by the waves; in particular, carbon monoxide, water vapor, ozone, and airglow emissions such as the green line or sodium lines. Finally, observations of the temperature variations, preferably using both nadir-viewing and limb-viewing instruments to obtain high-horizontal and high-vertical resolution data, are needed. Such a set of observations would test the propagation, transport, and dynamical characteristics of mesospheric gravity waves in a manner not possible with local, or non-simultaneous, observations.

Eos Observations

The observation strategy used to understand the generation of gravity waves, their filtering by stratospheric zonal winds, breaking in the mesosphere, and eventual influence on the basic state of the atmosphere will utilize a number of Eos instruments. These waves are created in the troposphere by weather systems, mountain lee waves, and other orographically related features. Thus, small-scale observations of intense weather processes occurring near the surface are required. Sensors for these observations include MODIS, AVHRR, AMSU, HIRS, and, if possible, LAWS and LASA.

These waves propagate through the stratosphere and are filtered by zonal winds that cause local dissipation. The waves themselves should be observed along with the stratospheric wind fields. The

instruments required include F/P INT, IR-RAD, and perhaps MLS and the operational AMSU.

The waves break when their thermal amplitude is such that convective instability occurs. This is observable by the large thermal perturbations that occur near the level of breaking. These effects can also be seen in chemical tracer fields and in the temperatures on the smallest observable scales. The nonlinear wave-breaking process generates turbulence and adds zonal momentum to the mesosphere. These processes are observable in the distribution of chemical trace species and in the dynamic and thermal state of the atmosphere in the mesosphere. In particular, the temperature of the cold summer mesopause is dominated by these processes. The instruments that can observe these phenomena include the various upper atmosphere composition monitors and temperature sounders and F/P INT.

V. CONCLUSIONS AND RECOMMENDATIONS

The Earth Observing System as described in this report represents a new approach to the study of the Earth. It is at the heart of a scientific program consisting of remotely sensed and correlative *in situ* observations designed to address important, interrelated global-scale processes. Scientific interest in these processes has arisen because of a recognition of the need to study the Earth as a complete, integrated system in order to understand and predict changes caused by human activities and natural processes. In part, interest is fueled by our new ability to obtain scientifically useful data sets from satellites. The Eos approach is crucial. It is based on an information system concept and designed to provide a long-term study of the Earth using a variety of measurement methods from both operational and research satellite payloads and continuing ground-based Earth science studies.

The complexity and scale of Earth system processes require that this program transcend traditional disciplinary boundaries within Earth science as well as agency and national boundaries. The Eos concept builds on the foundation of the earlier, single-discipline space missions that were designed for relatively short observation periods. Continued progress in our understanding of the Earth as a system will come from observations spanning several decades using a variety of contemporaneous measurements. Several proposed measurement systems are discussed in separate panel reports listed at the front of this report.

The Eos objective of producing a set of long-term, consistently processed global data sets has led to the concept of Eos as an information system for Earth science. Eos is not merely a collection of spaceborne hardware. Rather, it is a tool by which the Earth scientist acquires data from satellites and *in situ* sensors including Eos and non-Eos sources.

Although Eos will require significant amounts of human and financial resources, it should not be perceived as a replacement for the research activities of the traditional Earth science disciplines. Instead, the study of global processes will build on the foundation laid by traditional studies. The Eos approach will not address every problem of interest to Earth science. Many processes occur at spatial and temporal scales that cannot be resolved adequately with the measurements included as part of Eos. Other processes cannot be studied using remote sensing methods. These processes are no less important for our understanding of the Earth system. Eos does represent an exciting and essential new program for the study of global-scale processes.

It will afford the opportunity for a revolution in our understanding of the Earth system.

RECOMMENDATIONS

The Eos Science Steering Committee strongly endorses the recommendations put forth by the Eos Science and Mission Requirements Working Group (Butler *et al.*, 1984). They remain the critical principles that should be followed in Eos development. In this section we focus on the many tasks that need to be started now in advance of any launch of new space instruments. In this context we discuss Eos as an information system and its associated functions. These functions are data acquisition, archiving and retrieval, and analysis and understanding. Although these recommendations are directed at NASA, there are interagency and international issues that need to be addressed now as well.

Assumptions

We assume that the upcoming UARS, N-SCATT, and TOPEX missions will continue, and we support efforts to extend these missions beyond their primary mission lifetimes. We also assume that future short-duration missions, in particular GREM and TREM, will take place roughly at the same time as the early phase of the Eos mission, and we support continued preparations for these measurements.

Although these missions are oriented toward specific discipline studies, they are studies of key areas that will build a foundation for future Eos studies. UARS will study the coupling of chemical, radiative, and dynamic processes in the stratosphere and the mesosphere and allow inferences to be made about the troposphere. TOPEX will measure the mean barotropic circulation of the world ocean and is an essential component of the WOCE. GREM will make precision measurements of the Earth's magnetic and gravitational fields that will also be of great use to altimetric studies such as TOPEX. The TREM is a limited-duration experiment to determine the diurnal variation in precipitation at low latitudes and to test the accuracy of instantaneous and cumulative rainfall measurements. Thus far, accurate precipitation measurements have been difficult and advances in our ability are essential to any global study of climate, biogeochemistry, and hydrology.

We also assume that the suite of oceanographic, atmospheric, and land sensors aboard the NOAA polar orbiters and the geostationary satellites of NOAA, Japan and other countries, and Eumetsat will be continued. These data sets are invaluable in the study of a variety of phenomena that occur in the Earth system. We are aware that the concepts and approach we have taken with Eos may be extended to geostationary, orbit observing systems using

geoplatforms, and that such an approach is being actively studied. Similarly, we assume that the commercial sensors aboard the Landsat and/or SPOT satellites will be continued and that European, Japanese, and other nations' experimental Earth observations missions (such as ERS-1 and JERS-1) will be successfully completed.

Data Acquisition

1. Engineering studies must continue on platform design and instrument accommodation because they have important implications for the scientific objectives of Eos.

There are a number of engineering studies that need to be started or continued in the pre-Eos timeframe. While we do not describe these in detail in this section, we do point out those areas that are of particular significance to the scientific goals of Eos.

As described in Chapter II, Eos will use observation platforms that are significantly larger than the current generation of Earth observation satellites. The size of these platforms affects at least two areas of direct importance to the scientific mission. The first concerns precision orbit determination. This is an area of particular importance to altimetric and other topographic work. For example, the sea surface height signal of interest for oceanographic studies is on the order of 5 to 10 cm. Much of the altimetric work will depend on measuring the time-varying component of the signal. This variation must not be confounded with platform variations (e.g., structural flexure). The second area concerns pointing accuracy and co-registration. For example, HIRIS and SAR will have relatively narrow swaths, and pointing errors could cause the target area to be missed. As these instruments will primarily be used in process studies in conjunction with *in situ* observations, it is essential that such errors be minimized. As many of the scientific studies will require observations from several sensors, it is essential that the geolocation of the pixels be extremely accurate and easily accomplished. This will allow accurate co-registration of the various data sets.

The polar platforms will accommodate a large number of instruments. This presents a number of technological challenges concerning the integration of these sensors. These include power consumption, electromagnetic and mechanical interference, and data handling (and transmission) as the suite of instruments in use (and their data collection mode) changes over time. The command and operation of this observing system will be complicated. Because of the large number of instruments and the presence of some very high-data-rate sensors, the total volume of data to be acquired will be extremely large. Special attention must be given to the onboard data system, particularly to data selection and handling techniques and coping with commandable instruments such as HIRIS and SAR. Although these are pri-

marily engineering issues, they can significantly affect the scientific user by restricting the available observing scenarios and the structure and content of the data stream.

As the variety of possible observing scenarios is quite large, scientists must have access to appropriate tools to develop scenarios for the studies of interest and optimize experiment design. Such tools should also help the user evaluate the data rate and volume implications. As it is likely that different users will develop sampling scenarios that will be in conflict, a management system should be in place to anticipate and resolve these conflicts so as to provide maximum scientific return. *We recommend that the Eos science community continue to guide the platform developers to ensure that the scientific goals of Eos are met within the engineering constraints.*

2. Calibration of the Eos and operational sensors is a difficult problem, and it is essential to the scientific success of Eos. We must be able to separate instrument variability from natural variability.

We must pay particular attention to stability of calibration as well as intercalibration of multiple copies of individual sensors. *We recommend that a calibration panel be formed to investigate these issues and that standard calibration and documentation procedures be established as soon as possible.* Sensors that may be provided by the international community should also be included in this study.

3. The ADCLS will play a vital role in process studies and in obtaining data on processes and at scales that cannot be observed using spaceborne instrumentation.

Several instruments have not been the subject of specific panel reports, and yet, these sensors are equally important to the success of Eos. Specifically, *we recommend that a definition and design panel be established for ADCLS.* This panel should also establish methods for data retrieval and command transmission within the Eos data and information system for these *in situ* sensors. We also recommend that adequate science community involvement be obtained to guide the development and design of the other Eos and operational sensors that have not been the subject of specific Eos instrument panels. Special attention must also be given to the operational sensors as providers of valuable scientific data. Their design must not be overlooked.

There are other studies described in the individual panel reports that pertain to specific instruments. Many of these studies should begin as soon as possible so that these instruments are ready for the mid-1990s.

4. We must begin algorithm development so that algorithms, developed with the advice of

and accepted by the user community, are in place before launch.

The lack of access to processing algorithms has severely hindered the use of satellite data by most Earth scientists. Many of the algorithms are sufficiently complex that they cannot be easily replicated by the non-specialist. Also, some existing algorithms have *ad hoc* corrections that result in unforeseen "variability" in the geophysical fields. Many instruments currently have established algorithms; others are either new instruments or have new capabilities that will require considerable algorithm development efforts. Many processes to be studied, such as soil moisture will require data from multiple sensors. Such synergism between sensors is one of the strengths of Eos. We must begin studies so that this strength can be exploited.

It is essential that this development activity involve the data-using scientists as well as those who are primarily concerned with the sensors per se. This will increase the awareness within the larger Earth science community of the capabilities and limitations of the processing algorithms. The expertise of the users can also improve the design of sensor and algorithm validation studies. *We recommend that algorithm development begin as soon as possible for each of the potential set of Eos instruments and for groups of these instruments.*

Data Archiving and Retrieval

5. The proposals of the Eos Data Panel must be implemented as soon as possible.

We strongly endorse the report of the Eos Data Panel. *We recommend that a committee be formed to guide the implementation of the Panel's recommendations.* While we have no doubt that the technology will exist to cope with the projected Eos data streams, it is essential that the data and information system begin development as soon as possible if these data streams are to be exploited efficiently. The proposed data and information system represents a new way to cope with data streams from a variety of space- and ground-based systems. It is the centerpiece of Eos.

6. Existing data sets relevant to Earth science must be maintained and made accessible to scientists.

Processes that vary on time scales of several years to decades require long series of observations to produce statistically reliable results. There are many such data sets in existence in Earth science, particularly from the operational satellites. However, many of these data sets are either incompletely catalogued or are stored in a form that cannot be accessed readily and reliably. As these data sets age, the storage media degrade to such an extent that most of

the data become irretrievable. Inadequate funding forces a choice between the preservation of old data and the acquisition and storage of new data sets. This is a particular dilemma for operational archives where the primary use of the data is for near real-time analysis. This is in conflict with the main scientific use of data where real-time access is less important than easy access to long time series. *We recommend that immediate steps be taken to preserve these data, to convert them to less volatile storage media, and to provide a cataloging system that facilitates access to them.*

Many data sets exist only in a raw form, and the size of the data set along with the complexity of the processing algorithms makes the task of converting the raw data into usable, geophysical data sets far beyond the reach of individual investigators. *We recommend that such processing be given a high priority and be undertaken wherever justified.* Such tasks will need to include advice from the scientific user community to ensure the scientific utility of the final reduced data. For other data sets, access to the relevant algorithms will allow processing of subsets for specific research problems.

We realize that the preservation and processing of existing data sets is not a small project. However, these data sets represent our only opportunity for analysis of time series covering several decades. Also, the evolution of data processing and storage technology has reached the point where these are obtainable goals.

7. A unified plan for the existing Earth science pilot and future flight project data systems and for the various communication networks that are planned or in use must be developed and implemented as soon as possible.

Although the present pilot data systems are in various stages of maturity, they could form an important foundation for a future Eos data and information system. The objectives of such a plan should be:

- To implement a coherent communication network based on the experiences of existing networks so that the various archives can be easily searched by a user;
- To develop compatible data cataloging and access systems to facilitate the use of multiple-sensor data sets from different archives; and
- To develop a management structure that involves the science users, particularly those from outside NASA and NOAA laboratories.

The existing pilot data systems have been designed primarily to meet discipline needs. Their experiences—both successes and failures—will be invaluable for an evolving, multidisciplinary data

system. Although the pilots can continue to be a test bed for new data handling technologies, this should not be their primary focus. Rather, they should concentrate on improving their scientific utility for non-NASA users, particularly for scientific studies involving multiple archives and data sets.

We recommend that future Earth science flight projects, such as UARS and TOPEX, develop their mission data systems in a manner that will be compatible with a much larger, unified Earth science data system.

Similar statements can be made concerning the various communication networks (e.g., PSCN, SPAN, etc.). Their experiences are also valuable. Like the pilot data systems, their capabilities need to be brought to the attention of Earth scientists who could benefit from them. The experiences of users should be incorporated into the design of future networks. The ESADS activities are a significant step in addressing this area of concern.

8. The development of the data and information system must be based on the experiences of research studies that need access to remotely sensed data.

One of the main limitations of existing satellite data archives is that they tend to be based on the experience of specialists in remote sensing and data base management. They also tend to be organized around the needs of a single discipline and/or around a single instrument. Thus, they are difficult for most Earth scientists to use, and it is very difficult to analyze multiple data sets when they are located in more than one archive. It is clear that a data and information system designed to meet the needs of Earth scientists is essential if the scientific goals of Eos are to be met.

The development of such a system must be an evolutionary process. Support of several focused—preferably multidisciplinary—scientific studies that require access to several satellite data sets could accelerate this process. Such studies could point out potential problem areas such as access to operational satellite data archives and to small, academic archives. *We recommend that a number of these data-intensive research studies begin as soon as possible, with special attention paid to non-NASA investigators.* It is gratifying that some of the vitality package, university applications, and Eos study funds are being devoted to this need; this should be continued and expanded.

9. We must ensure that scientists involved primarily in data-handling tasks receive appropriate recognition for these tasks by the scientific community.

It has become clear in recent years that successful data archives are not characterized by their hardware but by their scientific management. For

scientific data and information systems, it is essential that there be strong science involvement in system management. Such involvement will help ensure that scientific needs for data access, documentation, etc., are met, as well as ensure high scientific standards for the data to be archived. Also, such “data scientists” can significantly improve the utility of the system by acting as consultants to users concerning matters such as data processing, algorithms, etc. In addition, they can provide scientific leadership, thus enhancing the credibility of the data systems.

Such data scientists perform an invaluable role for the larger scientific community, yet they often go unrewarded in the traditional funding, pay, and promotion systems because their publication rate in scientific journals tends to be lower than average. Funding agencies and institution management must become aware of the fact that such people are essential to the scientific progress of the community. *We recommend that the science community at large, and science managers in particular, judge those who devote themselves to data handling and data system tasks on the quality of the services they provide, not simply on their number of scientific publications.*

Analysis and Understanding

10. We must begin several multidisciplinary Earth science studies so that we are prepared to exploit the large Eos scientific data sets in the study of complex, global-scale processes.

Analogous to the engineering studies for the Eos instruments, we need scientific studies that will not only aid in the design and evolution of the data system as described earlier but will encourage the synergistic cooperation between the various Earth science disciplines. The foundation for Earth system studies has been laid; integration of the discipline components will provide significant progress toward the Eos scientific goals. Studies using existing data sets will help define new observing scenarios as well as identify key processes that need to be measured.

We recommend that such interdisciplinary science investigations be included along with instrument activities in all solicitations and studies preparatory to Eos. There should also be an expanded emphasis on graduate student training, particularly in the area of multidisciplinary, global-scale studies. Such a program can be a component of the science investigations. It is essential that we continue to expand the scientific talent available for Eos studies and ensure that this perspective continues to guide Eos development.

11. We must continue to develop and provide access to numerical models of large-scale and global-scale processes.

We must begin to regard coupled atmosphere-ocean-land models as another tool available to the Earth scientist. We must continue development of these models with the intention of adding to them the ability to assimilate satellite data. Traditionally, modelers and experimentalists have not worked together; the complexity of the processes under study requires such collaboration. These models must become accessible to a broader range of the Earth science community. The principal investigators for Eos instruments must be committed to and involved in the scientific study of the Earth. They cannot be solely hardware developers. Those leading modeling efforts will require an intimate working knowledge of observing system capabilities and limitations.

Both data analysis and modeling will need access to significant computing. Supercomputers will play a vital role in these studies. We must continue to expand the base of supercomputers available to academic researchers. We must ensure that these resources can be easily accessed through the data and information system, particularly for real-time models that will need rapid access to Eos data for predictive studies. *We recommend that large model development activities provide broad community access to their results and that these activities and those scientists performing them be involved in Eos directly.*

12. We must develop techniques for handling data sets from multiple sensors.

Access to a variety of Eos data sets is essential for all of the science scenarios described earlier. Proper comparisons will require an understanding of the sampling characteristics of each sensor as well as the spatial and temporal variability of the processes under study. Such information will be used for binning and gridding data, as well as interpolation between samples. Although such a task seems straightforward, it is complicated in many cases because we do not know the characteristics of the geophysical fields sufficiently well. Again, this suggests a need for access to existing data sets. *We recommend that technique development begin now for the interrelation of various geophysical fields to be measured by Eos.*

Science Management

13. Eos represents a new way of doing Earth science.

Access to a variety of data sets, both *in situ* and remotely sensed, is essential to Earth System Science. It crosses traditional discipline boundaries. It will also require involvement by several agencies. The

traditional model of a single discipline, a single agency, and a single centralized data system has been replaced. Such cooperative ventures have been done in the past, but not at this scale and not involving the full spectrum of Earth science. Coordination between agencies is essential for success. New initiatives such as the Global Geosciences Program proposed by the National Science Foundation complement the Eos program. Other agency programs are emphasizing the use of remote sensing in a variety of large-scale and regional-scale studies. The strength of an overall Earth science program could be greatly increased through coordination of these efforts.

Similarly, Eos will need international involvement if it is to be a truly global activity. Preliminary contacts have been made, and they should continue. It appears that the need for global studies based on remote sensing and ground-based observations has become widely recognized. Pilot studies such as the ESA Earth Observing Preparatory Programme should have close ties with the U.S. effort. *We recommend that committees that can oversee and help coordinate these international efforts be formed as soon as possible.* Such committees could also help stimulate international involvement in Eos. There are a number of current activities, each of which fulfills part of this recommendation. The Coordination Working Group formed by the Earth Observations offices of the Space Station partners is a good step in coordinating the planning and development of the space and data systems aspects of Eos. The International Forum on Earth Observations Using Space Station Means and the Committee on Earth Observing Satellites through its working groups on data and calibration and validation are providing an opportunity for setting standards and harmonizing the Earth observations plans of a larger set of nations in preparation for the Eos era. The adoption by the International Council of Scientific Unions of the IGBP provides a framework for the conduct of major field experiments with truly global support and participation in the 1990s; Eos planning must remain an integral part of these international coordination activities and they must be drawn together so as to be mutually supportive.

There is much work to be done in advance of any launch of Eos hardware. This includes engineering and algorithm studies, development of the data and information system, building up of the intellectual resources, and coordination of interagency and international programs. There is considerable agreement on the need and nature of such Earth system studies. The opportunities for a significant advancement in our understanding of the Earth are here; now is the time to begin.

REFERENCES

Abbott, M.R., and P.M. Zion, Spatial and temporal variability of phytoplankton pigment off Northern California during CODE-1, *J. Geophys. Res.*, (in press), 1987.

Abrams, M.J., A.B. Kahle, F.D. Palluconi, and J.P. Schieldge, Geologic mapping using thermal images, *Remote Sens. Environ.*, 16, 13, 1984.

Angel, M.V., and M.J.R. Fasham, Eddies and biological processes, in *Eddies in Marine Science*, edited by A.R. Robinson, p. 492, Springer-Verlag, New York, NY, 1983.

Asrar, G., M. Fuchs, E.T. Kanemasu, and J.L. Hatfield, Estimating absorbed photosynthetic radiation and leaf area index from spectral reflectance in wheat, *Agron. J.*, 76, 300, 1984.

Badhwar, G.D., J.G. Carnes, and W.W. Austiu, Use of Landsat-derived temporal profiles for corn-soybean feature extraction and classification, *Remote Sens. Environ.*, 12, 57, 1982.

Bernal, P.A., and J.A. McGowan, Advection and upwelling in the California current, in *Coastal Upwelling*, edited by F.A. Richards, p. 381, AGU, 1981.

Bernstein, R.L., Eddy structure of the north Pacific Ocean, in *Eddies in Marine Science*, edited by A.R. Robinson, p. 158, Springer-Verlag, New York, NY, 1983.

Bernstein, R.L., and D.B. Chelton, Large-scale sea surface temperature variability from satellite and shipboard measurements, *J. Geophys. Res.*, 90, 619, 1985.

Beven, K., Surface water hydrology-runoff generation and basin structure, *Rev. Geophys. Space Phys.*, 21, 721, 1983.

Bretherton *et al.*, Earth system science: A program for global change, NASA Advisory Council, Washington, D.C., 1987.

Bretherton *et al.*, Earth system science: A closer view, NASA Advisory Council, Washington, D.C., 1987.

Brink, K.H., B.H. Jones, J.C. Van Leer, C.N.K. Mooers, D.W. Stuart, M.R. Stevenson, R.C. Dugdale, and G.W. Heburn, Physical and biological structure and variability in an upwelling center off Peru near 15°S during March 1977, in *Coastal Upwelling*, edited by F.A. Richards, p. 473, AGU, 1981.

Broecker, W.S., and T. Takahashi, Is there a tie between atmospheric CO₂ content and ocean circulation? in *Climate Processes and Climate Sensitivity*, p. 314, Amer. Geophys. Union, Washington, DC, Monograph 25, 1984.

Butler, D.M. *et al.*, Earth Observing System: Science and Mission Requirements Working Group Report, Vol. I & Appendix, *NASA TM-86129*, 1984.

Camillo, P.J., R.J. Gurney, and T.J. Schmugge, A soil and atmospheric boundary layer model for evapotranspiration and soil moisture studies, *Water Resour. Res.*, 19, 371, 1983.

Carder, K.L., and R.G. Steward, A remote-sensing reflectance model of a red-tide dinoflagellate off West Florida, *Limnol. Oceanogr.*, 30, 286, 1985.

Carlson, T.N., J.K. Dodd, S.G. Benjamin, and J.N. Cooper, Satellite estimation of the surface energy balance, moisture availability and thermal inertia, *J. Appl. Meteor.*, 20, 67, 1981.

Carmouze, J.P., J.R. Durand, and C. Leveque (Editors), *Lake Chad, Ecology and Productivity of a Shallow Tropical Ecosystem*, 575 pp., Dr. W. Junk Publ., The Hague, 1983.

Carsey, F., Microwave observations of the southern ocean, *Mon. Wea. Rev.*, 108, 2032, 1980.

Charnock, H., and R.T. Pollard (Editors), Results of the Royal Society joint air-sea interaction project (JASIN), p. 229, Roy. Soc. Lond., 1983.

Chase, R.R.P. *et al.*, Data and information system: Report of the Eos Data Panel, 62 pp., *NASA TM-87777*, Vol. IIa, 1986.

Chase, R.R.P., *et al.*, Altimetric System, Report of the Eos Altimetry Panel, Vol. IIh, 1987.

Chelton, D.B., Large-scale response of the California current to forcing by wind stress curl, *CalCOFI Rept.*, 23, 130, 1982.

Chelton, D.B., and R.E. Davis, Monthly mean sea level variability along the west coast of North America, *J. Phys. Oceanogr.*, 12, 757, 1982.

Chelton, D.B., P.A. Bernal, and J.A. McGowan, Large-scale interannual physical and biological interaction in the California current, *J. Mar. Res.*, 40, 1095, 1982.

Cheney, R.E., J.G. Marsh, and B.D. Beckley, Global mesoscale variability from collinear tracks of Seasat altimeter data, *J. Geophys. Res.*, 88, 4343, 1983.

Christodoulidis, D.C., D.E. Smith, R. Kolenkiewicz, S.M. Klosko, M.H. Torrence, and P.J. Dunn, Observing tectonic plate motions and deformations from satellite laser ranging, LAGEOS Scientific Results, Reprinted from *J. Geophys. Res.*, 90(B11), 9249, 1985.

Colton, M.T., and R.R.P. Chase, Interaction of the Antarctic circumpolar current with bottom topography: An investigation using satellite altimetry, *J. Geophys. Res.*, 88(C3), 1825, 1983.

Csanady, G.T., *Turbulent Diffusion in the Environment*, 248 pp., Reidel Publishing Co., Dordrecht, Holland, 1973.

Davis, R.E., Drifter observations of coastal surface currents during CODE: The method and descriptive view, *J. Geophys. Res.*, 90, 4741, 1985a.

Davis, R.E., Drifter observations of coastal surface currents during CODE: The statistical and dynamical views, *J. Geophys. Res.*, 90, 4756, 1985b.

Davis, R.E., R. deSzeoke, D. Halpern, and P.P. Niiler, Variability in the upper ocean during MILE. Part I: The heat and momentum balances, *Deep Sea Res.*, 28, 1427, 1981.

Denman, K.L., A time-dependent model of the upper ocean, *J. Phys. Oceanogr.*, 3, 173, 1973.

Denman, K.L., and T.M. Powell, Effects of physical processes on planktonic ecosystems in the coastal ocean, *Oceanogr. Mar. Biol. Ann. Rev.*, 22, 125, 1984.

Denman, K.L., and A.E. Gargett, Time and space scales of vertical mixing and advection of phytoplankton in the upper ocean, *Limnol. Oceanogr.*, 28, 801, 1983.

Denny, P., Permanent swamp vegetation of the Upper Nile, *Hydrobiologia*, 110, 79, 1984.

Donnelley, M., Geology of the Sierra del Pinacate volcanic field, northern Sonora, Mexico, and southern Arizona, U.S.A., (Ph.D. dissert.), 772 pp., Stanford Univ., Stanford, CA, 1974.

Dooge, J., Parameterization of hydrologic processes, in *Land Surface Processes in Atmospheric General Circulation Models*, edited by P.S. Eagleson, Cambridge Univ. Press, New York, NY, 1982.

Duing, W., Spatial and temporal variability of major ocean currents and mesoscale eddies, *Boundary-Layer Meteorol.*, 13, 7, 1978.

Eagleson, P., Climate, soil and vegetation: 1-7, *Water Resour. Res.*, 14, 705, 1978.

Elachi, C., W.E. Brown, J.B. Cimino, T. Dixon, D.L. Evans, J.P. Ford, R.S. Saunders, C. Breed, H. Masursky, J.F. McCauley, G. Schaber, L. Dellwig, A. England, H. McDonald, P. Martin-Kaye, and F. Sabins, Shuttle imaging radar experiment, *Science*, 218, 996, 1982.

Enfield, D.B., and J.S. Allen, On the structure and dynamics of monthly mean sea level anomalies along the Pacific coast of North and South America, *J. Phys. Oceanogr.*, 10, 557, 1980.

Eppley, R.W., and B.J. Peterson, Particulate organic matter flux and planktonic new production in the deep ocean, *Nature*, 282, 677, 1979.

Eppley, R.W., E. Stewart, M.R. Abbott, and U. Heyman, Estimating ocean primary production from satellite chlorophyll. Introduction to regional differences and statistics for the southern California blight, *J. Plankton Res.*, 7, 57, 1985a.

Eppley, R.W., E. Stewart, M.R. Abbott, and R.W. Owen, Estimating ocean production from satellite-derived chlorophyll: Insights from the EASTROPAC data set, *Oceanologica Acta*, (in press), 1985b.

Ewel, K.C., and H.T. Odum (Editors), *Cypress Swamps*, 472 pp., Univ. of Florida Press, Gainesville, FL, 1981.

Farr, T.G., Geologic interpretation of texture in Seasat and SIR-A radar images, *Proc. Int. Soc. Photogram. Remote Sens.*, 24-VII/1, 261, 1982.

Flament, P., L. Armi, and L. Washburn, The evolving structure of an upwelling filament, *J. Geophys. Res.*, 90, 765, 1985.

Freilich, M.H., and D.B. Chelton, Wavenumber spectra of Pacific winds measured by the Seasat scatterometer, *J. Phys. Oceanogr.*, 16, 742, 1986.

Fu, L.-L., and B. Holt, Seasat views oceans and sea ice with synthetic-aperture radar, Jet Propulsion Laboratory, *TM 81-120*, 1982.

Gallo, K.P., C.S.T. Daughtry, and M.E. Bauer, Spectral estimation of absorbed photosynthetically active radiation in corn canopies, *Remote Sens. Environ.*, 17, 221, 1985.

Gaudet, J.J., D.S. Mitchell, and P. Denny, Macrophytes (aquatic vegetation), in *Ecology and Utilization of African Inland Waters*, edited by J.J. Symoens, M. Burgis, and J.J. Gaudet, p. 27, UNEP, Nairobi, 1981.

Gaudet, J.J., and A. Falconer, Remote sensing for tropical freshwater bodies. The problem of floating islands in Lake Naivasha, Regional Remote Sensing Facility, Nairobi, Kenya.

Gill, A.E., Eddies in relation to climate, in *Eddies in Marine Science*, edited by A.R. Robinson, p. 441, Springer-Verlag, New York, NY, 1983.

Gille, J.C., and J.M. Russell III, The Limb Infrared Monitor of the stratosphere: Experiment description, performance, and results, *J. Geophys. Res.*, 89, 5125, 1984.

Gillespie, A.R., A.B. Kahle, and F.D. Palluconi, Mapping alluvial fans in Death Valley, CA, using multichannel thermal infrared images, *Geophys. Res. Letters*, 11, 1153, 1984.

Goel, N.S., and R.L. Thompson, Inversion of vegetation canopy reflectance models for estimating agronomic variables. V: Estimation of LAI and average leaf angle using measured canopy reflectances, *Remote Sens. Environ.*, 16, 69, 1984.

Goetz, A., and B. Rock, Remote sensing for exploration: An overview, *Econ. Geol.*, 78, 573, 1983.

Goldberg, E.D. (Editor), *Proceedings of the Workshop on Assimilative Capacity of U.S. Coastal Waters for Pollutants*, 284 pp., NOAA, Boulder, CO, 1979.

Gordon, A.L., The U.S.-U.S.S.R. Weddell polynya expedition, *Antarct. J. U.S.*, 17, 996, 1982a.

Gordon, A.L., 1982b.

Gore, A.J.P. (Editor), *Mires: Swamp, Bog, Fen and Moor*, Elservier Sci. Publ. Co., Amsterdam, 440 pp., 1983.

Gosselink, J.G., and R.E. Turner, The role of hydrology in freshwater wetland ecosystems, in *Freshwater Wetlands*, edited by R.E. Good, D.E. Whigham, and R.L. Simpson, p. 63, Academic Press, New York, NY, 1978.

Greeley, R., P.R. Christensen, J.F. McHone, Y. Asmerom, and J.R. Zimbelman, Analysis of the Gran Desierto-Pinacate region, Sonora, Mexico, via shuttle imaging radar, *NASA CR-177356*, 1985.

Gross, M.F., and V. Klemas, Discrimination of coastal vegetation and biomass using AIS data, in *Proceedings Airborne Imaging Spectrometer Data Analysis Workshop*, edited by G. Vane and A.F.H. Goetz, p. 129, *JPL Publ. 85-41*, 1985.

Gurney, R.J., and P.J. Camillo, Modelling daily evapotranspiration using remotely sensed data, *J. Hydrol.*, 69, 305, 1984.

Gurney, R.J., and D.K. Hall, Satellite-derived surface energy balance estimates in the Alaskan subarctic, *J. Climate Appl. Meteor.*, 22, 115, 1983.

Haidvogel, D.B., A.R. Robinson, and C.G.H. Rooth, Eddy-induced dispersion and mixing, in *Eddies in Marine Science*, edited by A.R. Robinson, p. 481, Springer-Verlag, New York, NY, 1983.

Hardisky, M.A., F.C. Daiber, C.T. Roman, and V. Klemas, Remote sensing of biomass and annual aerial primary productivity of a salt marsh, *Remote Sens. Environ.*, 16, 91, 1984.

Haury, L.R., and E. Schulenberger, Horizontal transport of phosphorous in the California current, *CalCOFI Report*, 23, 149, 1982.

Hayward, T.L., and E.L. Venrick, Relation between surface chlorophyll, integrated chlorophyll, and integrated primary production, *Mar. Biol.*, 69, 247, 1982.

Hickey, B.M., The California current system—hypotheses and facts, *Prog. Oceanogr.*, 8, 191, 1979.

Hilland, J.E., Chelton, D.B., and E.G. Njoku, Production of global sea surface temperature fields for the Jet Propulsion Laboratory Workshop comparisons, *J. Geophys. Res.*, 90, 665, 1985.

Hunt, G.R., and Salisbury, J.W., Mid-infrared spectral behavior of igneous rocks, *Environ. Res. Paper*, 496-AFCRL-PR-74-0625, 142 pp., 1974.

Huyer, A., Coastal upwelling in the California current system, *Prog. in Oceangr.*, 12, 259, 1983.

Jackson, R.D., Evaluating evapotranspiration at local and regional scales, *Proc. IEEE*, 73, 1086, 1985.

Jones, B.H., K.H. Brink, R.C. Dugdale, D.W. Stuart, J.C. Van Leer, D. Blasco, and J.C. Kelley, Observations of a persistent upwelling center off Point Conception, California, in *Coastal Upwelling: Its Sediment Record. Responses of the Sedimentary Regime to Present Coastal Upwelling*, edited by E. Suess and J. Thiede, p. 37, Plenum Press, New York, NY, 1983.

Kahle, A.B., and A.F.H. Goetz, Mineralogic information from a new airborne thermal infrared multispectral scanner, *Science*, 222, 24, 1983.

Kahn, W.D., F.O. Von Bun, and D.E. Smith, Performance analysis of the spaceborne laser ranging system, *Bull. Geodesique*, 54, 165, 1980.

Katsaros, K.B., The aqueous thermal boundary layer, *Boundary-Layer Meteorol.*, 18, 107, 1980.

Klein, P., and B. Coste, Effects of wind-stress variability on nutrient transport into the mixed layer, *Deep Sea Res.*, 31, 21, 1984.

Koblenz-Mishke, O.J., V.V. Volkovinsky, and J.G. Kabanova, Plankton primary production of the world ocean, in *Scientific Exploration of the Southern Pacific*, edited by W.S. Wooster, p. 183, National Academy of Sciences, 1970.

Leberl, F., J. Raggam, C. Elachi, and W.J. Campbell, Sea ice motion measurements from SEASAT SAR images, *J. Geophys. Res.*, 88, 1915, 1983.

Liu, W.T., Assessing the capability of Eos sensors in measuring ocean-atmosphere moisture exchange, *JPL Publ.* 85-93, 18 pp., Jet Propulsion Laboratory, Pasadena, CA, 1985.

Liu, W.T., and P.P. Niiler, Tropical ocean and global atmosphere (TOGA) heat exchange project—a summary report, *JPL Publ.* 85-49, Jet Propulsion Laboratory, Pasadena, CA, 1985.

Lynch, D.J., Genesis and geochronology of alkaline volcanism in the Pinacate volcanic field, northwestern Sonora, Mexico, (Ph.D. dissert.) 248 pp., Univ. of Arizona, Tucson, AZ, 1981.

Lyon, R.J.P., Evaluation of infrared spectroscopy for compositional analysis of lunar and planetary soils, Stanford Research Inst. Final Report, Contract NASR 49(04), 1962.

Mackas, D.L., K.L. Denman, and M.R. Abbott, Plankton patchiness: Biology in the physical vernacular, *Bull. Mar. Sci.*, 37, 652, 1985.

Marietta, M.G., and A. R. Robinson, *Proceedings of a Workshop on Physical Oceanography Related to Seabed Disposal of High-level Nuclear Waste*, 318 pp., Sandia National Laboratory, TM SAND-80-1776, 1980.

Martinson, D.G., P.D. Killworth, and A.L. Gordon, A convective model for the Weddell Polynya, *J. Phys. Oceanogr.*, 11, 466, 1981.

Matthews, E., and I. Fung, Methane emission for natural wetlands: global distribution, area and environmental characteristics of sources, *Global Biogeochem. Cycles*, 1, 61, 1987.

McGowan, J.A., The California El Niño, *Oceanus*, 27, 48, 1983.

Monteith, J.L., Climate and efficiency of crop production, *Phil. Trans. Royal Soc. (London)*, Ser. B. 281:277294, 1977.

Mooers, C.N.K., and A.R. Robinson, Turbulent jets and eddies in the California current and inferred cross-shore transports, *Science*, 223, 51, 1984.

Moore, B., III (Chairman), The Land Processes Terrestrial Biology Working Group Overview, Earth System Science Committee, 1986.

NASA Ocean Energy Fluxes Science Working Group, Air-sea interaction with SSM/I and altimeter, Ocean Energy Fluxes Science Working Group, Rept. No. 1, 68 pp., Jet Propulsion Laboratory, 1985.

National Research Council, Carbon dioxide and climate: A scientific assessment, Climate Research Board, National Academy of Sciences, Washington, D.C., 1979.

National Research Council, Geodynamics in 1980s, U.S. Geodynamics Committee, Geophysics Board, National Academy of Sciences, Washington, D.C. 1980.

National Research Council, Scientific basis of water-resource management, Studies in Geophysics, Geophysics Research Board, National Academy of Sciences, Washington, D.C., 1982a.

National Research Council, A strategy for Earth sciences from space in the 1980s. Part 1: Solid Earth and oceans, Committee on Earth Sciences, Space Science Board, National Academy of Sciences, Washington, D.C., 1982b.

National Research Council, Opportunities for research in geological sciences, Board on Earth Sciences, National Academy of Sciences, Washington, D.C., 1983a.

National Research Council, Research briefings 1983, Committee on Science, Engineering and Public Policy, National Academy of Sciences, Washington, D.C., 1983b.

National Research Council, Global tropospheric chemistry: A plan for action, National Academy of Sciences, Washington, D.C. 1984a.

National Research Council, El Niño and the southern oscillation: A scientific plan, in *Proceedings of a Workshop*, National Academy of Sciences, Washington, D.C., 1984b.

National Research Council, A strategy for Earth science from space in the 1980s and 1990s, Part II: Atmospheric and interaction with the solid Earth, oceans and biota, Committee on Earth Sciences, Space Science Board, National Academy of Sciences, Washington, D.C. 1985.

National Research Council, Global change in the geosphere-biosphere: Initial priorities for an IGBP, U.S. Committee for an International Geosphere-Biosphere Program, National Academy of Sciences, Washington, D.C., 1986a.

National Research Council, Remote sensing of the biosphere, Committee on Planetary Biology, National Academy of Sciences, Washington, D.C., 1986b.

Niiler, P.P., and E.B. Kraus, One-dimensional models of the upper ocean, in *Modeling and Prediction of the Upper Layers of the Ocean*, edited by E.B. Kraus, p. 143, Pergamon Press, 1977.

Niiler, P.P. (Editor), *Tropical Pacific Ocean Heat and Mass Budgets: A Research Program Outline*, Hawaii Institute of Geophysics Special Publication, 56 pp., 1981.

Oceanography from Space, Plankton and temperature patterns, 1 pp., Jet Propulsion Laboratory, TM 400-225, 1984.

Penman, H.L., Natural evaporation from open water bare soil and grass, *Proceedings of the Royal Society of London (A)*, 193, 120, 1948.

Pilgrim, D.H., I. Cordery, and B.C. Baron, Effects of catchment size on runoff relationships, *J. Hydrol.*, 58, 205, 1982.

Platt, T., and D.V. Subba Rao, Primary production of marine microphytes, in *Photosynthesis and Productivity in Different Environments*, p. 249, Cambridge University Press, Cambridge, MA, 1975.

Rasmusson, E.M., and T.H. Carpenter, Variations in tropical sea surface temperature associated with the Southern Oscillation/El Niño, *Mon. Wea. Rev.*, 110, 354, 1982.

Rienecker, M.M., C.N.K. Mooers, D.E. Hagan, and A.R. Robinson, A cool anomaly off northern California: An investigation using IR imagery and *in situ* data, *J. Geophys. Res.*, 90, 4807, 1985.

Robinson, A.R., Overview and summary of eddy science, in *Eddies in Marine Science*, edited by A.R. Robinson, p. 3, Springer-Verlag, New York, NY, 1983.

Rock, B.N., D.L. Williams, and J.E. Vogelman, Field and airborne spectral characterization of suspected acid deposition damage in Red Spruce (Picea Rubens) from Vermont in *Machine Processed Remotely Sensed Data Symposium*, LARS, p. 71, Purdue University, West Lafayette, IN, 1985.

Rosema, A., J.H. Bijleveld, P. Reiniger, G. Tassone, R.J. Gurney, and K. Blyth, Tellus, a combined surface temperature, soil moisture, and evaporation mapping approach, in *Proc. 12th Internat'l. Symp. Remote Sens. Environ.*, 2267, 1978.

Rowan, L., P. Wetlaufer, A. Goetz, F. Billingsley, and J. Stewart, Discrimination of rock types and detection of hydrothermally altered areas in south-central Nevada by the use of computer-enhanced ERTS images, *U.S. Geol. Survey Prof. Paper*, 883, 35 pp., 1974.

Schaber, G.G., Variations in surface roughness within Death Valley, California; geologic evaluation of 25 cm wavelength radar images, *Geol. Soc. Amer. Bull.*, 87, 29, 1976.

Schmitz, W.J., W.R. Holland, and J.F. Price, Mid-latitude mesoscale variability, *Rev. Geophys. Space Phys.*, 21, 1109, 1983.

Sebacher, D., R.C. Harris, K.B. Bartlett, P.M. Crill, and J.O. Wilson, Atmospheric methane sources: Amazon River floodplain, *Eos Trans. Amer. Geophys. Union*, 66, 822, 1985.

Simmer, C., and S.A.W. Gerstl, Remote sensing of angular characteristics of canopy reflectances, *IEEE Trans. Geosci. Remote Sens.*, GE-23, 648, 1985.

Simonett, D.S., and B.E. Davis, Image analysis—active microwave, in *Manual of Remote Sensing*, p. 1125, 1984.

Smith, R.C., and K.S. Baker, Optical classification of natural waters, *Limnol. Oceanogr.*, 23, 260, 1978.

Soer, G.J.R., Estimation of regional evapotranspiration and soil moisture conditions using remotely sensed crop surface temperature, *Remote Sens. Environ.*, 9, 27, 1980.

Spanner, M.A., D.L. Peterson, W. Acevedo, and P. Matson, High resolution spectrometry of leaf and canopy chemistry for biogeochemical cycling, in *Proceedings Airborne Imaging Spectrometer Data Analysis Workshop*, edited by G. Vane and A.F.H. Goetz, p. 92, *JPL Publ.* 35-41, 1985.

Tapley, B.D., B.E. Schutz, and R.J. Eanes, Station coordinates, baselines, and Earth rotation from LAGEOS laser ranging: 1976-1984, LAGEOS Scientific Results, Reprinted from *J. Geophys. Res.*, **90(B11)**, 9235, 1985.

Taub, F.B. (Editor), *Lakes and Reservoirs*, 643 pp., Elsevier Sci. Publ. Co., Amsterdam, 1984.

Von Bun, F.O., W.D. Kahn, P.D. Argentiero, and D.W. Koch, Spaceborne Earth applications ranging system (SPEAR), *J. Spacecraft and Rockets*, **14**, 492, 1977.

Waring, R.H., Precursors of change in terrestrial ecosystems. Paper presented at Pecora 10 Symposium, Aug. 20-22, 1985, Fort Collins, CO, Remote Sensing in Forestry and Range Management. Sponsored by Amer. Foresters, Range Management, Amer. Soc. of Photogrammetry, Geol. Survey, Dept. of Interior, and NASA, 1985.

Weiss, R.F., Temporal and spatial distributions of tropospheric nitrous oxide. *J. Geophys. Res.*, **86**, 7105, 1982.

Wilson, W.S., Oceanography from satellites?, *Oceanus*, **24**, 9, 1981.

World Climate Research Programme, Report of the workshop on interim ocean surface wind data sets, *WCP-68*, World Climate Research Programme, WMO, Geneva, 1984a.

World Climate Research Programme, International satellite cloud climatology project (ISCCP), *WCP-85*, World Climate Research Programme, WMO, Geneva, 1985.

Worthington, L.V., *On The North Atlantic Circulation*, Johns Hopkins Oceanography Studies No. 6, 110 pp., Johns Hopkins University Press, Baltimore, MD, 1976.

Yentsch, C.S., Phytoplankton growth in the sea: A coalescence of disciplines, in *Primary Productivity in the Sea*, edited by P.G. Falkowski, p. 17, Plenum Press, New York, NY, 1980.

Zawadzki, I.I., Statistical properties of precipitation patterns, *J. Appl. Meteor.*, **12**, 459, 1973.